PROTEOMIC AND BIOCHEMICAL CHARACTERIZATION OF *BACILLUS THURINGIENSIS* TOXIN CRY4BA INTERACTION WITH MIDGUT PROTEINS FROM *AEDES (STEGOMYIA) AEGYPTI* LARVAE

by

KRISHNAREDDY BAYYAREDDY

(Under the Direction of MICHAEL J. ADANG)

ABSTRACT

Cry4Ba toxin derived from *Bacillus thuringiensis israelensis* (Bti) is highly toxic to larval stages of the yellow fever mosquito *Aedes aegypti*, a vector for disease causing pathogens, including dengue, chikungunya and yellow fever. Cry4Ba toxin kills larvae first by binding to gut membrane surface receptors, but these receptor identities in the larval gut are mostly uncharacterized. The overall objective of this research was to investigate Cry4Ba toxin interaction with midgut brush border membrane vesicles (BBMV) and lipid rafts of *Aedes* larvae. BBMV were prepared from whole larvae, and the proteins were separated by two-dimensional electrophoresis followed by ligand blot analysis with the Cry4Ba toxin. Mass spectrometry analysis of Cry4Ba toxin bound proteins resulted in the identification of three alkaline phosphatase (ALP) isoforms, an aminopeptidase, lipid raft proteins (flotillin and prohibitin), V-ATPase B subunit, and actin. The identified ALPs were further validated by immunoblotting with ALP antibodies from *Anopheles* larvae.

Multiple sequence alignment revealed that *A. aegypti* flotillin-1 (Aeflot-1) has high sequence similarity to other insect flotillin-1s and Aeflot-1 antibody can detect other insect flotillin-1s. Immunolocalization of Aeflot-1 was detected on the apical microvilli of larval

posterior midgut and gastric caeca. Furthermore, lipid rafts from *Aedes* BBMV were enriched in the Aeflot-1 and cholesterol. These results indicate that specialized plasma membrane domains are present in *A. aegypti,* and Aeflot-1 antibody can be used as an important tool to characterize membrane lipid rafts.

Previous research suggests that lipid rafts prepared from insect gut BBMV have an important role in Bt toxicity. We isolated and analyzed the protein components of *Aedes* larval BBMV lipid rafts that interact with Cry4Ba toxin. Lipid raft marker proteins, such as flotillin-1 and APN-1, were selectively associated with lipid rafts in the low density fraction. Also, upon Cry4Ba toxin incubation with BBMV, the toxin was enriched in the lipid raft fraction. Using LC-MS/MS we identified a total of 312 proteins including both known lipid raft markers and novel proteins implicated as Cry toxin putative receptors. We also identified a large number of other proteins that have substantial interest across numerous areas of research in mosquito biology and control.

INDEX WORDS: *Bacillus thuringiensis israelensis* (Bti), Cry4Ba, BBMV, *Aedes aegypti*, Flotillin, proteomics, Lipid rafts/DRMs, mass spectrometry

PROTEOMIC AND BIOCHEMICAL CHARACTERIZATION OF *BACILLUS THURINGIENSIS* TOXIN CRY4BA INTERACTION WITH MIDGUT PROTEINS FROM *AEDES (STEGOMYIA) AEGYPTI* LARVAE

by

KRISHNAREDDY BAYYAREDDY

B.S., University of Agricultural Sciences, Bangalore, India, 2001

M.S., University of Agricultural Sciences, Bangalore, India, 2004

A Dissertation Submitted to the Graduate Faculty of The University of Georgia in Partial Fulfillment of the Requirements for the Degree

DOCTOR OF PHILOSOPHY

ATHENS, GEORGIA

2011

PROTEOMIC AND BIOCHEMICAL CHARACTERIZATION OF *BACILLUS THURINGIENSIS* TOXIN CRY4BA INTERACTION WITH MIDGUT PROTEINS FROM *AEDES (STEGOMYIA) AEGYPTI* LARVAE

by

KRISHNAREDDY BAYYAREDDY

Major Professor:	Michael J. Adang
Committee:	Michael Tiemeyer Donald E. Champagne Gang Hua

Electronic Version Approved:

Maureen Grasso
Dean of the Graduate School
The University of Georgia
August 2011

DEDICATION

I dedicate this dissertation to my parents BayyaReddy and Siddamma and my elder brother ShivaReddy and his wife Bharathamma, for their unconditional support and encouragement in achieving my doctoral degree. Without their support, I would not have made it this far.

ACKNOWLEDGEMENTS

I am deeply grateful to a number of people during my journey through doctoral studies. I would like to thank my parents, siblings, extended Bayannagaari family, and all my friends who stood by me and supported all my decisions. Thanks to my wife Shruthi, for understanding and being patient for the last two years.

I am profoundly grateful to my advisor, Dr. Michael J. Adang, for his guidance, encouragement, and support right from the beginning to the final stages of my Ph.D. I am particularly thankful to him for being generous in providing an excellent atmosphere to work with collaborators and also in encouraging my participation in proteomics teaching at Cold Spring Harbor Laboratory, NY.

I am sincerely thankful to all my committee members. Everyone contributed differently, but collectively helped me to carry out my dissertation studies systematically. I am very indebted to Dr. Michael Tiemeyer, for his invaluable suggestions in planning my experiments and also allowing me to work in his lab to purify lipids, and to study their interactions with Bt Cry4Ba toxin. Dr. Donald E. Champagne, has also been very helpful to me in planning my studies, editing dissertation, and enriching my knowledge in mosquito research with his helpful conversations. My special thanks to Dr. Gang Hua, as a committee member and also as a lab colleague, for his invaluable support throughout my doctoral study. I would like to thank Dr. Tracy Andacht, who taught me basics of mass spectrometry analysis and also giving me an opportunity to work with her as teaching assistant to proteomics course.

I deeply owe my lab colleagues Dr. Mohd Amir F. Abdullah and Dr. Lohitash Karumbaiah, for their friendship and efforts in teaching me all the techniques, troubleshooting my research problems, and willingness to provide their best suggestions whenever I needed. I also would like to thank Dr. Suresh Ambati (InsectiGen Inc.,) and other members of Dr. Adang's lab (both present and past) for their support in providing truly encouraging work environment which helped me to grow and mature as a Ph.D., student. My research would not have been complete without their help and cooperation. A special thanks to the members of Dr. Brown's and Dr. Strand's lab for their support and help in using their facilities and equipment.

Also, I would like to extend my thanks to the Department of Entomology at UGA for accepting me as a Ph.D. student, and for providing teaching assistantship. I sincerely thank the graduate coordinator and staff at the department for helping with computer problems, paperwork, and making graduate life easier.

Special thanks to all my friends at UGA and other places; the years we have spent together are very precious and will never be forgotten. This dissertation would not have reached a successful completion without your support.

Sincere thanks to Mr. Ramesh Kumar and Mr. Krishna Murthy, for their support and encouragement throughout my career.

I deeply thank J. N. Tata Endowment for Higher Education of Indians for providing financial support of my initial travel to the United States.

Finally, I would like to thank all my teachers and professors for their encouragement and thoughtful insight towards education and life.

TABLE OF CONTENTS

Page

CHAPTER 1

INTRODUCTION AND LITERATURE REVIEW

Several groups of arthropods transmit human disease causing pathogens, but mosquitoes are the most notable vectors. They are important because they annoy by biting and also transmit deadly disease causing pathogens to humans and other livestock. The most significant mode of mosquito-borne pathogen transmission is by biological transmission while feeding blood from their host. There are three important mosquito vectors belonging to two groups: Anophelinae, which includes *Anopheles spp* and Culicinae which includes *Aedes spp* and *Culex spp* (Harbach 2007), which are commonly found all over the world except Antarctica. These three mosquito spp transmit various pathogens causing deadly diseases such as protozoan in malaria, dog heartworm in filarial diseases and viruses like West Nile Virus, dengue, Chikungunya, encephalitis, and yellow fever which represent some of the biggest threats to the public health agenda (Foster and Walker 2002; Speranca and Capurro 2007; Evans, Clark et al. 2009). For this reason, they are certainly among the best known family of insects that have great biomedical importance in research. Relative to other species of mosquitoes, *Aedes spp* are a good experimental insects and also serve as a model organism in various vector-pathogen interaction researches due to their advantageous characteristics in the laboratory both in terms of mass multiplication and maintenance in addition to a sequenced genome (Clemons, Haugen et al. 2010).

In developing countries of Africa, Asia, and tropical states of USA, malaria still kills several million people, while other mosquito borne pathogens are on the rise. *A. aegypti* is a widely distributed mosquito and the main urban vector involved in dengue, chikungunya and yellow fever virus transmission throughout the world. Yellow fever virus infects 200,000 people and results in 30,000 deaths annually and dengue virus causes incidence of 50 million cases resulting in ~24,000 deaths annually (CDC 2006; Clemons, Haugen et al. 2010). A potential solution to this growing human-health crisis is to stop the spread of mosquito-borne diseases by controlling vector populations. Larval stages of mosquitoes are of relatively low mobility and concentrated in relatively small breeding areas compared with flying adults and are easy to target by various control methods (Killeen, Fillinger et al. 2002). A common control strategy has been the use of broad spectrum synthetic chemical insecticides, this harms the environment with adverse impacts on man and nature. It also leads to the development of insecticide resistant mosquitoes and killing of beneficial organisms (Federici, Park et al. 2003). With this perspective in mind biopesticides assume greater importance. World Health Organization strongly recommends use of eco-friendly biopesticides as an alternative to the use of chemical insecticides (WHO 1985). The most well-known and widely used environment friendly alternative method to control these vectors is the use of bacterium *Bacillus thuringiensis* (Bt) based biopesticides. In other group of insects it's already proven as an effective alternative or supplement to synthetic chemical insecticide usage in managing agricultural and forest pests. They also provide toxin gene source for insect resistance to many insect pests in genetically modified crops (Schnepf, Crickmore et al. 1998).

In mosquitoes, the challenge of controlling these medically important vectors is compounded by emerging resistance to chemical pesticides. Therefore, controlling the larval

stage is critical to mosquito control programs. After discovery of *Bacillus thuringiensis* serovar *israelensis* (Bti), from a mosquito-breeding pond in the Negev Desert of Israel, it's been used very extensively throughout the world to control mosquito larvae (Goldberg and Margalit 1977; Federici 2005). Bti carries a megaplasmid that encodes the insecticidal proteins Cry4Aa, Cry4Ba, Cry10Aa, Cry11Aa, Cyt1Aa and Cyt2Ba (Berry, O'Neil et al. 2002). Each of these insecticidal proteins is deposited in inclusions that become part of the parasporal crystal of *Bti*. These mosquito larvicides are commercially available under the trade names of Aquabac, Bactimos, LarvX, Teknar, and Dunks in water-dispersible granule, aqueous suspension, pellet, granule and briquette formulations (Rose 2001).

1.1 History of *Bacillus thuringiensis*

The genus *Bacillus* belonging to the *Bacillaceae* family is characterized by rod shaped bacteria. It includes free living Gram positive, spore-forming and pathogenic species , which make parasporal inclusion bodies during the stationary phase of its growth cycle (Schnepf, Crickmore et al. 1998). Three species of *Bacillus* are considered microbes of high economic, medical and agricultural importance (Rasko, Altherr et al. 2005). All three species secrete pore forming toxins (PFTs) to harm the host. *Bacillus anthracis* and *B. cereus* cause anthrax and food borne illness respectively. Bt produces delta-endotoxin which is an important pathogenic determinant used to control insect and nematode pests of agriculture, medical and veterinary importance (Lacey and Goettel 1995). Japanese biologist, Shigetane Ishiwata, first isolated Bt and determined it was the cause of the disease in 1901, in silkworm *Bombyx mori* larvae (Ishiwata 1901). Later during 1911, Berliner rediscovered the insecticidal property of Bt when he isolated and showed that the bacterium was toxic when the spores were fed to insects. These spores cause of a disease called *Schlaffsucht* in flour moth *Anagasta kuehniella* larvae in the

German region of Thuringia (Berliner 1911). The interest on Bt stimulated when the strain of Bt was reisolated in 1927 from *Ephestia* and subsequent field tests with this isolate on the European corn borer which lead to the first commercial Bt product, named Sporeine, in France during 1938 (Milner 1994). Although a parasporal body was observed in 1915 (Berliner 1915), interest in the protein crystal structure, biochemical properties, and mode of action of *Bt* crystals increased when researchers, Hannay and Angus, found that the parasporal crystal is the main active ingredient responsible for insecticidal activity against lepidopteran insects (Angus 1954; Angus 1956). Later in the year 1958, United States, started using Bt for commercial purpose and during 1961, Environmental Protection Agency (EPA) registered it as a pesticide (Milner 1994).

1.2 Bt Cry toxins and structural details

To date, more than 200 different Bt endotoxin genes have been discovered and each strain harbors diverse combination of these pesticidal genes (http://www.lifesci.sussex.ac.uk/home/Neil_Crickmore/Bt/). Based on amino acid sequence similarity and insect specificity, the Bt toxins were classified into four groups: Cry 1 (specific to Lepidoptera), Cry 2 (specific to Lepidoptera and Diptera), Cry 3 (specific to Coleopteran) and Cry 4 (Dipteran-specific) (Hofte and Whiteley 1989) and later Cry 5 and Cry 6 (specific to nematodes) were added (Feitelson, Payne et al. 1992). The crystal structures of several of these Cry toxins have been solved (Fig. 1.1): Coleopteran-active Cry3Aa (Li, Carroll et al. 1991), Cry3Bb(Galitsky, Cody et al. 2001) and Cry8Ea1 (Guo, Ye et al. 2009), lepidopteran-active Cry1Aa (Grochulski, Masson et al. 1995), Cry1Ac (Li, Derbyshire et al. 2001), Cry2Aa (Morse, Yamamoto et al. 2001), and mosquitocidal Cry4Ba (Boonserm, Davis et al. 2005), and Cry4Aa toxins (Boonserm, Mo et al. 2006). All these Cry toxins in activated form generally have a three domain structure (Fig. 1.1) which consist of Domain-I (in red color) a seven helix bundle in the

N-terminus, Domain-II (blue color), a triple anti-parallel beta sheet domain in the middle and Domain-III (yellow color), which is a sandwich of two antiparallel beta-sheet in the C-terminus end (Li, Carroll et al. 1991). The core toxin structure has a highly conserved feature across different insect group of active Bt toxins indicating that all the proteins in this Cry family will likely adopt the same general protein folding and topology (Pigott and Ellar 2007).

There is high degree of overall structural similarity in Bt toxins, comprising three distinct domains. Each domain has unique properties in the process of intoxication and insect death. Domain-I consists of 30 Å long, hydrophobic and amphipathic alpha helices, responsible for transmembrane insertion and pore formation (Li, Carroll et al. 1991). Structurally Domain-I resembles the Colicin-A pore forming domain with six helices surrounding a central helix and is important for the membrane insertion step (Parker, Pattus et al. 1989). Domain-II has a beta prism structure with three beta sheets and are solvent exposed (Li, Carroll et al. 1991). This is an important domain with respect to toxicity and is believed to be involved in receptor binding specificity , based on the information derived from mutagenesis studies (Rajamohan, Cotrill et al. 1996) and similarity to immunoglobulin's complementarity determining region (Li, Carroll et al. 1991). The C-terminal toxin end contains Domain III, composed of a β-sandwich structure by two antiparallel β-sheets forming a "jelly roll" topology and plays key roles in maintaining the toxin structural stability (Li, Carroll et al. 1991). Domain III also involves in ion channel conductance regulation in association with Domain I (Chen, Lee et al. 1993), and finally host receptor recognizing and binding (reviewed in (Pigott and Ellar 2007).

1.3 Mosquito larval midgut

In reality, adult mosquitoes are terrestrial and vectors of many diseases causing pathogens, whereas larval mosquitoes are non-vectors and aquatic in habitat. In many ways,

adult biology is quite different from that of larva. A key aspect of larval biology that attracts scientists relevant to larval control and population management is understanding the gut involved in ingestion of food, digestion and absorption (Linser, Smith et al. 2009). The digestive tract, and in particular midgut of mosquito larvae is a target area of many mosquitocidal toxins including the most commonly used Bti, based biopesticide. The mosquito larval midgut is a major part of its body mass and structurally and functionally diverse along the length (Billingsley 1990) containing different cell types, including columnar cells, tracheal cells and non-digestive regenerative cells performing different functions (Zhuang, Linser et al. 1999).

The alimentary canal of *A. aegypti* larvae is a long tubular epithelium divided into foregut, a straight midgut and a hindgut (Zhuang, Linser et al. 1999). At the anterior end of the alimentary canal, the foregut consists of esophagus and terminates in the proventriculus. Ingested food particles after mixing with saliva in mouth, move posteriorly due to muscular activity and by pushing from new food particles in the mouth (Clements 1992). The midgut region begins in the prothorax at the cardiac sphincter and extends through the thorax and up to the 7^{th} abdominal segment. It is composed of the cardia, gastric caeca, anterior midgut (AMG) and posterior midgut (PMG). The posterior end of the foregut is surrounded by cardia, and is involved in the secretion of peritrophic matrix (PT), a protective matrix that continuously surrounds the food during its passage from anterior to posterior end of the gut. Space between the PT and the gut epithelium is a compartment called the ectoperitrophic space (Zhuang, Linser et al. 1999).

In general, gastric caeca (generally 8 in number) are involved in the digestion and absorption of proteins, carbohydrates, and in the secretion of antimicrobial peptides. The midgut region is mainly involved in digestion of food, absorption of lipids, carbohydrates and proteins (Lehane and Billingsley 1996). The columnar cells in the midgut are elongated and flat with

narrow extensions originating from the plasma membrane surface towards gut lumen called microvilli (Zieler, Garon et al. 2000). At the apical microvilli membrane is packed with enzymes that help the breakdown of complex nutrients into simpler compounds and their absorption in the gut lumen (Clements 1992). The posterior end is the hindgut, which consists of ileum followed by colon then finally by the rectum. At the junction of midgut and the hindgut are Malpighian tubules (5 in number) that extend from gut epithelium into the surrounding hemolymph. The Malpighian tubules are involved in ion regulation. hindgut is involved in the final steps of digestion, absorption and elimination of digestive waste (Wigglesworth 1933).

1.4 Bt toxin mechanism of intoxication in lepidopteran insects

The mode of action of Bt Cry toxins is best studied for the lepidopteran-active Cry1A group (Fig. 1.2) and to date, there are several models that have attempted to explain the toxin interaction with susceptible insect midgut cells. In general, the intoxication process is a complex event of Cry toxins. After ingestion of protoxin or crystal by a susceptible insect, it undergoes solubilization in the gut alkaline environment and proteolytic activation. Toxin then binds to membrane surface receptor called cadherin, followed by dual action of Mg^{2+}-dependent signaling pathway activation. It also results in conformational changes of the toxin molecules, leading to binding to secondary receptors forming a pre-pore complex, lipid raft insertion, ionic disequilibrium, cell lysis and insect death.

According to a model by Bravo et al. (Bravo, Gómez et al. 2004) based on the sequential receptor binding (Fig. 1.2), activated Cry1A monomer toxin upon binding to cadherin induces an internal protease cleavage of toxin which results in oligomerization of the toxin and subsequent binding to glycosylphosphatidyl inositol (GPI) anchored aminopeptidases (APN) and alkaline phosphatase (ALP). Secondary receptors direct toxin oligomer to insert into lipid rafts domains

to make lytic pores finally leading to change in membrane potential, ionic imbalance across the membrane, which results in cell swelling, and cell lysis.

According to the Zhang et al. model (Zhang, Candas et al. 2005; Zhang, Candas et al. 2006) Bt toxin binds as monomeric Cry1Ab to cadherin (BT-R_1) receptor and triggers an $Mg2^{+}$-dependent signaling pathway in which G protein and adenylyl cyclase get stimulates by interaction of toxin and host receptor, which results in increased cyclic AMP levels, and activation of protein kinase A (PKA). Activated PKA affects downstream signaling molecules that, in turn, destabilize both the cytoskeleton and ion channels in the cell membrane leading to cell death. This model also speculates that, monomeric toxin after binding to cadherin, forms an oligomer and interacts non-specifically with host lipids. The oligomer inserts into membrane and does not cause cell toxicity due to failure to form lytic pores in the membrane.

There are two other models which are less popular, the one is Jurat-Fuentes and Adang's model, which says that, toxicity caused by Bt toxins is due to the combination of both sequential receptor binding-osmotic lysis and activation of cell signaling pathway regulated by phosphatases (Jurat-Fuentes and Adang 2006). The other model (Nair and Dean 2008) which was proposed recently, claim that all the domains of activated Cry1A toxin insert into *Manduca sexta* brush border membranes.

1.5 Bt toxin mechanism of intoxication in mosquito larvae

A detailed model that describes the mechanisms that kills mosquito larvae has not been elucidated, but several identified Cry toxin receptors in mosquitoes which are similar to Lepidoptera indicate, that mode of action undoubtedly occurs as a multi-step process. Recently, the mode of action of Bt toxins which is based on sequential receptor binding in mosquitoes has been described (Likitvivatanavong, Chen et al. 2011). Upon ingestion of Bt paraspores by a

susceptible mosquito larva, the highly alkaline environment in midgut solubilizes inclusions releasing the inactive toxins, which are cleaved and activated by the action of gut proteases. Activated toxin first either binds to high affinity APN and ALP receptors, followed by binding to a cadherin, or directly binds to the cadherin first, triggering helix cleavage and the formation of toxin oligomer, which then binds to APN or ALP proteins in lipid rafts, resulting in the oligomeric toxins insertion into the cell membrane leading to pore formation and cell death. The Cyt toxin component of Bti crystals has limited toxicity itself, but none the less serves as a synergist enhancing Cry protein toxicity to mosquito larvae. This synergism occurs via a mechanism whereby Cyt toxin itself binds to brush border membrane and functions as a receptor for Cry11Aa (Perez, Fernandez et al. 2005).

1.6 Known Bt Cry toxin receptors in Insect midgut

Five different types of membrane components which have been identified and characterized as Bt toxin receptors inside the midgut of lepidopteran caterpillars. They are GPI-APN (Knight, Crickmore et al. 1994; Sangadala, Walters et al. 1994), cadherin (Vadlamudi, Weber et al. 1995; Nagamatsu, Koike et al. 1999), GPI- ALP (McNall and Adang 2003; Jurat-Fuentes and Adang 2004), 270-kD glycoconjugate (Valaitis, Jenkins et al. 2001) and glycolipids (Griffitts, Haslam et al. 2005). In coleopteran grubs, ADAM metalloprotease (Ochoa-Campuzano, Real et al. 2007), cadherin (Fabrick, Oppert et al. 2009) and GPI-ALP (Martins, Monnerat et al. 2010) has been identified as a functional receptor to Cry toxin.

Relative to Cry1A toxin interaction with midgut tissue, less is known about the identities and roles of Cry toxin receptors in mosquito larvae. Several receptors (Table 1.1) implicated in binding to the toxin includes, a GPI-anchored ALP (Buzdin, Revina et al. 2002; Fernandez,

Aimanova et al. 2006; Hua, Zhang et al. 2009; Dechklar, Tiewsiri et al. 2011), cadherin (Hua, Zhang et al. 2008; Chen, Aimanova et al. 2009) and a 100-kDa GPI-anchored APN (Abdullah, Valaitis et al. 2006; Zhang, Hua et al. 2008; Chen, Aimanova et al. 2009; Saengwiman, Aroonkesorn et al. 2011) and GPI-anchored alpha-amylase (Fernandez-Luna, Lanz-Mendoza et al. 2010). All these receptor identities suggests that some of the same types of proteins which function as receptors in Cry1A toxins in lepidopteran larvae are involved in modulating Cry toxin action against mosquitoes. In Lepidoptera, all the known GPI-anchored Cry receptors are partitioned into lipid rafts which are enriched in cholesterol and sphingolipids, and have been suggested to serve as platforms for a range of cellular signaling complexes and protein sorting (Zhuang, Oltean et al. 2002).

1.7 Lipid rafts – specialized plasma membrane domains

In recent times, there is a clear evidence for the co-existence of more than one lipid bilayer phase. The different phases of lipid bilayers represent physical states which differ in the degree of lipid packing, the order and the relative mobility of lipid components within the lipid bilayer (Brown and London 1998; Rietveld and Simons 1998). Two main phases are the cholesterol rich liquid-ordered (L_0) and a cholesterol poor liquid-disordered (L_d) phase (Brown and London 1998; Brown and London 1998). The classical fluid mosaic model of the cell membranes structure states that, biological membranes are very organized and can be considered as a two-dimensional liquid where all functionally active protein and lipid molecules are randomly distributed (Singer and Nicolson 1972). Over a decade of research on cell plasma membrane organization indicates that membrane lipids are not randomly distributed, but instead have local heterogeneities forming a membrane subdomains, one among them is called lipid rafts

or L_0 phase or detergent resistant membranes (DRMs) (Simons and Ikonen 1997; Brown and London 1998).

Lipid rafts are subdomains of plasma membrane with a distinct characteristic of enriched cholesterol-sphingolipid structural composition and that appear to act as specialized platforms to co-localize a variety of post-translationally modified proteins involved in various cellular functions (Brown and Rose 1992; Simons and Ikonen 1997; Brown and London 1998). An indication of these rafts existence came from the observation that cell membranes were partially resistant to cold non-ionic detergents solubilization and can be isolated on a sucrose gradient solution (Brown and Rose 1992; Schroeder, Ahmed et al. 1998).

1.8 The lipid raft hypothesis

The concept of lipid raft domains existence was proposed by a group led by Simons Kai, when working on studies involving epithelial cell polarity (Simons, *et al.*, 1988). They hypothesize the existence of dynamic assemblies of cholesterol and sphingolipids in the exoplasmic leaflet of the lipid bilayer. The presence of mostly phospholipids with unsaturated fatty acyl chains and cholesterol make membrane surrounding lipid rafts more fluid and distinct (Simons and Toomre 2000).

Study related to the lipid rafts is challenging because of nano-scale size (10–200 nm) (Pike 2009) and these rafts need milliseconds time to diffuse across the cell membrane (Sengupta, Baird et al. 2007). They require additional resources and techniques for timely detection. Numerous studies in model membranes, plasma membrane vesicles and reconstituted plasma membrane vesicles have presented evidence for existence of complex lipid rafts by various techniques; e.g. by electron microscopy (Wilson, Pfeiffer et al. 2000), photonic force microscopy (Pralle, Keller et al. 2000), atomic force microscopy (AFM) (Anderton, Lou et al.

2011), Forster resonance energy transfer (FRET) (Rao and Mayor 2005), Fluorescence correlation and cross-correlation spectroscopy (FCS/FCCS) (Sankaran, Manna et al. 2009) and antibody cross-linking of placental GPI-ALP, Thy-1, influenza virus hemagglutinin (HA), and raft lipid ganglioside GM1 into patches and separating them from non-raft proteins (Harder, Scheiffele et al. 1998).

1.9 Lipid rafts purification and characterization

The most important biochemical property of lipid raft/DRMs is their insolubility in non-ionic detergents at 4°C. These are commonly extracted by employing detergent- and non-detergent based fractionation methods combined with sucrose or Optiprep density gradient ultra-centrifugation by exploiting their low density physical property resulting from high lipid-to-protein ratio (Ostrom and Liu 2007). DRMs can be extracted with several detergents but recent study have demonstrated that only CHAPS and Triton X-100 detergents can display specificity for the lipid-raft markers cholesterol and sphingomyelin (Schuck, Honsho et al. 2003). Typically lipid rafts/DRMs are purified from either membrane fractions or from total cell lysate extracted with 1% Triton X-100. Typically, the treated membrane mixture is floated through three gradients of sucrose/Optiprep at 40-45% (which contains the starting material), 30-35% and 5% density gradient fractionation carried out ~ 200,000 g at 4^0C (Brown and Rose 1992). Another method for isolating lipid rafts is detergent free extraction in high salt (500 mM sodium carbonate), and high pH (≥11), followed by gradient ultracentrifugation (Song, Scherer et al. 1996). The main disadvantage with this approach is its failure to enrich GPI-anchored proteins. A high pH buffer, resulted in more than 75% enriched proteins being non-raft proteins (Foster, de Hoog et al. 2003). Regardless of the extraction method, DRMs are recovered from the 5%-

30% sucrose/Optiprep gradient or least and preceding low % gradient interface, to which majority of the complex is localized.

Several approaches have been taken to characterize the DRMs after biophysical fractionation process. Biochemical detection of cholesterol and enzyme enrichments and immunodetection of DRMs components are the most commonly used approaches. Enzymatic and western blot detection of GPI-anchored ALP and APN proteins are well-characterized markers for the DRM fraction of the plasma membrane (Mayor, Rothberg et al. 1994; Danielsen 1995; Simons and Ikonen 1997; Milhiet, Giocondi et al. 2002; Nguyen, Amine et al. 2006) in addition, to integral membrane proteins flotillin-1 (Bickel, Scherer et al. 1997; Dermine, Duclos et al. 2001; Salzer and Prohaska 2001; Santamaria, Castellanos et al. 2005).

Since their discovery, flotillin-antibodies are extensively used as diagnostic tools for lipid raft fractions (Stuermer 2011). Flotillin-1, is a member of lipid raft-associated integral membrane protein that carry a evolutionarily conserved domain called the prohibitin homology domain (PHB) (Morrow and Parton 2005) also known as the SPFH (stomatin, prohibitin, flotillin, HflC/K) superfamily (Tavernarakis, Driscoll et al. 1999). In adipocytes, Flotillin-1 has been implicated in insulin signaling pathway by recruiting activated signaling molecules to lipid rafts and thus forming complexes with lipid raft-based downstream effector proteins to trigger glucose transporter redistribution (Baumann, Ribon et al. 2000), it also interacts and co-precipitates with GPI-linked proteins (Stuermer, Langhorst et al. 2004) in the plasma membrane domains. Among insects, flotillins were first identified in *Drosophila*, and found to be expressed in the developing nervous system (Galbiati, Volonte et al. 1998). They are essential for filopodia formation (Hazarika, Dham et al. 1999) and in signaling processes at cellular contact sites. Misexpression of flotillins interferes with wing and eye development (Hoehne, Gert de Couet et al. 2005) and

flotillins are required for secretion and spreading of Wnt and Hedgehog in *Drosophila* (Katanaev, Solis et al. 2008).

In zebrafish, flotillin proteins are required for cholera toxin intoxication of cells which helps in trafficking of the GM1-toxin complex from the plasma membrane to the endoplasmic reticulum (Saslowsky, Cho et al. 2010). In association with flotillin-2, flotillin-1 forms hetero-oligomeric complexes that are believed to be involved in various cellular activities, namely epidermal growth factor (EGF)-induced endocytosis (Babuke, Ruonala et al. 2009), EGF signaling (Neumann-Giesen, Fernow et al. 2007), cytoskeletal rearrangement (Rajendran, Beckmann et al. 2009). Further, flotillins are also required for NPC1L1-mediated cellular cholesterol uptake, biliary cholesterol reabsorption, and for the regulation of lipid levels in mice (Ge, Qi et al. 2011).

Two simple methods are used widely to define the proteins that reside in lipid rafts and to investigate their functional role in a variety of cellular processes. The most common method is based on sequestration of cholesterol, its depletion and removal using methyl-β-cyclodextrin (Ilangumaran and Hoessli 1998). Since lipid rafts are highly enriched in cholesterol, removal or reduction of its content sometimes redistributes proteins differently in lipid rafts indicating their characteristics of being associated to rafts (Brown 2006) and in disrupting the association of a protein to rafts also disrupts its function. Another approach is to cluster the protein of interest with lipid rafts, since several proteins must interact and/or co-localize to perform cellular functions.

1.10 Lipidomics of DRMs/Lipid rafts

Recent advances in the field of lipidomics, mass spectrometry coupled with computational methods, to analyze lipids resulted in better understanding of the lipidome of lipid

rafts. Relatively, lipid raft bilayers are thicker than non-raft bilayers because of presence of high percentage of saturated polar lipids (sphingomyelin [SM]) and cholesterol, and they are resistant to cold Triton X-100 extraction, whereas non-raft membranes were enriched in dioleoylphosphatidylcholine (DOPC) and were readily soluble in Triton X-100 (McIntosh, Vidal et al. 2003). These Triton X-100 insoluble membranes had 32 and 14 mol% more cholesterol and sphingomyelin and 5-fold enrichment of glycolipids such as gangliosides and sulfatides compared to the whole cell membranes (Brown and Rose 1992). Cholesterol is important component in maintaining raft integrity and thought to serve as a spacer between the hydrocarbon chains of the sphingolipids (Simons and Toomre 2000). Cholesterol also has higher affinity to raft sphingolipids than to unsaturated phospholipids and partitions between the low density raft and the high density non-raft phase (Simons and Ehehalt 2002).

In experiments when model membranes were reconstituted *in vitro* with defined lipids, it has been shown that, sphingolipids can indeed form a 'L_0' phase in the lipid bilayer, at the relative concentrations found in the plasma membrane (Ahmed, Brown et al. 1997). Early observations indicated that lipids in rafts tend to be in a more rigid state than the surrounding membrane and it has been correlated to the tight packing of saturated acyl chains of rafts phospholipids (Brown and London 1998). Several studies have indicated that, the main lipid classes present in the membrane rafts are phospholipids, glycosphingolipids, and cholesterol (Quinn 2010). Rafts prepared by non-detergent methods were enriched in cholesterol, sphingomyelin, phosphatidylserine, and arachidonic acid-containing plasmenylethanolamine as compared to the rafts prepared by detergent extraction method which contained higher levels of cholesterol and saturated fatty acyl chains (Pike, Han et al. 2002). Phosphatidylserine was enriched by 2- to 3-fold in rafts as compared with plasma membranes (Pike, Han et al. 2005).

Lipid composition also varies between DRMs derived from different organelle membranes, cellular types, and tissue types (Koumanov, Tessier et al. 2005).

In insects a few attempts to study the lipid composition of DRMs have been made and these studies have reported variations in lipid content, and the ratio of lipid to proteins. For example, *H. virescens* DRMs have a higher percentage of long fatty acid acyl chains and lower lipid-to-protein ratio than that observed in *M. sexta* DRMs and both species contain increased levels of cholesterol and phospholipids (Zhuang, Oltean et al. 2002). In both *D. melanogaster* and lepidopteran DRMs, the major non-steroid lipids detected are sphingomyelin (SM), phosphatidylserine (PS), phosphatidylcholine (PC), phosphatidylinositol (PI), phosphatidylethanolamine (PE) and shorter acyl chain lengths of lipid (Rietveld, Neutz et al. 1999; Zhuang, Oltean et al. 2002).

1.11 Proteomics of DRMs/Lipid rafts

Mass spectrometry, a highly sensitive method for qualitative and quantitative protein profiling that allow the study of hundreds to thousands of proteins and the analytical identification of protein composition of a sample based on mass to charge ratios (Guerrera and Kleiner 2005). Plasma membrane proteins can be grouped into three categories; raft resident proteins, proteins associated with non-raft membrane and proteins which move in and out of rafts representing intermediate state (Simons and Ehehalt 2002). Proteomics analyses have been done on detergent-resistant membranes (Gupta, Wollscheid et al. 2006; Le Naour, André et al. 2006; Zhang, Shaw et al. 2008; Williamson, Thompson et al. 2010), and non-detergent membranes (Foster, de Hoog et al. 2003; McMahon, Zhu et al. 2006). Lipid rafts proteomic studies have identified several proteins as a part of rafts, including GPI-anchored proteins (Brown and Rose 1992; Zhuang, Oltean et al. 2002; Sangiorgio, Pitto et al. 2004), heterotrimeric G protein α-

subunits, doubly acylated proteins such as Src tyrosine kinases (Resh 1999), palmitoylated and myristoylated proteins such as flotillins (Salzer and Prohaska 2001), cholesterol-binding proteins such as caveolins (Anderson 1993), and phospholipid-binding proteins such as annexins (Rajendran and Simons 2005). In general, it has been found that lipid rafts fractionation provides a cleaner starting material for sub-proteome analysis than other methods, having less false positives with respect to their raft association and biological function (Foster, de Hoog et al. 2003). However, showing a change in the membrane domain association of a particular protein following a pathogen infection (Bravo, Gómez et al. 2004) or particular treatment of cells with a physiological stimulus (Bini, Pacini et al. 2003; MacLellan, Steen et al. 2005) is an alternative approach to probe the selective raft resident proteins involvement in a specific biological process. In general, the protein and lipid composition of rafts from the different organism or species is often different. Despite several proteomic studies in vertebrate systems, no comprehensive proteomic studies regarding characterization of insect lipid rafts associated proteome have been reported yet.

1.12 Bt toxins interactions with Lipid Rafts

Communication between Bt toxins and their host cell occurs via macromolecules (proteins, lipids and glycan) embedded in the plasma membrane. Besides specific host protein receptor-mediated interactions, the research during last decade has highlighted the importance of specialized plasma membrane domains, called lipid rafts in the intoxication processes.

In the Bt derived pore-forming Cry toxins, the initial step in the mode of action process is insertion of the toxin into insect brush border membranes to form membrane-penetrating toxin channels and various size pores by targeting lipid rafts, to accumulate and oligomerize in these domains (Pigott and Ellar 2007). In *M. sexta* and *H. virescens*, lipid rafts are known to act as

concentration platforms for Cry toxin receptors including GPI-anchored proteins, such as APN and ALP. Lipid raft integrity is understood to be important for toxin insertion and membrane pore formation (Zhuang, Oltean et al. 2002). The lepidopteran (Sf9) cell line is known to became insensitive to Cry1C toxin when their growth is arrested at G2-M phase because of the lack of organized lipid rafts in these dividing cells (Avisar, Segal et al. 2005).

Recently, an anticancer Cry toxin parasporin derived from *B. thuringiensis* has been identified and shown to exhibit selective cytotoxicity towards human cancer cell lines (Ito, Sasaguri et al. 2004; Ohba, Mizuki et al. 2009). Similar to other insecticidal Bt toxins, this parasporin also binds specifically to GPI-anchored proteins located in the lipid rafts of the plasma membrane of susceptible cells followed by its oligomerization and pore formation resulting in a rapid increase in membrane permeability (Abe, Shimada et al. 2008).

1.13 Rationale and goals of the dissertation

The working hypothesis of the current dissertation research is, mosquitocidal Bt toxins interacts with their host cells. Their receptors (GPI-anchored proteins) similar to the other pore-forming toxins, the toxin will also be partitioning into lipid rafts, and integrity of these rafts is a key to Cry4Ba toxin insertion and pore formation. Due to the structural similarities of Cry4B and Cry1 toxins, and recent knowledge of mosquito receptors to Bt toxins, it is possible that both share a similar mode of action and perhaps use similar receptors, the same classes of proteins (Boonserm, Davis et al. 2005). The preceding literature review indicates that much of our knowledge on the Bt toxin receptors such as cadherin, GPI-anchored APN, and ALP has been derived from studies involving the Cry toxins in Lepidoptera. Despite these advances in the Lepidoptera, relatively less is known about the Bt toxin binding protein identities, their role as receptors in the target mosquitoes. Yet this information is absolutely essential for understanding

insect resistance against the Bt toxins and in designing rational strategies offering the potential to reduce medically important mosquito populations and/or prevent pathogen transmission without harming the environment and non-target organisms.

In search of identifying more Cry toxin receptors in mosquitoes we have used proteomics approach. Traditional one-dimensional approach may not resolve individual proteins identified by ligand blots. The recent improvements in the techniques of 2-DE (two-dimensional gel electrophoresis) and mass spectrometry, in combination with accumulating genome sequence database resources, have made it possible to characterize the many proteins in insects. In our laboratory, these techniques combined with ligand blotting were applied previously to identify lepidopteran midgut BBMV proteins (McNall and Adang 2003; Krishnamoorthy, Jurat-Fuentes et al. 2007).

The following chapters describe the results of my studies that are largely aligned with my above mentioned research goals. Chapter 2 describes, the identification of novel Bti Cry4Ba binding proteins in *A. aegypti* larval midgut through a two-dimensional gel based proteomics approach combined with ligand blots. Chapter 3 reports the developing of marker proteins to establish an optimized method to prepare and characterize detergent resistant membranes/lipid rafts from larval mosquito BBMV. The work in this chapter includes, cloning of flotillin-1 cDNA from *Aedes* larval midgut, expressing the protein heterologously in *E. coli*, making poly-clonal flotillin-1 antibody, immunolocalizing flotillin in *Aedes* midgut, and preparing lipid rafts. Chapter 4 describes the results of Cry4Ba interaction with *A. aegypti* BBMV DRMs/lipid rafts and proteome profiling of the same DRMs/ lipid rafts using Liquid chromatography Mass spectrometry (LC-MS/MS). The chapters 3rd and 4th were written and organized in a manner that would facilitate their publication in a peer-reviewed journal.

References

Abdullah, M. A., A. P. Valaitis, et al. (2006). "Identification of a *Bacillus thuringiensis* Cry11Ba toxin-binding aminopeptidase from the mosquito, *Anopheles quadrimaculatus*." BMC Biochem. **7**: 16.

Abe, Y., H. Shimada, et al. (2008). "Raft-targeting and oligomerization of Parasporin-2, a *Bacillus thuringiensis* crystal protein with anti-tumour activity." J. Biochem. **143**(2): 269-275.

Ahmed, S. N., D. A. Brown, et al. (1997). "On the origin of sphingolipid/cholesterol-rich detergent-insoluble cell membranes: physiological concentrations of cholesterol and sphingolipid induce formation of a detergent-insoluble, liquid-ordered lipid phase in model membranes." Biochemistry **36**(36): 10944-10953.

Anderson, R. G. (1993). "Caveolae: where incoming and outgoing messengers meet." Proc. Natl. Acad. Sci. U. S. A. **90**(23): 10909-10913.

Anderton, C. R., K. Lou, et al. (2011). "Correlated AFM and NanoSIMS imaging to probe cholesterol-induced changes in phase behavior and non-ideal mixing in ternary lipid membranes." Biochim. Biophys. Acta **1808**(1): 307-315.

Angus, T. (1954). "A bacterial toxin paralysing silkworm larvae." Nature **173**: 545-546.

Angus, T. (1956). "General characteristics of certain insect pathogens related to *Bacillus cereus*." Canad. J. Microbiol. **2**: 111-121.

Avisar, D., M. Segal, et al. (2005). "Cell-cycle-dependent resistance to *Bacillus thuringiensis* Cry1C toxin in Sf9 cells." J. Cell Sci. **118**(Pt 14): 3163-3171.

Babuke, T., M. Ruonala, et al. (2009). "Hetero-oligomerization of reggie-1/flotillin-2 and reggie-2/flotillin-1 is required for their endocytosis." Cell. Signal. **21**(8): 1287-1297.

Baumann, C. A., V. Ribon, et al. (2000). "CAP defines a second signalling pathway required for insulin-stimulated glucose transport." Nature **407**(6801): 202-207.

Bayyareddy, K., T. M. Andacht, et al. (2009). "Proteomic identification of *Bacillus thuringiensis* subsp. *israelensis* toxin Cry4Ba binding proteins in midgut membranes from *Aedes* (*Stegomyia*) *aegypti* Linnaeus (Diptera, Culicidae) larvae." Insect Biochem. Mol. Biol. **39**(4): 279-286.

Berliner, E. (1911). "Uber die schlaffsucht der mehlmottenraupe." Zeitschrift Gesamte Getreidewes **252**: 3160-3162.

Berliner, E. (1915). "Über die Schlaffsucht der mehlmottenraupe (*Ephestia kuhniella* Zell)." Z. Angew. Entomol. **2**: 29-56.

Berry, C., S. O'Neil, et al. (2002). "Complete sequence and organization of pBtoxis, the toxin-coding plasmid of *Bacillus thuringiensis* subsp. *israelensis*." Appl. Environ. Microbiol. **68**(10): 5082-5095.

Bickel, P. E., P. E. Scherer, et al. (1997). "Flotillin and epidermal surface antigen define a new family of caveolae-associated integral membrane proteins." *J. Biol. Chem.* **272**(21): 13793-13802.

Billingsley, P. F. (1990). "The midgut ultrastructure of hematophagous insects." Annu. Rev. Entomol. **35**(1): 219-248.

Bini, L., S. Pacini, et al. (2003). "Extensive temporally regulated reorganization of the lipid raft proteome following T-cell antigen receptor triggering." Biochem. J. **369**(2): 301-309.

Boonserm, P., P. Davis, et al. (2005). "Crystal structure of the mosquito-larvicidal toxin Cry4Ba and its biological implications." J. Mol. Biol. **348**(2): 363-382.

Boonserm, P., M. Mo, et al. (2006). "Structure of the functional form of the mosquito larvicidal Cry4Aa toxin from *Bacillus thuringiensis* at a 2.8-angstrom resolution." J. Bacteriol. **188**(9): 3391-3401.

Bravo, A., I. Gómez, et al. (2004). "Oligomerization triggers binding of a *Bacillus thuringiensis* Cry1Ab pore-forming toxin to aminopeptidase N receptor leading to insertion into membrane microdomains." Biochim. Biophys. Acta **1667**(1): 38-46.

Brown, D. A. (2006). "Lipid rafts, detergent-resistant membranes, and raft targeting signals." Physiology (Bethesda) **21**: 430-439.

Brown, D. A. and E. London (1998). "Functions of lipid rafts in biological membranes." Annu. Rev. Cell Dev. Biol. **14**: 111-136.

Brown, D. A. and E. London (1998). "Structure and origin of ordered lipid domains in biological membranes." J. Membr. Biol. **164**(2): 103-114.

Brown, D. A. and J. K. Rose (1992). "Sorting of GPI-anchored proteins to glycolipid-enriched membrane subdomains during transport to the apical cell surface." Cell **68**(3): 533-544.

Buzdin, A. A., L. P. Revina, et al. (2002). "Interaction of 65- and 62-kD proteins from the apical membranes of the *Aedes aegypti* larvae midgut epithelium with Cry4B and Cry11A endotoxins of *Bacillus thuringiensis*." Biochemistry (Moscow) **67(5)**: 540-546.

CDC (2006). "http://www.who.int/csr/disease/dengue/impact/en/."

Chen, J., K. G. Aimanova, et al. (2009). "*Aedes aegypti* cadherin serves as a putative receptor of the Cry11Aa toxin from *Bacillus thuringiensis* subsp. *israelensis*." Biochem. J. **424**(2): 191-200.

Chen, J., K. G. Aimanova, et al. (2009). "Identification and characterization of *Aedes aegypti* aminopeptidase N as a putative receptor of *Bacillus thuringiensis* Cry11A toxin." Insect Biochem. Mol. Biol. **39**(10): 688-696.

Chen, X. J., M. K. Lee, et al. (1993). "Site-directed mutations in a highly conserved region of *Bacillus thuringiensis* delta-endotoxin affect inhibition of short circuit current across *Bombyx mori* midguts." Proc. Natl. Acad. Sci. U.S.A. **90**(19): 9041-9045.

Clements, A. N. (1992). The Biology of Mosquitoes. London, New York, Chapman and Hall.

Clemons, A., M. Haugen, et al. (2010). "*Aedes aegypti*: an emerging model for vector mosquito development." Cold Spring Harb. Protoc. **2010**(10): 141.

Danielsen, E. M. (1995). "Involvement of detergent-insoluble complexes in the intracellular transport of intestinal brush border enzymes." Biochemistry **34**(5): 1596-1605.

Dechklar, M., K. Tiewsiri, et al. (2011). "Functional expression in insect cells of glycosylphosphatidylinositol-linked alkaline phosphatase from *Aedes aegypti* larval midgut: A *Bacillus thuringiensis* Cry4Ba toxin receptor." Insect Biochem. Mol. Biol. **41**(3): 159-166.

Dermine, J. F., S. Duclos, et al. (2001). "Flotillin-1-enriched lipid raft domains accumulate on maturing phagosomes." J. Biol. Chem. **276**(21): 18507-18512.

Evans, B. P., J. W. Clark, et al. (2009). "Operational vector-borne disease surveillance and control: closing the capabilities gap through research at overseas military laboratories." U.S. Army Medical Department journal: 16-27.

Fabrick, J., C. Oppert, et al. (2009). "A novel *Tenebrio molitor* cadherin is a functional receptor for *Bacillus thuringiensis* Cry3Aa toxin." J. Bio. Chem. **284**(27): 18401-18410.

Federici, B. A. (2005). "Insecticidal bacteria: An overwhelming success for invertebrate pathology." J. Invertebr. Pathol. **89**(1): 30-38.

Federici, B. A., H.-W. Park, et al. (2003). "Recombinant bacteria for mosquito control." J. Exp. Biol. **206**(21): 3877-3885.

Feitelson, J. S., J. Payne, et al. (1992). "*Bacillus thuringiensis*: insects and beyond." Nat. Biotech. **10**(3): 271-275.

Fernandez-Luna, M. T., H. Lanz-Mendoza, et al. (2010). "An alpha-amylase is a novel receptor for *Bacillus thuringiensis* ssp. *israelensis* Cry4Ba and Cry11Aa toxins in the malaria vector mosquito *Anopheles albimanus* (Diptera: Culicidae)." Environ. Microbiol. **12**(3): 746-757.

Fernandez, L. E., K. G. Aimanova, et al. (2006). "A GPI-anchored alkaline phosphatase is a functional midgut receptor of Cry11Aa toxin in *Aedes aegypti* larvae." Biochem. J. **394**(Pt 1): 77-84.

Foster, L. J., C. L. de Hoog, et al. (2003). "Unbiased quantitative proteomics of lipid rafts reveals high specificity for signaling factors." Proc. Natl. Acad. Sci. U.S.A. **100**(10): 5813-5818.

Foster, W. A. and E. D. Walker (2002). Mosquitoes (Culicidae). Medical and veterinary entomology. M. Gary and D. Lance. San Diego, Academic Press**:** 203-262.

Galbiati, F., D. Volonte, et al. (1998). "Identification, sequence and developmental expression of invertebrate flotillins from *Drosophila melanogaster*." Gene **210**(2): 229-237.

Galitsky, N., V. Cody, et al. (2001). "Structure of the insecticidal bacterial [delta]-endotoxin Cry3Bb1 of *Bacillus thuringiensis*." Acta Crystallogr. D Biol. Crystallogr. **57**(8): 1101-1109.

Ge, L., W. Qi, et al. (2011). "Flotillins play an essential role in Niemann-Pick C1-like 1-mediated cholesterol uptake." Proc. Natl. Acad. Sci. U.S.A. **108**(2): 551-556.

Goldberg, L. J. and J. Margalit (1977). "A bacterial spore demonstraitng rapid larvicidal activity against *Anopheles sergentii*, *Uranotaenia unguicalata*, *Culex univitattus*, *Aedes aegyptii* and *Culex pipiens*." Mosq. News **37**: 355-358.

Griffitts, J. S., S. M. Haslam, et al. (2005). "Glycolipids as receptors for *Bacillus thuringiensis* crystal toxin." Science **307**: 922-925.

Grochulski, P., L. Masson, et al. (1995). "*Bacillus thuringiensis*CrylA(a) insecticidal toxin: crystal structure and channel formation." J. Mol. Biol. **254**(3): 447-464.

Guerrera, I. and O. Kleiner (2005). "Application of mass spectrometry in proteomics." Biosci. Rep. **25**(1): 71-93.

Guo, S., S. Ye, et al. (2009). "Crystal structure of *Bacillus thuringiensis* Cry8Ea1: An insecticidal toxin toxic to underground pests, the larvae of *Holotrichia parallela*." J. Struct. Biol. **168**(2): 259-266.

Gupta, N., B. Wollscheid, et al. (2006). "Quantitative proteomic analysis of B cell lipid rafts reveals that ezrin regulates antigen receptor-mediated lipid raft dynamics." Nat. Immunol. **7**(6): 625-633.

Harbach, R. E. (2007). The Culicidae (Diptera): a review of taxonomy, classification and phylogeny, Zootaxa.

Harder, T., P. Scheiffele, et al. (1998). "Lipid domain structure of the plasma membrane revealed by patching of membrane components." J. Cell Biol. **141**(4): 929-942.

Hazarika, P., N. Dham, et al. (1999). "Flotillin 2 is distinct from epidermal surface antigen (ESA) and is associated with filopodia formation." J. Cell Biochem. **75**(1): 147-159.

Hoehne, M., H. Gert de Couet, et al. (2005). "Loss- and gain-of-function analysis of the lipid raft proteins Reggie/Flotillin in *Drosophila*: They are posttranslationally regulated, and misexpression interferes with wing and eye development." Mol. Cell. Neurosci. **30**(3): 326-338.

Hofte, H. and H. R. Whiteley (1989). "Insecticidal crystal proteins of *Bacillus thuringiensis*." Microbiol.Rev. **53**: 242-255.

http://www.lifesci.sussex.ac.uk/home/Neil_Crickmore/Bt/.

Hua, G., R. Zhang, et al. (2008). "*Anopheles gambiae* cadherin AgCad1 binds the Cry4Ba toxin of *Bacillus thuringiensis israelensis* and a fragment of AgCad1 synergizes toxicity." Biochemistry **47**(18): 5101-5110.

Hua, G., R. Zhang, et al. (2009). "*Anopheles gambiae* alkaline phosphatase is a functional receptor of *Bacillus thuringiensis jegathesan* Cry11Ba toxin." Biochemistry **48**(41): 9785-9793.

Ilangumaran, S. and D. C. Hoessli (1998). "Effects of cholesterol depletion by cyclodextrin on the sphingolipid microdomains of the plasma membrane." Biochem. J. **335**(2): 433-440.

Ishiwata, S. (1901). "On a kind of severe flacherie (sotto disease)." Dainihon Sanshi Keiho **9**: 1-5 (in Japanese).

Ito, A., Y. Sasaguri, et al. (2004). "A *Bacillus thuringiensis* crystal protein with selective cytocidal action to human Cells." J. Bio. Chem. **279**(20): 21282-21286.

Jurat-Fuentes, J. L. and M. J. Adang (2004). "Characterization of a Cry1Ac-receptor alkaline phosphatase in susceptible and resistant *Heliothis virescens* larvae." Eur.J.Biochem. **271**: 3127-3135.

Jurat-Fuentes, J. L. and M. J. Adang (2006). "Cry toxin mode of action in susceptible and resistant *Heliothis virescens* larvae." J. Invertebr. Pathol. **92**(3): 166-171.

Katanaev, V. L., G. P. Solis, et al. (2008). "Reggie-1/flotillin-2 promotes secretion of the long-range signalling forms of Wingless and Hedgehog in *Drosophila*." EMBO J. **27**(3): 509-521.

Killeen, G. F., U. Fillinger, et al. (2002). "Advantages of larval control for African malaria vectors: low mobility and behavioural responsiveness of immature mosquito stages allow high effective coverage." Malar. J. **1**: 8.

Knight, P. J., N. Crickmore, et al. (1994). "The receptor for *Bacillus thuringiensis* CrylA(c) delta-endotoxin in the brush border membrane of the lepidopteran *Manduca sexta* is aminopeptidase N." Mol. Microbiol. **11**(3): 429-436.

Koumanov, K. S., C. Tessier, et al. (2005). "Comparative lipid analysis and structure of detergent-resistant membrane raft fractions isolated from human and ruminant erythrocytes." Arch. Biochem. Biophys. **434**(1): 150-158.

Krishnamoorthy, M., J. L. Jurat-Fuentes, et al. (2007). "Identification of novel Cry1Ac binding proteins in midgut membranes from *Heliothis virescens* using proteomic analyses." Insect Biochem. Mol. Biol. **37**(3): 189-201.

Lacey, L. and M. Goettel (1995). "Current developments in microbial control of insect pests and prospects for the early 21st century." BioControl **40**(1): 3-27.

Le Naour, F., M. André, et al. (2006). "Membrane microdomains and proteomics: Lessons from tetraspanin microdomains and comparison with lipid rafts." Proteomics **6**(24): 6447-6454.

Lehane, M. and P. Billingsley (1996). Biology of the insect midgut, Chapman & Hall.

Li, J., J. Carroll, et al. (1991). "Crystal structure of insecticidal d-endotoxin from *Bacillus thuringiensis* at 2.5 Å resolution." Nature **353**: 815-821.

Li, J., D. J. Derbyshire, et al. (2001). "Structural implications for the transformation of the *Bacillus thuringiensis* delta-endotoxins from water-soluble to membrane-inserted forms." Biochem. Soc. Trans. **29**(Pt 4): 571-577.

Likitvivatanavong, S., J. Chen, et al. (2011). "Multiple receptors as targets of Cry toxins in mosquitoes." J. Agric. Food Chem. **59**(7): 2829-2838.

Linser, P. J., K. E. Smith, et al. (2009). "Carbonic anhydrases and anion transport in mosquito midgut pH regulation." J. Exp. Biol. **212**(11): 1662-1671.

MacLellan, D. L., H. Steen, et al. (2005). "A quantitative proteomic analysis of growth factor-induced compositional changes in lipid rafts of human smooth muscle cells." Proteomics **5**(18): 4733-4742.

Martins, É. S., R. G. Monnerat, et al. (2010). "Midgut GPI-anchored proteins with alkaline phosphatase activity from the cotton boll weevil (*Anthonomus grandis*) are putative receptors for the Cry1B protein of *Bacillus thuringiensis*." Insect Biochem. Mol. Biol. **40**(2): 138-145.

Mayor, S., K. Rothberg, et al. (1994). "Sequestration of GPI-anchored proteins in caveolae triggered by cross-linking." Science **264**(5167): 1948-1951.

McIntosh, T. J., A. Vidal, et al. (2003). "Sorting of lipids and transmembrane peptides between detergent-soluble bilayers and detergent-resistant rafts." Biophys. J. **85**(3): 1656-1666.

McMahon, K.-A., M. Zhu, et al. (2006). "Detergent-free caveolae proteome suggests an interaction with ER and mitochondria." Proteomics **6**(1): 143-152.

McNall, R. J. and M. J. Adang (2003). "Identification of novel *Bacillus thuringiensis* Cry1Ac binding proteins in *Manduca sexta* midgut through proteomic analysis." Insect Biochem. Molec. Biol. **33**(10): 999-1010.

Milhiet, P. E., M. C. Giocondi, et al. (2002). "Spontaneous insertion and partitioning of alkaline phosphatase into model lipid rafts." EMBO reports **3**(5): 485-490.

Milner, R. J. (1994). "History of *Bacillus thuringiensis*." Agric. Ecosyst. Environ. **49**(1): 9-13.

Morrow, I. C. and R. G. Parton (2005). "Flotillins and the PHB Domain Protein Family: Rafts, Worms and Anaesthetics." Traffic **6**(9): 725-740.

Morse, R. J., T. Yamamoto, et al. (2001). "Structure of Cry2Aa suggests an unexpected receptor binding epitope." Structure **9**(5): 409-417.

Nagamatsu, Y., T. Koike, et al. (1999). "The cadherin-like protein is essential to specificity determination and cytotoxic action of the *Bacillus thuringiensis* insecticidal Cry1Aa toxin." FEBS Lett. **460**: 385-390.

Nair, M. S. and D. H. Dean (2008). "All domains of Cry1A toxins insert into insect brush border membranes." J. Biol. Chem. **283**(39): 26324-26331.

Neumann-Giesen, C., I. Fernow, et al. (2007). "Role of EGF-induced tyrosine phosphorylation of reggie-1/flotillin-2 in cell spreading and signaling to the actin cytoskeleton." J. Cell. Sci. **120**(3): 395-406.

Nguyen, H. T. T., A. B. Amine, et al. (2006). "Proteomic characterization of lipid rafts markers from the rat intestinal brush border." Biochem. Biophys. Res. Commun. **342**(1): 236-244.

Ochoa-Campuzano, C., M. D. Real, et al. (2007). "An ADAM metalloprotease is a Cry3Aa *Bacillus thuringiensis* toxin receptor." Biochem. Biophys. Res. Commun. **362**(2): 437-442.

Ohba, M., E. Mizuki, et al. (2009). "Parasporin, a new anticancer protein group from *Bacillus thuringiensis*." Anticancer Res. **29**(1): 427-433.

Ostrom, R. S. and X. Liu (2007). "Detergent and detergent-free methods to define lipid rafts and caveolae." Methods Mol. Biol. **400**: 459-468.

Parker, M. W., F. Pattus, et al. (1989). "Structure of the membrane-pore-forming fragment of colicin A." Nature **337**(6202): 93-96.

Perez, C., L. E. Fernandez, et al. (2005). "*Bacillus thuringiensis* subsp. *israelensis* Cyt1Aa synergizes Cry11Aa toxin by functioning as a membrane-bound receptor." Proc. Natl. Acad. Sci. U. S. A. **102**(51): 18303-18308.

Pigott, C. R. and D. J. Ellar (2007). "Role of receptors in *Bacillus thuringiensis* crystal toxin activity." Microbiol. Mol. Biol. Rev. **71**(2): 255-281.

Pike, L. J. (2009). "The challenge of lipid rafts." J. Lipid Res. **50 Suppl**: S323-328.

Pike, L. J., X. Han, et al. (2002). "Lipid Rafts are enriched in arachidonic acid and plasmenylethanolamine and their composition is independent of caveolin-1 expression: a quantitative electrospray ionization/mass spectrometric analysis." Biochemistry **41**(6): 2075-2088.

Pike, L. J., X. Han, et al. (2005). "Epidermal growth factor receptors are localized to lipid rafts that contain a balance of inner and outer leaflet lipids." J. Bio. Chem. **280**(29): 26796-26804.

Pralle, A., P. Keller, et al. (2000). "Sphingolipid–cholesterol rafts diffuse as small entities in the plasma membrane of mammalian cells." J. Bio. Chem. **148**(5): 997-1008.

Quinn, P. J. (2010). "A lipid matrix model of membrane raft structure." Prog. Lipid Res. **49**(4): 390-406.

Rajamohan, F., J. A. Cotrill, et al. (1996). "Role of domain II, loop 2 residues of *Bacillus thuringiensis* Cry1Ab δ-endotoxin in reversible and irreversible binding to *Manduca sexta* and *Heliothis virescens*." J.Biol.Chem. **271**(5): 2390-2396.

Rajendran, L., J. Beckmann, et al. (2009). "Flotillins are involved in the polarization of primitive and mature hematopoietic cells." PLoS One **4**(12): e8290.

Rajendran, L. and K. Simons (2005). "Lipid rafts and membrane dynamics." J. Cell. Sci. **118**(Pt 6): 1099-1102.

Rao, M. and S. Mayor (2005). "Use of Forster's resonance energy transfer microscopy to study lipid rafts." Biochim. Biophys. Acta **1746**(3): 221-233.

Rasko, D. A., M. R. Altherr, et al. (2005). "Genomics of the *Bacillus cereus* group of organisms." FEMS Microbiol. Rev. **29**(2): 303-329.

Resh, M. D. (1999). "Fatty acylation of proteins: new insights into membrane targeting of myristoylated and palmitoylated proteins." Biochim. Biophys. Acta **1451**(1): 1-16.

Rietveld, A., S. Neutz, et al. (1999). "Association of sterol- and glycosylphosphatidylinositol-linked proteins with *Drosophila* raft lipid microdomains." J. Biol. Chem. **274**(17): 12049 - 12054.

Rietveld, A. and K. Simons (1998). "The differential miscibility of lipids as the basis for the formation of functional membrane rafts." Biochim. Biophys. Acta **1376**(3): 467-479.

Rose, R. I. (2001). "Pesticides and public health: integrated methods of mosquito management." Emerging Infect. Dis. **7**(1): 17-23.

Saengwiman, S., A. Aroonkesorn, et al. (2011). "In vivo identification of *Bacillus thuringiensis* Cry4Ba toxin receptors by RNA interference knockdown of glycosylphosphatidylinositol-linked aminopeptidase N transcripts in *Aedes aegypti* larvae." Biochem. Biophys. Res. Commun. **407**(4): 708-713.

Salzer, U. and R. Prohaska (2001). "Stomatin, flotillin-1, and flotillin-2 are major integral proteins of erythrocyte lipid rafts." Blood **97**(4): 1141-1143.

Sangadala, S., F. S. Walters, et al. (1994). "A mixture of *Manduca sexta* aminopeptidase and phosphatase enhances *Bacillus thuringiensis* insecticidal Cry1A(c) toxin binding and $^{86}Rb^{+}$-K^{+} efflux in vitro." J. Biol. Chem. **269**: 10088-10092.

Sangiorgio, V., M. Pitto, et al. (2004). "GPI-anchored proteins and lipid rafts." Ital. J. Biochem. **53**(2): 98-111.

Sankaran, J., M. Manna, et al. (2009). "Diffusion, transport, and cell membrane organization investigated by imaging fluorescence cross-correlation spectroscopy." Biophys. J. **97**(9): 2630-2639.

Santamaria, A., E. Castellanos, et al. (2005). "PTOV1 enables the nuclear translocation and mitogenic activity of flotillin-1, a major protein of lipid rafts." Mol. Cell Biol. **25**(5): 1900-1911.

Saslowsky, D. E., J. A. Cho, et al. (2010). "Intoxication of zebrafish and mammalian cells by cholera toxin depends on the flotillin/reggie proteins but not Derlin-1 or -2." J. Clin. Invest. **120**(12): 4399-4409.

Sayle, R. A. and E. J. Milner-White (1995). "RASMOL: biomolecular graphics for all." Trends Biochem. Sci. **20**(9): 374.

Schnepf, E., N. Crickmore, et al. (1998). "*Bacillus thuringiensis* and its pesticidal crystal proteins." Microbiol. Mol. Biol. Rev. **62**(3): 775-806.

Schroeder, R. J., S. N. Ahmed, et al. (1998). "Cholesterol and sphingolipid enhance the Triton X-100 insolubility of glycosylphosphatidylinositol-anchored proteins by promoting the

formation of detergent-insoluble ordered membrane domains." J. Bio. Chem. **273**(2): 1150-1157.

Schuck, S., M. Honsho, et al. (2003). "Resistance of cell membranes to different detergents." Proc. Natl. Acad. Sci. U.S.A. **100**(10): 5795-5800.

Sengupta, P., B. Baird, et al. (2007). "Lipid rafts, fluid/fluid phase separation, and their relevance to plasma membrane structure and function." Semin. Cell Dev. Biol. **18**(5): 583-590.

Simons, K. and R. Ehehalt (2002). "Cholesterol, lipid rafts, and disease." J. Clin. Invest. **110**(5): 597-603.

Simons, K. and E. Ikonen (1997). "Functional rafts in cell membranes." Nature **387**(6633): 569-572.

Simons, K. and D. Toomre (2000). "Lipid rafts and signal transduction." Nat. Rev. Mol. Cell Biol. **1**(1): 31-39.

Singer, S. J. and G. L. Nicolson (1972). "The fluid mosaic model of the structure of cell membranes." Science **175**(23): 720-731.

Song, K. S., P. E. Scherer, et al. (1996). "Expression of Caveolin-3 in Skeletal, Cardiac, and Smooth Muscle Cells." J. Biol. Chem. **271**(25): 15160-15165.

Speranca, M. A. and M. L. Capurro (2007). "Perspectives in the control of infectious diseases by transgenic mosquitoes in the post-genomic era--a review." Mem. Inst. Oswaldo Cruz **102**(4): 425-433.

Stuermer, C. A. (2011). "Reggie/flotillin and the targeted delivery of cargo." J. Neurochem. **116**(5): 708-713.

Stuermer, C. A., M. F. Langhorst, et al. (2004). "PrPc capping in T cells promotes its association with the lipid raft proteins reggie-1 and reggie-2 and leads to signal transduction." FASEB J. **18**(14): 1731-1733.

Tavernarakis, N., M. Driscoll, et al. (1999). "The SPFH domain: implicated in regulating targeted protein turnover in stomatins and other membrane-associated proteins." Trends Biochem. Sci. **24**(11): 425-427.

Vadlamudi, R. K., E. Weber, et al. (1995). "Cloning and expression of a receptor for an insecticidal toxin of *Bacillus thuringiensis*." J.Biol.Chem. **270**: 5490-5494.

Valaitis, A. P., J. L. Jenkins, et al. (2001). "Isolation and partial characterization of gypsy moth BTR-270, an anionic brush border membrane glycoconjugate that binds *Bacillus thuringiensis* Cry1A toxins with high affinity." Arch. Insect Biochem. Physiol. **46**(4): 186-200.

WHO (1985). "Informal consultation on the development of *Bacillus sphaericus* as a microbial larvicide." Geneva: World Health Organization **TDR/BCV/sphaericus/85.3.**

Wigglesworth, V. B. (1933). "The function of the anal gills of the mosquito larva." J. Exp. Biol. **10**(1): 16-26.

Williamson, R., A. J. Thompson, et al. (2010). "Isolation of detergent resistant microdomains from cultured neurons: detergent dependent alterations in protein composition." BMC Neurosci **11**: 120.

Wilson, B. S., J. R. Pfeiffer, et al. (2000). "Observing Fcεri signaling from the inside of the mast cell membrane." J.Biol.Chem. **149**(5): 1131-1142.

Zhang, N., A. R. E. Shaw, et al. (2008). "Liquid chromatography electrospray ionization and matrix-assisted laser desorption ionization tandem mass spectrometry for the analysis of lipid raft proteome of monocytes." Anal. Chim. Acta **627**(1): 82-90.

Zhang, R., G. Hua, et al. (2008). "A 106-kDa aminopeptidase is a putative receptor for *Bacillus thuringiensis* Cry11Ba toxin in the mosquito *Anopheles gambiae*." Biochemistry **47**(43): 11263-11272.

Zhang, X., M. Candas, et al. (2005). "Cytotoxicity of *Bacillus thuringiensis* Cry1Ab toxin depends on specific binding of the toxin to the cadherin receptor BT-R1 expressed in insect cells." Cell Death Differ. **12**(11): 1407-1416.

Zhang, X., M. Candas, et al. (2006). "A mechanism of cell death involving an adenylyl cyclase/PKA signaling pathway is induced by the Cry1Ab toxin of *Bacillus thuringiensis*." Proc. Natl. Acad. Sci. U.S.A. **103**(26): 9897-9902.

Zhuang, M., D. I. Oltean, et al. (2002). "*Heliothis virescens* and *Manduca sexta* lipid rafts are involved in Cry1A toxin binding to the midgut epithelium and subsequent pore formation." J. Biol. Chem. **277**(16): 13863-13872.

Zhuang, Z., P. J. Linser, et al. (1999). "Antibody to H(+) V-ATPase subunit E colocalizes with portasomes in alkaline larval midgut of a freshwater mosquito (*Aedes aegypti*)." J. Exp. Biol. **202**(18): 2449-2460.

Zieler, H., C. F. Garon, et al. (2000). "A tubular network associated with the brush-border surface of the *Aedes aegypti* midgut: implications for pathogen transmission by mosquitoes." J. Exp. Biol. **203**(10): 1599-1611.

Figures and Tables

Table 1.1: Midgut receptors for various mosquitocidal *Bacillus thuringeinsis* toxins

Mosquito Species	Alpha-amylase	Aminopeptidase	Alkaline phosphatase	Cadherin
Anopheles gambiae		**Cry11Ba** (Zhang, Hua et al. 2008)	**Cry11Ba** (Hua, Zhang et al. 2009)	**Cry4Ba** (Hua, Zhang et al. 2008)
Anopheles quadrimaculatus		**Cry11Ba** (Abdullah, Valaitis et al. 2006)		
Anopheles albimanus	**Cry4Ba**, **Cry11Aa** (Fernandez-Luna, Lanz-Mendoza et al. 2010)			
Aedes aegypti		**Cry4Ba** (Bayyareddy, Andacht et al. 2009), **Cry11Aa** (Chen, Aimanova et al. 2009), **Cry11Ba** (Likitvivatanavong, Chen et al. 2011)	**Cry4Ba** (Bayyareddy, Andacht et al. 2009; Dechklar, Tiewsiri et al. 2011) **Cry11Aa** (Fernandez, Aimanova et al. 2006), **Cry11Ba** (Likitvivatanavong, Chen et al. 2011)	**Cry11Aa** (Chen, Aimanova et al. 2009), **Cry11Ba** (Likitvivatanavong, Chen et al. 2011)

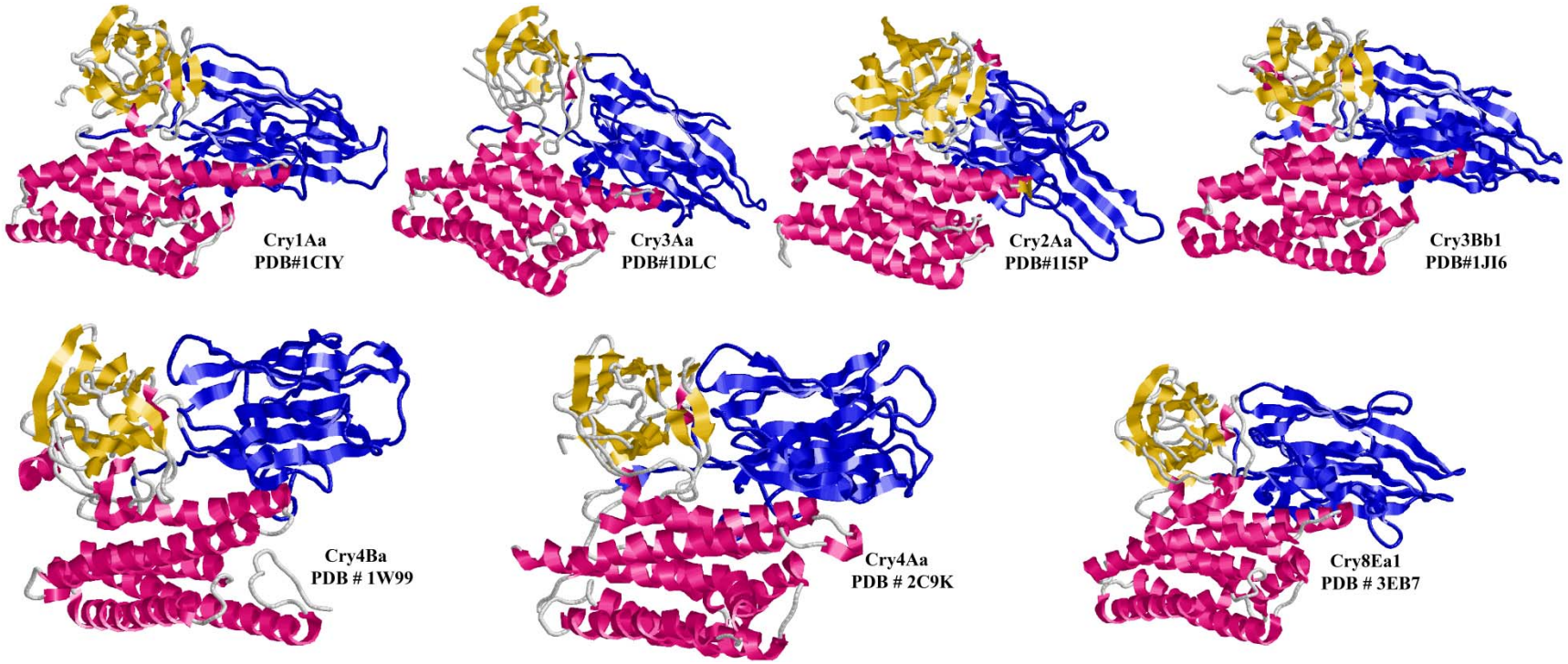

Figure 1.1: Overview of the Bt Cry toxins crystal structure. Cry1Aa, (PDB ID, 1CIY), Cry3Aa (PDB ID, 1DLC), Cry2Aa (PDB ID, 1I5P), Cry3Bb1 (PDB ID, 1JI6), Cry4Ba (PDB ID, 1W99), Cry4Aa (PDB ID, 2C9K) and Cry8Ea1 (PDB ID, 3EB7). Domain I, domain II, and domain III are shown in red, blue, and yellow, respectively. All cartoon images of protein structures in this figure were generated using the RasMol program with PDB files (Sayle and Milner-White 1995).

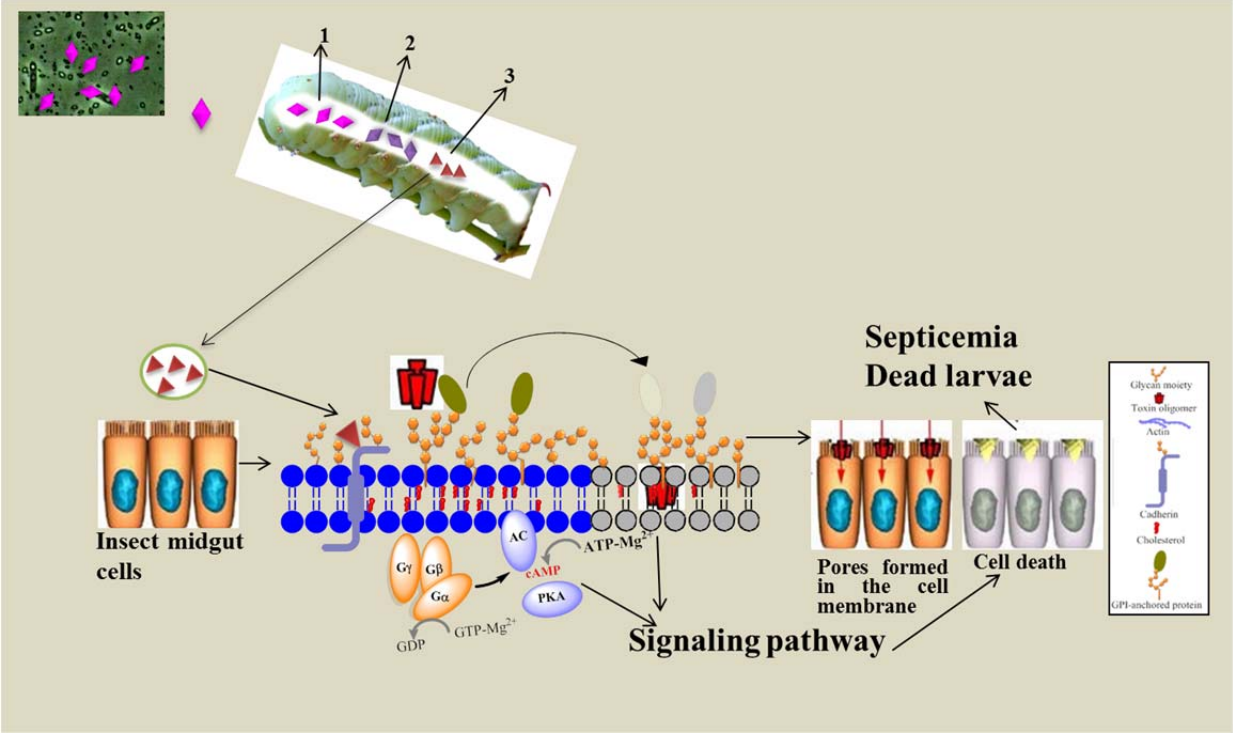

Figure 1.2: Current proposed mode of action of Bt Cry toxins in lepidopteran insects.

Bt crystals when ingested by susceptible larvae, are solubilized in the alkaline midgut and activated by the action of serine proteinases. Activated toxin then binds to a Cadherin like protein which results in activation of intracellular signaling pathways regulated by phosphatases or subsequently formed toxin oligomers then bind secondary receptors, GPI-anchored proteins such as APN's and ALP's. Toxin binding may induce lipid raft aggregation resulting in toxin insertion causing osmotic imbalance and also activates apoptotic responses (also regulated by phosphatases) culminating in cell death. The gut becomes paralyzed and the insect stops feeding; most insects will die within a few hours of ingestion (Jurat-Fuentes and Adang 2006; Zhang, Candas et al. 2006).

CHAPTER 2

PROTEOMIC IDENTIFICATION OF *BACILLUS THURINGIENSIS* SUBSP. *ISRAELENSIS* TOXIN CRY4BA BINDING PROTEINS IN MIDGUT MEMBRANES FROM *AEDES* (*STEGOMYIA*) *AEGYPTI* LINNAEUS (DIPTERA, CULICIDAE) LARVAE

Bayyareddy K, Andacht TM, Abdullah MA, Adang MJ. 2009. Insect Biochem. Mol. Biol. 39(4):279-86.

Abstract

Novel *Bacillus thuringiensis* subsp. *israelensis* (Bti) Cry4Ba toxin-binding proteins have been identified in gut brush border membranes of the *Aedes* (*Stegomyia*) *aegypti* mosquito larvae by combining 2-dimensional gel electrophoresis (2DE) and ligand blotting followed by protein identification using mass spectrometry and database searching. Three alkaline phosphatase isoforms and aminopeptidase were identified. Other Cry4Ba binding proteins identified include the putative lipid raft proteins flotillin and prohibitin, V-ATPase B subunit and actin. These identified proteins might play important roles in mediating the toxicity of Cry4Ba due to their location in the gut brush border membrane. Cadherin-type protein was not identified, although previously, we identified a midgut cadherin AgCad1 as a putative Cry4Ba receptor in *Anopheles gambiae* mosquito larvae [Hua, G., Zhang, R., Abdullah, M.A., Adang, M.J., 2008. *Anopheles gambiae* cadherin AgCad1 binds the Cry4Ba toxin of *Bacillus thuringiensis israelensis* and a fragment of AgCad1 synergizes toxicity. Biochemistry 47, 5101–5110]. Other identified proteins in this study that might have lesser roles include mitochondrial proteins such as ATP synthase subunits, mitochondrial processing peptidase and porin; which are likely contaminants from mitochondria and are not brush border membrane components. Trypsin-like serine protease was also identified as a protein that binds Cry4Ba. Identification of these toxin-binding proteins will lead to a better understanding of the mode of action of this toxin in mosquito.

Keywords: *Aedes aegypti*; *Bacillus thuringiensis israelensis*; Cry4Ba; Alkaline phosphatase; 2D electrophoresis; Mass spectrometry

2.1 Introduction

Aedes (*Stegomyia*) species vector dengue, yellow fever and chikungunya viral diseases. The challenge of controlling this medically important vector is compounded by emerging resistance to chemical pesticides. Controlling the larval stage is critical to mosquito control programs and biopesticides based on *Bacillus thuringiensis* subsp. *israelensis* (Bti) are widely used for this purpose. Bti carries a plasmid that encodes the insecticidal proteins Cry4Aa, Cry4Ba, Cry10Aa, Cry11Aa, Cyt1Aa and Cyt2Ba (Berry, O'Neil et al. 2002). Each of these insecticidal proteins is deposited in inclusions that become part of the parasporal crystal of Bti.

The action of Cry toxins is best studied for the lepidopteran-active Cry1A toxins. The intoxication process is a complex event involving Cry1A binding to receptors, pre-pore formation, membrane insertion, activation of biochemical pathways culminating in midgut cell lysis and insect mortality. According to the Bravo et al. (Bravo, Gómez et al. 2004) model, Cry1A toxin-binding to cadherin induces an internal protease cleavage of toxin, toxin pre-pore formation and subsequent binding to glycosylphosphatidyl inositol (GPI) anchored aminopeptidases (APN) and alkaline phosphatase (ALP). These events probably take toxin to the membrane surface where glycolipids function as Cry1 toxin receptors (Griffitts, Haslam et al. 2005). The role of receptors in Cry1A toxin action was recently reviewed (Pigott and Ellar 2007).

Relative to Cry1A toxin interaction with midgut tissue, less is known about the identities and roles of Cry toxin receptors in dipteran larvae. A 65-kDa protein that bound Cry4B and Cry11A toxin was identified in the midgut of *Aedes* larvae (Buzdin, Revina et al. 2002). This protein was identified as a GPI-anchored alkaline phosphatase (Fernandez, Aimanova et al.

2006) and determined to be a functional receptor for Cry11Aa toxin. A second GPI-anchored protein, a 100-kDa aminopeptidase in *Anopheles* species was determined to specifically bind Cry11Ba and is considered a potential toxin receptor (Abdullah, Valaitis et al. 2006) and (Zhang, Hua et al. 2008). The Cyt toxin component of Bti crystals has limited toxicity itself, yet serves as a synergist enhancing Cry protein toxicity to mosquito larvae. This synergism occurs via a mechanism whereby Cyt toxin itself binds to brush border membrane and functions as a receptor for Cry11Aa (Perez, Fernandez et al. 2005). Evidence suggests that some of the same types of proteins which function as receptors in Cry1A toxins in Lepidopteran larvae may be involved in Cry toxin action against mosquitoes.

Novel Cry1 binding proteins have been identified in brush border membranes of lepidopteran larvae by combining 2-dimensional gel electrophoresis (2DE) and ligand blotting followed by protein identification using mass spectrometry. Using this approach ALP was identified as a Cry1Ac binding protein in brush border of *Manduca sexta* and *Heliothis virescens* (Krishnamoorthy, Jurat-Fuentes et al. 2007) and (McNall and Adang 2003) . This identification was validated in *H. virescens* when ALP was demonstrated as a functional receptor molecule and loss of the enzyme correlated with Bt resistance to Cry1Ac (Jurat-Fuentes and Adang 2004). Additional Cry1Ac binding proteins in lepidopteran brush border preparations detected by 2DE ligand blots approach includes actin, aminopeptidase, vacuolar-ATPase subunit A and a desmocollin-like protein (Krishnamoorthy, Jurat-Fuentes et al. 2007) and (McNall and Adang 2003). A proteomics-based approach using differential-in-gel electrophoretic (DIGE) analysis quantified altered levels of specific proteins in Bt susceptible and resistant larvae of *Plodia interpunctella* (Candas, Loseva et al. 2003). Those authors detected changes in the levels of APN, V-ATPase and an F_1F_0-ATPase in resistant larvae.

Following the same rationale above to identify novel toxin-binding proteins, in this study Cry4Ba binding proteins in the midgut proteome of *Aedes aegypti* were detected on blots of 2DE gels. Proteins that bound toxin on blots were identified from the corresponding protein in stained 2DE gels by mass spectrometry. The tryptic peptide patterns of 12 groups of toxin-binding proteins matched with high-confidence scores to 12 proteins in *A. aegypti* protein databases. ALP isoforms were predominant among the identified Cry4Ba binding proteins.

2.2 Materials and methods

2.2.1 Bacterial strain, toxin purification and ^{125}I-labeling

Escherichia coli DH5α harboring the *cry4Ba* gene was cultured to produce Cry4Ba inclusion bodies and activated toxin produced as previously described (Abdullah, Alzate et al. 2003). Protein was quantified using the Bradford protein assay (Bradford 1976) with BSA as standard. Purified Cry4Ba toxin (10 μg) was labeled with 5 μCi of $Na^{125}I$ (GE Healthcare) using the chloramine-T reagent according to Garczynski et al.(Garczynski, Crim et al. 1991). Labeled toxin was separated from free iodine by gel filtration on sephadex G-50 (Sigma) resulting in ^{125}I-Cry4Ba with a specific activity of 6 μCi/μg input toxin. Labeled toxin was stored at 4 °C for further use.

2.2.2 Mosquitoes

A. aegypti (UGAL strain) was maintained at 27 °C, 70–80% humidity with a photoperiod of 14L: 10D. Larvae were fed ground brewers yeast, lactalbumin and rat food-chow (1:1:1 ratio) daily for 6 days. Fourth instar larvae were collected on a nylon mesh and then washed thoroughly with deionized water to remove food particles and molted skin. Larvae were dried

briefly on filter paper with gentle suction and stored at −80 °C until needed for brush border membrane fraction (BBMF) preparation.

2.2.3 BBMF preparation

Whole body homogenate was prepared by adding 4 g of frozen larvae to 16 ml ice cold homogenization buffer (300 mM mannitol, 5 mM EGTA, 17 mM Tris-HCl, pH 7.5) containing 1 mM PMSF. Larvae were homogenized with 40 strokes of a glass–teflon homogenizer and BBMF isolated using the magnesium precipitation method according to Silva-Filha et al. (Silva-Filha, Nielsen-Leroux et al. 1997). The final BBMF protein concentration was determined as above. Enrichment of the brush border marker enzymes ALP and APN was determined using leucine-*ρ*-nitroanalide and *ρ*-nitrophenyl phosphate as substrates, respectively (Terra and Ferreira 1994). Enrichment in the final BBMF preparation relative to the initial homogenate ranged from 5- to 7-fold for APN activity and 8- to 10-fold for ALP activity.

2.2.4 Preparation of protein samples for 2DE

Proteins were precipitated from BBMF (100 µg protein) using Plus-One cleanup kit (GE Healthcare) according to the manufacturer's instruction. The final precipitant in a microfuge tube was dissolved in 100 µl solubilization buffer [7 M urea, 2 M thiourea, 2% CHAPS, 2% caprylyl sulfobetaine, 18 mM DTT, 2% carrier ampholytes (pH 3–10 or 4–7, Plus-one; GE Healthcare)]. To increase solubilization, the microfuge tube containing the BBMF protein sample was floated in a sonicating water bath containing cold water, replacing the water every 5 min to avoid potential artifacts created by urea in warm water. Protein samples were then centrifuged at

13,000 g for 10 min at room temperature; the supernatant was collected and protein amount determined with a 2D quantification kit (GE Healthcare).

2.2.5 IEF

For IEF, solubilized BBMF (60–80 μg protein) in 150 μl rehydration solution (solubilization buffer plus 0.002%(w/v) of bromophenol blue) were loaded onto a 13 cm immobilized pH gradient (IPG) strip (pH 4–7 or pH 3–10, nonlinear, GE Healthcare) and overlaid with 2 ml of plus-one IPG strip cover fluid (GE Healthcare). After 15–17 h passive rehydration, IEF was performed on a Multiphor-II flatbed system according to the manufacturer's guidelines (2D Electrophoresis Principles and Methods, GE Healthcare) with an additional initial step of 30 min low voltage (150 V) step to facilitate improved entry of high molecular-sized proteins into the IPG strip. Strips were stored at −80 °C or used directly in the equilibration step. Strips were first equilibrated for 15 min in equilibration buffer (6 M urea, 75 mM Tris-HCl pH 8.8, 29.3% glycerol, 2% SDS and 0.002%(w/v) of bromophenol blue) containing 1% DTT (w/v). The strips were then equilibrated in equilibration buffer containing 4% iodoacetamide (w/v).

2.2.6 Second-dimensional electrophoresis

SDS-PAGE was performed on an Ettan DALT*six* large vertical electrophoresis system (GE Healthcare). The equilibrated IPG strip was transferred onto a 12% SDS-PAGE gel. Electrophoresis was carried out at 20 °C using a three-phase program: 5 mA for 30 min, 10 mA for 60 min, and 15 mA until the dye front was near the bottom of the gel. Proteins were stained with Deep Purple stain (GE Healthcare) or transferred overnight onto a PVDF (polyvinylidene

difluoride; Immobilon P, Millipore) membrane. Stained gels and gels for ligand blotting were run in parallel.

2.2.7 MALDI-TOF/TOF mass spectrometric analysis and database searching

Deep Purple-stained 2DE gels were imaged on a Typhoon 9400 imager (GE Healthcare) using 532 nm excitation and 610 nm emission wavelengths. The image was analyzed using Decyder 6.5 software (GE Healthcare) to provide a gel image and coordinates for selected spots. Protein spots were selected for picking by overlaying gel images with images from toxin-binding autoradiograms. Selected spots were excised from the stained 2DE gel and trypsin-digested using the Ettan Spot Handling workstation (GE Healthcare). Methods for processing of gel plugs and peptide preparation for spotting to a matrix-assisted laser/desportion ionization (MALDI) plate are described elsewhere (Krishnamoorthy, Jurat-Fuentes et al. 2007). MALDI-time of flight (TOF) mass spectrometry was carried out using a 4700 Proteomics Analyzer (Applied Biosystems) to obtain PMFs. Optimal resolution of spectra acquired in positive reflection mode, from 900 to 3500 m/z, was achieved by altering the laser intensity. Trypsin auto-digested peaks of m/z 1045.556 and 2211.096 were used for spectral calibration. The top 10 most abundant peaks from the mass spectrometric (MS) spectrum were subsequently selected for MS/MS to obtain peptide fragmentation data. MS/MS spectra were calibrated using the instrument default calibration.

PMF and ion fragmentation mass lists obtained from MALDI-TOF/TOF were used for protein identification by searching the latest version of NCBInr with a licensed copy of Mascot v. 1.9.05 (http://www.matrixscience.com) as the search tool. Searches were performed allowing

one missed trypsin cleavage, fixed cysteine carbamidomethylation, and partial methionine oxidation.

The quality of search results was interpreted with consideration of the observed and expected pI values, molecular size, the specific percentage of amino acid coverage, mass accuracy, and the probability of obtaining the same Mascot score result in a random match. The percentage of coverage indicates the portion of protein sequence covered by matched peptides to the whole length of protein sequence in the database. The Mascot score assigns significance to the search results using a combination of the PMF score and the individual MS/MS scores. Mascot scores of 59 or higher indicate the search results are significant and are >95% probability that the results are not false positive. Protein scores with higher Mascot scores represent better matches. We performed BLAST searches with the protein sequence having the highest score for each spot as query to the *Aedes* subset of NCBInr to identify potential homologues.

2.2.8 Ligand blotting

Proteins were transferred from either a 1D or 2DE gel overnight onto PVDF membrane (Immobilon P, Millipore) at 22 V constant voltage in 25 mM Tris-HCl, 192 mM glycine and 10% methanol. The following experiments were performed at room temperature. Blots were blocked for 1 h in 3% BSA in PBS (137 mM NaCl, 2.7 mM KCl, 4.3 mM Na_2HPO_4, 1.4 mM KH_2PO_4) with 0.1% Tween-20 (PBST) plus 0.1% BSA and then incubated either with 0.2 nM ^{125}I-Cry4Ba only or in a mixture with a 500-fold excess of the unlabeled Cry4Ba toxin (to determine non-specific binding) in PBST plus 0.1% BSA for 2 h. Blots were washed 1 h in 6 changes of PBST plus 0.1% BSA, air dried and subjected to overnight autoradiography using Hyper film (GE Healthcare) to visualize ^{125}I-Cry4Ba binding proteins.

2.2.9 Western blotting and analysis of *Aedes* ALP proteins

After separation by 2DE, proteins were transferred to PVDF filters as described for ligand blotting. The following experiments were performed at room temperature. Filters were blocked for 1 h in PBST containing 3% BSA. To detect ALP, filters were incubated 1 h in a 1:5000 dilution of rabbit anti-*A. gambiae* membrane ALP serum (kindly provided by Dr. Gang Hua, University of Georgia) in PBST plus 0.1% BSA. Filters were washed three times in PBST plus 0.1% BSA followed by incubation in a 1:25,000 dilution of goat anti-rabbit IgG horse radish peroxidase conjugate in PBST plus 0.1% BSA. Following three washes in PBST −0.1% BSA, spots were visualized with ECL plus chemiluminescence substrate and exposure to film. Blots were repeated to establish reproducibility.

Since toxin-receptor ALPs in larval midgut prepared from *Aedes* and other insects species are GPI-anchored (Fernandez, Aimanova et al. 2006) and (Jurat-Fuentes and Adang 2004) we analyzed ALPs identified by mass spectrometry and anti-mALP serum for predicted GPI anchorage. We applied the GPI-SOM (Fankhauser and Maser 2005) and Big-PI (Eisenhaber, Bork et al. 1999) computational tools to predict C-terminal GPI-anchoring signals on the ALP protein sequences.

2.3 Results

2.3.1 Detection of Cry4Ba binding proteins on ligand blots of BBMF proteins

Aedes midgut proteins that bind Cry4Ba toxin were identified by combining 2DE proteomics with the ligand blot technique. Brush border membrane proteins were resolved by 1DE into bands ranging from >20- to <200-kDa (Fig. 2.1A). By 2DE, approximately 300

individual protein spots were resolved with molecular sizes ranging from 20- to 160-kDa (Fig. 2.1B). Since the resolved 2DE protein pattern showed that most proteins were in the acidic to neutral range, we used pH 4–7 IPG strips to increase separation (Fig. 2.1C).

Blots of 1D and 2D gels were probed with ^{125}I-labeled Cry4Ba to identify brush border proteins that bind Cry4Ba. On a 1D blot, Cry4Ba recognized a series of proteins with calculated sizes of 141-, 102-, 89-, 82-, 64-, 55-, 45-, 30- and 25-kDa (Fig. 2.2A). On blots of 2DE gels prepared with pH 3–10 and pH 4–7 strips, Cry4Ba bound proteins that were primarily distributed on the gel as chains or clusters of proteins (Fig. 2.2B and D). The sizes of proteins detected by Cry4Ba binding on the 2DE blots were less than 100-kDa. Chains of spots were detected at 65-kDa (group 6 spots), 55-kDa (group 2) and 42-kDa (group 4) on both pH 4–7 and pH 3–10 gels (Fig. 2.2B and D). The relatively basic group 12 toxin-binding proteins at 30-kDa were resolved on the pH 3–10 2DE gel (Fig. 2.2B and C). A homologous competition binding blot showed that in the presence of 500-fold unlabeled Cry4Ba, the binding of ^{125}I-labeled Cry4Ba to the 2DE spots was reduced significantly (Fig. 2.5). This suggests that the toxin-binding spots were binding specifically to the Cry4Ba toxin.

2.3.2 Identification of Cry4Ba binding proteins by mass spectrometry

Proteins corresponding to spots that bound Cry4Ba were selected for protein identification by PMF and MS/MS ion fragmentation (Table 2.1). Spots were excised from 2DE gels, trypsin-digested and resulting peptide fragments subjected to MALDI-TOF MS analysis to yield PMF data for each protein spot. The top 10 most abundant peaks from the MS spectrum were subsequently selected for MALDI-TOF/TOF analysis to yield peptide fragmentation data. The NCBInr database was searched with PMF and MS/MS ion fragmentation data using Mascot

to establish the best protein match for each spot. The analyzed gel spots, molecular masses, iso-electric points (pI), NCBI accession numbers, source species as well as protein identities are listed in Table 1. The predicted molecular masses of identified proteins ranged from 25- to 103-kDa and the pI were from 5 to 9. The mass spectrometry data from spot 1 (Fig. 2.2E) matched V-ATPase subunit B from *A. aegypti* with a high Mascot score of 289 and 55% sequence coverage. The expected pI and molecular size for this protein agreed with the position observed on the 2D gel. The train of spots marked 2 in Fig. 2.2D and E bound Cry4Ba strongly. Spots designated 2a–2e in this train yielded spectra that matched ATP synthase subunit alpha from *A. aegypti*. The Mascot scores for these identifications ranged from 187 to 302. The mass spectrometry analysis from spot 3, matched a M1 family zinc metalloprotease from *A. aegypti* with a Mascot score of 212. The predicted pI of 5.19 agrees with the position observed on the gel, yet the predicted 103-kDa size is greater than the apparent 70-kDa size of spot 3. The identified metalloprotease appears to be a degraded fragment of an aminopeptidase. Spots 4a–4c matched to actin. The Cry4Ba binding proteins in group 6 mass spectra matched to three *Aedes* ALPs with predicted sizes of 59- to 61-kDa (Table 2.1). The mass spectra of series 7 spots (7a and 7b) matched to ATP synthase beta subunit and spot 8a and 8b to serine proteases with high MASCOT scores. Another series of spots approximately 30-kDa (spots 12a–12c) were bound by Cry4Ba and their mass spectra matched to mitochondrial porins with MASCOT scores ranging from 154 to 244. Other protein spots which bound Cry4Ba include V-ATPase subunit E (spot 10), mitochondrial peptidase beta subunit (spots 9a and 9b), flotillin (spot 5), and prohibitin (spot 11).

2.3.3 Alkaline phosphatase blot

An antibody that recognizes the membrane form of *A. gambiae* ALP identified spots that correspond to group 6 spots which mass spectra analysis identified as ALP (Fig. 2.3A). On 2D gels the detected proteins migrated as chains of spots at about 59- and 63-kDa. The antibody cross-reacted with a chain of 3 spots identified as ATP synthase beta subunit (group 7) (Fig. 2.3A). The cross-reaction of the anti-mALP antibody to ATP synthase could be due to high homology of antigenic epitopes on both proteins. Results from ^{125}I-Cry4Ba ligand blot showed binding to both the ALPP as well as ATP synthase spots (Fig. 2.2D and 3B).

2.4 Discussion

In this study Cry4Ba binding proteins were identified in the midgut brush border proteome of *A. aegypti* larvae. Cry4Ba is highly toxic to *Aedes* larvae, yet little is known about its target molecules in the brush border. Our approach combined 2DE, ligand blotting and mass spectrometry to identify a set of proteins that bound ^{125}I-labeled Cry4Ba toxin. The availability of an *Aedes* protein database derived from genomic sequence information yielded high-confidence scores for protein identifications (Table 2.1). We were able to identify all spots by PMF alone, but further analyses by MS/MS that correlate the two types of data are superior to identifications made with PMF data alone(He, Yang et al. 2008). A limitation of PMF data alone is that it is possible that two different peptides in a tryptic digest the same molecular size.

Proteins identified as binding Cry4Ba on blots were present in a brush border membrane fraction prepared from whole *Aedes* larvae. Since blotted proteins are denatured, epitopes expected to bind Cry toxins include short peptide sequences and attached glycan moieties. A caveat is that epitopes exposed on denatured proteins may be buried under non-denaturation

conditions (Daniel, Sangadala et al. 2002). The identified Cry4Ba binding proteins, ALP and APN have a predicted GPI anchorage and are well-characterized as Cry1A binding proteins in lepidopteran larvae (Pigott and Ellar 2007). Several identified proteins (flotillin, prohibitin and V-ATPse) are typically associated with the cytoplasmic side of plasma membranes. Actin, also identified as Cry4Ba binding protein, is a cytoskeletal element that has a dynamic association with plasma membrane (Schlichting, Wilsch-Bräuninger et al. 2006). How might Cry4Ba contact proteins attached to the cytoplasmic side of brush border membrane? The lepidopteran-active Cry1A toxins bind cadherin, undergo proteolytic processing and form an oligomeric pre-pore structure that then binds GPI-anchored APN (Bravo, Gómez et al. 2004) and probably ALP. After binding APN, Cry1A toxins localize in lipid rafts and are present as oligomers (Aronson, Geng et al. 1999) and (Zhuang, Oltean et al. 2002). Since virtually the whole Cry1A molecule enters the membrane (Nair and Dean 2008), it is quite likely that toxin is exposed on the cytoplasmic side of the membrane allowing interaction with nearby proteins.

Three ALP isoforms (group 6 spots) were identified as Cry4Ba binding proteins. Spots 6a and 6b at 58-kDa and spot 6c at 62-kDa matched a single ALP isoform, while spots 6d and 6e at 64-kDa matched additional ALP isoforms. Each ALP isoform detected in the brush border membrane preparation has a predicted signal peptide and GPI-anchor attachment sequence near the C-terminus of the protein. These results are in agreement with previous studies where a 64-kDa protein in *A. aegypti* brush border bound Cry4Ba and Cry11Ba toxins on ligand blots (Buzdin, Revina et al. 2002) and (Krieger, Revina et al. 1999). Our identification of the 62- to 65-kDa proteins as ALP confirmed the prediction of Pigott and Ellar (Pigott and Ellar 2007). Since the 65-kDa ALP is a functional Cry11Aa receptor, isoforms of ALP may function as receptors for Cry4Ba, Cry11Ba and Cry11Aa toxins. Related ALPs function as a Cry1Ac

receptor in the lepidopteran, *H. virescens* and loss of ALP is correlated with resistance to Cry1Ac (Jurat-Fuentes and Adang 2004) and (Jurat-Fuentes and Adang 2006).

APNs are identified as receptors for Cry1A toxins in Lepidoptera (Pigott and Ellar 2007). Recently, a 100-kDa APN in *A. quadrimaculatus* (Abdullah, Valaitis et al. 2006) and a 106-kDa APN in *A. gambiae* (Zhang, Hua et al. 2008) were identified as Cry11Ba binding proteins. Spot 3 at 70-kDa was identified by mass spectrometry as an *A. aegypti* aminopeptidase (XP 001662884) with additional matches to related insect aminopeptidases. A Clustal X alignment of the *Aedes* APN against 53 insect APNs listed in (Zhang, Hua et al. 2008) placed the *Aedes* APN among the class 7 type APNs along with AeAPNRc2 (AAL85580) from *A. aegypti* and AgAPN1 from *A. gambiae* (Dinglasan, Kalume et al. 2007) (data not shown).

Since spot 3 at 70-kDa is smaller than the matched 100-kDa *Aedes* APN, how do we explain this apparent discrepancy? Considering that the PMF data matched to residues spanning the N- and C-termini of the predicted protein (Fig. 2.4) the APN peptide should be about 93-kDa, a size considerably larger than the observed 70-kDa. This would be accounted for if the APN is degraded and the N- and/or C-termini PMF matches (which were not among the best scores to be picked for MS/MS) are incorrect. Proteolytic degradation could occur from either the N- or C-terminus, regardless of the GPI anchorage, during storage or sample preparation. Another possible explanation for the apparent size discrepancy is that there exists another APN isoform not yet annotated in databases.

Flotillin-1 (spot 5) and prohibitin (spot 11) were identified as Cry4Ba binding proteins on 2D blots. Flotillins (also called Reggies) are structural proteins of detergent resistant lipid rafts (Eckert, Igbavboa et al. 2003) and (Morrow and Parton 2005). They are highly conserved

proteins that anchor lipid rafts with actin cytoskeleton via their stomatin/prohibitin/flotillin/HflK/C (SPFH) domain (Langhorst, Solis et al. 2007). Prohibitin, like flotillin also has an SPFH domain and it typically is associated with lipid rafts (Browman, Hoegg et al. 2007). SPFH-domain proteins are membrane-associated through N-terminal hydrophobic regions or, in the case of flotillin, by palmitoylation (Browman, Hoegg et al. 2007). Lipid rafts are also rich in cholesterol, sphingolipids, GPI-anchored proteins and several cell-signaling receptors. These specialized areas of cell membranes are involved in polarized sorting of proteins to the apical membrane of epithelia. In *M. sexta* and *H. virescens*, lipid rafts contain APNs and ALPS that bind Cry toxin and mediate toxin insertion into the raft microdomain (Zhuang, Oltean et al. 2002). We believe it likely that the lipid raft proteins, flotillin and prohibitin, will co-localize with the GPI-anchored APNs and ALPS in insect brush border membrane.

Recently, the binding of actin by Cry toxins in different insects has been documented (Krishnamoorthy, Jurat-Fuentes et al. 2007) and (McNall and Adang 2003) and in our experiments we found a similar result where Cry4Ba binds to actin in *A. aegypti.* In eukaryotic organisms a cadherin–catenin complex forms a dynamic link with actin that is involved in maintenance of cytoskeleton architecture. A route for Cry4Ba contact with actin is suggested by these protein interactions. Considering that Cry4Ba binds AgCad1 cadherin in *A. gambiae* (Hua, Zhang et al. 2008), it possibly binds cadherin in *A. aegypti*. Insertion of the entire Cry4Ba molecule into membrane as a single or oligomeric unit, as is the case for Cry1A toxins (Nair and Dean 2008), may expose regions of the toxin to the cytoplasm allowing contact with actin. Contact between toxin and actin could lead to disruption of cytoskeletal links causing loss of host cell shape and integrity (Shimada, Usui et al. 2001) and (Woods, Wu et al. 1997).

Cry4Ba bound V-ATPase subunits B and E (spots 1 & 10) on 2DE blots of *Aedes* brush border protein. Previously, Cry1Ac was reported to bind V-ATPase subunit A in *H. virescens* larvae (Krishnamoorthy, Jurat-Fuentes et al. 2007) and (McNall and Adang 2003). V-ATPases are located in the plasma membranes of insect epithelia where they serve as proton motive forces generating an electrochemical gradient (Wieczorek, Brown et al. 1999). V-ATPase is abundant in the apical membrane of the posterior midgut of *A. aegypti* larvae (Patrick, Aimanova et al. 2006). According to hypothetical models of V-ATPase, subunits A through H are located on the cytoplasmic side of the plasma membrane (Beyenbach and Wieczorek 2006). If Cry4Ba binds V-ATPase *in vivo* it may destabilizes the cationic pathway of pH regulation described in mosquito larvae (Okech, Boudko et al. 2008) and (Patrick, Aimanova et al. 2006). A compensatory response to help overcome Cry1Ac intoxication is reported in a Bt-resistant strain of *P. interpunctella* where V-ATPases were up-regulated in resistant larvae(Candas, Loseva et al. 2003).

ATP synthase (F_1F_0 ATP synthase) α and β (spots 2a–2f and 7a and 7b, respectively) were identified as abundant proteins on 2DE gels that showed intense Cry4Ba binding signals (Fig. 2.2). The ATP synthase protein complex is localized to the mitochondrial membrane where it functions in ATP generation via H^+ transport. The presence of this protein in a brush border membrane preparation is evidence of contamination by mitochondrial membrane. With the current state of Bt Cry toxin action it is not likely that Cry4Ba toxin would contact ATP synthase subunits in the mitochondria.

Mitochondrial processing peptidase β subunit (spots 9a and 9b) was identified as a Cry4Ba toxin-binding peptide. This type of peptidase is a mitochondrial membrane-associated

enzyme that cleaves N-terminal signal sequences from proteins as they reach the inside of the mitochondrion (Gakh, Cavadini et al. 2002).

Porins or voltage-dependent anion-selective channels were detected as abundant proteins that bound Cry4Ba in the brush border preparations (Fig. 2.2, spots 12a–12c). While the closest match for spot 12 was to *A. aegypti* mitochondrial porin, the second best match was to Agporin of *A. gambiae* (Sardiello, Tripoli et al. 2003). Mitochondrial porins allow small metabolites, such as ATP, to diffuse across the mitochondrial membrane (Aiello, Messina et al. 2004). Related porins are located in the epithelial membranes of animal intestines (Matsuzaki, Tajika et al. 2004).

Trypsin-like serine proteases of 30-kDa (spot 8a) and 42-kDa (spot 8b) bound Cry4Ba. While the spot 8a at 30-kDa corresponds to the expected size of the mature protein, spot 8b at 42-kDa is closer to the size of a serine protease precursor associated with a membrane secretory vesicle (Shen, Edwards et al. 2000). Trypsin is shown to associate tightly to plasma membranes and the binding level is correlated to the level of cholesterol in the membrane (Mahmmoud 2005). This might explain the presence of trypsin-like serine proteases in our BBMF preparation even though the proteases lack any type of anchor that might explain its association with the membrane. The toxin-binding trypsins might serve as a transient receptor that pulls the toxin close to the membrane for the toxin to form pores. However, there is also an example where a gut protease (elastase) selectively precipitates certain Cry toxins to reduce toxicity (Milne, Wright et al. 1998). Further experiments are needed to understand the significance of Cry4Ba binding to these proteases.

Based on reported Cry toxin mode of action models and a recent report on 200-kDa AgCad1 interaction with Cry4Ba, cadherin is a potential key binding molecule to initiate Cry toxicity in mosquito (Hua, Zhang et al. 2008). However, no report has yet identified a cadherin-like protein as a potential Cry-binding protein in *A. aegypti*. A BLAST search of the available *A. aegypti* database (NCBI) using a partial sequence from AgCad1 identified a closely related cadherin from a partial mRNA sequence (XM 001652753). However, there might not be sufficient homology in the *Aedes* sequence to AgCad1 to allow Cry4Ba binding. Another reason could be that due to the limitation of ability to resolve high molecular size proteins in 2D analysis (Garbis, Lubec et al. 2005), high molecular weight *Aedes* cadherins (200 kDa or larger) were likely excluded from the analysis.

The present study demonstrates the value of 2DE-based separation and mass spectrometry for the identification of Bti toxin-binding proteins. The quality of protein identifications was high due to available *Aedes* genomic sequence and predicted protein databases. Identification of toxin-binding ALPs lends confidence to the meaningfulness of 'hits' detected by toxin blots. However, the identification of 4 mitochondrial proteins among the group of 12 Cry4Ba binding proteins encourages further development of methods for preparing brush border membranes from mosquito larvae. The detection of mitochondrial proteins that bind Cry toxin is probably not physiologically relevant, as their localization is not compatible with known mechanisms of Cry toxin action. Finally, functional analyses are needed to test the role of identified toxin-binding proteins as receptors or as proteins involved in Cry4Ba toxicity.

Acknowledgements

This research was supported by National Institutes of Health Grant R01 AI 29092 to D.H. Dean (Ohio State University) and M.J.A. The authors thank two anonymous reviewers for their critical reviews of a previous version of this manuscript.

References

Abdullah, M. A., O. Alzate, et al. (2003). "Introduction of *Culex* toxicity into *Bacillus thuringiensis* Cry4Ba by protein engineering." Appl. Environ. Microbiol. **69**(9): 5343-5353.

Abdullah, M. A., A. P. Valaitis, et al. (2006). "Identification of a *Bacillus thuringiensis* Cry11Ba toxin-binding aminopeptidase from the mosquito, *Anopheles quadrimaculatus*." BMC Biochem **7**: 16 (electronic resource).

Aiello, R., A. Messina, et al. (2004). "Functional characterization of a second porin isoform in *Drosophila melanogaster*. DmPorin2 forms voltage-independent cation-selective pores." J. Biol. Chem. **279**(24): 25364-25373.

Aronson, A. I., C. Geng, et al. (1999). "Aggregation of *Bacillus thuringiensis* Cry1A toxins upon binding to target insect larval midgut vesicles." Appl. Environ. Microbiol. **65**(6): 2503-2507.

Berry, C., S. O'Neil, et al. (2002). "Complete sequence and organization of pBtoxis, the toxin-coding plasmid of *Bacillus thuringiensis* subsp. *israelensis*." Appl. Environ. Microbiol. **68**(10): 5082-5095.

Beyenbach, K. W. and H. Wieczorek (2006). "The V-type H+ ATPase: molecular structure and function, physiological roles and regulation." J. Exp. Biol. **209**(4): 577-589.

Bradford, M. (1976). "A rapid and sensitive method for the quantitation of microgram quantities of protein utilizing the principle of protein-dye binding." Anal. Biochem. **72**: 248-254.

Bravo, A., I. Gómez, et al. (2004). "Oligomerization triggers binding of a *Bacillus thuringiensis* Cry1Ab pore-forming toxin to aminopeptidase N receptor leading to insertion into membrane microdomains." Biochim. Biophys. Acta **1667**(1): 38-46.

Browman, D. T., M. B. Hoegg, et al. (2007). "The SPFH domain-containing proteins: more than lipid raft markers." Trends Cell. Biol. **17**(8): 394-402.

Buzdin, A. A., L. P. Revina, et al. (2002). "Interaction of 65- and 62-kD proteins from the apical membranes of the *Aedes aegypti* larvae midgut epithelium with Cry4B and Cry11A endotoxins of *Bacillus thuringiensis*." Biochemistry (Moscow) **67(5)**: 540-546.

Candas, M., O. Loseva, et al. (2003). "Insect resistance to *Bacillus thuringiensis*: Alterations in the Indianmeal moth larval gut proteome." Mol. Cell. Proteomics **2(1)**: 19-28.

Daniel, A., S. Sangadala, et al. (2002). "Denaturation of either *Manduca sexta* aminopeptidase N or *Bacillus thuringiensis* Cry1A toxins exposes binding epitopes hidden under nondenaturing conditions." Appl. Environ. Microbiol. **68**(5): 2106-2112.

Dinglasan, R. R., D. E. Kalume, et al. (2007). "Disruption of *Plasmodium falciparum* development by antibodies against a conserved mosquito midgut antigen." Proc. Natl. Acad. Sci. U. S. A. **104**(33): 13461-13466.

Eckert, G. P., U. Igbavboa, et al. (2003). "Lipid rafts of purified mouse brain synaptosomes prepared with or without detergent reveal different lipid and protein domains." Brain Res. **962**(1-2): 144-150.

Eisenhaber, B., P. Bork, et al. (1999). "Prediction of potential GPI-modification sites in proprotein sequences." J. Mol. Biol. **292**(3): 741-758.

Fankhauser, N. and P. Maser (2005). "Identification of GPI anchor attachment signals by a Kohonen self-organizing map." Bioinformatics **21**(9): 1846-1852.

Fernandez, L. E., K. G. Aimanova, et al. (2006). "A GPI-anchored alkaline phosphatase is a functional midgut receptor of Cry11Aa toxin in *Aedes aegypti* larvae." Biochem. J. **394**(Pt 1): 77-84.

Gakh, O., P. Cavadini, et al. (2002). "Mitochondrial processing peptidases." Biochim. Biophys. Acta **1592**(1): 63-77.

Garbis, S., G. Lubec, et al. (2005). "Limitations of current proteomics technologies." J. Chromatogr. A **1077**(1): 1-18.

Garczynski, S. F., J. W. Crim, et al. (1991). "Identification of putative insect brush border membrane-binding molecules specific to *Bacillus thuringiensis* delta-endotoxin by protein blot analysis." Appl. Environ. Microbiol. **57**(10): 2816-2820.

Griffitts, J. S., S. M. Haslam, et al. (2005). "Glycolipids as receptors for *Bacillus thuringiensis* crystal toxin." Science **307**: 922-925.

He, Z., C. Yang, et al. (2008). "Peak bagging for peptide mass fingerprinting." Bioinformatics **24**(10): 1293-1299.

Hua, G., R. Zhang, et al. (2008). "*Anopheles gambiae* cadherin AgCad1 binds the Cry4Ba toxin of *Bacillus thuringiensis israelensis* and a fragment of AgCad1 synergizes toxicity." Biochemistry **47**(18): 5101-5110.

Jurat-Fuentes, J. L. and M. J. Adang (2004). "Characterization of a Cry1Ac-receptor alkaline phosphatase in susceptible and resistant *Heliothis virescens* larvae." Eur. J. Biochem. **271**: 3127-3135.

Jurat-Fuentes, J. L. and M. J. Adang (2006). "Cry toxin mode of action in susceptible and resistant *Heliothis virescens* larvae." J. Invertebr. Pathol. **92**(3): 166-171.

Krieger, I. V., L. P. Revina, et al. (1999). "Membrane proteins of *Aedes aegypti* larvae bind toxins Cry4B and Cry11A of *Bacillus thuringiensis* ssp. *israelensis*." Biochemistry. (Moscow) **64(10)**: 1163-1168.

Krishnamoorthy, M., J. L. Jurat-Fuentes, et al. (2007). "Identification of novel Cry1Ac binding proteins in midgut membranes from *Heliothis virescens* using proteomic analyses." Insect Biochem. Mol. Biol. **37**(3): 189-201.

Langhorst, M. F., G. P. Solis, et al. (2007). "Linking membrane microdomains to the cytoskeleton: regulation of the lateral mobility of reggie-1/flotillin-2 by interaction with actin." FEBS lett. **581**(24): 4697-4703.

Mahmmoud, Y. A. (2005). "Stabilization of trypsin by association to plasma membranes: Implications for tryptic cleavage of membrane-bound Na,K-ATPase." Biochim. Biophys. Acta **1720**(1-2): 110-116.

Matsuzaki, T., Y. Tajika, et al. (2004). "Aquaporins in the digestive system." Med. Electron Microsc. **37**(2): 71-80.

McNall, R. J. and M. J. Adang (2003). "Identification of novel *Bacillus thuringiensis* Cry1Ac binding proteins in *Manduca sexta* midgut through proteomic analysis." Insect Biochem. Molec. Biol. **33**(10): 999-1010.

Milne, R., T. Wright, et al. (1998). "Spruce budworm elastase precipitates *Bacillus thuringiensis* delta-endotoxin by specifically recognizing the C-terminal region." Insect Biochem. Molec. Biol. **28**(12): 1013-1023.

Morrow, I. C. and R. G. Parton (2005). "Flotillins and the PHB domain protein family: rafts, worms and anaesthetics." Traffic **6**(9): 725-740.

Nair, M. S. and D. H. Dean (2008). "All domains of Cry1A toxins insert into insect brush border membranes." J. Biol. Chem. **283**(39): 26324-26331.

Okech, B. A., D. Y. Boudko, et al. (2008). "Cationic pathway of pH regulation in larvae of *Anopheles gambiae*." J. Exp. Biol. **211**(6): 957-968.

Patrick, M. L., K. Aimanova, et al. (2006). "P-type Na+/K+-ATPase and V-type H+-ATPase expression patterns in the osmoregulatory organs of larval and adult mosquito *Aedes aegypti*." J. Exp. Biol. **209**(23): 4638-4651.

Perez, C., L. E. Fernandez, et al. (2005). "*Bacillus thuringiensis* subsp. *israelensis* Cyt1Aa synergizes Cry11Aa toxin by functioning as a membrane-bound receptor." Proc. Natl. Acad. Sci. U. S. A. **102**(51): 18303-18308.

Pigott, C. R. and D. J. Ellar (2007). "Role of receptors in *Bacillus thuringiensis* crystal toxin activity." Mol. Biol. Rev. **71**(2): 255-281.

Sardiello, M., G. Tripoli, et al. (2003). "A comparative study of the porin genes encoding VDAC, a voltage-dependent anion channel protein, in *Anopheles gambiae* and *Drosophila melanogaster*." Gene **317**(1-2): 111-115.

Schlichting, K., M. Wilsch-Bräuninger, et al. (2006). "Cadherin Cad99C is required for normal microvilli morphology in *Drosophila* follicle cells." J. of Cell Sci. **119**(6): 1184-1195.

Shen, Z., M. J. Edwards, et al. (2000). "A gut-specific serine protease from the malaria vector *Aanopheles gambiae* is downregulated after blood ingestion." Insect Mol. Biol. **9**(3): 223-229.

Shimada, Y., T. Usui, et al. (2001). "Asymmetric colocalization of Flamingo, a seven-pass transmembrane cadherin, and Dishevelled in planar cell polarization." Curr. Biol. **11**(11): 859-863.

Silva-Filha, M. H., C. Nielsen-Leroux, et al. (1997). "Binding kinetics of *Bacillus sphaericus* binary toxin to midgut brush-border membranes of *Anopheles* and *Culex* sp. mosquito larvae." Eur. J. Biochem. **247**: 754-761.

Terra, W. R. and C. Ferreira (1994). "Insect digestive enzymes: properties , compartmentalization and function." Comp. Biochem. Physiol. **109B**: 1-62.

Wieczorek, H., D. Brown, et al. (1999). "Animal plasma membrane energization by proton-motove V-ATPases." BioEssays **21**: 637-648.

Woods, D. F., J. W. Wu, et al. (1997). "Localization of proteins to the apico-laterall junctions of *Drosophila* epithelia." Dev. Genet. **20**: 111-118.

Zhang, R., G. Hua, et al. (2008). "A 106-kDa aminopeptidase is a putative receptor for *Bacillus thuringiensis* Cry11Ba toxin in the mosquito *Anopheles gambiae*†." Biochemistry **47**(43): 11263-11272.

Zhuang, M., D. I. Oltean, et al. (2002). "*Heliothis virescens* and *Manduca sexta* lipid rafts are involved in Cry1A toxin binding to the midgut epithelium and subsequent pore formation." J. Biol. Chem. **277**(16): 13863-13872.

Figures and Tables

Table 2.1: Results from PMF and MS/MS ion fragmentation, database searches using the Mascot program and NCBInr database, the Mascot score for the best match is shown.

Spot No.	Accession number	Vectoorbase No.	*Mascot Score	Top ranking match	Predicted PI	Predicted mass	¥% Sequence coverage	Species
1	4680480	AAEL005798	289	V- ATPase B subunit	5.25	55	55	*A. aegypti*
2a, c, d, e, f	94468442	AAEL012175	302	ATP synthase alpha subunit	9.01	59.5	41	*A. aegypti*
3	108870801	AAEL012776	212	protease m1 zinc metalloprotease	5.19	103	28	*A. aegypti*
4a, b	71383976	AAEL001673	225	actin 6	5.23	42.1	50	*A. aegypti*
4c	108879764	AAEL004616	135	actin	5.3	42	54	*A. aegypti*
5	108871581	AAEL012046	120	flotillin-1	5.82	45.05	45	*A. aegypti*
6a, b, c	108868480	AAEL015070	171	alkaline phosphatase	5.82	58.9	30	*A. aegypti*
6d	108881200	AAEL003313	124	alkaline phosphatase	5.46	61.1	29	*A. aegypti*
6e	108881197	AAEL003298	277	alkaline phosphatase	5.23	58.3	55	*A. aegypti*
7a, b	108881105	AAEL003393	304	ATP synthase beta subunit	5.02	53.9	60	*A. aegypti*
8a	108881971	AAEL002593	127	serine protease(Tryp-Spc)	5.58	46.2	42	*A. aegypti*
8b	108881966	AAEL002595	245	serine protease	5.27	47.9	38	*A. aegypti*
9a, b	108878872	AAEL005435	116	mito-processing peptidase beta	5.87	52.8	51	*A. aegypti*
10	94469084	AAEL012035	163	V-ATP synthase subunit E	5.91	25.7	75	*A. aegypti*
11	94468930	AAEL009345	239	prohibitin	5.36	29.8	69	*A. aegypti*
12a, b,c	94468842	AAEL001872	244	mito-porin	8.63	30.7	55	*A. aegypti*

*The Mascot Score is given as $S = -10*\log(P)$, where P is the probability that the observed match is a random event. It is an indication of match quality; a value less than 59 is considered a non-significant hit.

¥ % Sequence coverage is defined as the ratio of the length of query sequence covered by matched peptides to the whole protein sequence.

Figure 2.1: **Silver stained 1D (10 µg of proteins were loaded) (A) and Deep purple blue stained 2DE (B, C) separations of *A. aegypti* BBMF proteins**. Proteins (80 µg) were focused on 13 cm IPG pH 3–10 (B) and pH 4–7 (C) strips for the first dimension followed by 12% SDS-PAGE for the second dimension. Positions of molecular size markers (kDa) are indicated on the left of each gel and pH range of iso-electric focusing at the bottom of the gels.

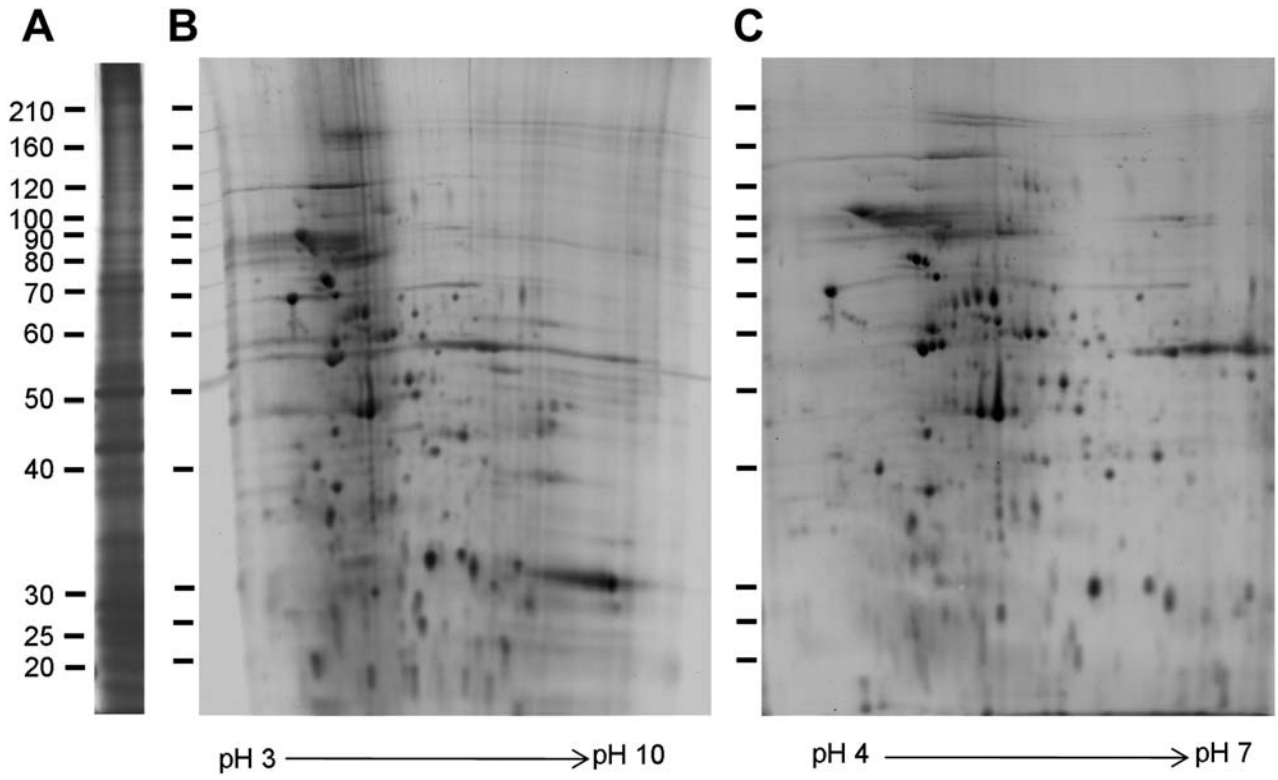
A
B
C
210
160
120
100
90
80
70
60
50
40
30
25
20
pH 3
pH 10
pH 4
pH 7

Figure 2.2: Blot analysis of Cry4Ba binding proteins in *Aedes* BBMF. Proteins were separated by 1D (A) and 2DE (B–E). Arrows to the right in Fig. 2.2A denote positions of the major Cry4Ba binding proteins mentioned in Results. For 2DE, proteins were resolved by iso-electric focusing using pH 3–10 and pH 4–7 strips followed by separation on SDS-12%PAGE gels. Gels were either stained with Deep purple blue for spot-picking (C, E) or blotted to membrane filters (B, D). For detection of Cry4Ba binding proteins filters were probed with 0.2 nM ^{I25}I-Cry4Ba. Positions of molecular size markers (kDa) are indicated on the side of each gel.

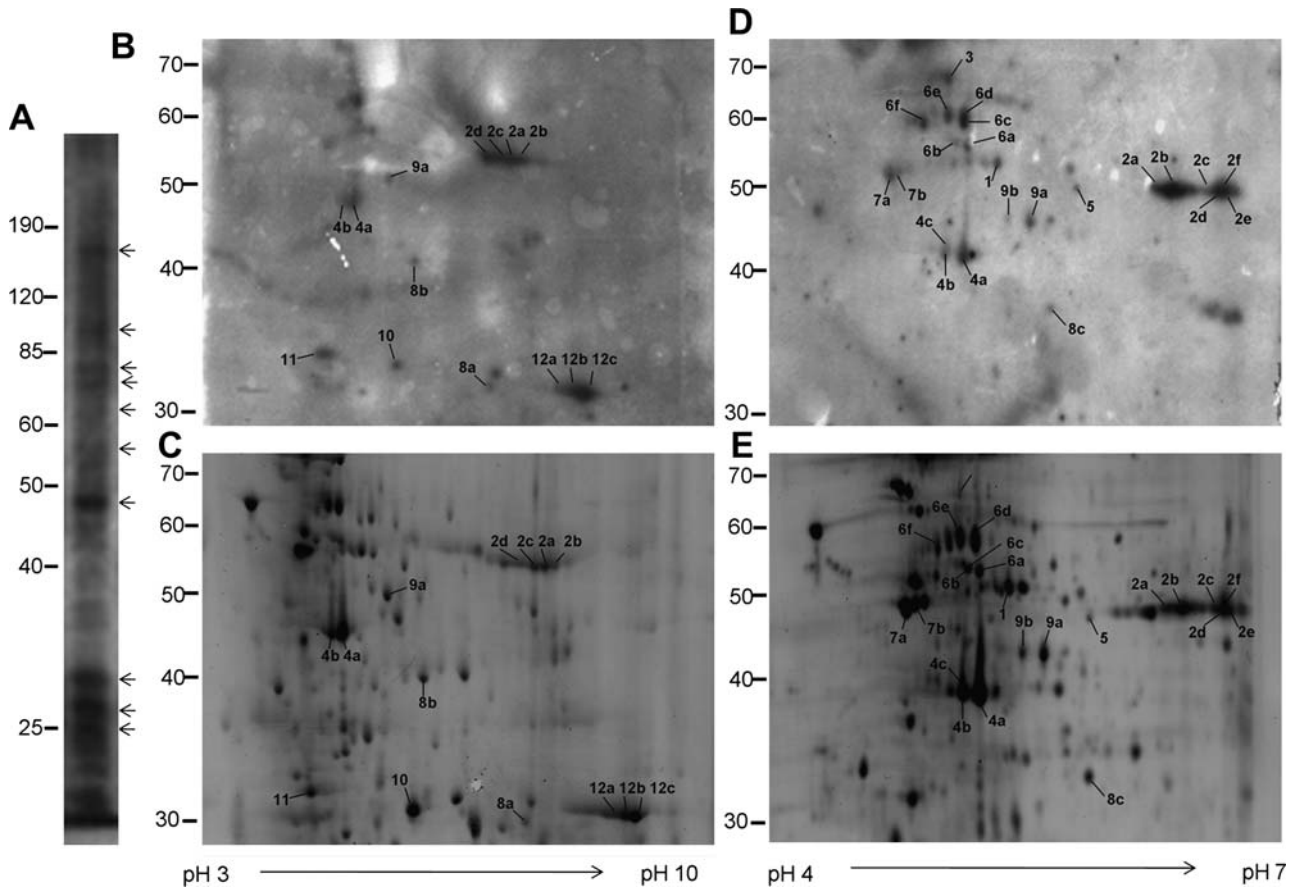
A
B
C
D
E
190
120
85
60
50
40
25
70
60
50
40
30
2d 2c 2a 2b
9a
4b 4a
8b
10
11
8a
12a 12b 12c
3
6e
6d
6f
6c
6a
6b
1
9b
9a
5
2a
2b
2c
2f
2d
2e
7a
7b
4c
4b
4a
8c
pH 3
pH 10
pH 4
pH 7

Figure 2.3: **Membrane alkaline phosphatase blot (ALP) of 2DE separated *A. aegypti* brush border proteins**. A rabbit polyclonal antibody against *A. gambiae* membrane ALP was used to probe a blot (A) of BBMF proteins separated by iso-electric focusing using pH 4–7 strips and separated on SDS-12%PAGE gels. Detection was by goat anti-rabbit conjugated HRP followed by chemiluminescent detection. For comparison a ^{125}I-Cry4Ba ligand blot (B) and a stained 2DE gel (C) are aligned to the alkaline phosphatase blot. Spots corresponding to ALPs identified by MALDI-TOF/TOF are designated 6a–6f, while spots corresponding to ATP synthase are designated 7a and 7b. Positions of molecular size markers (kDa) are indicated on the side of each gel.

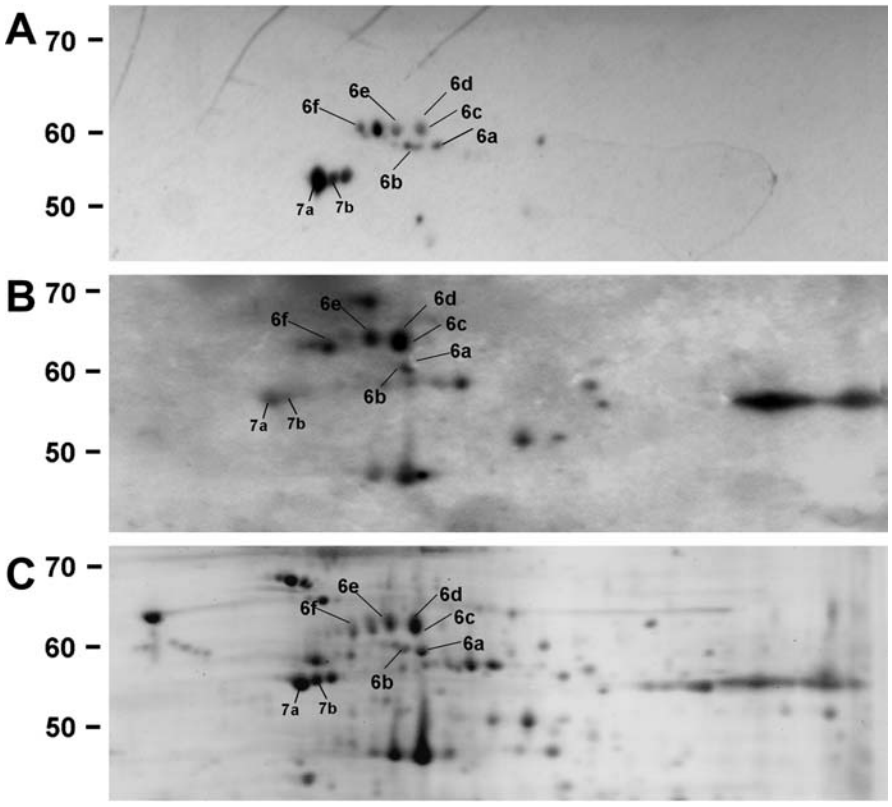
A
70
60
50
6e
6d
6f
6c
6a
6b
7a
7b
B
70
60
50
6e
6d
6f
6c
6a
6b
7a
7b
C
70
60
50
6e
6d
6f
6c
6a
6b
7a
7b

Figure 2.4: Peptides for spot no. 3 that matched *Aedes* APN (gi|157133539|ref|XP_001662884.1) are shown in red and blue. Red color denotes matches to only PMF data; blue denotes peptides that match both PMF and MS/MS data. The predicted leader peptide would be cleaved between residues 17 and 18. Matching peptides can be found throughout the sequence, while the more accurately matched peptides based on both PMF and MS/MS data (blue colored) covered the region from amino acid residue 136 to 578.

MLKICVPLAL LAVASLAWPV DQSVRAFDTY RLPNQTVPTH YDLYLDTNLH
LADLDYSGNV KIRIQVLEST SQIVLHSKRS EIVRLELRNS NQLAISLKSF
ELDADKDFLI VNTKETLPAG SSYVLDIAFT NSLDRTDAAG FYRSSYVNAE
GVTKFLGVTQ FESTDARSAF PCFDEPGIKT TYSVQIACGL DYNARSNAPA
LGIQLLPAGK KLTTFQTTPR MQTYLLAFLV SDFISERQVV FQPHQIAVST
FARPTASHQL TYSVDASVRF LRELEIYFDQ RYAMSKIDNV AIANSDFAAG
AMENWGLVTY RESTILLDPE SQGESQQLQV VGIVGHEYTH QFFGNLLAPQ
WWSYLWLNEG FARLYQYYVS EFSHPELKMR DRFASVRESA LNLDASATVR
PMTYYVETPG EISRLFDNIA YAKSASVLRM MNYAITEPTF QKGLRYYIQQ
NKDHGVANEE NLFDSLEQAA KEDAQLPQSL TMHEIFRSWS NQPGAPVVTF
KRVGDTNEFV FNQERFYNTP PETPGQQSWW IPISFFTPSS NGQYNSSAAF
WLPPHVSDFS YRIDVAESET LLVNPLARGY YRVNYDAQTW ENIISNLYES
PEKFHRLTRS QLVDDAMNLA HAGKLDYFTA FQVFVYLNEE TDFIPWSTAS
SNLQFLKRML RHDSEALANL ESYSSMLAAN LLATYGLESI KGESADDESA
RLIALEWACN SDESCQAEAA QKLRSSRRSQ TFTIGSKTEQ LLVCSQMRKA
DYSDFSMMLS SLKNTRDSIS RSYLVDTISC VENGQSINKL LNALKSDDFG
AAEKVQVLKS VYSNSLTGLN AIIDMFDSTT NVAENMNINK RQLHALLEDM
AEYTVQPESA ERFAEFVKRE APTHLVHTIQ AKLRENESWI RRNAAIVSDM
LKTPPQIDM

Figure 2.5: Homologous competition of the ^{125}I Cry4Ba in *Aedes* BBMF proteins. Arrows in the panel A denote position of the major Cry4Ba-binding proteins identified in pH4-7 gel and mentioned in Results. 80ug of *Aedes* BBMF proteins were resolved by iso-electric focusing using pH 4-7 strips followed by separation on SDS-12%PAGE gels. Gels were blotted to membrane filters and either incubated with 0.2nM ^{125}I-Cry4Ba alone (A) or in the presence of 500 folds of excess unlabeled Cry4Ba toxin (B). Positions of molecular size markers (kDa) are indicated on the side of each gel.

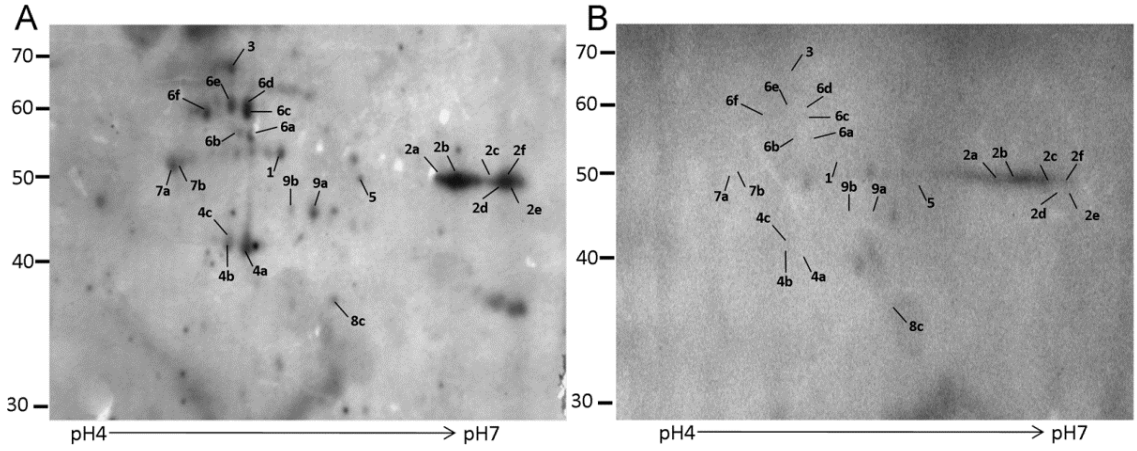
A
70
60
50
40
30
pH4
pH7
3
6e
6d
6f
6c
6a
6b
1
9b
9a
5
2a
2b
2c
2f
7a
7b
2d
2e
4c
4b
4a
8c
B
70
60
50
40
30
pH4
pH7
3
6e
6d
6f
6c
6a
6b
1
9b
9a
5
2a
2b
2c
2f
7a
7b
2d
2e
4c
4b
4a
8c

CHAPTER 3

CLONING AND CHARACTERIZATION OF *AEDES* (*STEGOMYIA) AEGYPTI* LIPID RAFT MARKER PROTEIN FLOTILLIN-1

Bayyareddy K, Hua G, Abdullah MA, and Adang MJ
To be submitted to Biochemistry

Abstract

Flotillin-1 is a marker protein for membrane rafts in eukaryotic cells. Membrane rafts (also called lipid rafts) are detergent resistant and partition into a buoyant fraction in density gradients. Typically, lipid rafts are enriched in sphingolipids, cholesterol and, preferentially sequester certain proteins while excluding others. Flotillin-1 has been implicated in numerous cellular processes including signal transduction, cell-matrix adhesion, phagocytosis, and uptake of cholera toxin and cholesterol. In this study, we report the identification, cDNA sequence and midgut expression pattern of *Aedes aegypti* flotillin-1 (AeFlot-1). In addition, immunohistochemical analysis of AeFlot-1 revealed that expression was confined primarily to the larval posterior midgut and gastric caeca. AeFlot-1 is most closely related to other insect flotillin-1, and western blot analysis showed that anti-AeFlot-1 antibody cross reacted with other insect flotillin-1 proteins. Lipid rafts prepared from larval *A. aegypti* brush border membrane by cold detergent solubilization and step gradient ultra-centrifugation differed in cholesterol and marker protein content from soluble membrane fractions. These data demonstrated the utility of anti-AeFlot-1 antibody as an insect lipid rafts protein marker that. may be used in *Bacillus thuringiensis* toxin-receptors research, as a number of receptors were found to be present in lipid rafts.

Key Words: Flotillin-1, *Aedes*, brush border membrane, lipid rafts, cholesterol

3.1 Introduction

Lipid rafts are liquid-ordered, detergent-insoluble microdomains in the plasma membrane that are enriched in cholesterol, sphingolipids and different posttranslationally modified glycosylphosphatidylinositol (GPI)-anchored, myristoylated, and palmitoylated) proteins (Brown and Rose 1992; Simons and Ikonen 1997; Brown and London 1998; Brown and London 2000). Lipid rafts play a fundamental role in biological pathways, such as apoptosis, cell migration, signal transduction, synaptic transmission, protein sorting and cytoskeletal stabilization (Brown and London 1998; Tsui-Pierchala, Encinas et al. 2002; Salaun, James et al. 2004). In addition, lipid rafts serve as a target point for many pathogens causing common and complex diseases, such as diabetes, atherosclerosis, cancer, and Alzheimer's disease in humans (Simons and Ehehalt 2002). Until recently existence of lipid rafts in the biological cell membrane was controversial (Radeva and Sharom 2004). Studies involving lipid rafts are now extensively accepted in the scientific community. Currently, this knowledge has been extended to invertebrates, especially insects (Rietveld, Neutz et al. 1999; Zhuang, Oltean et al. 2002; Eroglu, Brugger et al. 2003; Bravo, Gómez et al. 2004; Wang, Yoo et al. 2010). To our knowledge, there are no data on the nature and composition of lipid rafts from mosquitoes, vectors of deadly human disease causing pathogens.

The success of lipid raft research depends on the availability of well characterized markers. Flotillin-1 (also known as Reggie-2) was discovered as a constituent of the lipid raft floating fraction after solubilization of membranes in Triton- X-100 at low temperature and density centrifugation (Bickel, Scherer et al. 1997). Since their discovery, antibodies against flotillin-1 have become important diagnostic tools for biochemical characterization of lipid raft fractions. Flotillin-1, belongs to a family of lipid raft-associated integral membrane protein that

is ubiquitously expressed and. is localized to lipid rafts on the cell plasma membrane (Langhorst, Reuter et al. 2005). Although flotillins' role and localization are widely studied in mammalian systems and in epithelial cells, and flotillin-1 is mainly localized at the plasma membrane, the localization of flotillins is still a debatable topic (Neumann-Giesen, Falkenbach et al. 2004; Vassilieva, Ivanov et al. 2009). Studies have shown that the association of flotillin-1 to plasma membrane is by a combination of amino acids in N-terminal hydrophobic transmembrane stretch and myristoyl and palmitoyl residues (Morrow, Rea et al. 2002; Neumann-Giesen, Falkenbach et al. 2004). More recent data highlight that the protein does not contain any transmembrane domain (Morrow and Parton 2005) but flotillin-1 faces cytosol by attaching to plasma membrane through the palmitoyl group near to its N-terminus (Stuermer and Plattner 2005).

Research, over the last decade showed that flotillins are involved in a variety of cellular processes, including cell-matrix adhesion, phagocytosis, exocytosis, and several signaling pathways (Dermine, Duclos et al. 2001; Neumann-Giesen, Falkenbach et al. 2004; Kato, Nakanishi et al. 2006). Recent publications demonstrate that flotillins are crucial for the uptake of cholera toxin, and define a clathrin-independent endocytic pathway (Glebov, Bright et al. 2006; Frick, Bright et al. 2007; Langhorst, Jaeger et al. 2008). Flotillin-1 also plays essential roles in NPC1L1-mediated cellular cholesterol uptake, biliary cholesterol reabsorption, and the regulation of lipid levels in mice (Ge, Qi et al. 2011). During malaria parasite *Plasmodium falciparum* infection, which is vectored by mosquito, the association of flotillin-1 with erythrocyte lipid rafts is disrupted, and flotillins are selectively recruited to the vacuole (Nagao, Seydel et al. 2002; Murphy, Samuel et al. 2004). Additionally, flotillins are involved in retrograde transport of bacterial Shiga toxin and plant toxin ricin. Their redistribution is affected by toxin treatment, and is p38 MAPK dependent (Pust, Dyve et al. 2010). Recently, it has been

proposed that sensitivity of *Manduca sexta* to Cry1Ab and *A. aegypti* to Cry11Aa toxins is MAPK p38 pathway dependent (Cancino-Rodezno, Alexander et al. 2010). In plasma membrane, flotillins play a vital role as scaffolds for the lipid rafts in organizing multimolecular complexes and for communication across the plasma membrane (Stuermer and Plattner 2005). Due to the presence of several putative phosphorylation sites, it also functions as a signaling protein associate capable of regulating multiprotein complexes involved in transmembrane signaling (Stuermer 2011). With the association of other GPI-anchored proteins on the cell surface, it is also involved in actin cytoskeletal rearrangements and recruitment of E-cadherin on the cell surface (Stuermer 2011).

The use of flotillin-1 as a lipid raft marker is now widely accepted. As far as we are aware, tools to study flotillins from any insect including anti-flotillin antibody are not available. There is one study on cDNA sequence and embryonic expression pattern of flotillin in *Drosophila melanogaster (Galbiati, Volonte et al. 1998)*. In mammalian systems, molecular cloning of flotillin and analysis of the cDNA for this protein has provided new avenues to explore the structure and function of lipid rafts and in *A. aegypti* it has been identified as a Cry4Ba binding protein (Bayyareddy, Andacht et al. 2009).

In the present work, we describe the identification, sequence and larval gut expression pattern of *A. aegypti* flotillin (AeFlot-1) and the use of anti-AeFlot-1 antibody as a tool in density flotation experiments to identify lipid rafts in mosquito.

3.2 Materials and methods

3.2.1 Insects, midgut dissection, RNA isolation, and cDNA synthesis

A colony of *A. aegypti* was reared and maintained as described in (Bayyareddy, Andacht et al. 2009). Midguts from early fourth instar larvae were dissected by removing hindgut and were immediately frozen on dry ice for RNA isolation by placing in RNAlater (Sigma-Aldrich, St. Louis, MO). RNeasy Mini Kit (Qiagen, Valencia, CA) was used to extract total RNA according to the manufacturer's instructions. cDNA was synthesized by reverse transcription from total RNA using superscript™ III reverse transcriptase (Invitrogen, Carlsbad, Ca) and oligo$(dT)_{20}$ primer according to the manufacturer's recommendations.

3.2.2 Molecular cloning of AeFlot-1 cDNA

Two pairs of specific primers were designed to a coding region of *A. aegypti* flotillin-1 (AeFlot-1) (gi|108871581|gb|EAT35806.1), which matched the Cry4Ba-binding flotillin-1 spot from 2D ligand blots (Bayyareddy, Andacht et al. 2009). The primers were used sequentially as shown in Fig. 3.1B & 3.1D in a PCR reaction to amplify AeFlot-1 from the cDNA. PCR amplifications were carried out in a thermocycler (Eppendorf AG, Hamburg, Germany) in 50 µl reaction volumes under the following conditions: using a synthesized midgut cDNA as a template for 25 cycles of 94 ℃ for 2 min, at 94 ℃ for 15 sec, annealing at 55 ℃ for 30 sec, 1min extension at 72 ℃. The resulting PCR product was ligated to pGEM®-T Easy Vector (Promega, Madison, WI) and sequenced from both forward and reverse directions at the Molecular Genetics Instrumentation Facility (University of Georgia, Athens, Ga). Amplification was done with the new set of redesigned primers with restriction enzyme sites NdeI and XhoI. A stop codon artifact was found within the flotillin gene and eliminated using PCR-site directed point mutagenesis to

generate a full length clone. The primers used for PCR site directed mutagenesis and their details are shown in Fig.1B. DNA and protein sequences were assembled and analyzed using online tools available on JUSTBIO website (www.justbio.com).

3.2.3 Production of Rabbit Polyclonal Serum against *E. coli*-expressed AeFlot-1 peptide

To raise antisera, the AeFlot-1 gene was truncated with Nde-I and Xho-I, inserted into protein expression vector pET-30a(+) (Novagen, Madison, WI) and transformed into *E. coli* strain DH5α. The confirmed pET-AeFlot-1 plasmid was re-transformed into BL21-CodonPlus (DE3)/pRIL for expression. AeFlot-1 was over expressed by IPTG induction according to the pET system manual ninth edition (Novagen, Madison, WI) and the inclusion bodies were purified and solubilized in 8M urea. The solubilized AeFlot-1 protein was refolded by stepwise dialysis as described previously (Moonsom, Chaisri et al. 2007) with minor modification. The protein was refolded in 200 volumes of freshly made carbonate buffer (20mM $Na_2Co_{3,}$ pH 9.0) containing 200mM NaCl with decreasing urea concentrations of 6, 4, and 2M at 4 °C for 1 h at each step, and was finally dialyzed against the carbonate buffer with 50mM NaCl (without urea). overnight at 4 °C. Precipitated protein was removed by centrifugation (17,000 *g*, 20 min at 4 °C). The truncated AeFlot-1 peptide was separated on 10% SDS-PAGE, coomassie stained and sent for mass spectrometry analysis at Proteomics and Mass Spectrometry facilities, University of Georgia, Athens, GA. After mass spectrometry confirmation as described previously (Zhang, Hua et al. 2008), the re-folded truncated AeFlot-1 protein (amino acid residues from 1-356) (500 µg) was then dialyzed for overnight in 1x PBS (137 mM NaCl, 2.7 mM KCl,4.3 mM $Na_2HPO_{4,}$ 1.47 mM KH_2PO_4, pH7.4) buffer and used to raise antisera in rabbits at the Animal Resources Facility, University of Georgia. The booster injections and collection of final sera were carried out similar to the method described previously (Hua, Zhang et al. 2009).

3.2.4 Protein sequence analysis

All available predicted insect flotillin-1 protein sequences (except *Drosophila* which is from cloned mRNA sequence) were downloaded from NCBI and aligned with AeFlot-1 sequence by multiple sequence alignment using ClustalW2 program (www.ebi.ac.uk/Tools/msa/clustalw2/). We predicted and analyzed secondary structure and post-translational modifications using various bioinformatics tools including computational soft wares used previously (Rivera-Milla, Stuermer et al. 2006). Various web based bioinformatics tools used in this study are transmembrane helix prediction by HMMTOP v.2.0 (www.enzim.hu/hmmtop); Pfam server from the Sanger institute (www.pfam.sanger.ac.uk) to predict the protein family; NCBI conserved-domain database CDD (www.ncbi.nlm.nih.gov/Structure/cdd/cdd.shtml) to predict conserved protein domains, and the SMART server (http://smart.embl-heidelberg.de) to identify and annotate protein domains. Functional motifs were identified using the Eukaryotic Linear Motif server (http://elm.eu.org/).

3.2.5 SDS-PAGE and immuno blotting

AeFlot-1 (2 μg) expressed in *E. coli* as full length and truncated forms were separated on SDS-PAGE (10% acrylamide) and transferred to PVDF filter. PVDF (Millipore, Bedford, MA) filter then were blocked in 1×PBST (PBS+1%Tween20)/ 3%BSA and then subsequently incubated in the sera raised against AeFlot-1 (1:5000). After washing, the filters were incubated in HRP conjugated anti-rabbit goat secondary antibody, then developed with ECL™ western blotting detection reagents (GE Healthcare, Piscataway, NJ) and exposed to X-ray film. Ten micrograms of *Aedes* BBMV proteins prepared as before (Bayyareddy, Andacht et al. 2009)

were resolved on 10% SDS-PAGE and Western blot was performed using the same procedure described above.

3.2.6 Processing of mosquito larvae for paraffin embedding and immunohistochemistry

Early fourth instar *A. aegypti* larvae were punctured in the thorax and the end of the abdomen by a fine needle and immediately fixed with 4% (v/v) paraformaldehyde at 4ºC. The fixed larvae were rinsed twice in 1xPBS and processed for paraffin embedding using a Tissue Tek VIP5 automated processor (Sakura Finetek, Torrance, CA) according to the manufacturer's instructions. Finally the processed larvae were embedded in Paraplast Plus® tissue-embedding medium (McCormick Scientific, Richmond, IL) and longitudinal sections (~8 μm thick) were cut from the paraffin plus embedded whole larval tissues on a fully-motorized rotary microtome (Leica RM2155, Buffalo Grove, IL). Sections were transferred to previously gelatin-coated glass slides and baked at 37^0 C for overnight.

Immunolocalization of AeFlot-1 protocol was adapted from previously described procedure (Zhang, Hua et al. 2008). Slides containing sections were deparaffinized and blocked the non-specific binding sites (1xPBST with 3%BSA) for 30min at room temperature, the sections were incubated in 250 μl of primary antibody (α-Ae-flotiilin-1, 1:200) for overnight in moist incubation chamber at 4 °C. The slides were then washed, blocked and incubated with 250 μl of Alexa Fluor-488-conjugated goat-anti-rabbit IgG (Invitrogen Corp, Camarillo, CA.) secondary antibody diluted 1:1000 in 1xPBST with 3%BSA serum. The sections were washed in 1xPBST for 10 min. A few drops of 1:1 (v/v) glycerol and PBST solution were added and a coverslip was placed for further observation under Olympus BX60 light microscope (Olympus

Optical, Tokyo, Japan) equipped with epifluorescence and the fluorescent filters. Images were collected by Auto-Montage software (Synoptics, Cambridge, UK).

3.2.7 Isolation of detergent insoluble membranes/lipid rafts

Lipid rafts were isolated as described previously (Chmelar and Nathanson 2006). BBMV were prepared from early fourth instar larvae (Bayyareddy, Andacht et al. 2009) and then approximately one mg of BBMV were re-suspended in 0.5ml TNE buffer (25mM Tris (pH 8.0) 150mM NaCl 5mM EDTA) containing Complete Protease Inhibitor Cocktail (Roche, Indianapolis, IN). The suspension was mixed with 0.5ml of pre-chilled 2% Triton X-100 in TNE buffer and incubated on ice for 30min. The homogenate (1 ml) was then mixed with 2 ml of 60% OptiPrep™ gradient (Iodixanol) (Sigma-Aldrich, St. Louis, MO) in TNE buffer and placed in a 12 ml ultracentrifuge tube (Beckman Coulter 344059). A discontinuous 5-30-40% OptiPrep™ gradient was formed by layering 6 ml of 30% (w/v) OptiPrep™ in TNE buffer on top of the 3 ml of 40% OptiPrep™ with homogenate, followed by 3 ml 5% (w/v) OptiPrep™ in TNE buffer. The samples were ultracentrifuged at 192,072 g in a SW41Ti (Beckman) rotor for 4 h at 4 °C. After centrifugation, the floating opaque band corresponding to the lipid rafts fraction was collected at the interface between the 30% and 5% OptiPrep™ gradients while the bottom fraction corresponding to 40% OptiPrep™ was collected as soluble membranes. Equal volumes of soluble and insoluble fractions were collected and analyzed by Western blotting for lipid raft marker proteins as described above.

3.2.8 Protein, cholesterol and APN activity measurements

Total protein in detergent soluble and insoluble fractions was determined using the Bradford protein assay kit (Bio-Rad, Hercules, CA) according to the manufacturer's

recommendations. Similarly, total cholesterol content was measured fluorimetrically using the Amplex Red Cholesterol Assay Kit (Invitrogen, Carlsbad, CA) by taking the equal volume from the soluble and insoluble fractions. Enzymatic activity of aminopeptidase was also measured according to the method described previously (Bayyareddy, Andacht et al. 2009).

3.3 Results

3.3.1 Comparison of AeFlot-1 to *D. melanogester* FLO^{Dm} and insect predicted flotillin-1 proteins.

A. aegypti flotillin-1 (AeFlot-1) (Accession. No: EAT35806 & GI: 108871581), a Cry4Ba toxin binding protein, was identified in the brush border membrane of *Aedes* larvae using a 2D gel electrophoresis mass spectrometry approach (Bayyareddy, Andacht et al. 2009). Figure 3.2, shows a ClustalW multiple protein sequence alignments of the predicted AeFlot-1 protein with *D. melanogaster* FLO^{DM}, the only previously cloned insect flotillin-1, and other predicted insect flotillin-1 proteins (Fig. 3.2). Of these, AeFlot-1 is most similar to flotillin-1 proteins from *Culex quinquefasciatus* (96% identity, gi:170045542) and *Anopheles gambiae* (95% identity, gi: 158285579) with less, but still high identity to *Drosophila melanogaster* (89% identity gi: 3115385), *Pediculus humanus* (87% identity, gi: 242019841), *Harpegnathos saltator* (85% identity, gi: 307199471), *Apis mellifera* (84% identity, gi: 66512137), *Bombyx mori* (83% identity, gi: BGIBMGA000743), and *Tribolium castaneum* (83% identity, gi: 189240020).

There are two hydrophobic N-terminal transmembrane regions predicted; one from Hidden Markov model prediction at residue 137-154 with amino-termini being extracellular (Tusnády and Simon 1998; Tusnády and Simon 2001) and another in accordance with previously published results (Rivera-Milla, Stuermer et al. 2006) from residue 8 to 36 in all the insect

flotillin-1 sequences (Fig. 3.2). In an attempt to identify the potential phosphorylation sites, we systematically compared all insect flotillin-1 with vertebrate flotillin-1 (Rivera-Milla, Stuermer et al. 2006). As shown in Figure 3. 2, there are two conserved phosphorylation sites by casein kinase-II at residues 119, 153 and one by conserved tyrosine kinase site at residue 169 and a less conserved site at residue 247 predicted by computational tools. All the flotillin-1 sequences have a PDZ3 domain at residues 382-388, by which it interacts with transmembrane proteins in the cell membrane.

3.3.2 Cloning of AeFlot-1 cDNA from larval midgut tissue.

The nucleotide sequence of predicted AeFlot-1 (Accession. No: EAT35806 & GI: 108871581) was used to design the F_1 - R_1 primer pair (Fig. 3.1A and 3.1B). The primers were used in PCR amplification of larval gut cDNA to obtain an expected 1.2 kb DNA fragment (Fig.3.1C). The cloned PCR fragment contained an open reading frame (ORF) encoding a protein with high identity to the predicted AeFlot-1; an exception being a stop codon introduced as a PCR artifact at amino acid residue 356 near the C-terminus (Fig. 3.1D). For heterologous expression of AeFlot-1 in *E. coli*, we re-designed F_1 - R_1 primers with terminal restriction sites (NdeI & XhoI), PCR amplified the cloned AeFlot-1 region and subcloned the fragment into pET30a vector resulting in clone pET-AeFlot-1 with a 1218 bp ORF that encoded a protein of 405 amino acid residues, with molecular size of 45 kDa.

3.3.3 Heterologous expression of AeFlot-1.

AeFlot-1 protein was overexpressed in *E. coli* and SDS-PAGE showed the protein migrated as a 40-kDa band (Fig. 3.3A). We confirmed the identity of the *E. coli* expressed AeFlot-1 by subjecting the protein band to Peptide Mass Fingerprinting (PMF) analysis using

trypsin digestion and MALDI-TOF mass spectrometry. Peptide masses in the scan shown in Fig. 3.3B were searched against local mosquito databases using Mascot resulting in an unambiguous match to AeFlot-1 with a significant Mascot score of 138 and 50% sequence coverage (Fig.3.3C and 3.3D). In addition, the two high intensity spectra (1089.4, 2030.8) were matched to peptides AFVWPSVQR and SEAEIQHIALVTLEGHQR of AeFlot-1 (Fig. 3.3B).

3.3.4 AeFlot-1 in BBMV and midgut tissue.

In Western blot using anti-AeFlot-1 antiserum, specific AeFlot-1 bands were detected in *E.coli* expressing AeFlot-1(Fig. 3.4A) and in BBMV prepared from *Aedes* larvae (a 47-kDa sized band) (Fig. 3.4B). While minor bands were visible on the Western blot of BBMV proteins the antisera appeared to be specific for flotillin (Fig. 3.4B). The anti-AeFlot-1 serum might detect the similar-sized *Aedes* Flotillin-2 (VectorBase Id: AAEL004041) protein that was likely in the larval brush border epithelial cells. As control, pre-immune serum did not detect any BBMV proteins (Fig. 3.4B).

To examine the immunolocalization of AeFlot-1 in larval midgut, we probed whole larval sections with anti-AeFlot-1 antibody. AeFlot-1 was detected in the apical microvilli of the posterior midgut and in the gastric caeca, but not in the microvilli of anterior larval midgut (Fig. 3.5A, 3.5D & 3.5E). As controls, no signal was detected with the preimmune serum (Fig. 3.5B) and secondary antibody only (Fig. 3.5C) in the entire midgut.

3.3.5 AeFlot-1 is a marker of lipid rafts from *A. aegypti.*

Lipid rafts are characterized by resistance to detergent solubilization, usually Triton X-100, at low temperatures and fractionation into low density gradient solutions (Brown and Rose 1992; Fiedler, Kobayashi et al. 1993; Simons and Ikonen 1997). Detergent Resistant Membranes

(DRMs) is a more precise name for such biochemically fractionated materials. We applied a DRM fractionation method to *Aedes* brush border membrane to isolate DRMs, tested for cholesterol enrichment, and evaluated AeFlot-1 as a marker for DRMs. Since DRMs are also enriched in GPI-anchored proteins, aminopeptidase N (APN) enrichment was also measured and APN was detected on western blots. After ultra-centrifugation, a floating opaque band corresponding to the DRM fraction was visible at the interface between the 5% and 30% OptiPrep™ gradients (Fig. 3.7A). Figure 3.7B, represents the silver stained protein profile of DRM and non-DRM fractions. The highest protein concentration of 0.46 mg/ml was present in non-DRM fractions compared to DRM fraction of 0.39 mg/ml (Table 3.1). When compared to the starting BBMV material, the DRM fraction was enriched in cholesterol by 17% and APN activity by 64%, whereas, in the non-DRM fraction cholesterol concentration and APN activity were decreased by 57 and 38 % respectively (Table 3.1). In addition, we also analyzed the gradients for presence of marker proteins known to be present in lipid raft fractions by Western blotting. We discovered that flotillin-1 partitioned into the DRM fractions of larval BBMV (Fig. 3.7C). As shown in Fig. 3.7D, the DRM fractions were also enriched in APN. These data confirmed that DRM marker proteins could be measured by enzyme kinetic assays and by immunoblotting. AeFlot-1 especially appeared to associate closely with the DRMs, suggesting that this protein is uniquely suited for the cholesterol-rich microenvironment of DRMs.

3.3.6 Anti-AeFlot-1 antiserum detects flotillins in Diptera, Lepidoptera and Coleoptera.

In metazoans, flotillin-1 is conserved across many species and in insects a multiple sequence alignment showed more than 83% amino acid sequence similarity (Fig. 3.2). To test whether anti-AeFlot-1 antiserum will cross react with other insect flotillin-1, a western blot analysis was performed on other insect gut BBMVs. The anti-AeFlot-1 antiserum recognized the

expected band at 47kDa in the BBMVs from: *A. aegypti, Culex quinquefasciatus, Heliothis virescens, Helicoverpa zea, Spodoptera frugiperda, Ostrinia nubilalis,* and *Alphitobius diaperinus* (Fig. 3.6).

3.4 Discussion

In the work presented here, AeFlot-1 cDNA was cloned, the presence of AeFlot-1 protein in brush border membrane was confirmed and its distribution in *A. aegypti* larval gut was determined. In addition, we also validated the use of anti-AeFlot-1 antibody for the characterization of *A. aegypti* lipid rafts specifically and insect lipid rafts in general.

Flotillin-1 has been used extensively as a marker and as a structural component of lipid rafts in numerous studies in mammalian systems (Bickel, Scherer et al. 1997). In the lipid rafts of adipocytes, flotillin-1 specifically interacts with the signaling complex which includes CAP, the Src family kinase Fyn, and cortical F-actin (Liu, Deyoung et al. 2005). A high degree of sequence similarity was found in the protein encoded by our cloned AeFlot-1 cDNA with flotillin-1 in *D. melanogaster* (Galbiati, Volonte et al. 1998) and with other predicted insect flotillin-1 protein sequences (Fig. 3.2) indicating that the function and structure of this protein might be highly conserved. A similar observation was reported in vertebrate flotillin-1 sequences (Edgar and Polak 2001; Rivera-Milla, Stuermer et al. 2006). A ClustalW multiple sequence alignment of flotillin-1 proteins was analyzed using available flotillin-1 protein sequences from insects of the orders Diptera, Coleoptera, Lepidoptera, Hymenoptera, and Phthiraptera (Fig. 3.2). The comparative alignment suggested the conserved presence of transmembrane domains, putative lipid anchoring sites and kinase active-site signature sequence for phosphorylation. Although no attempt was made to determine functional significance of flotillin-1 in insects, the predicted results were in agreement with the vertebrate flotillin-1 studies (Edgar and Polak 2001;

Rivera-Milla, Stuermer et al. 2006) that it has two hydrophobic domains, putative palmitoylation and myristoylation sites, and two phosphorylation sites. The functional study on flotillin-1 domains revealed that the first hydrophobic stretch is important in lipid raft association and remains in the cytoplasm upon its removal (Liu, Deyoung et al. 2005).

In the *A. aegypti* genome there are two predicted flotillin-1 proteins, one from the initiation codon methionine (AAEL012046) and another from leucine (AAEL015235). These two isoforms are possibly due to incomplete annotation of the *A. aegypti* genome database. However, it should be noted that the clone used for this study had methionine as an initiation codon. *A. gambiae* and *D. melanogaster* flotillin-1 has 21 amino acid residues more in N-terminal region and has two translation initiation sites. Western blot analysis in human cells detected doublet of molecular weights 47 and 45 kDa flotillin-1, indicating a presence of alternate translation initiation site at amino acid residue 11 (Bickel, Scherer et al. 1997). In contrast, there was no evidence of an alternate translation initiation site in insects as the antiserum anti-AeFlot-1 detected only a single band of approximately 47kD in all the insect membranes tested (Fig. 3.4B, Fig. 3.6).

Expression of the gene coding for AeFlot-1 should occur in all larval midgut cells of *A. aegypti* (Fig. 3.5A). Flotillin-1 interaction with cadherins and GPI-anchored proteins was confirmed in mammalian epithelial cells, suggesting that interaction between these three proteins occur in all cells and across species when cell contacts need to be formed (Stuermer 2011). However, as assessed by immunolocalization techniques, we found intriguing patterns of distribution of AeFlot-1 with regards to the region of organ, cell type, or membrane location, mostly localized in the apical microvilli of posterior midgut and gastric caeca (Fig. 3.5A, 3.5D & 3.5E). In the *A. aegypti* larval midgut, a similar localization pattern has been described for

cadherin (Chen, Aimanova et al. 2009) and APN (Chen, Aimanova et al. 2009), indicating the similar localization of AeFlot-1. It is possible that AeFlot-1 is specific to certain cell types, because columnar cells have long, 'absorptive-type' microvilli in the posterior midgut (Zhuang, Linser et al. 1999). Our results provide new information on the localization of flotillin-1 in the insect larval midgut.

A number of investigators have isolated lipid rafts from different cells and tissues based on their biochemical characters, such as the presence of marker proteins like flotillin-1 and APN detected by mass spectrometry or western blot, and fractions high in cholesterol/protein ratio. Our study, using detergent solubilization and OptiPrep™ gradient fractionation technique, shows that AeFlot-1 is specifically fractionated into the low density fraction and can be used as a lipid raft marker (Fig. 3.7C). This selective association of flotillin-1 to lipid rafts might be due to the presence of a Prohibitin Homology (PHB) Domain (Dermine, Duclos et al. 2001). Similar to AeFlot-1, GPI-anchored APN was also enriched in the low density fraction (Fig. 3.7D & Table 3.1). The presence of a GPI-anchor on APN helps to attract the protein to the lipid rafts (Sargiacomo, Sudol et al. 1993). In addition to AeFlot-1 and APN selective partitioning, AeFlot-1 in this study had similar immunolocalization as APN which is a Cry toxin receptor in. *A. aegypti* (Chen, Aimanova et al. 2009).

It was interesting to note that cholesterol and APN were enriched in lipid raft fractions, suggesting that these are an important components of lipid rafts (Danielsen 1995; Radeva and Sharom 2004), and these results were in agreement with other reports (Brown and London 1998; Nguyen, Amine et al. 2006). When the cholesterol amount in lipid rafts from *A. aegypti* and mammalian system was compared, we found that mosquito has several fold lower cholesterol concentration. The fact that mosquitos are cholesterol auxotrophs (Clayton 1964), they have to

depend on external source for cholesterol; thus all cholesterol found in mosquito is typically obtained from diet in larva and blood-meal diet in female adult. Similarly, the virus particles raised on mammalian cells had ten-fold higher cholesterol content in their envelopes than virus particles isolated from mosquito cells (Sousa, Carvalho et al. 2011).

Detailed information on AeFlot-1 gene, its localization and function was previously unavailable. In this study, we developed a polyclonal antiserum of AeFlot-1 as an important tool to study lipid rafts in insects. To our knowledge, this is the first report describing flotillin-1 localization in the larval midgut.

Acknowledgements

This research was partially supported by National Institutes of Health Grant R01 AI 29092 to D.H. Dean (Ohio State University) and M.J.A. We would like to thank Dr. Mark R. Brown, for allowing us to use his fluorescent microscope and Dr. Kallappagoudar, at Emory University, for helping with larval gut cDNA preparation.

Reference

Bayyareddy, K., T. M. Andacht, et al. (2009). "Proteomic identification of *Bacillus thuringiensis* subsp. *israelensis* toxin Cry4Ba binding proteins in midgut membranes from *Aedes* (*Stegomyia*) *aegypti* Linnaeus (Diptera, Culicidae) larvae." Insect Biochem. Mol. Biol. **39**(4): 279-286.

Bickel, P. E., P. E. Scherer, et al. (1997). "Flotillin and epidermal surface antigen define a new family of caveolae-associated integral membrane proteins." *J. Biol. Chem.* **272**(21): 13793-13802.

Bravo, A., I. Gómez, et al. (2004). "Oligomerization triggers binding of a *Bacillus thuringiensis* Cry1Ab pore-forming toxin to aminopeptidase N receptor leading to insertion into membrane microdomains." Biochim. Biophys. Acta **1667**(1): 38-46.

Brown, D. A. and E. London (1998). "Functions of lipid rafts in biological membranes." Annu. Rev. Cell Dev. Biol. **14**: 111-136.

Brown, D. A. and E. London (2000). "Structure and function of sphingolipid- and cholesterol-rich membrane rafts." J. Biol. Chem. **275**(23): 17221-17224.

Brown, D. A. and J. K. Rose (1992). "Sorting of GPI-anchored proteins to glycolipid-enriched membrane subdomains during transport to the apical cell surface." Cell **68**(3): 533-544.

Cancino-Rodezno, A., C. Alexander, et al. (2010). "The mitogen-activated protein kinase p38 is involved in insect defense against Cry toxins from *Bacillus thuringiensis*." Insect Biochem. Mol. Biol. **40**(1): 58-63.

Chen, J., K. G. Aimanova, et al. (2009). "*Aedes aegypti* cadherin serves as a putative receptor of the Cry11Aa toxin from *Bacillus thuringiensis* subsp. *israelensis*." Biochem. J. **424**(2): 191-200.

Chen, J., K. G. Aimanova, et al. (2009). "Identification and characterization of *Aedes aegypti* aminopeptidase N as a putative receptor of *Bacillus thuringiensis* Cry11A toxin." Insect Biochem. Mol. Biol. **39**(10): 688-696.

Chmelar, R. S. and N. M. Nathanson (2006). "Identification of a novel apical sorting motif and mechanism of targeting of the M2 muscarinic acetylcholine receptor." J. Biol. Chem. **281**(46): 35381-35396.

Clayton, R. B. (1964). "The Utilization of Sterols by Insects." J. Lipid Res. **15**: 3-19.

Danielsen, E. M. (1995). "Involvement of detergent-insoluble complexes in the intracellular transport of intestinal brush border enzymes." Biochemistry **34**(5): 1596-1605.

Dermine, J. F., S. Duclos, et al. (2001). "Flotillin-1-enriched lipid raft domains accumulate on maturing phagosomes." J. Biol. Chem. **276**(21): 18507-18512.

Edgar, A. J. and J. M. Polak (2001). "Flotillin-1: gene structure: cDNA cloning from human lung and the identification of alternative polyadenylation signals." Int. J. Biochem. Cell Biol. **33**(1): 53-64.

Eroglu, C., B. Brugger, et al. (2003). "Glutamate-binding affinity of *Drosophila metabotropic* glutamate receptor is modulated by association with lipid rafts." Proc. Natl. Acad. Sci. U.S.A. **100**(18): 10219 - 10224.

Fiedler, K., T. Kobayashi, et al. (1993). "Glycosphingolipid-enriched, detergent-insoluble complexes in protein sorting in epithelial cells." Biochemistry **32**(25): 6365-6373.

Frick, M., N. A. Bright, et al. (2007). "Coassembly of flotillins induces formation of membrane microdomains, membrane curvature, and vesicle budding." Curr. Biol. **17**(13): 1151-1156.

Galbiati, F., D. Volonte, et al. (1998). "Identification, sequence and developmental expression of invertebrate flotillins from *Drosophila melanogaster*." Gene **210**(2): 229-237.

Ge, L., W. Qi, et al. (2011). "Flotillins play an essential role in Niemann-Pick C1-like 1-mediated cholesterol uptake." Proc. Natl. Acad. Sci. U.S.A. **108**(2): 551-556.

Glebov, O. O., N. A. Bright, et al. (2006). "Flotillin-1 defines a clathrin-independent endocytic pathway in mammalian cells." Nat. Cell Biol. **8**(1): 46-54.

Hua, G., R. Zhang, et al. (2009). "*Anopheles gambiae* alkaline phosphatase is a functional receptor of *Bacillus thuringiensis jegathesan* Cry11Ba toxin." Biochemistry **48**(41): 9785-9793.

Kato, N., M. Nakanishi, et al. (2006). "Flotillin-1 regulates IgE receptor-mediated signaling in rat basophilic leukemia (RBL-2H3) cells." J. Immunol. **177**(1): 147-154.

Langhorst, M. F., F. A. Jaeger, et al. (2008). "Reggies/flotillins regulate cytoskeletal remodeling during neuronal differentiation via CAP/ponsin and Rho GTPases." Eur. J. Cell Biol. **87**(12): 921-931.

Langhorst, M. F., A. Reuter, et al. (2005). "Scaffolding microdomains and beyond: the function of reggie/flotillin proteins." Cell Mol. Life Sci. **62**(19-20): 2228-2240.

Liu, J., S. M. Deyoung, et al. (2005). "The stomatin/prohibitin/flotillin/HflK/C domain of flotillin-1 contains distinct sequences that direct plasma membrane localization and protein interactions in 3T3-L1 adipocytes." J. Biol. Chem. **280**(16): 16125-16134.

Moonsom, S., U. Chaisri, et al. (2007). "Binding characteristics to mosquito-larval midgut proteins of the cloned domain II-III fragment from the *Bacillus thuringiensis* Cry4Ba toxin." J. Biochem. Mol. Biol. **40**(5): 783-790.

Morrow, I. C. and R. G. Parton (2005). "Flotillins and the PHB Domain Protein Family: Rafts, Worms and Anaesthetics." Traffic **6**(9): 725-740.

Morrow, I. C., S. Rea, et al. (2002). "Flotillin-1/reggie-2 traffics to surface raft domains via a novel golgi-independent pathway. Identification of a novel membrane targeting domain and a role for palmitoylation." J. Biol. Chem. **277**(50): 48834-48841.

Murphy, S. C., B. U. Samuel, et al. (2004). "Erythrocyte detergent-resistant membrane proteins: their characterization and selective uptake during malarial infection." Blood **103**(5): 1920-1928.

Nagao, E., K. B. Seydel, et al. (2002). "Detergent-resistant erythrocyte membrane rafts are modified by a *Plasmodium falciparum* infection." Exp. Parasitol. **102**(1): 57-59.

Neumann-Giesen, C., B. Falkenbach, et al. (2004). "Membrane and raft association of reggie-1/flotillin-2: role of myristoylation, palmitoylation and oligomerization and induction of filopodia by overexpression." Biochem. J. **378**(Pt 2): 509-518.

Nguyen, H. T. T., A. B. Amine, et al. (2006). "Proteomic characterization of lipid rafts markers from the rat intestinal brush border." Biochem. Biophys. Res. Commun. **342**(1): 236-244.

Pust, S., A. B. Dyve, et al. (2010). "Interplay between toxin transport and flotillin localization." PLoS One **5**(1): e8844.

Radeva, G. and F. J. Sharom (2004). "Isolation and characterization of lipid rafts with different properties from RBL-2H3 (rat basophilic leukaemia) cells." Biochem. J. **380**(Pt 1): 219-230.

Rietveld, A., S. Neutz, et al. (1999). "Association of sterol- and glycosylphosphatidylinositol-linked proteins with *Drosophila* raft lipid microdomains." J. Biol. Chem. **274**(17): 12049 - 12054.

Rivera-Milla, E., C. A. Stuermer, et al. (2006). "Ancient origin of reggie (flotillin), reggie-like, and other lipid-raft proteins: convergent evolution of the SPFH domain." Cell Mol. Life Sci. **63**(3): 343-357.

Salaun, C., D. J. James, et al. (2004). "Lipid rafts and the regulation of exocytosis." Traffic **5**(4): 255-264.

Sargiacomo, M., M. Sudol, et al. (1993). "Signal transducing molecules and glycosyl-phosphatidylinositol-linked proteins form a caveolin-rich insoluble complex in MDCK cells." J. Cell Biol. **122**(4): 789-807.

Simons, K. and R. Ehehalt (2002). "Cholesterol, lipid rafts, and disease." J. Clin. Invest. **110**(5): 597-603.

Simons, K. and E. Ikonen (1997). "Functional rafts in cell membranes." Nature **387**(6633): 569-572.

Sousa, I. P., C. A. M. Carvalho, et al. (2011). "Envelope lipid-packing as a critical factor for the biological activity and stability of alphavirus particles isolated from mammalian and mosquito cells." J. Biol. Chem. **286**(3): 1730-1736.

Stuermer, C. A. (2011). "Microdomain-forming proteins and the role of the reggies/flotillins during axon regeneration in zebrafish." Biochim. Biophys. Acta **1812**(3): 415-422.

Stuermer, C. A. (2011). "Reggie/flotillin and the targeted delivery of cargo." J. Neurochem. **116**(5): 708-713.

Stuermer, C. A. and H. Plattner (2005). "The 'lipid raft' microdomain proteins reggie-1 and reggie-2 (flotillins) are scaffolds for protein interaction and signalling." Biochemical Society symposium(72): 109-118.

Tsui-Pierchala, B. A., M. Encinas, et al. (2002). "Lipid rafts in neuronal signaling and function." Trends Neurosci. **25**(8): 412-417.

Tusnády, G. E. and I. Simon (1998). "Principles governing amino acid composition of integral membrane proteins: application to topology prediction." J. Mol. Cell Biol. **283**(2): 489-506.

Tusnády, G. E. and I. Simon (2001). "The HMMTOP transmembrane topology prediction server." Bioinformatics **17**(9): 849-850.

Vassilieva, E. V., A. I. Ivanov, et al. (2009). "Flotillin-1 stabilizes caveolin-1 in intestinal epithelial cells." Biochem. Biophys. Res. Commun. **379**(2): 460-465.

Wang, C., Y. Yoo, et al. (2010). "Regulation of Integrin beta 1 recycling to lipid rafts by Rab1a to promote cell migration." J. Biol. Chem. **285**(38): 29398-29405.

Zhang, R., G. Hua, et al. (2008). "A 106-kDa Aminopeptidase Is a Putative Receptor for *Bacillus thuringiensis* Cry11Ba Toxin in the Mosquito *Anopheles gambiae*†." Biochemistry **47**(43): 11263-11272.

Zhuang, M., D. I. Oltean, et al. (2002). "*Heliothis virescens* and *Manduca sexta* lipid rafts are involved in Cry1A toxin binding to the midgut epithelium and subsequent pore formation." J. Biol. Chem. **277**(16): 13863-13872.

Zhuang, Z., P. Linser, et al. (1999). "Antibody to H(+) V-ATPase subunit E colocalizes with portasomes in alkaline larval midgut of a freshwater mosquito (*Aedes aegypti*)." J. Exp. Biol. **202**(18): 2449-2460.

Figures and Tables

Table 3.1: Protein, cholesterol and APN composition of BBMV, DRMs and DSMs. Biochemical analysis of *Aedes* DRMs reveals low protein content, high cholesterol amounts, high aminopeptidase activity, and high protein to cholesterol ratio. The cholesterol and protein determination assay were performed on BBMV, low density and high density fractions extracted by Optiprep density gradient ultracentrifugation. The assays were carried out according to the manufacturer's instruction. (All the values are means ± SD (%) of four BBMV and DRM preparations).

	Protein mg/ml	Cholesterol ug/ml	Cholesterol ug/mg protein	% Cholesterol change	APN umol/min/mg of protein	% APN change
BBMV	0.41 ± 0.03	16.32 ± 3.13	44.30 ± 12.033		2.25 ± 0.15	
DRM	0.39 ± 0.06	19.16 ± 2.47	56.65 ± 12.588	28	3.81 ± 0.20	64
DSM	0.46 ± 0.13	7.02 ± 2.20	12.42 ± 4.208	`-72	1.48 ± 0.22	`-38

Figure 3.1: **Nucleotide and amino acid sequence underneath for AeFlot-1 with primer details.** Cloning strategy and location of oligonucleotides used as PCR primers (*arrows*), also indicated the position of stop codon and it's mutated sequence (A). Primers used in PCR amplifications for cloning and site directed mutagenesis for midgut flitillin-1cDNA (B). PCR amplified product (C). Sequence of *A. aegypti* flotillin-1 cDNA and deduce d amino acid sequence (D).

A

B

Primer name	Oligonucleotid (5′–3′)
Cloning cDNA of *Aedes* flotillin	
Ae-flotillin/F1	5′-ATGAAACCACTGTTGGTTCCCG-3′
Ae-flotillin/F2	5′-CCGAGGCGGAGATTCAGCACATT-3′
Ae-flotillin/R1	5′-ACCAGCGTGTACCGACCGAGAAA-3′
Ae-flotillin/R2	5′-CGGCGGCCACCTTTGGCAACGT-3′
Site directed mutagenesis	
Ae-flotillin/pm-F	5'-CCGCTGTCGCAGGCCAAAAAGATTACAATG-3'
Ae-flotillin/pm-R	5'-TTTGGCCTGCGACAGCGGAGCCGCAAC-3

C

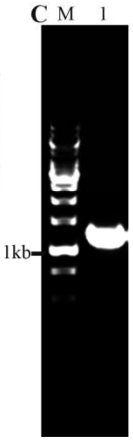

D

```
1 - ATGAAACCACTGTTGGTTCCCGGAGGTCGAGCTTTCGTATGGCCATCGGTGCAAAGAGTT - 60
1 - M K P L L V P G G R A F V W P S V Q R V   - 20
61 - CAACGAATCTCTCTCAACACGATGACGCTGCAGGTGGAAAGCCCAACAGTTTACACCAGC - 120
21 - Q R I S L N T M T L Q V E S P T V Y T S   - 40
121 - CAGGGTGTTCCAATTTCCGTGACCGGCATTGCCCAAGTAAAAATACAGGGCCAGAACGAA - 180
41 - Q G V P I S V T G I A Q V K I Q G Q N E   - 60
181 - GATATGCTGCTGACGGCGTGCGAACAATTCCTCGGCAAGTCTGAGGCGGAGATTCAGCAC - 240
61 - D M L L T A C E Q F L G K S E A E I Q H   - 80
241 - ATTGCGCTGGTCACGCTGGAGGGACACCAGCGCGCCATTATGGGCTCGATGACGGTGGAG - 300
81 - I A L V T L E G H Q R A I M G S M T V E   - 100
301 - GAAATTTACAAGGACCGGAAGAAATTCTCCAAACAGGTGTTCGAGGTTGCCTCGTCGGAT - 360
101 - E I Y K D R K K F S K Q V F E V A S S D   - 120
361 - TTGGTCAACATGGGTATTACGGTGGTGTCGTACACGCTGAAGGACATTCGCGACGAGGAG - 420
121 - L V N M G I T V V S Y T L K D I R D E E   - 140
421 - GGCTACCTGAAAAGCCTCGGTATGGCTCGTACGGCCGAGGTGAAGCGTGACGCCCGTATT - 480
141 - G Y L K S L G M A R T A E V K R D A R I   - 160
481 - GGCGAGGCGGAGGCCCGCTGTGACGCCACCATCAAGGAGGCCATCGCCGAGGAGCAACGG - 540
161 - G E A E A R C D A T I K E A I A E E Q R   - 180
541 - ATGGCCGCTCGGTTCCTCAACGACACCGAGATCGCCAAGGCTCAGCGTGACTTCGAACTG - 600
181 - M A A R F L N D T E I A K A Q R D F E L   - 200
601 - AAGAAGGCCGTCTACGACGTCGAGGTGCAAACGAAGAAGGCCGAAGCCGAGATGGCTTAT - 660
201 - K K A V Y D V E V Q T K K A E A E M A Y   - 220
661 - GAACCGCAGGCTGCCAAGACCAAGCAGCGCATCAAGGAGGAACAGATGCAGATCAAGGTC - 720
221 - E P Q A A K T K Q R I K E E Q M Q I K V   - 240
721 - ATCGAACGTACCCAGGAGATTGCCGTTCAGGAGCAGGAAATGGCTCGCCGTGAACGTGAA - 780
241 - I E R T Q E I A V Q E Q E M A R R E R E   - 260
781 - CTGGAGGCCACCATCCGGAGACCGGCCGAGGCCGAGAAGTACAAGCTGGAGAAACTGGCT - 840
261 - L E A T I R R P A E A E K Y K L E K L A   - 280
841 - GAAGCCAACAGAAACCGAGTCATTTTGGAGGCCGAAGCTGAAGCGGAAGCGATTAAGGTC - 900
281 - E A N R N R V I L E A E A E A E A I K V   - 300
901 - CGCGGAGAAGCTGAAGCATTTGCCATCGCAGCCAAATCGAAAGCCGAAGCCGAACAGATG - 960
301 - R G E A E A F A I A A K S K A E A E Q M   - 320
961 - GCTAAGAAGGCGGAAGCCTGGCGTGAATATCGCGAGGCTGCCATGGTCGACATGCTGTTG - 1020
321 - A K K A E A W R E Y R E A A M V D M L L   - 340
1021 - GATACGTTGCCAAAGGTGGCCGCCGAGGTTGCGGCTCCGCTGTCGTAGGCCAAAAAGATT - 1080
341 - D T L P K V A A E V A A P L S * A K K I   - 360
1081 - ACAATGGTATCCAGTGGCACCGGTGGGGTCGGTGCGGCAAAGCTCACCGGCGAAGTGCTG - 1140
361 - T M V S S G T G G V G A A K L T G E V L   - 380
1141 - CAAATCGTCAACAAGATTCCGGATCTGGTCAGATCGATCACTGGCGTGGACATTTCTCGG - 1200
381 - Q I V N K I P D L V R S I T G V D I S R   - 400
1201 - TCGGTACACGCTGGTCTCGAGCACCACCACCACCACCACTGA - 1242
401 - S V H A G L E H H H H H H * X             - 420
```

Figure 3.2: Multiple sequence alignment of AeFlot-1 with the protein sequences of currently known insect flotillin-1. Conserved amino acid sequences among known insect Flot-1, highlighting the conserved post-translational modifications: phosphorylation sites indicated by 'P', myristoylation and putative palmitoylation sites in black framed boxes. N-terminal conserved hydrophobic regions are underlined. Ae, *Aedes aegypti;* Cq, *Culex quinquefasciatus* (GI: 170045542); Ag, *Anopheles gambiae* (GI: 158285579); DM, *Drosophila melanogaster* (GI: 3115385); Hs, *Harpegnathos saltator* (GI: 307199471); Am, *Apis mellifera* (GI: 66512137); Ph, *Pediculus humanus* (GI: 242019841); Bm, *Bombyx mori* (GI: BGIBMGA000743); Tc, *Tribolium castaneum* (GI: 189240020).

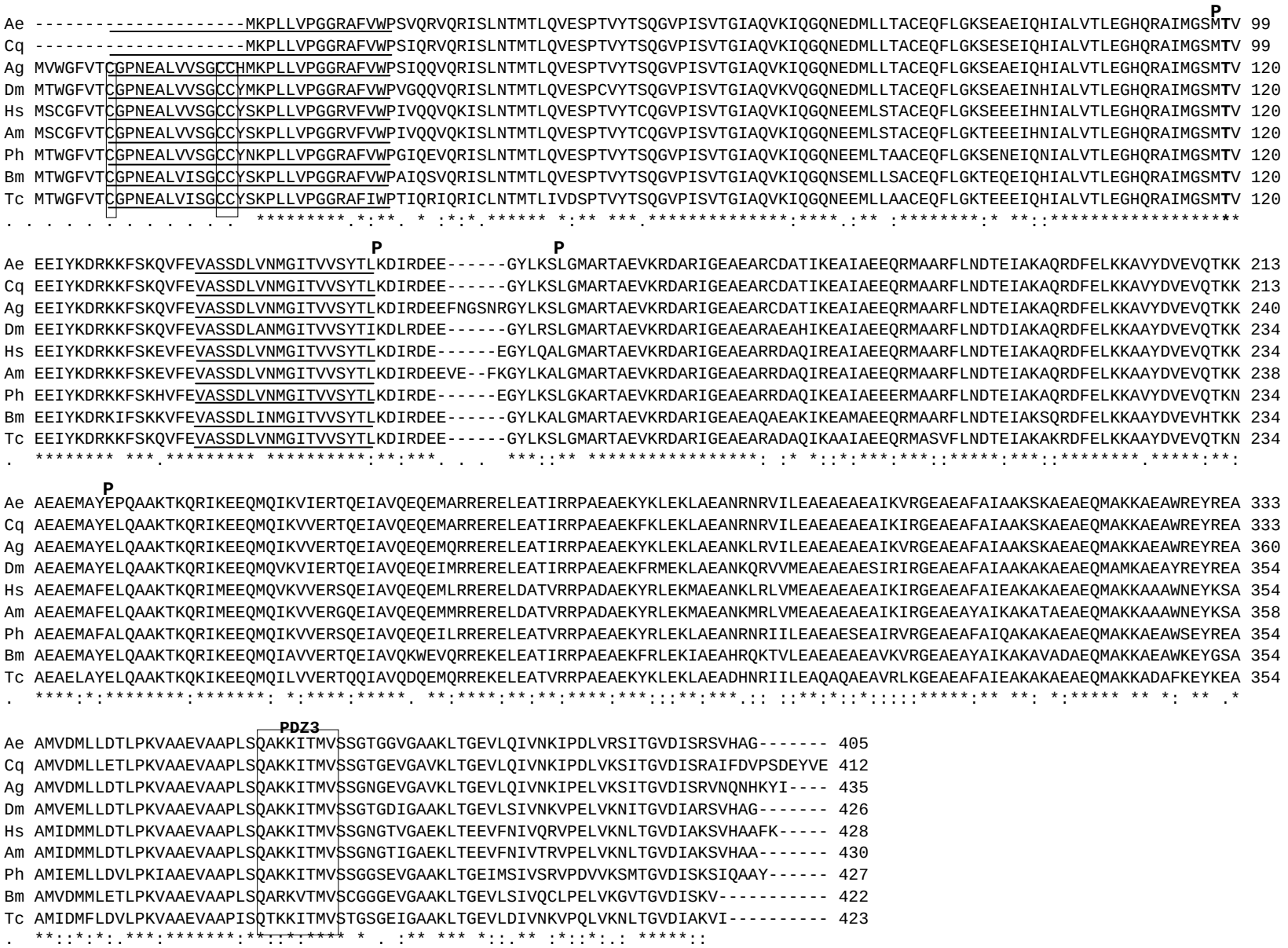
P
Ae ----------MKPLLVPGGRAFVWPSVQRVQRISLNTMTLQVESPTVYTSQGVPISVTGIAQVKIQGQNEDMLLTACEQFLGKSEAEIQHIALVTLEGHQRAIMGSMTV 99
Cq ----------MKPLLVPGGRAFVWPSIQRVQRISLNTMTLQVESPTVYTSQGVPISVTGIAQVKIQGQNEDMLLTACEQFLGKSESEIQHIALVTLEGHQRAIMGSMTV 99
Ag MVWGFVTCGPNEALVVSGCCHMKPLLVPGGRAFVWPSIQQVQRISLNTMTLQVESPTVYTSQGVPISVTGIAQVKIQGQNEDMLLTACEQFLGKSEAEIQHIALVTLEGHQRAIMGSMTV 120
Dm MTWGFVTCGPNEALVVSGCCYMKPLLVPGGRAFVWPVGQQVQRISLNTMTLQVESPCVYTSQGVPISVTGIAQVKVQGQNEDMLLTACEQFLGKSEAEINHIALVTLEGHQRAIMGSMTV 120
Hs MSCGFVTCGPNEALVVSGCCYSKPLLVPGGRVFVWPIVQQVQKISLNTMTLQVESPTVYTCQGVPISVTGIAQVKIQGQNEEMLSTACEQFLGKSEEEIHNIALVTLEGHQRAIMGSMTV 120
Am MSCGFVTCGPNEALVVSGCCYSKPLLVPGGRVFVWPIVQQVQKISLNTMTLQVESPTVYTCQGVPISVTGIAQVKIQGQNEEMLSTACEQFLGKTEEEIHNIALVTLEGHQRAIMGSMTV 120
Ph MTWGFVTCGPNEALVVSGCCYNKPLLVPGGRAFVWPGIQEVQRISLNTMTLQVESPTVYTSQGVPISVTGIAQVKIQGQNEEMLTAACEQFLGKSENEIQNIALVTLEGHQRAIMGSMTV 120
Bm MTWGFVTCGPNEALVISGCCYSKPLLVPGGRAFVWPAIQSVQRISLNTMTLQVESPTVYTSQGVPISVTGIAQVKIQGQNSEMLLSACEQFLGKTEQEIQHIALVTLEGHQRAIMGSMTV 120
Tc MTWGFVTCGPNEALVISGCCYSKPLLVPGGRAFIWPTIQRIQRICLNTMTLIVDSPTVYTSQGVPISVTGIAQVKIQGQNEEMLLAACEQFLGKTEEEIQHIALVTLEGHQRAIMGSMTV 120
P
P
Ae EEIYKDRKKFSKQVFEVASSDLVNMGITVVSYTLKDIRDEE------GYLKSLGMARTAEVKRDARIGEAEARCDATIKEAIAEEQRMAARFLNDTEIAKAQRDFELKKAVYDVEVQTKK 213
Cq EEIYKDRKKFSKQVFEVASSDLVNMGITVVSYTLKDIRDEE------GYLKSLGMARTAEVKRDARIGEAEARCDATIKEAIAEEQRMAARFLNDTEIAKAQRDFELKKAVYDVEVQTKK 213
Ag EEIYKDRKKFSKQVFEVASSDLVNMGITVVSYTLKDIRDEEFNGSNRGYLKSLGMARTAEVKRDARIGEAEARCDATIKEAIAEEQRMAARFLNDTEIAKAQRDFELKKAVYDVEVQTKK 240
Dm EEIYKDRKKFSKQVFEVASSDLANMGITVVSYTIKDLRDEE------GYLRSLGMARTAEVKRDARIGEAEARAEAHIKEAIAEEQRMAARFLNDTDIAKAQRDFELKKAAYDVEVQTKK 234
Hs EEIYKDRKKFSKEVFEVASSDLVNMGITVVSYTLKDIRDE------EGYLQALGMARTAEVKRDARIGEAEARRDAQIREAIAEEQRMAARFLNDTEIAKAQRDFELKKAAYDVEVQTKK 234
Am EEIYKDRKKFSKEVFEVASSDLVNMGITVVSYTLKDIRDEEVE--FKGYLKALGMARTAEVKRDARIGEAEARRDAQIREAIAEEQRMAARFLNDTEIAKAQRDFELKKAAYDVEVQTKK 238
Ph EEIYKDRKKFSKHVFEVASSDLVNMGITVVSYTLKDIRDE------EGYLKSLGKARTAEVKRDARIGEAEARRDAQIKEAIAEEERMAARFLNDTEIAKAQRDFELKKAVYDVEVQTKN 234
Bm EEIYKDRKIFSKKVFEVASSDLINMGITVVSYTLKDIRDEE------GYLKALGMARTAEVKRDARIGEAEAQAEAKIKEAMAEEQRMAARFLNDTEIAKSQRDFELKKAAYDVEVHTKK 234
Tc EEIYKDRKKFSKQVFEVASSDLVNMGITVVSYTLKDIRDEE------GYLKSLGMARTAEVKRDARIGEAEARADAQIKAAIAEEQRMASVFLNDTEIAKAKRDFELKKAAYDVEVQTKN 234
P
Ae AEAEMAYEPQAAKTKQRIKEEQMQIKVIERTQEIAVQEQEMARRERELEATIRRPAEAEKYKLEKLAEANRNRVILEAEAEAEAIKVRGEAEAFAIAAKSKAEAEQMAKKAEAWREYREA 333
Cq AEAEMAYELQAAKTKQRIKEEQMQIKVVERTQEIAVQEQEMARRERELEATIRRPAEAEKFKLEKLAEANRNRVILEAEAEAEAIKIRGEAEAFAIAAKSKAEAEQMAKKAEAWREYREA 333
Ag AEAEMAYELQAAKTKQRIKEEQMQIKVVERTQEIAVQEQEMQRRERELEATIRRPAEAEKYKLEKLAEANKLRVILEAEAEAEAIKVRGEAEAFAIAAKSKAEAEQMAKKAEAWREYREA 360
Dm AEAEMAYELQAAKTKQRIKEEQMQVKVIERTQEIAVQEQEIMRRERELEATIRRPAEAEKFRMEKLAEANKQRVVMEAEAEAESIRIRGEAEAFAIAAKAKAEAEQMAMKAEAYREYREA 354
Hs AEAEMAFELQAAKTKQRIMEEQMQVKVVERSQEIAVQEQEMLRRERELDATVRRPADAEKYRLEKMAEANKLRLVMEAEAEAEAIKIRGEAEAFAIEAKAKAEAEQMAKKAAAWNEYKSA 354
Am AEAEMAFELQAAKTKQRIMEEQMQIKVVERGQEIAVQEQEMMRRERELDATVRRPADAEKYRLEKMAEANKMRLVMEAEAEAEAIKIRGEAEAYAIKAKATAEAEQMAKKAAAWNEYKSA 358
Ph AEAEMAFALQAAKTKQRIKEEQMQIKVVERSQEIAVQEQEILRRERELEATVRRPAEAEKYRLEKLAEANRNRIILEAEAESEAIRVRGEAEAFAIQAKAKAEAEQMAKKAEAWSEYREA 354
Bm AEAEMAYELQAAKTKQRIKEEQMQIAVVERTQEIAVQKWEVQRREKELEATIRRPAEAEKFRLEKIAEAHRQKTVLEAEAEAEAVKVRGEAEAYAIKAKAVADAEQMAKKAEAWKEYGSA 354
Tc AEAELAYELQAAKTKQKIKEEQMQILVVERTQQIAVQDQEMQRREKELEATVRRPAEAEKYKLEKLAEADHNRIILEAQAQAEAVRLKGEAEAFAIEAKAKAEAEQMAKKADAFKEYKEA 354
PDZ3
Ae AMVDMLLDTLPKVAAEVAAPLSQAKKITMVSSGTGGVGAAKLTGEVLQIVNKIPDLVRSITGVDISRSVHAG------- 405
Cq AMVDMLLETLPKVAAEVAAPLSQAKKITMVSSGTGEVGAVKLTGEVLQIVNKIPDLVKSITGVDISRAIFDVPSDEYVE 412
Ag AMVDMLLDTLPKVAAEVAAPLSQAKKITMVSSGNGEVGAVKLTGEVLQIVNKIPELVKSITGVDISRVNQNHKYI---- 435
Dm AMVEMLLDTLPKVAAEVAAPLSQAKKITMVSSGTGDIGAAKLTGEVLSIVNKVPELVKNITGVDIARSVHAG------- 426
Hs AMIDMMLDTLPKVAAEVAAPLSQAKKITMVSSGNGTVGAEKLTEEVFNIVQRVPELVKNLTGVDIAKSVHAAFK----- 428
Am AMIDMMLDTLPKVAAEVAAPLSQAKKITMVSSGNGTIGAEKLTEEVFNIVTRVPELVKNLTGVDIAKSVHAA------- 430
Ph AMIEMLLDVLPKIAAEVAAPLSQAKKITMVSSGGSEVGAAKLTGEIMSIVSRVPDVVKSMTGVDISKSIQAAY------ 427
Bm AMVDMMLETLPKVAAEVAAPLSQARKVTMVSCGGGEVGAAKLTGEVLSIVQCLPELVKGVTGVDISKV----------- 422
Tc AMIDMFLDVLPKVAAEVAAPISQTKKITMVSTGSGEIGAAKLTGEVLDIVNKVPQLVKNLTGVDIAKVI---------- 423

Figure 3. 3: Mass spectrometry analysis of *E.coli* expressed flotilin-1. (A)**.** Purified flotillin-1 protein band on 10% SDS−PAGE (Coomassie staining). (B). MALDI-TOF peptide-mass fingerprint (PMF) spectrum of the tryptic digest of flotillin protein from 1D gel band. (C). The predominant peaks at 1089.4 and 2030.8 corresponds to *Aedes* flotillin-1. Peptides that matched *Aedes* flotillin (gi|157131242|ref|XM_001655783.1) are shown in red, red color denotes matches to PMF data. (D).Mascot search results matching *Aedes* flotillin-1.

A

B

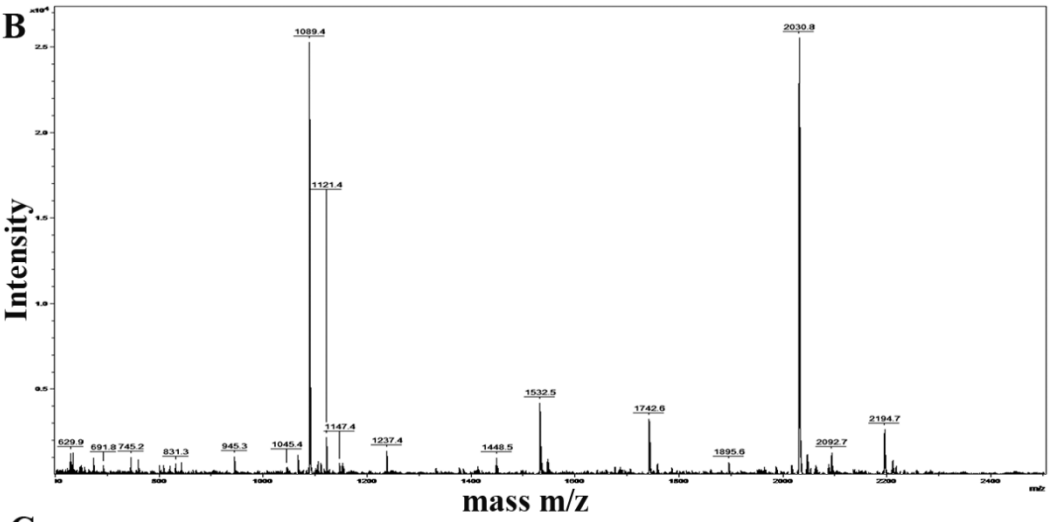

C

```
  1 MKPLLVPGGR AFVWPSVQRV QRISLNTMTL QVESPTVYTS QGVPISVTGI
 51 AQVKIQGQNE DMLLTACEQF LGKSEAEIQH IALVTLEGHQ RAIMGSMTVE
101 EIYKDRKKFS KQVFEVASSD LVNMGITVVS YTLKDIRDEE GYLKSLGMAR
151 TAEVKRDARI GEAEARCDAT IKEAIAEEQR MAARFLNDTE IAKAQRDFEL
201 KKAVYDVEVQ TKKAEAEMAY ELQAAKTKQR IKEEQMQIKV IERTQEIAVQ
251 EQEMARRERE LEATIRRPAE AEKYKLEKLA EANRNRVILE AEAEAEAIKV
301 RGEAEAFAIA AKSKAEAEQM AKKAEAWREY REAAMVDMLL DTLPKVAAEV
351 AAPLSQAKKI TMVSSGTGEV GAAKLTGEVL QIVNKIPDLV KSITGVDISR
401 SVHAG
```

D

Accession no.	Mascot score	Top ranking match	Predicted PI	Observed mass (kDa)	Predicted mass (kDa)	pValue	% Seq. coverage	Species
157131242	138	flotillin-1	5.82	45	44.8	1.7e-07	50	*A. aegypti*

Figure 3.4: Development of antisera and immunodetection of flotillin-1 protein in *Aedes* BBMV and heterologously expressed *E. coli*. (A) SDS-PAGE and Western blot analysis of the expression of the flotillin-1 peptide used for antisera production. Lane 1: coomassie stained flotillin-1 & lane 2: western blot of flotillin-1. (B) Immuno detection of the flotillin-1 of *A. aegypti* in BBMV. Lane 3; coomassie stained BBMV, lane 4.western blot profile of flotillin-1 in BBMV and lane 5, pre-immune as a control (10 µg or 2 µg) proteins were separated by SDS-12%PAGE, electro transferred overnight on to PVDF membrane with constant 22v &4 °C, which were then identified by subsequent incubation with α-flotillin and. horseradish peroxidase-conjugated secondary antibody and the signal was detected by ECL.

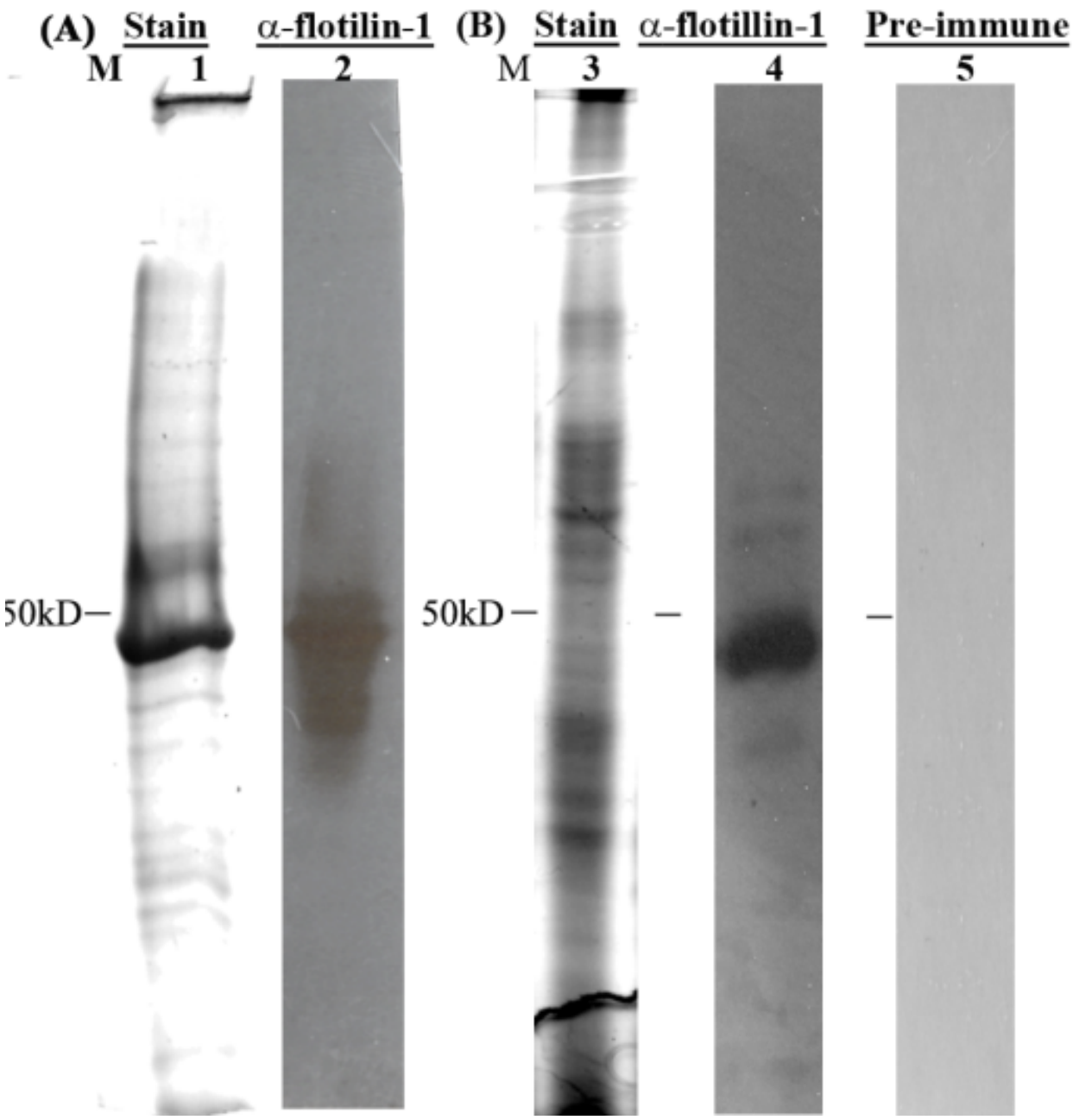
(A) Stain
α-flotilin-1
M
1
2
50kD
(B) Stain
α-flotillin-1
Pre-immune
M
3
4
5
50kD

Figure 3.5: Flotillin-1 is localized predominantly in the apical microvilli of posterior midgut and gastric caeca as detected by immunohistochemical analysis of longitudinal sections of the larval midgut of *A. aegypti*. (AMG, anterior midgut; PMG, posterior midgut; Amv, apical tip of microvilli; BL, basal lamina; BMv, base of microvilli; Nu, nucleus; GC, gastric ceca). Paraffin sections of early 4th instar mosquito larvae were probed with a polyclonal antibody specific to the Aedes flotillin-1. Fig. A: Longitudinal flotillin immuno-sections of the whole larvae, Fig B., pre-immune, C., secondary only, D., α- flotillin-1 staining in gastric caeca, and E., α- flotillin-1 staining in PMG @40X magnification. The scale bar represents 25 μm (A) 100 μm (B-E).

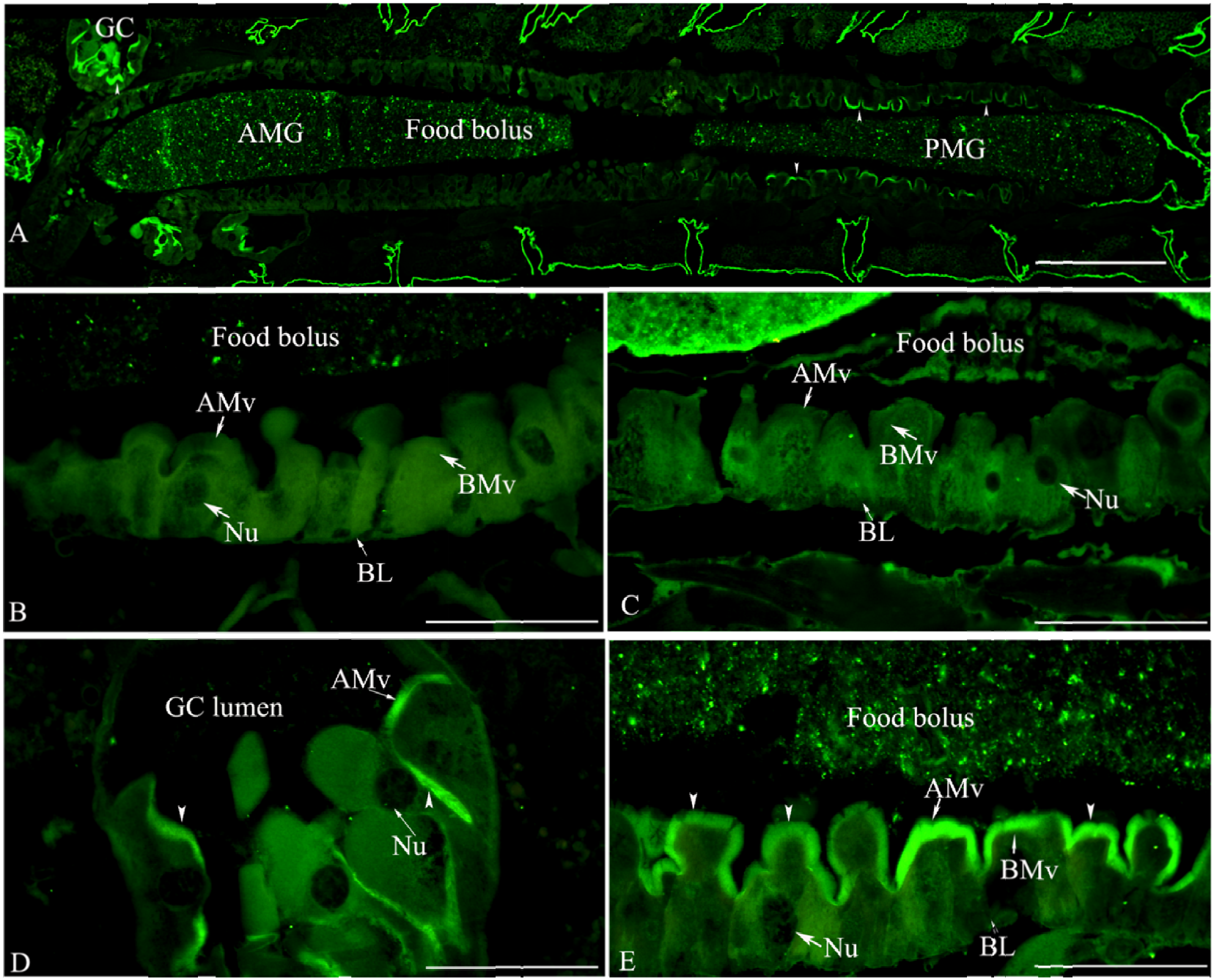
GC
AMG
Food bolus
PMG
A
Food bolus
AMv
BMv
Nu
BL
B
Food bolus
AMv
BMv
Nu
BL
C
AMv
GC lumen
Nu
D
Food bolus
AMv
BMv
Nu
BL
E

Figure 3.6: Detection of Flotillin-1 from other insect BBMV by western blot analysis using AeFlot-1 antibody. Larval BBMV (10 µg). proteins were separated by SDS-12%PAGE, electro transferred overnight on to PVDF membrane with constant 22v & 4 °C, which were then identified by subsequent incubation with a-flotillin-1 and. horseradish peroxidase-conjugated secondary antibody and the signal was detected by ECL. Lane 1: *A. aegypti, 2: Culex quinquefasciatus, 3: Heliothis virescens, 4: Helicoverpa zea, 5: Spodoptera frugiperda, 6: Ostrinia nubilalis, 8: Alphitobius diaperinus*

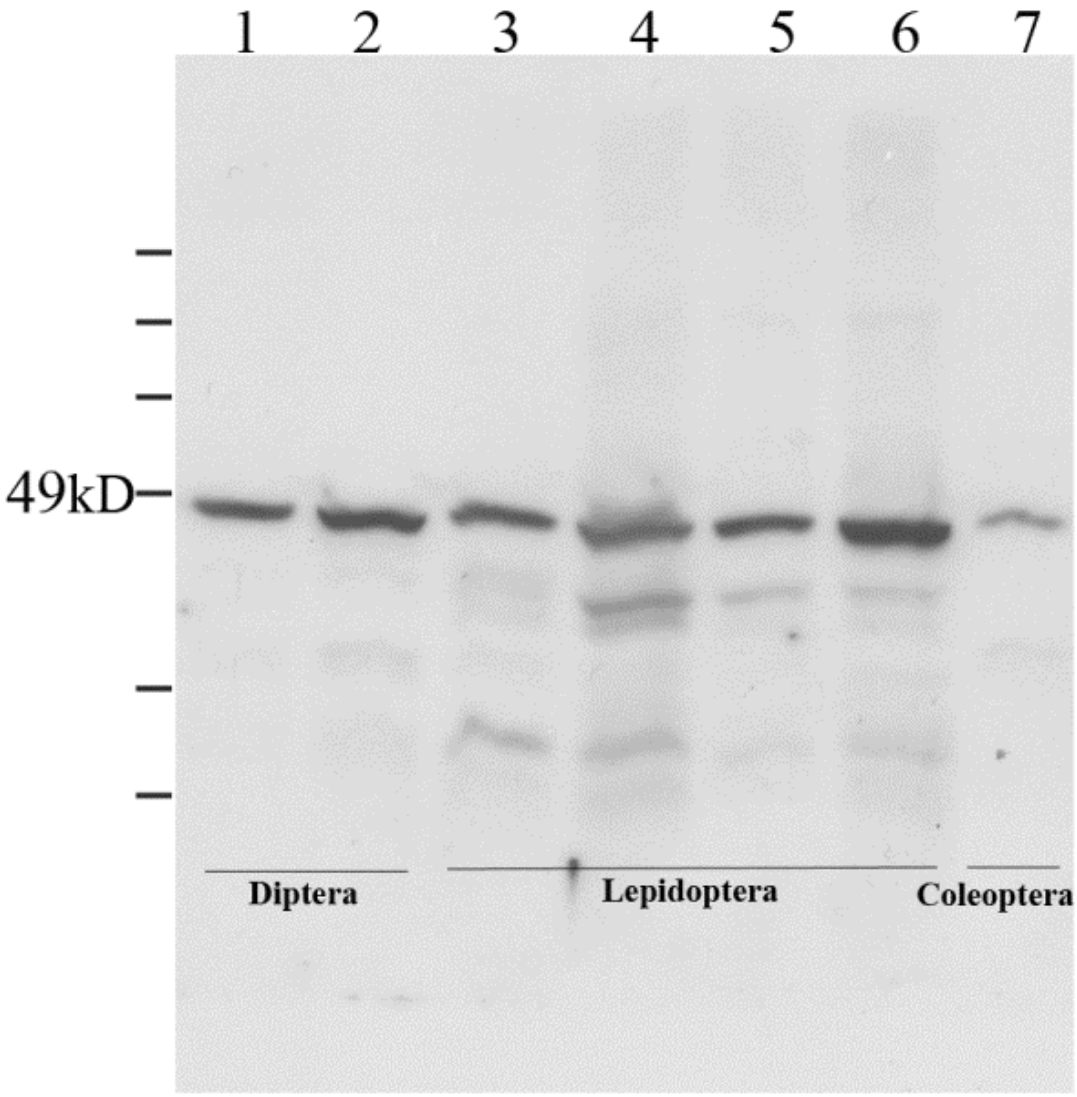
1
2
3
4
5
6
7
49kD
Diptera
Lepidoptera
Coleoptera

Figure 3. 7: Analysis of *Aedes* DRMs by SDS-PAGE and immunoblot reveals enrichment in DRM marker proteins. (A). Representative image of gradient tube after ultracentrifugation, an opaque band could clearly be seen at an Optiprep density between 5 and 30% Optiprep. (B) Silver stained protein profile of DRM, DSM and BBMV. (C). Immunoblot analysis with Aedes flotillin-1 antibody and (D). Aminopetidase antibody. Lipid rafts from *Aedes* BBMV were prepared based on their detergent insolubility and low density. After Triton X-100 solubilization for 30 min on ice, the mixture was brought to the final concentration of 40% Optiprep (Sigma) and then over laid with 30% and 5% Optiprep in TNE buffer. The samples were centrifuged at 39,000 rpm in a SW41Ti (Beckman) rotor for 4 h at 4 °C. After step density gradient ultracentrifugation, a pipette man was used to fractionate the Optiprep® gradients from the top to the bottom with 12 fractions and analyzed by Western blot. Equal volume of gradient fractions or 10 μg of larval BBMV were separated by SDS-10%PAGE, electro transferred overnight on to PVDF membrane with constant 22v, which were then identified by subsequent incubation with *Aedes* anti-flotillin-1 or AgAPN2 and. horseradish peroxidase-conjugated secondary antibody and the signal was detected by ECL

A
40% Optiprep
30% Optiprep
5% Optiprep
DRM
B
BBMV
DRM
DSM
kD
250
100
75
50
37
C
BBMV
DRM
DSM
D
BBMV
DRM
DSM

CHAPTER 4

PROTEOME ANALYSIS OF THE CRY 4BA TOXIN INTERACTING *AEDES AEGYPTI* LIPID RAFTS USING geLC-MS/MS

Bayyareddy K, Zhu X, Orlando R,and Adang MJ
To be submitted to Molecular & Cellular Proteomics

Abstract

Lipid rafts are microdomains in the plasma membrane of eukaryotic cells. Among their many functions, lipid rafts are involved in cell toxicity caused by pore forming bacterial toxins including *Bacillus thuringiensis* (Bt) Cry toxins. We isolated lipid rafts from brush border membrane vesicles (BBMV) of *Aedes aegypti* larvae as a detergent resistant membrane (DRM) fraction on density gradients. Cholesterol, aminopeptidase, alkaline phosphatase and the raft marker flotillin were preferentially partitioned into the lipid raft fraction. When mosquitocidal Cry4Ba toxin was pre-incubated with BBMV, Cry4Ba localized to lipid rafts. A proteomic approach based on in-gel trypsin digestion followed by liquid chromatography-mass spectrometry (geLC-MS/MS) identified a total of 312 proteins. Of which many are typical lipid raft marker proteins including flotillins and glycosylphosphatidylinositol (GPI)-anchored proteins. Identified raft proteins were annotated *in silico* for functional and physicochemical characteristics. Parameters such as distribution of isoelectric point, molecular mass, and predicted post-translational modifications relevant to lipid raft proteins (GPI anchorage and myristoylation or palmitoylation) were analyzed for identified proteins in the DRM fraction. From a functional point of view, this study identified proteins implicated in Cry toxin interactions as well as membrane-associated proteins expressed in the mosquito midgut that have potential relevance to mosquito biology and vector management.

Keywords: Lipid rafts, Detergent resistant membranes, Brush border membrane vesicles, Cry4Ba toxin, Cholesterol, Proteomics, LC-MS/MS

4.1 Introduction

Lipid rafts are membrane micro-domains enriched in glycosylphosphatidylinositol (GPI)-anchored proteins, glycosphingolipids and sterols, and are defined by their insolubility in Triton X-100 at low temperature (Rietveld, Neutz et al. 1999; Lingwood and Simons 2010). Lipid rafts have been implicated physiologically important cell membrane related processes including organizing and segregating membrane components for signaling, trafficking of plasma membrane proteins (Schroeder, Ahmed et al. 1998), and portals of entry for various pathogens, including viruses, bacteria and their toxins (Fantini, Garmy et al. 2002).

Bacterial pore forming toxins interact with host membrane receptors located in lipid rafts and this is a critical step in the oligomerization and insertion of these toxins into the membrane (Cabiaux, Wolff et al. 1997). In some mammalian pore-forming bacterial toxins, lipid rafts play an essential role in toxin interaction by functioning as platforms to recruit distinct classes of proteins, such as GPI-anchored proteins and palmitoylated or diacylated transmembrane proteins (Galbiati, Razani et al. 2001). Moreover, aerolysin, one of the most studied pore-forming toxins, functions via a GPI-anchored proteins present in lipid rafts (Abrami, Fivaz et al. 1998). In insects, investigations regarding the presence of such microdomains and their interaction with insecticidal pore forming toxins are limited to a small number of recent studies. The presence and proper integrity of lipid rafts has been proposed as a prerequisite for Cry1A pore formation and toxicity, and also Cry1A receptor APN is localized to lipid raft domains of the plasma membrane in epithelial cells of *Heliothis virescens* and *Manduca sexta* larval midgut (Zhuang, Oltean et al. 2002). Bravo et al., reported cadherin and Cry1Ab oligomeric toxin complex binds to APN which drives the toxin into lipid raft microdomains causing pore formation (Bravo, Gómez et al. 2004). Similarly, Cry1Ca was toxic to Sf9 cells after binding to lipid rafts, and

without lipid rafts Sf9 cells showed resistance to Cry1Ca toxicity (Avisar, Segal et al. 2005). Toxin-mediated pores in the brush border membrane lead to osmotic cell shock, and finally cell death. Bt Cry protein mode-of-action and the usage of Bt were recently reviewed (Bravo, Likitvivatanavong et al. 2011).

The yellow fever mosquito, *Aedes aegypti* is the major vector of dengue, yellow fever, and chikungunya viruses and represents a significant public health problem (Chadee, Kittayapong et al. 2007). The most commonly used biolarvicide to control this vector is based on *Bacillus thuringiensis var. israelensis* (Bti). Bti harbors a megaplasmid which encodes multiple toxins: Cry4Aa, Cry4Ba, Cry10Aa, Cry11Aa, Cyt1Aa and Cyt2Ba (Berry, O'Neil et al. 2002). Among these toxins Cry4Ba is more toxic to *A. aegypti* relative to the other individual toxins (Poncet, Delécluse et al. 1995). Cry4Ba and Cry11Aa toxins of Bti bind to specific receptor proteins on *Aedes* larval midgut cell surfaces and receptor binding has been shown to correlate with larval toxicity. These receptors (Likitvivatanavong, Chen et al. 2011) are cadherin (Chen, Aimanova et al. 2009), GPI- anchored ALPs (Fernandez, Aimanova et al. 2006; Dechklar, Tiewsiri et al. 2011) and GPI-anchored APNs (Chen, Aimanova et al. 2009; Saengwiman, Aroonkesorn et al. 2011).

There is substantial experimental evidence for the existence of lipid rafts in biological membranes. In the literature lipid rafts have been frequently termed detergent-resistant membranes on the basis of detergent insolubility (Brown 2006). Incomplete solubilization of plasma membranes with detergents results in DRMs and these will exist only after detergent extraction. Lipid rafts are special functional microdomains of membrane *in vivo* containing high sphingolipids and cholesterol in addition to enriched lipid modified proteins and these are

resistant to cold detergents solubilization (Lichtenberg, Goñi et al. 2005). At present, the terms 'lipid rafts' and 'DRMs' are often used as synonyms, despite their differences.

The composition and distribution of lipid raft component lipids and proteins are heterogeneous in mammalian and insect counter parts. In insects, a few attempts have been made to describe lipid composition of detergent resistant membranes but to our knowledge there is no information available on protein composition of insect lipid rafts. Mass spectrometry-based proteomic identification can result in unique protein profiles of the lipid raft microenvironment and insight into their functional processes of pathogen interactions. In non-insect systems several groups reported the protein composition of lipid rafts derived from brush border membranes (Paradela, Bravo et al. 2005; Nguyen, Amine et al. 2006; Gylfason, Knutsdottir et al. 2010). These studies have indicated typical plasma membrane proteins such as GPI-ALPs, APNs, and other receptor proteins. In addition, signaling/trafficking proteins belonging to the G protein family, protein kinases and the annexins were also identified. The above cited studies have also shown that the global proteome composition of raft microdomains is quite different from that of the whole brush border membrane. To investigate insect rafts in that direction, an inventory of the proteins associated to these domains seems essential.

Here, we report a series of experiments to provide evidence for typical lipid raft characteristics in addition to demonstrating the interaction of Cry4Ba toxin with lipid rafts isolated from *A. aegypti* midgut membranes. We also report the comprehensive proteome of rafts from mosquito larval BBMV. Moreover, we focused our investigations on geLC-MS/MS analysis of lipid raft proteome, to our knowledge; this is the first reported proteomic study from insects. The tandem mass spectrometry methodology we employed here is capable of identification of a substantial number of high molecular weight, low abundance and also

membrane bound proteins. These proteins are difficult to resolve and identify using classical two dimensional gel electrophoresis based proteomics.

4.2 Materials and methods

4.2.1 Preparation of *A. aegypti* whole larval BBMV

A. aegypti (UGAL strain) was maintained as described (Bayyareddy, Andacht et al. 2009). Four grams early fourth instar larvae (stored -80°C) were suspended in 16 ml ice cold MET buffer (300 mM mannitol, 5 mM EGTA, 17 mM Tris-HCl, pH 7.5) containing 1 mM PMSF. Larvae were homogenized with 40 strokes of a teflon-glass homogenizer (clearance 0.1-0.15 mm; Wheaton) while rotating the pestle at 1525 rpm (GCA Precision Scientific). BBMV were prepared from the larval homogenate using the magnesium chloride precipitation method (Silva-Filha, Nielsen-Leroux et al. 1997) with modifications (Bayyareddy, Andacht et al. 2009). The final BBMV pellet was suspended in 1 ml cold MET with Complete™ protease inhibitor cocktail (Roche Applied Science). Total protein concentrations were determined using a Bio-Rad protein assay kit (Bio-Rad) with bovine serum albumin as a protein standard (Sigma). The relative purity of the final BBMV preparation was assessed by comparing APN and ALP activities relative to the initial homogenate. APN and ALP activities of BBMV and extracted BBMV fractions (below) were determined using leucine-*ρ*-nitroanalide and *ρ*-nitrophenyl phosphate as substrates, respectively (Terra and Ferreira 1994).

4.2.2 Extraction of a detergent resistant membrane fraction from *A.aegypti* larval BBMV and isolation on Optiprep™ density gradients

Detergent resistant membrane fractions (DRM) were prepared from larval BBMV using cold Triton X-100 extraction and Optiprep™ (Sigma) gradients (Chmelar and Nathanson 2006). BBMV (1mg) were re-suspended in 0.5 ml TNE buffer (25 mM Tris-HCl (pH 8.0), 150 mM NaCl, 5 mM EDTA), 0.5 ml ice-cold 2% Triton X-100 in TNE buffer was added, the mixture was gently suspended and placed on ice for 30 min. Extracted membrane solution was pipetted into a centrifuge tube and brought to 40% Optiprep™ by the addition of 2 ml 60% Optiprep™ in TNE buffer and then overlaid with 6 ml of 30% and 3 ml of 5% Optiprep™. Gradient were centrifuged 39,000 rpm (270, 519g) in a SW41Ti (Beckman) rotor for 4 h at 4°C. After centrifugation, the opalescent DRM band was located at the interface between the 30% and 5% Optiprep™ gradients. Gradients fractions were collected from 12 one ml fractions starting from the top of the gradient.

4.2.3 Cholesterol quantitation and depletion from BBMV by methyl-β-cyclodextrin (MBCD)

Concentrations of cholesterol and cholesterol esters from the gradient fractions were determined in 96-well flat-well plates by Amplex® Red cholesterol assay kit (Invitrogen) according to the manufacturer's instruction. Briefly, 5 µl of each gradient fraction was mixed with 45 µl of 1x reaction buffer. A standard curve was made with cholesterol concentrations ranging from 1.25 µM to 12 µM with buffer as a negative control and 10 µM H_2O_2 as a positive control. Reactions were initiated by adding 50 µl Amplex® Red reagent/HRP/cholesterol oxidase/cholesterol esterase working solution to each well. Microplates were incubated for 30

min at 37°C in the dark. Reaction fluorescence was measured in BioTek Synergy 4 plate reader at an excitation wavelength of 550 nm and an emission wavelength of 590 nm over 30 min (5 min time points). Background fluorescence from the negative control reaction was subtracted from each value and determined unknown samples cholesterol concentration by comparing with a standard curve. For cholesterol depletion experiments, BBMV were treated with 20 mM MBCD (Sigma) at 37°C for 60 min prior to detergent extraction and Optiprep™ fractionation.

4.2.4 Analysis Cry4Ba toxin association with DRM extracted from BBMV

Cry4Ba association with DRM extracted from BBMV was analyzed as for Cry1Ab toxin-DRM interactions (8, 9). Trypsin-activated Cry4Ba toxin was prepared from *E. coli*-produced inclusions (Abdullah, Alzate et al. 2003). BBMV (1mg) were incubated with 5 µg/ml Cry4Ba toxin in TNE buffer at 4°C overnight, subsequently the suspension was centrifuged 13,000 rpm for 20 min and the pellet washed with TNE buffer twice. The washed BBMV pellet was treated with cold Triton X-100 and separated in Optiprep™ gradients as above. The effect of MBCD treatment on Cry4Ba association with DRM was examined by pre-incubating BBMV with 5 µg/ml of Cry4Ba toxin followed by MBCD treatment and DRM isolation. Equal volumes of gradient fractions were separated by SDS-10% PAGE, electro- transferred overnight on to polyvinylidene difluoride (PVDF) membrane, which were then identified by western blot analysis with anti-Cry4Ba serum as described below.

4.2.5 SDS-PAGE and Western Blotting

Equal sample volumes from the resulting gradient fractions were solubilized in 2x Laemmli buffer (Laemmli 1970) and resolved on SDS-10% PAGE. Separated proteins were visualized either by silver staining, Deep Purple (GE Healthcare), or immunodetection on

western blots as follows. Proteins were transferred by electro-blotting onto a PVDF membrane (overnight, 22v and 4°C; Criterion blotter (Bio-Rad) in transfer buffer (25 mM Tris, 192 mM glycine, 10% methanol). The membranes were blocked by incubating in PBST (137 mM NaCl, 2.7 mM KCl, 4.3 mM Na_2HPO4, 1.4 mM KH_2PO_4, 0.1% Tween 20) containing 3% BSA, followed by incubation with primary antibody diluted in PBST containing 1% BSA for 1 h. After washing the membranes for 3x 10 min, and then incubated in a PBST (1%BSA) containing secondary antibody conjugated to horseradish peroxidase (Molecular Probes). Finally, membranes were washed 3 times for 10 min in PBST and then incubated for 5 min with ECL™ detection reagent (GE Healthcare) and exposed to X-ray film to detect immunoreactive bands. All the incubations were at room temperature.

4.2.6 Preparation of in-gel protein digests

Purified *A. aegypti* lipid raft proteins (20 µg) were resolved by SDS-10% PAGE and the gels stained with Deep Purple™ total protein stain according to the manufacturer's instructions (GE Healthcare). An individual gel lane was sliced into 20 pieces manually, and each piece was then subjected to dithiothreitol reduction, iodoacetamide alkylation, and in-gel trypsin digestion, using a standard protocol as previously reported (Bayyareddy, Andacht et al. 2009). The resulting tryptic peptides were extracted and concentrated to 20 µl each using a SpeedVac (Thermo Savant), and subjected to LC–MS /MS analysis.

4.2.7 LC-MS/MS analysis

Proteolyzed peptide samples were separated and analyzed on an Agilent 1100 capillary LC interfaced directly to a LTQ linear ion trap mass spectrometer (Thermo Electron). Mobile phases A and B were H_2O-0.1% formic acid and acetonitrile-0.1% formic acid, respectively.

Peptides were eluted from the C18 column into the mass spectrometer via a 80 min linear gradient from 5 to 55% mobile phase B at a flow rate of 4 µl/min. The instrument was set to acquire MS/MS spectra on the nine most abundant precursor ions from each MS scan with a repeat count of 2 and repeat duration of 30 s. Dynamic exclusion was enabled for 90 s. Generated raw tandem mass spectra were converted into the mzXML format and then into peak lists using ReAdW software followed by mzMXL2Other software (Pedrioli, Eng et al. 2004). The peak lists were then searched using Mascot 2.2 (Matrix Science).

4.2.8 Database searching, protein identification and GPI-anchorage prediction

A target database was created using the Diptera annotated sequences obtained from *Drosophila melanogaster*, *Anopheles gambiae*, *A. aegypti* and *Culex quinquefasciatus* protein databases in Flybase (www.flybase.org) and Vectorbase (www.vectorbase.org). A decoy database (decoy) was then constructed by reversing the sequences in the normal database. Using these databases we excluded redundancies and contaminations in the search results. Searches were performed against the normal and decoy databases using the following parameters: fully tryptic enzymatic cleavage with two possible missed cleavages, peptide tolerance of 1000 ppm, fragment ion tolerance of 0.6 Da. Fixed modification was set as carbamidomethyl due to carboxyamidomethylation of cysteine residues (+57 Da) and variable modifications were chosen as oxidation of methionine residues (+16 Da) and deamidation of asparagine residues (+1 Da). Statistically significant proteins from both searches were determined at a ≤1% protein false discovery rate (FDR) using the ProValT algorithm, as implemented in ProteoIQ (BioInquire). After sequences were identified they were annotated for possible function using QuickGO (http://www.ebi.ac.uk/QuickGO/Dataset.html). The big-PI predictor server (http://mendel.imp.ac.at/sat/gpi/gpi_server.html), GPI-SOM (http://gpi.unibe.ch/), and PredGPI

(http://gpcr.biocomp.unibo.it/predgpi/pred.htm) were used to predict GPI anchorage of proteins. The computational tool CSS-Palm 3.0 (http://csspalm.biocuckoo.org/online3.php) was used to predict palmitoylation sites on proteins.

4.3 Results

4.3.1 Cholesterol, flotillin, and the GPI-anchored proteins ALP and APN are concentrated in lipid rafts isolated from *Aedes* larval brush border membrane

Lipid rafts are defined by their insolubility in cold Triton X-100 and their density which helps them to float on gradient solution. We used Optiprep™ gradient fractionation of 1% Triton X-100 solubilized BBMV. The lipid raft fraction was visible as an opalescent band at the 5%-30% interface (data not shown). Since cholesterol is typically enriched in DRM fractions (i.e. lipid rafts), we measured cholesterol content in the 12 collected gradient fractions. As shown in Fig. 4.1A, cholesterol content was highest in fraction 4 at the 5%-30% Optiprep™ interface. Fraction 4 contained about 50% of the total cholesterol present in all 12 fractions. In contrast, the majority (>50%) of the total protein was distributed in fractions 10-12 from the 40% Optiprep™ region; about 25% of total protein was in the DRM fraction 4. The enrichment of cholesterol versus total protein in the opalescent DRM fraction is consistent with a successful Optiprep™ gradient fractionation procedure for the isolation of *A.aegypti* lipid rafts.

Since GPI-anchored proteins are localized in DRM preparations, we measured the activities of ALP and APN across the Optiprep™ gradient. The enzymatic activities of ALP and APN were the highest in DRM fraction 4 with substantial APN activity spread across soluble fractions 4-9 (Fig. 4.1B). ALP activity was low in fractions 4-9 collected from the 30% Optiprep™ region but increased in the fractions 10-12 from the 40% Optiprep™ region. The

result of probing a western blot of Optiprep™ fractions with anti-AgAPN1 antiserum is shown in Fig. 4.2C. The distribution of APN protein was in agreement with the activity data. The strongest signal for APN was in DRM fraction 4, yet an APN signal was detectable in 30% Optiprep™ fractions 4-9. We probed blots of the Optiprep™ fractions with anti-AeFlot-1 antibody to determine the distribution of flotillin in the gradient. As shown in Fig. 4.2B, the flotillin amount was greatest in the DRM fraction 4, with lesser amounts in fractions 5-9, there little flotillin detected in the soluble protein fractions 10-12. The highest concentration of flottilin, cholesterol, APN and ALP were each located in fraction 4, providing further support that fraction 4 from the Optiprep™ gradients is the lipid raft fraction.

4.3.2 Cry4Ba toxin is associated with the *A. aegytpi* lipid rafts

Cry4Ba binds APNs and ALPs in *Aedes* midgut (Bayyareddy, Andacht et al. 2009; Likitvivatanavong, Chen et al. 2011), therefore we hypothesized that membrane-bound Cry4Ba would localize in the DRM fraction of *Aedes* brush border membranes. To test this hypothesis, BBMV were pre-incubated with Cry4Ba toxin. After unbound toxin was removed by washing BBMV and cold Triton X-100 extraction, soluble and insoluble materials were separated by flotation on Optiprep™ step gradients and the distribution of Cry4Ba toxin was analyzed by probing blots with anti-Cry4Ba antibody. As seen in Fig. 4.2D, most of the toxin was in the DRM fraction 4 with some toxin in soluble fractions 10-12. The association of Cry4Ba with *A. aegypti* the DRM fraction suggests that raft microdomains play a key role in membrane insertion and pore formation.

4.3.3 Effect of MBCD on *A.aegypti* lipid rafts cholesterol and protein distribution

MBCD extracts cholesterol from lipid rafts causing a loss of integrity when raft integrity depends on cholesterol (Schuck, Honsho et al. 2003). To test the effect of cholesterol depletion by MBCD on *Aedes* larval lipid rafts, BBMV were pre-incubated with MBCD, extracted with cold Triton-X100 and the extract separated by Optiprep™ gradient fractionation. Surprisingly, a fraction of the *Aedes* membrane was resistant to Triton X-100 and floated at the interface between 5% and 30% Optiprep™. Fraction 4, the floating fraction, showed the highest cholesterol and total protein content (Fig. 4.3A). Less than 10% of total protein was in the high-density soluble fractions. Following the MBCD treatment, the amounts of cholesterol and protein in raft fractions 4 and 5 were slightly higher than untreated BBMV (Fig. 4.3A). Thus, incubation of BBMV with MBCD under conditions that induce cholesterol depletion did not disrupt the DRM lipid raft fraction

We also tested APN and ALP enzyme activities in the MBCD pre-treated gradient fractions and the results differed for the two enzymes. While APN activity was concentrated in the DRM fraction, ALP activity could no longer be detected in any gradient fractions (Fig. 4.3B). The ALP activity results suggesting that under MBCD incubation conditions either ALP degrades or MBCD might interfere with substrate reaction.

Further evidence for the resistance of the DRM fraction to MBCD is presented in Fig. 4.3C showing where anti-AeFlot1 antibody detected a 47-kDa protein in fraction 4. Additionally, BMCD treatment did not affect localization of Cry4Ba to the DRM fraction (Fig. 4.3D).

In summary, the distribution pattern of cholesterol and marker protein activity assays and the western blots of flotillin-1, APN-1, and Cry4Ba, clearly evidenced co-partitioning of both Cry4Ba toxin and lipid raft marker proteins in the DRM lipid raft fractions. When MBCD was

used on BBMV, DRM association of cholesterol, marker proteins and Cry4Ba were essentially unaffected. Furthermore, the data suggested a preferential association of Cry4Ba with lipid rafts in *A.aegypti*.

4.3.4 Proteomics analysis of lipid rafts isolated from *A. aegypti* BBMV

The member proteins of the DRM fraction were identified as diagrammed in Fig. 4.4. The opalescent band at the 5%-30% Optiprep™ interface was collected and the proteins separated by SDS-PAGE. After staining the gel, twenty equal gel bands were excised from and subjected to trypsin in-gel digestion. The resulting peptides in each gel band were separated and analyzed by LC-MS/MS. The peptide sequences deduced from MS were matched to *A. aegypti* proteins using the Mascot search engine against either the *A. aegypti* database alone, or the combined Diptera databases. For Mascot search results obtained against Diptera database, if two or more potential matches were reported for one mass spectrum, only peptide hits with the highest matching score (i.e., No.1 ranking) for the corresponding spectra were selected.

Our analysis revealed 1513 unique peptides representing 312 proteins in the DRM samples which passed a <1% false discovery rate (Table 4.1). Of the 312 proteins, 250 proteins were identified with two or more unique peptide sequences and 36 additional hits were matched to conserved hypothetical proteins not assigned to any known protein in the constructed Diptera database. For these uncharacterized proteins, no homolog that satisfied BLAST criteria was found when their sequence was searched against NCBInr database. Using stringent statistical analysis via ProteoIQ, 62 proteins identified with a single peptide were accepted if the peptide occurred multiple times in the data set.

The distribution of predicted isolectric points (pI) and molecular masses of identified DRM proteins (Table 4.1) are presented in Fig. 4.5. The pI of the proteins identified range from 3.9 to 12.2 with a peak of proteins (about 39%) in the acidic pH 4-6 range; 2D gels of *Aedes* larval BBMV proteins have a similar concentration of proteins in the acidic range (Bayyareddy, Andacht et al. 2009). Of the total DRM proteins 52% have predicted pI values less than 7 and 48% greater than 7 (Fig. 4.5A). The molecular masses of the identified proteins ranged between 8 and 300 kDa with a majority of proteins (70%) exhibiting a molecular mass <120 kDa (Fig. 4.5B). Some of the identified proteins, such as apolipophorin II, are probably pro-proteins and do not represent final size of proteins expected to be present in the DRMs.

The identified proteins listed in Table 4.1 were also classified on the basis of their subcellular localization, molecular function and biological process as predicted from their gene ontology (GO) term descriptions provided in FlyBase and UniProtKB database. Apart from this, for each identified protein GO terms were compared with results from other studies. Functional classification of the all uniquely identified proteins is shown in Figure 4.6. Of the 275 proteins identified with protein names, 246 had descriptions for their molecular function and these were summarized into 13 GO categories. These proteins are involved in: binding, (47 proteins); translation elongation (43 proteins); peptidase activity (40 proteins); cellular metabolic processes (34 proteins); cell transport (34 proteins); proteins with Unknown GO terms (30 proteins); hydrolase activity (11 proteins); transferase activity (8 proteins); cell signaling (7 proteins); phosphatase activity (7 proteins); isomerase activity (5 proteins); Receptors or surface glycoproteins functions (5 proteins), and oxidoreductase activity (4 proteins); see Fig. 4.6B for assignments for individual proteins.

When we analyzed the identified 275 proteins for subcellular locations, 55 proteins did not have descriptions for GO terms. A large proportion of the identified proteins are known or were predicted to be associated with plasma membranes, with 28% described as membrane-bound, 3% integral to membrane, and 2% are associated extracellular. For the remainder of the proteins, 16% are localized in cytoplasm, 15% in lipid particles, and 9% are associated with mitochondria. Proteins involved in the cytoskeleton accounted for 7%; 20% of the identified proteins did not have GO terms defined (Fig. 4.6A).

The results of GO analysis for the 275 annotated proteins identified into known biological processes are shown in Fig. 4.6C. The most numerously identified proteins belong to the following categories: Metabolism and biogenesis (37%), biological regulation (29%), iontransport (9%), Immune system process (8%), Cytoskeletal component organization (6%) and cell biological process unknown (12%).

4.4 Discussion

The brush border membrane of *Aedes* larvae has a lateral organization that includes a DRM fraction containing lipid rafts. The DRM fraction was prepared from *Aedes* larval BBMV using cold Triton X-100 extraction and Optiprep™ gradient fractionation. The DRM fraction was enriched in cholesterol, and alkaline phosphatase and aminopeptidase activities (Fig. 4.1). Western blot analysis identified AeFlot-1 and APN1 in the DRM fraction (Fig. 4.2B and 4.2C). These results and the proteomic analyses of the DRMs identified GPI-anchored proteins and other lipid-raft associated proteins, a result in agreement with studies conducted on vertebrate systems (Brown and Rose 1992; Danielsen 1995; Nguyen, Amine et al. 2006; Gylfason, Knutsdottir et al. 2010).

4.4.1 Cry4Ba toxin association with *A.aegypti* lipid rafts.

The presence of lipid rafts in the DRM fraction provided an approach to bridge the model that Cry1 toxins insert into lipid rafts (Zhuang, Oltean et al. 2002; Bravo, Gómez et al. 2004; Avisar, Segal et al. 2005) to mosquitocidal Cry toxins. The detection of membrane-bound Cry4Ba toxin in the DRM fraction (Fig. 4.2D) is in concordance with the Cry1 insertion model and in agreement with the presence of Cry4Ba receptors APN (Saengwiman, Aroonkesorn et al. 2011) and ALP (Dechklar, Tiewsiri et al. 2011) in the raft fraction (Fig. 4.2C, 4.1B and Table 4.1). Possibly the small amount of bound Cry4Ba in the soluble membrane fraction (Fig. 4.2D) may be attributed to non-specific Cry4Ba binding to BBMV or binding to receptors that are not raft-associated. The integration of Cry4Ba into the lipid raft component of the DRMs supports the model that lipid rafts have a functional role in the Cry intoxication process in mosquito larvae, as they do for Cry toxin action in lepidopteran larvae.

4.4.2 Effect of MBCD on Cry 4Ba and receptors distribution.

The integrity of DRM fractions in plasma membranes typically depends on cholesterol and sphingolipids (Simons and Ikonen 1997; Brown and London 1998). Consequently, extraction of cholesterol with MBCD often disrupts the DRM and releases associated proteins into the soluble phase of a sucrose or Optiprep™ gradient (Kamata, Manno et al. 2008; Crepaldi Domingues, Ciana et al. 2009). We tested the influence of MBCD on the brush border DRM fraction by treating BBMV with MBCD prior to Triton X-100 extraction and Optiprep ™gradient fractionation. After MBCD treatment, we observed no obvious physical change in the opalescent DRM band and detected no changes in cholesterol, APN or flotillin and no loss of the ability of Cry4Ba to partition into the DRM fraction (Fig. 4.3). What may account for the

stability of the *Aedes* DRM fraction after extraction of BBMV with MBCD? It is possible that the low concentration of cholesterol in mosquito midgut membrane may limit the ability of MBCD to effectively bind and extract cholesterol. MBCD depletion of cholesterol from membranes is limited or slower in membranes with low cholesterol content (Jouni, Zamora et al. 2002; Besenicar, Bavdek et al. 2008) and high sphingomyelin content (Sano, Kobayashi et al. 2007). It is also possible that while MBCD selectively extracts cholesterol, *A .aegypti* larvae may have other sterols or membrane components involved in maintaining raft integrity resulting in a cholesterol-independent DRM fraction. For example, similar to mammalian brush rafts membranes insect brush border membranes contain glycosphingolipids (Rietveld, Neutz et al. 1999) and galectin (Table 4.1). In mammalian brush border membranes, galectin stabilizes lipid rafts by cross-linking glycosophingolids resulting in cholesterol-independent rafts (Hansen, Immerdal et al. 2001; Braccia, Villani et al. 2003). With respect to Cry4Ba partitioning into DRMs after MBCD treatment of BBMV (Fig. 4.3D), this is consistent with MBCD-resistance of the DRMs. Additionally, previous studies with other pore forming toxins in mammalian cells indicated that the MBCD had no effect on toxin association and gradient distribution (Shogomori and Futerman 2001; Hansen, Dalskov et al. 2004).

4.4.3 Proteomic profile of the DRM fraction from *Aedes* midgut brush border.

Proteomic analyses of insect midguts have characterized either total BBMV proteomes (Pauchet, Muck et al. 2009; Popova-Butler and Dean 2009) or a proteome subset such as Bt toxin binding proteins (Biron, Agnew et al. 2005; Bayyareddy, Andacht et al. 2009; Tchankouo-Nguetcheu, Khun et al. 2010). Our geLC-MS/MS analysis of the DRM sub-proteome identified lipid raft marker proteins flotillin-1, flotillin-2, APN and ALP and many other proteins reported in similar analyses of DRMs (Foster, de Hoog et al. 2003; Blonder, Hale et al. 2004; Babuke and

Tikkanen 2007; Zhai, Ström et al. 2009; Williamson, Thompson et al. 2010). The 312 identified proteins (275 annotated proteins) are just slightly less in number than the approximately 400 spots seen on a 2D gel of *Aedes* brush border proteins (Bayyareddy, Andacht et al. 2009; Popova-Butler and Dean 2009). Of the 275 annotated proteins (Table 4.1) an expected overlap in identified DRM proteins was observed with the published *Aedes* larval BBMV proteome study (Popova-Butler and Dean 2009). Those authors identified 89 abundant proteins by a combination of 2D gel and LC-MS/MS approaches and of these 22 were identified in our DRM fraction. In addition to identifying about 290 proteins not detected in *Aedes* larval BBMV (Popova-Butler and Dean 2009), our DRM proteomic analysis identified more members of each type of GPI-anchored protein family (6 alkaline phosphatases, 10 m1 class aminopeptidases, and 5 alpha-amylases and 2 carbonic anhydrases) versus the single member identified in the *Aedes* BBMV larval proteome. Flotillins were identified in our DRM fraction and in our proteomics-based search for Cry4Ba binding proteins in *Aedes* BBMV, but not in (Popova-Butler and Dean 2009).

GPI-anchored proteins are targeted to lipid rafts and enriched in DRMs (Brown and Rose 1992; Rietveld, Neutz et al. 1999). Consistent with the localization of GPI-anchored proteins in DRMS, bioinformatic analyses of *Aedes* DRM proteins predicts 59 proteins as having GPI-anchors (Table 4.2). Each of the 4 GPI predictor programs identified a set of proteins including alanyl aminopeptidase, alkaline phosphatase, alpha-amylase, an m1 metalloprotease (APN), and carbonic anhydrase as likely to have a GPI-anchor. APN, ALP and amylase proteins were previously confirmed as GPI-anchored proteins and identified as receptors for Cry toxins in mosquito larvae. For example, aminopeptidase AEL01278 (named AeAPN1) was identified as a putative receptor for Cry11Aa in *Aedes* larvae (Chen, Aimanova et al. 2009). This is the only GPI-anchored APN identified by each of the 4 GPI predictor programs. Two APNs

(AAEL008155; called AeAPN2) and AAEL012774 (AeAPN2) were identified in *Aedes* BBMV as binding Cry11Aa (Likitvivatanavong, Chen et al. 2011). However, according to analyses of the annotated APNs they are not predicted to have GPI anchors (Table 4.2). Incorrect annotation of the APNs in the *Aedes* database is a possible explanation for lack of a predicted GPI anchor. Alternatively, these APNs are attached to brush border membrane via another anchorage system (discussed below). In regards to the glucosidase with predicted GPI anchorage, interestingly, the glucosidase present in DRM is not the GPI-anchored glucosidase which was examined, but refuted, as a receptor to mosquitocidal Bin toxin (Ferreira, Romao et al. 2010). Overall, most of the predicted GPI-anchored proteins present in *Aedes* DRM are glycosidases and hydrolases. Other notable proteins in the DRM fraction with predicted GPI-anchorage include carbonic anhydrase, an enzyme involved in alkalinization of *Aedes* midgut (Seron, Hill et al. 2004). Lachesin, a protein involved in epithelial integrity (Strigini, Cantera et al. 2006) was detected and probably identified correctly as a GPI-anchored protein. An apyrase and apolipoprotein D also had signals for GPI-anchorage recognized by each software program.

4.4.4 Predicted S-acylated proteins in the DRM fraction

Some proteins are targeted and attached to membranes via a post-translationally attached fatty acid. The most common type of attachment is via S-acylation at cysteine residues where the attached moiety is palmitic acid, hence the common name palmitoylation (Salaun, Greaves et al. 2010). Palmitoylated proteins are frequently isolated in DRMs and are considered lipid rafts components (Yang, Di Vizio et al. 2010). Using the computer program CSS-Palm (Ren, Wen et al. 2008), the set of identified DRM proteins was searched for predicted palmitoylation sites yielding a list of 178 proteins (Table 4.3). The caveat with this analysis is that because of a lack of experimental validation it is unclear how well the predictions correlate with actual

palmitoylation. Several cytoskeletal proteins, including actin, myosin and tubulin, were identified as having putative palmitoylation sites and in cultured human cells their homologues are palmitoylated and raft-associated (Yang, Di Vizio et al. 2010). This assemblage of cytoskeletal proteins in the DRM fraction also correlates with the link between lipid rafts, cytoskeletal proteins intracellular structures(Lin, Chien et al. 2010). Several 40s and 60S ribosomal proteins have predicted palmitoylation sites and they also have counterparts in human cells (Yang, Di Vizio et al. 2010). The CSS-Palm program also identified a number of ALPs and APNs as having palmitoylation sites. If APNs are indeed attached to brush border membrane via palmitoylation, it would explain why in insect BBMV preparations only half of the APN activity is released by the phosphatidylinositolspecific phospholipase C which cleaves GPI-anchored proteins (Garczynski and Adang 1995). Overall, there is correlation between proteins having predicted palmitoylation sites and their protein localizatin according to GO annotation.

4.4.5 Proteins not expected to be in lipid rafts that are likely contaminants of the DRM.

The presence of ribosomal, mitochondrial, and endoplasmic reticulum proteins in the DRM fraction is consistent with the DRM literature (Foster, de Hoog et al. 2003; Mannova, Fang et al. 2006; Zhang, Shaw et al. 2008; Williamson, Thompson et al. 2010). As discussed above some of the proteins typically with these organelles may be present in DRMs because they are lipidated (i.e palmitoylated). Another explanation is that these subcellular organelles are entrapped in BBMV during the folding process that occurs during the process of gut homogenization and vesicle purification (Wilfong and Neville 1970; Donowitz, Singh et al. 2007). In the case of mitochondria, they do not have lipid rafts and are considered contaminants in DRM preparations (Zheng, Berg et al. 2009). This conclusion was based on proteomic analyses of DRMs and mitochondria from cultured human cells where F1/F0 ATPase subunits

and other mitochondrial proteins were identified as co-purifying contaminants in DRM/lipid raft preparations (Zheng, Berg et al. 2009).With respect to BBMV(Popova-Butler and Dean 2009) and the DRM fraction analyzed in this study, it is possible that extra purification steps in BBMV and further development of the step gradient technique could yield improved BBMV and DRM fractions. However, it likely that small contamination will always show up in the proteomes of insect BBMV and lipid rafts, since LC-MS/MS is such an ultra-sensitive technique. Therefore, it is very important to re-evaluate the DRM fractions using qualitative immunoblotting and immunolocalization techniques. New techniques based on in vivo labeling and quantitative mass spectrometries are likely to add insights into DRM composition and their included lipid rafts. Based on these observations, the existence of rafts in cell organelles, BBMV preparation, and co-precipitation of cell organelle proteins with lipid rafts deserves serious consideration.

4.5 Conclusion

We believe that our observations, together with the information available for Bt toxins in other insects, also demonstrated the existence of lipid rafts in insects and their interaction with Bt Cry pore forming toxins.

In recent years, our knowledge of the Bt toxin receptors on the membrane surface and their complex interaction has improved significantly. Even though most of the knowledge of Bt toxin receptors and toxin mode of action derived from lepidopteran studies, there are broad differences in the midgut physiology of lepidopterans and dipteran insects. Although many receptors for of the Bt toxin are still unknown, many toxins seem to have an affinity for the same class of proteins on the midgut cells. Proteome composition of lipid rafts, which is an important target site for both mosquito killing and vectored pathogens helps in designing better mosquito control strategies. Several studies have suggested many pathogens interact with lipid rafts.

However, specific interacting proteins have not yet been identified; our study should help in the characterization and also in identifying candidate proteins that control susceptibility to Bt toxins. In this relatively new field, more research is needed to knock down the function of key lipid raft proteins. It will have better clarity on developing effective management strategies directed at vector controlling and also preventing toxin resistance in the mosquitoes**.** Furthermore, it may also serve as an important early step toward limiting the spread and burden of human disease caused by pathogens that are vectored by mosquitoes in general and *A. aegypti* in particular.

Acknowledgements

This research was partially supported by National Institutes of Health Grant R01 AI 29092 to D.H. Dean (Ohio State University) and M.J.A.

References

Abdullah, M. A., O. Alzate, et al. (2003). "Introduction of *Culex* toxicity into *Bacillus thuringiensis* Cry4Ba by protein engineering." Appl. Environ. Microbiol. **69**(9): 5343-5353.

Abrami, L., M. Fivaz, et al. (1998). "The pore-forming toxin proaerolysin is activated by furin." J. Biol. Chem. **273**(49): 32656-32661.

Avisar, D., M. Segal, et al. (2005). "Cell-cycle-dependent resistance to *Bacillus thuringiensis* Cry1C toxin in Sf9 cells." J. Cell Sci. **118**(Pt 14): 3163-3171.

Babuke, T. and R. Tikkanen (2007). "Dissecting the molecular function of reggie/flotillin proteins." Eur. J. Cell Biol. **86**(9): 525-532.

Bayyareddy, K., T. M. Andacht, et al. (2009). "Proteomic identification of *Bacillus thuringiensis* subsp. *israelensis* toxin Cry4Ba binding proteins in midgut membranes from *Aedes* (*Stegomyia*) *aegypti* Linnaeus (Diptera, Culicidae) larvae." Insect Biochem. Mol. Biol. **39**(4): 279-286.

Berry, C., S. O'Neil, et al. (2002). "Complete sequence and organization of pBtoxis, the toxin-coding plasmid of *Bacillus thuringiensis* subsp. *israelensis*." Appl. Environ. Microbiol. **68**(10): 5082-5095.

Besenicar, M. P., A. Bavdek, et al. (2008). "Kinetics of cholesterol extraction from lipid membranes by methyl-beta-cyclodextrin--a surface plasmon resonance approach." Biochim. Biophys. Acta **1778**(1): 175-184.

Biron, D. G., P. Agnew, et al. (2005). "Proteome of *Aedes aegypti* larvae in response to infection by the intracellular parasite *Vavraia culicis*." Int. J. Parasitol. **35**(13): 1385-1397.

Blonder, J., M. L. Hale, et al. (2004). "Proteomic analysis of detergent-resistant membrane rafts." Electrophoresis **25**(9): 1307-1318.

Braccia, A., M. Villani, et al. (2003). "Microvillar membrane microdomains exist at physiological temperature." J. Biol. Chem. **278**(18): 15679-15684.

Bravo, A., I. Gómez, et al. (2004). "Oligomerization triggers binding of a *Bacillus thuringiensis* Cry1Ab pore-forming toxin to aminopeptidase N receptor leading to insertion into membrane microdomains." Biochim. Biophys. Acta **1667**(1): 38-46.

Bravo, A., S. Likitvivatanavong, et al. (2011). "*Bacillus thuringiensis*: A story of a successful bioinsecticide." Insect Biochem. Mol. Biol. **41**(7): 423-431.

Brown, D. A. (2006). "Lipid rafts, detergent-resistant membranes, and raft targeting signals." Physiology (Bethesda) **21**: 430-439.

Brown, D. A. and E. London (1998). "Functions of lipid rafts in biological membranes." Annu. Rev. Cell Dev. Biol. **14**: 111-136.

Brown, D. A. and J. K. Rose (1992). "Sorting of GPI-anchored proteins to glycolipid-enriched membrane subdomains during transport to the apical cell surface." Cell **68**(3): 533-544.

Cabiaux, V., C. Wolff, et al. (1997). "Interaction with a lipid membrane: a key step in bacterial toxins virulence." Int. J. Biol. Macromol. **21**(4): 285-298.

Chadee, D. D., P. Kittayapong, et al. (2007). "A breakthrough for global public health." Science **316**(5832): 1703-1704.

Chen, J., K. G. Aimanova, et al. (2009). "*Aedes aegypti* cadherin serves as a putative receptor of the Cry11Aa toxin from *Bacillus thuringiensis* subsp. *israelensis*." Biochem. J. **424**(2): 191-200.

Chen, J., K. G. Aimanova, et al. (2009). "Identification and characterization of *Aedes aegypti* aminopeptidase N as a putative receptor of *Bacillus thuringiensis* Cry11A toxin." Insect Biochem. Mol. Biol. **39**(10): 688-696.

Chmelar, R. S. and N. M. Nathanson (2006). "Identification of a novel apical sorting motif and mechanism of targeting of the M2 muscarinic acetylcholine receptor." J. Biol. Chem. **281**(46): 35381-35396.

Crepaldi Domingues, C., A. Ciana, et al. (2009). "Resistance of Human Erythrocyte Membranes to Triton X-100 and C12E8." J. Membr. Biol. **227**(1): 39-48.

Danielsen, E. M. (1995). "Involvement of detergent-insoluble complexes in the intracellular transport of intestinal brush border enzymes." Biochemistry **34**(5): 1596-1605.

Dechklar, M., K. Tiewsiri, et al. (2011). "Functional expression in insect cells of glycosylphosphatidylinositol-linked alkaline phosphatase from *Aedes aegypti* larval midgut: A *Bacillus thuringiensis* Cry4Ba toxin receptor." Insect Biochem. Mol. Biol. **41**(3): 159-166.

Donowitz, M., S. Singh, et al. (2007). "Proteome of murine jejunal brush border membrane vesicles." J. Proteome Res. **6**(10): 4068-4079.

Fantini, J., N. Garmy, et al. (2002). "Lipid rafts: structure, function and role in HIV, Alzheimer's and prion diseases." Expert Rev. Mol. Med. **4**(27): 1-22.

Fernandez, L. E., K. G. Aimanova, et al. (2006). "A GPI-anchored alkaline phosphatase is a functional midgut receptor of Cry11Aa toxin in *Aedes aegypti* larvae." Biochem. J. **394**(Pt 1): 77-84.

Ferreira, L. M., T. P. Romao, et al. (2010). "The orthologue to the Cpm1/Cqm1 receptor in *Aedes aegypti* is expressed as a midgut GPI-anchored alpha-glucosidase, which does not bind to the insecticidal binary toxin." Insect Biochem. Mol. Biol. **40**(8): 604-610.

Foster, L. J., C. L. de Hoog, et al. (2003). "Unbiased quantitative proteomics of lipid rafts reveals high specificity for signaling factors." Proc. Natl. Acad. Sci. U. S. A. **100**(10): 5813-5818.

Galbiati, F., B. Razani, et al. (2001). "Emerging themes in lipid rafts and caveolae." Cell **106**(4): 403-411.

Garczynski, S. F. and M. J. Adang (1995). "*Bacillus thuringiensis* CryIA(c) d-endotoxin binding aminopeptidase in the *Manduca sexta* midgut has a glycosyl-phosphatidylinositol anchor." Insect Biochem.Mol.Biol. **25**: 409-415.

Gylfason, G. A., E. Knutsdottir, et al. (2010). "Isolation and biochemical characterisation of lipid rafts from Atlantic cod (*Gadus morhua*) intestinal enterocytes." Comp. Biochem. Physiol., Part B: Biochem. Mol. Biol. **155**(1): 86-95.

Hansen, G. H., S.-M. Dalskov, et al. (2004). "Cholera toxin entry into Pig enterocytes occurs via a lipid raft- and clathrin-dependent mechanism†." Biochemistry **44**(3): 873-882.

Hansen, G. H., L. Immerdal, et al. (2001). "Lipid rafts exist as stable cholesterol-independent microdomains in the brush border membrane of enterocytes." J. Biol. Chem. **276**(34): 32338-32344.

Jouni, Z. E., J. Zamora, et al. (2002). "Absorption and tissue distribution of cholesterol in *Manduca sexta*." Arch. Insect Biochem. Physiol. **49**(3): 167-175.

Kamata, K., S. Manno, et al. (2008). "Functional evidence for presence of lipid rafts in erythrocyte membranes: Gsα in rafts is essential for signal transduction." Am. J. Hematol. **83**(5): 371-375.

Laemmli, U. K. (1970). "Cleavage of structural proteins during the assembly of the head of bacteriophage T4." Nature **227**: 680-685.

Lichtenberg, D., F. M. Goñi, et al. (2005). "Detergent-resistant membranes should not be identified with membrane rafts." Trends Biochem. Sci. **30**(8): 430-436.

Likitvivatanavong, S., J. Chen, et al. (2011). "Cadherin, alkaline phosphatase, and aminopeptidase N as receptors of Cry11Ba toxin from *Bacillus thuringiensis* subsp. *jegathesan* in *Aedes aegypti*." Appl. Environ. Microbiol. **77**(1): 24-31.

Likitvivatanavong, S., J. Chen, et al. (2011). "Multiple receptors as targets of Cry toxins in mosquitoes." J. Agric. Food Chem. **59**(7): 2829-2838.

Lin, S. L., C. W. Chien, et al. (2010). "Temporal proteomics profiling of lipid rafts in CCR6-activated T cells reveals the integration of actin cytoskeleton dynamics." J. Proteome Res. **9**(1): 283-297.

Lingwood, D. and K. Simons (2010). "Lipid rafts as a membrane-organizing principle." Science **327**(5961): 46-50.

Mannova, P., R. Fang, et al. (2006). "Modification of host lipid raft proteome upon hepatitis C virus replication." Mol. Cell. Proteomics **5**(12): 2319-2325.

Nguyen, H. T. T., A. B. Amine, et al. (2006). "Proteomic characterization of lipid rafts markers from the rat intestinal brush border." Biochem. Biophys. Res. Commun. **342**(1): 236-244.

Paradela, A., S. B. Bravo, et al. (2005). "Proteomic analysis of apical microvillous membranes of syncytiotrophoblast cells reveals a high degree of similarity with lipid rafts." J. Proteome Res. **4**(6): 2435-2441.

Pauchet, Y., A. Muck, et al. (2009). "Chromatographic and electrophoretic resolution of proteins and protein complexes from the larval midgut microvilli of *Manduca sexta*." Insect Biochem. Mol. Biol. **39**(7): 467-474.

Pedrioli, P. G. A., J. K. Eng, et al. (2004). "A common open representation of mass spectrometry data and its application to proteomics research." Nat. Biotech. **22**(11): 1459-1466.

Poncet, S., A. Delécluse, et al. (1995). "Evaluation of synergistic interactions among the CryIVA, CryIVB, and CryIVD toxic components of *B. thuringiensis* subsp. *israelensis* crystals." J. Invertebr. Pathol. **66**(2): 131-135.

Popova-Butler, A. and D. H. Dean (2009). "Proteomic analysis of the mosquito *Aedes aegypti* midgut brush border membrane vesicles." J. Insect Physiol. **55**(3): 264-272.

Ren, J., L. Wen, et al. (2008). "CSS-Palm 2.0: an updated software for palmitoylation sites prediction." Protein Eng., Des. Sel. **21**(11): 639-644.

Rietveld, A., S. Neutz, et al. (1999). "Association of sterol- and glycosylphosphatidylinositol-linked proteins with *Drosophila* raft lipid microdomains." J. Biol. Chem. **274**(17): 12049 - 12054.

Saengwiman, S., A. Aroonkesorn, et al. (2011). "In vivo identification of *Bacillus thuringiensis* Cry4Ba toxin receptors by RNA interference knockdown of glycosylphosphatidylinositol-linked aminopeptidase N transcripts in *Aedes aegypti* larvae." Biochem. Biophys. Res. Commun. **407**(4): 708-713.

Salaun, C., J. Greaves, et al. (2010). "The intracellular dynamic of protein palmitoylation." J. Cell Biol. **191**(7): 1229-1238.

Sano, O., A. Kobayashi, et al. (2007). "Sphingomyelin-dependence of cholesterol efflux mediated by ABCG1." J. Lipid Res. **48**(11): 2377-2384.

Schroeder, R. J., S. N. Ahmed, et al. (1998). "Cholesterol and sphingolipid enhance the Triton X-100 insolubility of glycosylphosphatidylinositol-anchored proteins by promoting the formation of detergent-insoluble ordered membrane domains." J. Biol. Chem. **273**(2): 1150-1157.

Schuck, S., M. Honsho, et al. (2003). "Resistance of cell membranes to different detergents." Proc. Natl. Acad. Sci. U. S. A. **100**(10): 5795-5800.

Seron, T. J., J. Hill, et al. (2004). "A GPI-linked carbonic anhydrase expressed in the larval mosquito midgut." J. Exp. Biol. **207**(Pt 26): 4559-4572.

Shogomori, H. and A. H. Futerman (2001). "Cholera toxin is found in detergent-insoluble rafts/domains at the cell surface of hippocampal neurons but is internalized via a raft-independent mechanism." J. Biol. Chem. **276**(12): 9182-9188.

Silva-Filha, M. H., C. Nielsen-Leroux, et al. (1997). "Binding kinetics of *Bacillus sphaericus* binary toxin to midgut brush-border membranes of *Anopheles* and *Culex sp*. mosquito larvae." Eur.J.Biochem. **247**: 754-761.

Simons, K. and E. Ikonen (1997). "Functional rafts in cell membranes." Nature **387**(6633): 569-572.

Strigini, M., R. Cantera, et al. (2006). "The IgLON protein Lachesin is required for the blood-brain barrier in *Drosophila*." Mol. Cell. Neurosci. **32**(1-2): 91-101.

Tchankouo-Nguetcheu, S., H. Khun, et al. (2010). "Differential protein modulation in midguts of *Aedes aegypti* infected with chikungunya and dengue 2 viruses." PLoS One **5**(10): e13149.

Terra, W. R. and C. Ferreira (1994). "Insect digestive enzymes: properties , compartmentalization and function." Comp. Biochem. Physiol., Part B: Biochem. Mol. Biol. **109B**: 1-62.

Wilfong, R. F. and D. M. Neville (1970). "The isolation of a brush border membrane fraction from rat kidney." J. Biol. Chem. **245**(22): 6106-6112.

Williamson, R., A. J. Thompson, et al. (2010). "Isolation of detergent resistant microdomains from cultured neurons: detergent dependent alterations in protein composition." BMC Neurosci **11**: 120.

Yang, W., D. Di Vizio, et al. (2010). "Proteome scale characterization of human S-acylated proteins in lipid raft-enriched and non-raft membranes." Mol. Cell. Proteomics **9**(1): 54-70.

Zhai, J., A.-L. Ström, et al. (2009). "Proteomic characterization of lipid raft proteins in amyotrophic lateral sclerosis mouse spinal cord." FEBS Journal **276**(12): 3308-3323.

Zhang, N., A. R. E. Shaw, et al. (2008). "Liquid chromatography electrospray ionization and matrix-assisted laser desorption ionization tandem mass spectrometry for the analysis of lipid raft proteome of monocytes." Anal. Chim. Acta **627**(1): 82-90.

Zheng, Y. Z., K. B. Berg, et al. (2009). "Mitochondria do not contain lipid rafts, and lipid rafts do not contain mitochondrial proteins." J. Lipid Res. **50**(5): 988-998.

Zhuang, M., D. I. Oltean, et al. (2002). "*Heliothis virescens* and *Manduca sexta* lipid rafts are involved in Cry1A toxin binding to the midgut epithelium and subsequent pore formation." J. Biol. Chem. **277**(16): 13863-13872.

Figures and Tables

Table 4.1: LC-MS/MS identification of the lipid rafts proteins from the *Ae. aegypti* midgut BBMV

VectorBase acc. no.	Protein description	Pred.mass (kDa)	pred. PI	Mascot score	Unique peptides	% seq coverage	Total spectra	*GPI anchor	+Palmitoylation	Cellu. comp.	Bio. process	Mol. fun.
AAEL006885	14-3-3 protein zeta(Protein kinase C)	28	5	217	3	19	14			4C	6P	7F
AAEL011902	1-acylglycerol-3-phosphate O-acyltransferase, putative	35	10	58	1	5	4		++	8C	1P	9F
AAEL010146	3-hydroxyacyl-coa dehyrogenase	82	10	408	7	14	20		+++	3C	1P	14F
AAEL003427	40S ribosomal protein	17	11	285	5	27	87			2C	4P	8F
AAEL003582	40S ribosomal protein	17	11	223	4	30	9			2C	4P	8F
AAEL005266	40S ribosomal protein	16	11	221	4	44	27			2C	4P	8F
CPIJ011589	40S ribosomal protein	23	11	100	2	15	18			2C	4P	8F
AAEL010299	40S ribosomal protein S12	15	7	57	1	10	15			2C	4P	8F
AAEL004175	40S ribosomal protein S17	15	11	101	2	29	24			2C	4P	8F
AAEL009506	40S ribosomal protein S20	13	11	75	1	13	62			2C	4P	8F
AAEL008192	40S ribosomal protein S3	27	10	349	6	30	129			2C	4P	8F
AAEL005901	40S ribosomal protein S3a	30	10	412	7	27	111			2C	4P	8F
AAEL009496	40S ribosomal protein S7	22	11	111	2	14	19			2C	4P	8F
AAEL008103	40S ribosomal protein S8	20	11	176	3	18	17			2C	4P	8F
AAEL008083	40S ribosomal protein SA	40	6	233	4	25	94		++	2C	4P	8F
CPIJ009378	46 kDa FK506-binding nuclear protein	41	4	116	2	7	10			8C	4P	10F
AAEL003746	4-Hydroxybutyrate CoA-transferase	52	8	116	2	5	6		+	8C	4P	11F
AAEL014583	60S acidic ribosomal protein P2	11	4	78	1	13	2			2C	4P	11F
AAEL004325	60S ribosomal protein	34	10	366	7	27	27			2C	4P	8F
CPIJ007488	60S ribosomal protein	51	11	337	6	9	50		++	2C	4P	8F
AAEL013097	60S ribosomal protein	15	11	254	4	34	108			2C	4P	8F
AAEL008481	60S ribosomal protein	22	12	112	2	16	9		+	2C	4P	8F
AAEL012944	60S ribosomal protein L11	18	10	105	2	17	22		++	2C	4P	8F
AAEL009825	60S ribosomal protein L13a	22	12	125	2	14	21		+	2C	4P	8F
AAEL011447	60S ribosomal protein L14	26	12	150	2	11	57		+	2C	4P	8F
AAEL007771	60S ribosomal protein L22	17	10	350	6	40	44			2C	4P	8F

AAEL005817	60S ribosomal protein L26	17	11	57	1	12	2			2C	4P	8F
AAEL006698	60S ribosomal protein L31	15	11	118	2	20	12			2C	4P	8F
AAEL003396	60S ribosomal protein L32	16	12	75	1	10	5			2C	4P	8F
AAEL013272	60S ribosomal protein L37a	10	11	62	1	21	9			2C	4P	8F
AAEL009994	60S ribosomal protein L4	49	12	397	7	20	60			2C	4P	8F
AAEL008188	60S ribosomal protein L6	30	12	62	1	4	4			2C	4P	8F
AAEL005722	60S ribosomal protein L7a	39	11	207	4	9	25			2C	4P	8F
AAEL000987	60S ribosomal protein L8	29	11	357	6	21	79			2C	4P	8F
AAEL007699	60S ribosomal protein L9	21	11	59	1	12	3			8C	4P	8F
AAEL005085	AAEL005085-PA	13	10	243	4	38	11			8C	6P	11F
AAEL003530	Acidic ribosomal protein P1,	11	4	225	4	48	15		+	8C	4P	11F
AAEL011197	Actin	42	5	1534	23	55	1265		++	6C	5P	7F
AGAP011516	Actin	42	5	1388	21	55	1171			6C	5P	7F
AAEL005961	Actin	42	5	1324	20	56	1149		++	6C	5P	7F
AAEL001673	Actin	42	5	1215	20	55	1195		++	6C	5P	7F
AAEL004616	Actin	42	5	1175	19	49	1004		+	6C	5P	7F
AAEL004631	Actin	42	5	1031	17	53	1117		++	6C	5P	7F
CPIJ012574	Actin	42	5	1013	16	37	738		+	6C	5P	7F
CPIJ005786	Actin	42	5	909	15	41	871		+	6C	5P	7F
AAEL005964	Actin	42	5	703	12	31	775		+	6C	5P	7F
AAEL003957	Actin depolymerizing factor	17	7	122	2	9	3		+	8C	4P	11F
AAEL004778	Acyl-coa dehydrogenase	68	8	252	4	6	23		+++	8C	6P	11F
AAEL008574	Acyl-CoA oxidase	75	7	368	6	11	28		+	8C	1P	3F
AAEL005662	Adenosine diphosphatase	50	7	102	2	9	4		++	8C	6P	6F
AGAP006782	ADP,ATP carrier protein 1	33	10	647	10	24	327			1C	3P	7F
AGAP008686	AGAP008686-PA	53	6	67	1	3	2			1C	1P	6F
AAEL010185	A-kinase anchoring protein AKAP120	60	9	214	4	3	351			8C	6P	1F
AAEL005821	Alanyl aminopeptidase	107	5	1367	24	28	234	*	+++	1C	1P	12F
AAEL005808	Alanyl aminopeptidase	108	5	98	2	3	3	*	+	1C	1P	12F
AAEL003313	Alkaline phosphatase	61	6	540	9	21	28	*	+	1C	1P	13F
AAEL003309	Alkaline phosphatase	62	5	529	10	21	22	*	+	1C	1P	13F
AAEL003298	Alkaline phosphatase	58	5	294	5	14	35	*	+	1C	1P	13F
AAEL003286	Alkaline phosphatase	43	6	158	3	15	11	*		1C	1P	13F
AGAP011302	Alkaline phosphatase	59	6	137	2	6	6	*	++	1C	1P	13F
AAEL011176	Alkaline phosphatase	26	9	66	1	6	3	*		1C	1P	13F

AAEL010532	Alpha-amylase	69	5	3996	64	52	1476	*	++	1C	1P	5F
AAEL010540	Alpha-amylase	70	5	1179	19	28	318	*		1C	1P	5F
AAEL010537	Alpha-amylase	67	5	469	9	24	55	*	+	1C	1P	5F
CPIJ013171	Alpha-amylase	69	5	399	7	9	256	*		1C	1P	5F
AAEL014710	Alpha-amylase	71	5	351	6	12	27	*	+	1C	1P	5F
AAEL005740	AMP dependent ligase	69	7	102	2	5	14		++	8C	1P	5F
AAEL009955	Apolipophorin II	367	8	1613	28	11	205		+++++	8C	2P	3F
CPIJ007204	Apolipophorins precursor	367	7	165	3	1	14		+++++	8C	2P	11F
AAEL009569	Apolipoprotein D, putative	26	5	90	1	9	9	*	+	8C	2P	7F
AAEL010986	Apyrase, putative	60	4	179	3	9	36	*	+	8C	1P	6F
AAEL011341	Apyrase, putative	60	5	146	3	12	6		+	8C	1P	6F
AAEL012621	Arginine/serine-rich splicing factor	40	12	110	2	6	3			8C	6P	7F
CPIJ002271	ATP synthase alpha subunit	59	9	678	12	24	80			3C	1P	3F
AAEL002827	ATP synthase beta subunit	54	5	539	10	34	75			3C	1P	3F
AAEL010823	ATP synthase delta chain	23	10	58	1	9	4			3C	1P	3F
AAEL008848	ATP synthase gamma subunit	33	9	141	2	11	18			3C	1P	3F
AAEL009808	ATP synthase subunit d	28	10	161	3	12	11			3C	1P	3F
CPIJ012510	ATP-dependent RNA helicas	93	9	63	1	1	1			8C	6P	11F
AAEL005845	Beta chain spectrin	266	5	471	8	6	82			1C	6P	5F
CPIJ008529	Beta-glucosidase	106	5	116	2	3	9	*		8C	6P	11F
AAEL006582	Calcium-transporting atpase sarcoplasmic/endoplasmic reticulum type (Calcium pump)	110	5	949	15	17	500		++++	1C	1P	7F
AAEL005520	Carbonic anhydrase	29	7	61	1	7	19	*		1C	1P	5F
AAEL009323	Carbonic anhydrase	33	7	60	1	5	10	*		1C	1P	5F
AAEL000898	Carboxylesterase	57	6	132	2	7	5		+	4C	3P	3F
AAEL012094	Casein kinase ii, alpha chain (Cmgc group iv)	41	8	348	6	17	29			8C	4P	1F
AAEL009420	Cd36 antigen	56	5	330	6	16	24	*	++++	1C	2P	11F
AAEL009432	Cd36 antigen	55	5	57	1	3	1		+++	1C	2P	11F
AAEL006958	Cell adhesion molecule	148	7	103	2	4	3		++	1C	6P	7F
AAEL008340	Cell adhesion molecule	133	5	59	1	2	2		+	1C	6P	7F
AAEL006383	Chymotrypsin, putative	31	8	211	4	22	20	*		8C	1P	12F
AAEL004546	Coatomer beta subunit	107	6	68	1	2	4		+++	1C	3P	1F
AAEL005097	Cold induced protein (BnC24A), putative	16	11	113	2	22	19		++	4C	4P	8F

AAEL004699	conserved hypothetical protein	112	10	1118	20	22	393			8C	6P	11F
AAEL011180	Conserved hypothetical protein	31	7	794	12	49	213			8C	6P	11F
AAEL017096	Conserved hypothetical protein	50	10	551	10	30	329		++	8C	6P	11F
AAEL005259	Conserved hypothetical protein	21	5	371	6	25	101		+	8C	6P	11F
AAEL011551	Conserved hypothetical protein	99	6	357	6	13	38	*		8C	6P	11F
AGAP002076	Conserved hypothetical protein	71	5	296	5	7	52		+	8C	6P	11F
AAEL016984	Conserved hypothetical protein	35	8	278	5	26	101		++	8C	6P	11F
AAEL005432	conserved hypothetical protein	161	5	267	5	5	12		+++++	8C	2P	11F
AAEL003785	Conserved hypothetical protein	101	7	266	5	9	14		+	8C	6P	11F
AAEL008801	Conserved hypothetical protein	18	6	243	4	33	23	*	++	8C	6P	11F
AAEL010833	conserved hypothetical protein	126	4	228	4	7	57		+++	8C	1P	11F
AAEL010754	Conserved hypothetical protein	10	10	228	4	43	14			8C	6P	11F
AAEL004873	Conserved hypothetical protein	26	7	204	4	24	16	*		8C	6P	11F
AAEL003774	Conserved hypothetical protein	22	7	153	3	27	4		+	8C	6P	11F
AAEL011935	Conserved hypothetical protein	28	4	153	3	16	7		++	8C	6P	11F
AAEL012262	Conserved hypothetical protein	32	5	131	2	10	25		++	8C	6P	11F
AAEL008478	Conserved hypothetical protein	35	5	129	2	11	16	*	++	8C	6P	11F
AAEL000294	Conserved hypothetical protein	45	7	125	2	8	4		++	8C	6P	11F
AAEL004239	Conserved hypothetical protein	26	4	107	2	12	10		++	8C	6P	11F
AAEL003459	Conserved hypothetical protein	14	5	105	2	37	4			8C	6P	11F
AAEL017395	Conserved hypothetical protein	34	10	102	2	6	7			8C	6P	11F
AAEL010520	conserved hypothetical protein	131	8	90	1	1	2	*	++++	8C	6P	12F
AAEL000529	conserved hypothetical protein	9	7	82	1	23	9		+	8C	6P	11F
AAEL011813	conserved hypothetical protein	35	7	79	1	6	2		++	8C	6P	11F
AAEL001293	conserved hypothetical protein	34	8	73	1	5	14		+	8C	6P	11F
CPIJ019325	Conserved hypothetical protein	45	10	67	1	4	7		+++	8C	6P	11F
AAEL012382	conserved hypothetical protein	8	8	66	1	30	3		+	8C	6P	11F
AAEL012964	conserved hypothetical protein	40	10	62	1	4	8		+	8C	6P	11F
AAEL001301	conserved hypothetical protein	33	9	62	1	6	2			8C	6P	11F
AAEL010266	Conserved hypothetical protein	187	4	61	1	1	5	*	+++++ ++++	8C	6P	11F
AAEL013780	Conserved hypothetical protein	31	5	61	1	4	6			8C	6P	11F
AAEL017508	Conserved hypothetical protein	32	10	59	1	9	2		++	8C	6P	11F
AAEL002619	conserved hypothetical protein	36	5	58	1	4	1		+	5C	1P	7F
AAEL006611	Conserved hypothetical protein	29	8	57	1	6	2			8C	6P	11F
AAEL009185	Creatine kinase	40	6	801	14	38	106			8C	4P	1F

AAEL010017	Cytochrome B5 (Cytb5)	12	5	170	3	29	9			2C	6P	7F
AAEL005170	Cytochrome c oxidase subunit iv	46	7	157	3	11	16		+	2C	6P	5F
AAEL011871	Cytochrome C1	33	9	105	2	10	7		+	2C	6P	5F
AAEL007024	Cytochrome P450	58	9	71	1	3	8			2C	6P	3F
AAEL014414	DEAD box ATP-dependent RNA helicase	46	6	76	1	4	2		+	8C	6P	5F
AAEL008857	Deoxyribonuclease I, putative	48	6	154	3	13	11	*	+	8C	6P	6F
AAEL004294	Dihydrolipoamide acetyltransferase component of pyruvate dehydrogenase	54	9	204	3	9	6			4C	1P	9F
AAEL002764	Dihydrolipoamide succinyltransferase component of 2-oxoglutarate dehydrogenase	52	10	66	1	5	10		+	4C	1P	9F
AAEL009310	Dipeptidyl carboxypeptidase	70	5	215	4	9	12		+	1C	1P	12F
AAEL002174	Dolichyl-diphosphooligosaccharide protein glycosyltransferase	49	5	167	3	8	11		+	4C	4P	9F
AAEL000293	Ebna2 binding protein P100	103	7	219	4	7	14			7C	2P	6F
AAEL007078	eIF3a	133	9	210	4	4	31		+	2C	6P	11F
AAEL011288	Elongation factor 1 gamma	49	8	310	6	20	47		+	4C	4P	8F
CPIJ009303	Elongation factor 1-alpha 1	52	10	553	10	33	396		+++	4C	4P	14F
AAEL000951	Elongation factor 1-beta2	25	4	292	5	21	22		++	4C	4P	8F
AAEL009313	Elongation factor-1 beta,delta	29	4	60	1	7	3		+	4C	4P	11F
AAEL013845	Endoplasmic reticulum resident protein (ERp44), putative	46	7	119	2	4	3			7C	4P	7F
AAEL012827	Endoplasmin	91	5	57	1	2	8		+	4C	2P	7F
CPIJ000948	Enolase	47	7	178	3	15	8		+	5C	1P	6F
AAEL001668	Enolase	47	7	178	3	12	12		+	5C	1P	6F
AAEL007023	Estradiol 17 beta-dehydrogenase	78	8	383	7	14	19			4C	1P	5F
AAEL004500	Eukaryotic translation elongation factor	94	6	235	4	7	33		+	4C	1P	7F
AAEL013675	Eukaryotic translation initiation	41	4	106	2	7	5			4C	1P	7F
AAEL013144	Eukaryotic translation initiation factor 3 subunit I	36	6	180	3	21	12		+	4C	1P	7F
AAEL004347	Eukaryotic translation initiation factor 3 subunit M	44	6	61	1	4	3		+++	4C	1P	7F
AAEL012046	Flotillin-1	45	6	138	2	7	11			1C	2P	1F

AGAP003789	Flotillin-2	47	5	251	5	18	13		+++	1C	2P	1F
AAEL004041	Flotillin-2	47	5	209	4	15	13		+++	1C	2P	1F
AAEL005766	Fructose-bisphosphate aldolase	39	8	491	8	26	93		++	8C	1P	5F
AAEL012135	Galectin	36	5	311	6	31	26		++	4C	1P	7F
AAEL005293	Galectin	16	9	299	5	15	47			4C	6P	7F
AAEL003844	Galectin	42	9	66	1	4	2			4C	6P	7F
AAEL012478	Glucose transporter, putative	38	8	186	3	9	26			7C	3P	3F
AAEL010386	Glucosyl/glucuronosyl transferases	59	10	125	2	5	6		+++	7C	4P	9F
AAEL010464	Glutamate dehydrogenase	61	8	224	4	11	15		+++	3C	1P	14F
AAEL007201	Glutamyl aminopeptidase	114	6	365	7	11	19	*		1C	1P	12F
AAEL015573	Glycoside hydrolases	52	5	1114	19	37	83	*	++	4C	1P	5F
AAEL009237	Glycoside hydrolases	61	5	977	16	23	98	*	++	4C	1P	5F
AAEL015020	Glycoside hydrolases	61	5	937	15	20	77	*	++	4C	1P	5F
AAEL017349	Heat shock cognate 70	72	5	892	14	25	178		+	8C	2P	7F
AAEL005515	Heterogeneous nuclear ribonucleoprotein	30	9	137	2	12	5			4C	6P	11F
AAEL013981	Hexamerin 2 beta	83	6	57	1	3	1		+	8C	3P	3F
AAEL015464	Histone H1, putative	22	11	59	1	9	9			4C	4P	7F
AGAP006452	hypothetical protein	197	4	164	3	4	28		+++	8C	4P	11F
AGAP006871	hypothetical protein	30	11	63	1	5	9			8C	6P	11F
AGAP007157	hypothetical protein	9	10	57	1	14	23			8C	6P	11F
AAEL013359	Initiation factor EIF-4A	39	6	71	1	4	6			4C	4P	7F
AGAP010214	Integral membrane protein	30	10	157	3	5	11			1C	6P	6F
AAEL002133	Juvenile hormone-inducible protein	48	7	240	4	18	41			8C	6P	11F
AAEL009295	Lachesin	40	5	146	3	12	13	*	++	1C	5P	11F
AAEL003262	Leucine-rich transmembrane	152	8	111	2	2	6		+++	7C	6P	11F
AAEL010991	Long-chain-fatty-acid coa ligase	80	8	895	16	21	273			4C	1P	5F
CPIJ015739	Long-chain-fatty-acid coa ligase	78	8	246	5	7	29			4C	1P	5F
AAEL008708	Lysosomal pro-X carboxypeptidase	53	4	234	4	9	29			1C	1P	12F
AAEL012554	Maltose phosphorylase	163	5	1641	26	13	289		+++	1C	1P	5F
AAEL004195	Membrane associated progesterone receptor	28	4	202	3	11	14			1C	6P	2F
AAEL002861	Membrane protein, putative	48	9	273	5	15	22		+++	1C	6P	5F
AAEL015070	Membrane-bound alkaline phosphatase	58	6	235	4	10	21	*		1C	6P	11F
AAEL006829	Microsomal glutathione s-	17	10	329	6	34	18			2C	6P	9F

AAEL012175	Mitochondrial ATP synthase-α	59	9	749	13	23	77			3C	3P	3F
AAEL005610	Mitochondrial ATP synthase b	27	9	257	4	21	43		+	3C	3P	3F
AAEL004423	Mitochondrial F0 ATP synthase D chain, putative	20	5	182	3	16	8		+	3C	3P	3F
AAEL013876	Mitochondrial NADH:ubiquinone oxidoreductase	18	10	64	1	10	4			3C	3P	11F
AAEL005435	Mitochondrial processing peptidase beta subunit	52	6	492	9	26	14			3C	3P	3F
AAEL007915	Moesin/ezrin/radixin homolog 1	69	6	306	5	10	11			1C	5P	7F
AAEL014842	Multiple inositol polyphosphate phosphatase	57	8	113	2	6	6		+	1C	6P	13F
AAEL005733	Myosin heavy chain, nonmuscle or smooth muscle	222	6	1954	31	19	307		++	6C	6P	7F
AAEL001411	Myosin heavy chain, nonmuscle or smooth muscle	218	5	162	3	2	6		+++	6C	5P	7F
AAEL012631	Myosin i	116	10	244	4	4	25			6C	5P	7F
AAEL011905	Myosin I (Brush border myosin I)	119	9	962	17	19	183		++	6C	5P	7F
CPIJ015035	Myosin-IB	119	9	425	7	7	137		+++	6C	5P	7F
AAEL012062	Na+/k+ atpase alpha subunit	111	5	538	10	11	82		++	3C	3P	3F
AAEL010673	NADH dehydrogenase	8	8	101	2	26	3			3C	6P	11F
AAEL007054	NADH dehydrogenase, putative	12	9	70	1	12	2			3C	6P	6F
AAEL012552	NADH-ubiquinone oxidoreductase	79	7	383	5	12	59		++++	3C	1P	3F
AAEL009414	NADH-ubiquinone oxidoreductase 39 kDa subunit	46	9	170	3	10	7			3C	1P	3F
AAEL011381	NADH-ubiquinone oxidoreductase fe-s protein 2 (Ndufs2)	53	7	127	2	8	3		+	3C	1P	3F
AAEL007681	NADH-ubiquinone oxidoreductase flavoprotein 1 (Ndufv1)	53	9	164	3	10	7			3C	1P	3F
AAEL009078	NADH-Ubiquinone oxidoreductase SGDH	22	10	62	1	7	3			3C	1P	3F
AAEL012616	Nadp transhydrogenase	112	8	99	2	3	7		+++	8C	1P	11F
AAEL009651	Nascent polypeptide associated complex alpha subunit	17	6	133	2	35	10			8C	6P	11F
AAEL008069	Notch	371	5	253	5	2	19		+++++ ++++	5C	2P	7F
AAEL006371	Oviductin	51	8	265	5	16	22	*	++	8C	1P	5F

CPIJ005078	Phenoloxidase	77	7	153	3	6	17			8C	3P	3F
AAEL012282	Prohibitin	33	10	299	5	21	15			1C	6P	11F
AAEL012312	Proliferation-associated 2g4 (Pa2g4/ebp1)	48	9	170	3	9	49		++	8C	2P	11F
AAEL008699	Prolylcarboxypeptidase, putative	58	4	291	5	15	21	*		1C	1P	12F
AAEL008698	Prolylcarboxypeptidase, putative	58	5	192	4	11	5			1C	1P	12F
AAEL008702	Prolylcarboxypeptidase, putative	57	5	102	2	7	5	*		1C	1P	12F
AAEL011764	Prophenoloxidase	78	6	540	9	12	42			8C	1P	5F
AAEL013498	Prophenoloxidase	78	7	531	9	17	52			8C	1P	5F
AAEL013499	Prophenoloxidase	78	7	425	8	18	34			8C	1P	5F
AAEL011763	Prophenoloxidase	79	7	377	6	14	45			8C	1P	5F
AAEL012778	Protease m1 zinc metalloprotease	112	5	2564	41	40	637	*	+	1C	1P	12F
AAEL008155	Protease m1 zinc metalloprotease	211	5	2435	41	21	312	*	+	1C	1P	12F
AAEL012776	Protease m1 zinc metalloprotease	103	5	673	12	18	54	*	+++	1C	1P	12F
AAEL012774	Protease m1 zinc metalloprotease	102	5	652	11	15	77	*	+	1C	1P	12F
AAEL012783	Protease m1 zinc metalloprotease	107	6	608	10	12	35	*		1C	1P	12F
AAEL008163	Protease m1 zinc metalloprotease	106	5	523	9	16	47	*		1C	1P	12F
AAEL012786	Protease m1 zinc metalloprotease	25	5	306	5	21	14	*	+	1C	1P	12F
AAEL013899	Protease m1 zinc metalloprotease	82	6	181	3	7	11	*	++	1C	1P	12F
AAEL008162	Protease m1 zinc metalloprotease	106	5	123	2	3	7	*	+	1C	1P	12F
AAEL012779	Protease m1 zinc metalloprotease	93	5	69	1	2	2	*	++	1C	1P	12F
AAEL000641	Protein disulfide isomerase	56	5	289	5	17	51			2C	4P	10F
AAEL001432	Protein disulfide isomerase	55	5	109	2	5	8		++	2C	4P	10F
AAEL002501	Protein disulfide isomerase	44	5	97	2	12	6		+	2C	4P	10F
AAEL010065	Protein disulfide-isomerase A6	48	5	367	6	16	48			2C	4P	10F
AAEL000859	Putative uncharacterized protein	57	5	289	4	6	15	*	+++++ +++	1C	4P	7F
AAEL005792	Putative uncharacterized protein	39	6	58	1	5	3		++	8C	4P	11F
AAEL007845	Rab5	24	9	59	1	9	8		+++	2C	2P	7F
AAEL004902	Ras-related protein Rab-2A,	24	6	106	2	14	3		++	2C	2P	7F
AAEL013069	Receptor for activated protein kinase c (Rack1)	35	8	116	2	9	32			4C	4P	2F
AAEL013071	Ribophorin	52	9	109	2	6	10		++	4C	4P	9F
AAEL010521	Ribophorin ii	73	10	141	2	5	5		+	4C	4P	9F
AAEL012736	Ribosomal protein L15	18	11	58	1	9	2		+	4C	4P	8F
AAEL008353	Ribosomal protein L28, putative	17	12	88	1	11	11			4C	4P	8F

AAEL009341	Ribosomal protein L34, putative	15	12	71	1	11	9			4C	4P	8F
AAEL012585	Ribosomal protein L7	30	11	152	3	11	25			4C	4P	8F
AAEL010821	Ribosomal protein P0	34	5	428	7	33	78			4C	4P	8F
AAEL012686	Ribosomal protein S12, putative	16	11	193	3	31	43			4C	4P	8F
AAEL009747	Ribosomal protein S18	17	11	167	3	22	18			4C	4P	8F
AAEL010168	Ribosomal protein S2	30	11	192	4	17	42			4C	4P	8F
AAEL001759	Ribosomal protein S4	23	11	195	4	19	16			4C	4P	8F
AAEL013625	Ribosomal protein S5	25	10	119	2	12	12		+	4C	4P	8F
AAEL000032	Ribosomal protein S6	37	11	149	3	10	26			4C	4P	8F
AAEL003837	Ryanodine receptor 3, brain	578	5	60	1	0	2		+++++ +++++	1C	3P	2F
AAEL007987	SEC63 protein, putative	86	6	172	3	6	50			8C	4P	7F
AAEL007926	Serine carboxypeptidase	50	5	56	1	3	1	*	+	1C	1P	12F
AAEL009682	Serine collagenase 1, putative	28	8	169	3	6	39		++	8C	1P	12F
AAEL008207	Serine protease	31	8	225	3	9	11			8C	1P	12F
AAEL002600	Serine protease	98	7	173	3	5	18		+++	8C	1P	12F
AAEL002595	Serine protease	47	5	95	2	8	13		+++	8C	1P	12F
AAEL002629	Serine protease	43	5	58	1	4	4		+++++	8C	1P	12F
CPIJ011380	Serine-type enodpeptidase	30	8	158	3	7	45		+	8C	1P	12F
AAEL011929	Serine-type enodpeptidase, putative	27	9	574	8	27	218		+	8C	1P	12F
AAEL006627	Serine-type enodpeptidase, putative	27	9	550	9	36	170		++	8C	1P	12F
AAEL011917	Serine-type enodpeptidase, putative	27	8	462	7	24	114		+++	8C	1P	12F
AAEL011913	Serine-type enodpeptidase, putative	27	7	258	5	30	26		+	8C	1P	12F
AAEL011889	Serine-type enodpeptidase, putative	28	6	113	2	13	10		+	8C	1P	12F
AAEL006902	Serine-type enodpeptidase, putative	30	6	58	1	6	2		++	8C	1P	12F
AAEL009625	Short-chain dehydrogenase	37	10	359	7	27	16			1C	1P	5F
AAEL006224	Short-chain dehydrogenase	29	9	107	2	11	9			1C	1P	5F
AAEL015065	Spectrin	278	5	1334	24	13	152		+	6C	5P	7F
AAEL009634	Steroid dehydrogenase	35	9	126	2	7	4			1C	6P	11F
AAEL010330	Succinate dehydrogenase	32	9	195	4	14	21		+++++	3C	4P	5F
AAEL002107	Sulfide quinone reductase	49	9	106	2	7	3		+	1C	4P	11F
CPIJ004284	Sulfide quinone reductase	49	9	106	2	7	3		+++	1C	4P	14F
AAEL006271	Superoxide dismutase (Cu-Zn)	21	7	213	4	29	15	*	+	4C	4P	7F
AAEL008687	Tar RNA binding protein (Trbp)	36	6	82	1	5	12		+	4C	6P	7F
AAEL008607	Tep3	162	6	75	1	1	2	*	++	5C	2P	5F
AAEL011641	Transferrin	86	5	516	8	13	66	*	++	5C	3P	3F

AAEL003872	Translationally-controlled tumor protein homolog (TCTP)	20	4	167	2	30	18		+	4C	6P	11F
AAEL013320	Translocon-associated protein-δ	18	9	61	1	7	1	*	++	7C	4P	11F
AAEL007441	Translocon-associated protein-γ	21	10	123	2	13	7			7C	4P	11F
AAEL002436	Transmembrane protein 38A	30	10	69	1	5	8			1C	4P	5F
AAEL002759	Tropomyosin	32	5	404	7	31	32			1C	2P	2F
AAEL002761	Tropomyosin	33	5	169	3	16	17			1C	2P	2F
AAEL010850	Troponin i	23	10	58	1	8	6			6C	2P	11F
AAEL002417	Troponin t	45	4	159	3	9	19	*		6C	2P	11F
AAEL005614	Trypsin	28	7	161	3	22	15	*	+++	8C	1P	5F
AAEL008079	Trypsin-alpha, putative	31	8	146	3	15	8	*	+++++	8C	1P	5F
AAEL008097	Trypsin-eta, putative	32	8	321	5	18	18	*		8C	1P	5F
AAEL006642	Tubulin alpha chain	50	5	593	10	34	364		+++++ ++++	6C	1P	7F
AAEL002851	Tubulin beta chain	50	4	955	17	31	263		+++++ ++	6C	1P	7F
AAEL005052	Tubulin beta chain	50	5	598	11	15	124		++++++	6C	1P	7F
AAEL007868	Ubiquinol-cytochrome c reductase complex 14 kd protein	13	7	129	2	11	2			3C	4P	12F
AAEL005269	Ubiquinol-cytochrome c reductase complex core protein	46	8	231	4	15	14	*		3C	4P	12F
AAEL003675	Ubiquinol-cytochrome c reductase iron-sulfur subunit	28	9	140	2	10	7			3C	4P	12F
AAEL008787	Vacuolar ATP synthase catalytic subunit A	68	5	1333	23	57	206		+	1C	3P	3F
CPIJ007772	Vacuolar ATP synthase catalytic subunit A	68	5	968	16	47	131		+	1C	3P	3F
AAEL005798	Vacuolar ATP synthase catalytic subunit beta	55	5	1246	21	51	100			1C	3P	3F
AAEL011025	Vacuolar ATP synthase subunit	40	5	910	15	45	113		+	7C	3P	3F
AAEL005173	Vacuolar ATP synthase subunit c	80	7	189	3	4	6		+	1C	3P	3F
AAEL012035	Vacuolar ATP synthase subunit e	26	6	151	3	6	10			1C	3P	3F
AAEL006516	Vacuolar ATP synthase subunit h	55	6	111	2	8	11		+++	1C	3P	3F
AAEL007777	Vacuolar ATP synthase subunit S1	43	5	200	4	8	23	*	+	1C	3P	3F
AAEL006390	Vacuolar proton atpases	92	6	1036	17	19	325		+	1C	3P	3F
AAEL014053	Vacuolar proton atpases	95	7	397	7	10	53		+	1C	3P	3F

AAEL006023	Vanin-like protein 1, putative	59	5	302	5	9	27	*	+	7C	1P	6F
AAEL001872	voltage-dependent anion channel	31	9	830	14	45	91			3C	4P	3F
AAEL001840	Zinc carboxypeptidase	48	5	447	7	18	37	*	+	1C	1P	12F
AAEL008600	Zinc carboxypeptidase	48	5	273	5	11	33	*	+	1C	1P	12F
AAEL008609	Zinc carboxypeptidase	51	5	197	3	9	14	*		1C	1P	12F
AAEL001844	Zinc carboxypeptidase	49	6	109	2	3	7	*		1C	1P	12F

* GPI anchor prediction for proteins in the A. aegypti lipid raft fraction using N-terminal secretory signal prediction program SignalP 3.0 and four C-terminal GPI anchor-specific prediction programs (Big PI, GPI SOM, FragAnchor and PredGPI)

+ Palmitoylation site prediction for proteins in the A. aegypti lipid raft fraction using CSS-Palm 3.0 and number of + indicates number of CSS-Palm3.0 predicted sites for that particular protein.

Table index:

Cellular compartment		**Molecular Function**		**Biological process**	
Plasma membrane	1C	Signal Transduction	1F	Metabolism and Biogenesis	1P
Lipid particles	2C	Receptors or surface glycoproteins	2F	Immune system process	2P
Mitochondria	3C	Cell Transport	3F	Iontransport	3P
Cytoplasma	4C	Cell adhesion	4F	Biological regulation	4P
Extracellular	5C	Metabolic process	5F	Cytoskeletal component organization	5P
Cytoskeleton	6C	Hydrolase activity	6F	Biological process unknown	6P
Integral to membrane	7C	Binding	7F		
Unknown	8C	Translation elongation factor	8F		
		Transferase acitvity	9F		
		Isomerase activity	10F		
		Others	11F		
		Peptidase activity	12F		
		Phosphatase activity	13F		
		oxidoreductase activity	14F		

Table 4.2: GPI anchor prediction for proteins in the A. aegypti lipid raft fraction. Results for the GPI-anchor prediction from SignalP 3.0 which predicts N-terminal secretory signal and Big PI, GPI SOM, FragAnchor and PredGPI, predicts C-terminal GPI anchor-specific signal. Symbol '●' denoting a positive prediction while '○' indicates a negative prediction.

VectorBase acc. no.	Protein Name	Signal peptide	NN Score	BigPI	Score	Frag Anchor	Score	PredGPI	Score	GPI anchored (C&N-term signal) + SignalP
AAEL005821	Alanyl aminopeptidase	●	0.999	●	3.86E-04	●	0.999889	●	Highly probable	●
AAEL005808	Alanyl aminopeptidase	●	1	●	4.77E-04	●	0.999982	●	Highly probable	●
AAEL003313	Alkaline phosphatase	●	0.998	●	7.03E-04	●	0.999894	●	Highly probable	●
AAEL003309	Alkaline phosphatase	●	1	●	7.62E-04	●	0.999979	●	Highly probable	●
AAEL003298	Alkaline phosphatase	●	0.999	○	5.70E-01	○	0.030191	○	Not GPI-anchored	○
AAEL003286	Alkaline phosphatase	●	0.992	○	6.61E-01	○	0.002292	○	Not GPI-anchored	○
AGAP011302	Alkaline phosphatase	○	0.107	○	7.30E-01	○	0.041705	○	Not GPI-anchored	○
AAEL011176	Alkaline phosphatase	●	0.96	○	9.45E-01	○	0.000028	○	Not GPI-anchored	○
AAEL010532	Alpha-amylase	●	1	●	2.32E-04	●	0.99999	●	Highly probable	●
AAEL010540	Alpha-amylase	●	0.998	○	3.85E-03	●	0.99999	●	Highly probable	●
AAEL010537	Alpha-amylase	●	0.997	●	1.51E-03	●	0.999985	●	Highly probable	●
CPIJ013171	Alpha-amylase	●	1	●	9.58E-04	●	0.999988	●	Highly probable	●
AAEL014710	Alpha-amylase	●	0.995	●	4.38E-04	●	0.999997	●	Probable	●
AAEL009569	Apolipoprotein D, putative	●	0.998	●	4.37E-04	●	0.999974	●	Highly probable	●
AAEL010986	Apyrase, putative	○	0.016	●	2.41E-03	●	0.999992	●	Probable	○
CPIJ008529	Beta-glucosidase	○	0.008	○	2.58E-02	●	0.992575	●	Probable	○
AAEL009323	Carbonic anhydrase	●	0.991	●	3.81E-04	●	0.999965	●	Highly probable	●
AAEL006383	Chymotrypsin, putative	●	0.997	●	2.35E-04	●	0.999993	●	Highly probable	●
AAEL011551	Conserved hypothetical protein	●	0.999	●	5.23E-04	●	0.999995	●	Highly probable	●
AAEL004873	Conserved hypothetical protein	●	1	●	4.13E-04	●	0.999891	●	Highly probable	●
AAEL008801	Conserved hypothetical protein	○	0	○	7.61E-02	●	0.999433	○	Not GPI-anchored	○
AAEL008478	Conserved hypothetical protein	●	0.994	○	8.83E-03	○	Pot. false +	●	Highly probable	●
AAEL010520	conserved hypothetical protein	●	0.998	○	7.33E-01	●	0.99997	●	Probable	○
AAEL010266	Conserved hypothetical protein	○	0	○	1.31E-02	○	Pot. false +	●	Weakly probable	○
AAEL008857	Deoxyribonuclease I, putative	○	0.001	●	2.61E-03	●	0.999143	●	Probable	○
AAEL007201	Glutamyl aminopeptidase	●	0.525	○	2.75E-01	●	0.23483	●	Weakly probable	○
AAEL009237	Glycoside hydrolases	●	1	○	6.07E-03	●	0.999973	●	Highly probable	○
AAEL015573	Glycoside hydrolases	○	0.019	●	6.21E-02	●	0.949126	●	Highly probable	○
AAEL015020	Glycoside hydrolases	●	1	●	6.07E-03	●	0.99997	○	Highly probable	○
AAEL009295	Lachesin	●	0.995	●	3.64E-04	●	0.999928	●	Highly probable	●

AAEL015070	Membrane-bound alkaline phosphatase	●	0.867	●	7.54E-04	●	0.999946	●	Probable	●
AAEL014842	Multiple inositol polyphosphate phosphatase	●	0.998	●	5.18E-03	●	0.999507	●	Weakly probable	●
AAEL006371	Oviductin	○	0	○	2.98E-01	●	0.999646	○	Not GPI-anchored	○
AAEL008702	Prolylcarboxypeptidase, putative	●	0.999	○	2.89E-01	○	n/a	○	Not GPI-anchored	●
AAEL012778	Protease m1 zinc metalloprotease	●	0.98	●	4.13E-04	●	0.999991	●	Highly probable	●
AAEL008155	Protease m1 zinc metalloprotease	●	0.994	○	2.78E-01	○	0.103862		Not GPI-anchored	●
AAEL012776	Protease m1 zinc metalloprotease	●	1	○	5.11E-01	○	0.005453	●	Weakly probable	○
AAEL012774	Protease m1 zinc metalloprotease	●	0.993	○	7.47E-01	○	0.000355	○	Not GPI-anchored	○
AAEL012783	Protease m1 zinc metalloprotease	●	0.998	●	1.07E-03	●	0.999982	●	Highly probable	●
AAEL008163	Protease m1 zinc metalloprotease	●	1	○	7.16E-01	○	0.000179	○	Not GPI-anchored	○
AAEL012786	Protease m1 zinc metalloprotease	●	0.989	○	2.30E-01	○	0.000943	○	Not GPI-anchored	○
AAEL013899	Protease m1 zinc metalloprotease	○	0	○	4.70E-01	○	0.000441	○	Not GPI-anchored	○
AAEL008162	Protease m1 zinc metalloprotease	●	1	○	2.33E-01	○	0.013946	○	Not GPI-anchored	○
AAEL012779	Protease m1 zinc metalloprotease	○	0	○	9.77E-04	●	0.999955	●	Probable	○
AAEL000859	Putative uncharacterized protein	●	0.997	○	3.98E-03	●	0.999989	●	Highly probable	●
AAEL006271	Superoxide dismutase (Cu-Zn)	●	1	●	8.65E-04	●	0.999962	●	Weakly probable	●
AAEL008607	Tep3	○	0	○	4.88E-03	●	0.999985	●	Weakly probable	○
AAEL011641	Transferrin	●	0.993	●	5.69E-02	○	Pot. false +	●	Weakly probable	●
AAEL013320	Translocon-associated protein, delta subunit	●	1	○	2.24E-01	○	n/a	●	Probable	●
AAEL005614	Trypsin	●	1	○	2.09E-01	○	Pot. false +	○	Not GPI-anchored	●
AAEL008079	Trypsin-alpha, putative	●	0.974	●	4.27E-04	●	1	●	Highly probable	●
AAEL008097	Trypsin-eta, putative	●	0.987	○	1.16E-02	○	Pot. false +	●	Weakly probable	●
AAEL005269	Ubiquinol-cytochrome c reductase complex core protein	●	0.914	●	1.67E-02	○	n/a	●	Weakly probable	●
AAEL007777	Vacuolar ATP synthase subunit S1	●	1	●	6.61E-01	○	n/a	●	Weakly probable	○
AAEL006023	Vanin-like protein 1, putative	●	0.842	●	2.83E-03	●	0.999998	○	Not GPI-anchored	●
AAEL001840	Zinc carboxypeptidase	●	0.994	○	4.84E-01	○	0.018004	○	Not GPI-anchored	○
AAEL008600	Zinc carboxypeptidase	●	0.996	○	4.90E-01	○	0.000595	○	Not GPI-anchored	○
AAEL008609	Zinc carboxypeptidase	○	0.002	○	1.17E-01	○	0.177718	○	Not GPI-anchored	○
AAEL001844	Zinc carboxypeptidase	●	1	○	2.67E-01	○	0.000055	○	Not GPI-anchored	○

Table 4.3. Computational prediction of palmitoylation modification sites in *A.aegypti* lipid raft proteome.
Note: High-confidence palmitoylated candidates were selected and modification sites are indicated in red font.

VectorBase acc. no.	Protein name	Position	Peptide	Score	Cutoff	
AAEL011902	1-acylglycerol-3-phosphate O-acyltransferase	4	****MTDCTLCHYVG	2.438	1.225	Cluster C
		7	*MTDCTLCHYVGLLV	2.388	1.225	Cluster C
AAEL010146	3-hydroxyacyl-coa dehyrogenase	100	VISAKPGCFVAGADI	0.381	0.308	Cluster A
		113	DITMLEKCKSAEEAT	0.352	0.308	Cluster A
		148	VAAINGVCLGGGLEL	0.639	0.497	Cluster B
AAEL008083	40S ribosomal protein	3	*****MPCHACNDRI	0.676	0.308	Cluster A
		6	**MPCHACNDRILPP	0.686	0.308	Cluster A
AAEL003746	4-Hydroxybutyrate CoA-transferas	294	VDLVKKGCVTNDKKA	0.759	0.497	Cluster B
AAEL008481	60S ribosomal protein	185	ARGRRSSCGFKN***	2.033	1.225	Cluster C
AAEL012944	60S ribosomal protein L11	151	FAHIGKYCCQRQM**	2.762	0.308	Cluster A
		152	AHIGKYCCQRQM***	1.771	0.308	Cluster A
AAEL009825	60S ribosomal protein L13a	130	PTAMRQLCLRPDRKF	0.528	0.497	Cluster B
AAEL011447	60S ribosomal protein L14	7	*MVSISVCVPVLKEK	1.595	0.308	Cluster A
AAEL003530	Acidic ribosomal protein P1, putati	10	LNKAELACVYSALIL	3.438	1.225	Cluster C
CPIJ005786	Actin	2	******MCDEEIAAL	0.776	0.308	Cluster A
CPIJ012574	Actin	2	******MCDDDAGAL	0.71	0.308	Cluster A
AAEL011197	Actin	2	******MCDEEVAAL	0.867	0.308	Cluster A
		218	RDIKEKLCYVALDFE	1.231	1.225	Cluster C
AAEL005961	Actin	2	******MCDDDAGAL	0.71	0.308	Cluster A
		218	RDIKEKLCYVALDFE	1.231	1.225	Cluster C
AAEL001673	Actin	2	******MCDDDVAAL	2.364	1.225	Cluster C
		218	RDIKEKLCYVALDFE	1.231	1.225	Cluster C
AAEL004616	Actin	2	******MCDDEIAAL	2.397	1.225	Cluster C
AAEL004631	Actin	2	******MCDDDVAAL	2.364	1.225	Cluster C
		218	RDIKEKLCYVALDFE	1.231	1.225	Cluster C

AAEL005964	Actin	2	******MCDDDAGAL	0.662	0.308	Cluster A
AAEL003957	Actin depolymerizing factor	11	GVTVSDVCKTTYEEI	0.529	0.308	Cluster A
AAEL004778	Acyl-coa dehydrogenase	14	QLVSKTGCSLAQNSR	0.833	0.308	Cluster A
		323	LAGTMRACIAKATDH	0.343	0.308	Cluster A
		608	SLIANNICENGGVVQ	0.457	0.308	Cluster A
AAEL008574	Acyl-CoA oxidase	388	PELHAIACCLKAVCT	0.357	0.308	Cluster A
AAEL005662	Adenosine diphosphatase	3	*****MTCLQQQDAN	2.89	0.308	Cluster A
		443	EISWALGCAYSILTS	1.21	0.308	Cluster A
AAEL005821	Alanyl aminopeptidase	14	YLLAAGVCCVLASPI	1.886	0.308	Cluster A
		15	LLAAGVCCVLASPID	0.819	0.308	Cluster A
		779	LILQGLGCAQDREQI	0.5	0.308	Cluster A
AAEL005808	Alanyl aminopeptidase	5	***MMILCSLLGVSL	1.343	0.308	Cluster A
AGAP011302	Alkaline phosphatase	520	HMMAYAACIGNGLKA	1.152	0.308	Cluster A
		528	IGNGLKACPEN****	1.614	0.308	Cluster A
AAEL003313	Alkaline phosphatase	131	RQVADSACTATAYLS	1.273	1.225	Cluster C
AAEL003309	Alkaline phosphatase	10	LKALAVLCLLAVVKA	2.496	1.225	Cluster C
		545	GAGSLSACLSLLVAA	1.339	1.225	Cluster C
AAEL003298	Alkaline phosphatase	507	HMMAYALCVGDGLTA	0.69	0.308	Cluster A
		515	VGDGLTACVDTTQ**	1.686	0.308	Cluster A
AAEL010532	Alpha-amylase	4	****MKKCAVVCLLG	5.017	1.225	Cluster C
		8	MKKCAVVCLLGLLAL	3.43	1.225	Cluster C
AAEL010537	Alpha-amylase	4	****MRLCSAGLLVT	4.653	1.225	Cluster C
AAEL014710	Alpha-amylase	15	LTALVVYCTSQELAE	0.519	0.308	Cluster A
AAEL005740	AMP dependent ligase	224	NIVINKCCCLVYTSG	0.595	0.308	Cluster A
		609	PKVSTSYCSKCRPKS	0.676	0.497	Cluster B
CPIJ007204	Apolipophorins precursor	4	****MLGCMASCKTG	1.91	0.308	Cluster A
		8	MLGCMASCKTGCPSP	1.067	0.308	Cluster A
		12	MASCKTGCPSPNKSS	1.843	0.497	Cluster B
		529	AYLSLVECPSAAVAN	0.314	0.308	Cluster A
		2993	PVEVPAQCKKCSVSG	0.352	0.308	Cluster A

		3293	**EISSDCVCKLRNGLH**	0.481	0.308	Cluster A
AAEL009955	Apolipophorin II	6	****MASSSCKTGCPTP**	0.576	0.308	Cluster A
		10	**SSSCKTGCPTPNKST**	1.537	0.497	Cluster B
		473	**LLDKVVLCASDKSSA**	0.429	0.308	Cluster A
		3291	**EVSSDCVCKLRNGLH**	0.452	0.308	Cluster A
		3303	**GLHAEESCEAKETRY**	0.443	0.308	Cluster A
AAEL009569	Apolipoprotein D, putative	27	**AVIYEKHCLIFEESY**	0.371	0.308	Cluster A
AAEL010986	Apyrase, putative	536	**VVALAFVCMLQRIFM**	1.381	0.308	Cluster A
AAEL011341	Apyrase, putative	415	**PFENNLVCVELRGDY**	0.381	0.308	Cluster A
AAEL008848	ATP synthase gamma subunit	243	**FAMKEGACSEQSSRM**	0.395	0.308	Cluster A
AAEL006582	Calcium-transporting atpase	102	**LILIANACVGVWQER**	0.319	0.308	Cluster A
		267	**SKVISLICIAVWAIN**	1.355	1.225	Cluster C
		317	**LPAVITTCLALGTRR**	0.424	0.308	Cluster A
		469	**DRRSAAICVRQEIET**	0.741	0.497	Cluster B
AAEL000898	Carboxylesterase	2	********MCAKYITAV**	4.727	1.225	Cluster C
AAEL009420	Cd36 antigen	2	********MCCCNCSNT**	9.333	0.497	Cluster B
		3	*******MCCCNCSNTA**	2.886	0.308	Cluster A
		4	******MCCCNCSNTAK**	5.009	0.497	Cluster B
		6	****MCCCNCSNTAKKV**	4.269	0.497	Cluster B
AAEL009432	Cd36 antigen	2	********MCGKCSNKA**	1.048	0.308	Cluster A
		5	*****MCGKCSNKAKRW**	3.491	0.497	Cluster B
		473	**VGILGVFCLALFLHY**	1.014	0.308	Cluster A
AAEL006958	Cell adhesion molecule	109	**YINAQKICQAYQGDL**	0.371	0.308	Cluster A
		1301	**IMYKFFKCYY*******	1.417	0.497	Cluster B
AAEL008340	Cell adhesion molecule	1082	**ILLLIIICIIKRNRG**	0.833	0.308	Cluster A
AAEL004546	Coatomer beta subunit	8	**MSLSEASCYTIINAQ**	1.119	0.308	Cluster A
		388	**LVRTLHSCCIKFPDV**	0.581	0.308	Cluster A
		948	**KINHTQKCLQEKPVA**	1.39	0.308	Cluster A
AAEL005097	Cold induced protein (BnC24A), putative	2	********MCLQICLAA**	4.793	1.225	Cluster C
		6	****MCLQICLAAGLTK**	1.429	0.308	Cluster A

AAEL017096	Conserved hypothetical protein	363	**GYTPVLDCHTAHIAC**	0.39	0.308	Cluster A
		370	**CHTAHIACKFAEIKE**	0.676	0.308	Cluster A
AAEL005259	Conserved hypothetical protein	8	**MHDFAAMCYYPVPYP**	1.38	1.225	Cluster C
AAEL016984	Conserved hypothetical protein	149	**KVVSNASCTTNCLAP**	0.348	0.308	Cluster A
		244	**VSVVDLTCRLNKPAT**	1.052	0.308	Cluster A
AAEL005432	conserved hypothetical protein	11	**KLWVVLFCAVAVLDR**	1.224	0.308	Cluster A
		483	**VDTNRAICVQPFLKA**	0.528	0.497	Cluster B
		782	**DVRPYYSCCMWQDEQ**	0.62	0.497	Cluster B
		1201	**PLIMCIVCGVYCFRK**	0.519	0.308	Cluster A
		1205	**CIVCGVYCFRKRKLK**	0.786	0.308	Cluster A
AAEL003785	conserved hypothetical protein	3	*****MDCLKRSPSF**	1.105	0.308	Cluster A
AAEL008801	conserved hypothetical protein	4	****MRDCVGENNNT**	1.267	0.308	Cluster A
		12	**VGENNNTCFTRIVNR**	0.543	0.308	Cluster A
AAEL010833	conserved hypothetical protein	4	****ARSCTTCDTVL**	4.562	1.225	Cluster C
		7	***ARSCTTCDTVLAEL**	3.074	1.225	Cluster C
		1079	**DYLAVFFCE********	1.962	0.308	Cluster A
CPIJ019325	Conserved hypothetical protein	8	**MRNRKRRCACLARTL**	3.033	1.225	Cluster C
		10	**NRKRRCACLARTLKA**	2.579	1.225	Cluster C
		18	**LARTLKACSSVLLVL**	1.901	1.225	Cluster C
AGAP002076	Conserved hypothetical protein	19	**DLGTTYSCVGVFQHG**	0.405	0.308	Cluster A
AAEL003774	conserved hypothetical protein	144	**RWTKVAKCSVEDSKN**	0.639	0.497	Cluster B
AAEL011935	conserved hypothetical protein	11	**LTLTAIACGLLVLAS**	3.347	1.225	Cluster C
		243	**INQRINQCVV*****	2.033	1.225	Cluster C
AAEL012262	conserved hypothetical protein	3	*****MECKLISRYS**	1.271	0.308	Cluster A
		251	**LCAIILICEKRRNKT**	1.024	0.308	Cluster A
AAEL008478	conserved hypothetical protein	135	**RRSTAIECINTFSND**	0.338	0.308	Cluster A
		146	**FSNDVDVCLEEEERE**	1.296	0.497	Cluster B
AAEL000294	conserved hypothetical protein	8	**MKFKFRPCSAVSTGL**	2.116	1.225	Cluster C
		30	**QASVYEGCQQEVNVK**	0.357	0.308	Cluster A
AAEL004239	conserved hypothetical protein	6	****MKFFLCLLLAIAG**	3.281	1.225	Cluster C

		231	**IRDTLHFCQ********	1.543	0.308	Cluster A
AAEL010520	conserved hypothetical protein	16	**TWLLLVVCSLLASKF**	0.462	0.308	Cluster A
		32	**TANDVFGCGGFIKNA**	0.395	0.308	Cluster A
		407	**VVSGFKVCGQVISKK**	0.362	0.308	Cluster A
		507	**LPDAGNACSKDVTVT**	1.521	1.225	Cluster C
AAEL000529	conserved hypothetical protein	13	**GEFVDLYCPRKCSSS**	0.433	0.308	Cluster A
AAEL011813	conserved hypothetical protein	233	**ALYGLFLCCGHIANS**	0.871	0.308	Cluster A
		234	**LYGLFLCCGHIANSK**	0.386	0.308	Cluster A
AAEL001293	conserved hypothetical protein	283	**HIGRYNECGFVAKTD**	0.829	0.308	Cluster A
AAEL012382	conserved hypothetical protein	58	**ADVASNRCYGGFARV**	0.357	0.308	Cluster A
AAEL012964	conserved hypothetical protein	345	**KEAAVAACRQLFDVQ**	0.595	0.308	Cluster A
AAEL010266	conserved hypothetical protein	171	**DNSLCNKCFGPHCNE**	0.556	0.497	Cluster B
		260	**CYQCTEDCVDTDESQ**	0.546	0.497	Cluster B
		364	**EGKFVRGCESDLPTE**	0.324	0.308	Cluster A
		492	**SGQVIRGCFGDKKDE**	0.348	0.308	Cluster A
		906	**GKAICYECDSEQDND**	0.528	0.497	Cluster B
		980	**LPDTRTQCYVCEGSE**	0.611	0.497	Cluster B
		1290	**SSLSCIQCMGARDCE**	0.319	0.308	Cluster A
		1540	**PAPTFLSCLRCQESS**	0.467	0.308	Cluster A
		1543	**TFLSCLRCQESSDDA**	0.524	0.308	Cluster A
AAEL017508	conserved hypothetical protein	24	**LASAGAACCTHPLDL**	0.348	0.308	Cluster A
		25	**ASAGAACCTHPLDLL**	1.636	1.225	Cluster C
AAEL002619	conserved hypothetical protein	14	**IGALLLLCGGISADE**	0.867	0.308	Cluster A
AAEL005170	Cytochrome c oxidase subunit iv	10	**PNVTLVICSDTQIRK**	1.105	0.308	Cluster A
AAEL011871	Cytochrome C1	9	**AAFVGRICGSGLLSS**	3.207	1.225	Cluster C
AAEL014414	DEAD box ATP-dependent RNA h	129	**MNVQCHACIGGTNLG**	1.314	1.225	Cluster C
AAEL008857	Deoxyribonuclease I, putative	21	**KKNAIQECQAELSDS**	0.5	0.308	Cluster A
AAEL002764	Dihydrolipoamide succinyltransfer	325	**LGFMSAFCKAAAYAL**	0.556	0.497	Cluster B
AAEL009310	Dipeptidyl carboxypeptidase	2	******LCHRAASLP**	1.633	0.308	Cluster A
AAEL002174	Dolichyl-diphosphooligosaccharide	127	**LRELASECGFEVDEE**	0.694	0.497	Cluster B

AAEL007078	eIF3a	187	**AKMAFGFCLKYNRKM**	0.357	0.308	Cluster A
AAEL011288	Elongation factor 1 gamma	357	**KQAFASVCLFGEDNN**	0.583	0.497	Cluster B
AAEL000951	Elongation factor 1-beta2	189	**GINKLQICCVIEDDK**	0.829	0.308	Cluster A
		190	**INKLQICCVIEDDKV**	1.38	0.497	Cluster B
AAEL009313	Elongation factor-1 beta,delta	231	**IHKLQLSCVIEDDKV**	0.815	0.497	Cluster B
CPIJ009303	Elongation factor 1-alpha 1	12	**FVRETGVCASGRVSG**	0.69	0.308	Cluster A
		382	**GYTPVLDCHTAHIAC**	0.443	0.308	Cluster A
		389	**CHTAHIACKFSEIKE**	0.671	0.308	Cluster A
AAEL012827	Endoplasmin	652	**ERLSNSPCALVASMF**	1.612	1.225	Cluster C
CPIJ000948	Enolase	400	**QIKTGAPCRSERLAK**	0.433	0.308	Cluster A
AAEL001668	Enolase	400	**QIKTGAPCRSERLAK**	0.414	0.308	Cluster A
AAEL004500	Eukaryotic translation elongation factor	135	**GALVVVDCVSGVCVQ**	0.31	0.308	Cluster A
		140	**VDCVSGVCVQTETVL**	1.602	0.497	Cluster B
AAEL013144	Eukaryotic translation initiation fac	224	**FDSESLMCLKTYKTE**	0.352	0.308	Cluster A
AAEL004347	Eukaryotic translation initiation factor 3 subunit M	53	**IIGVCDVCFKDGTQH**	0.648	0.497	Cluster B
		92	**ENLILAFCEKMTRAP**	0.319	0.308	Cluster A
AAEL004041	Flotillin-2	3	*******GGCCGSTKKR**	4.639	0.497	Cluster B
		4	******GGCCGSTKKRT**	2.315	0.497	Cluster B
		196	**AGIREAECEKSAMDV**	0.386	0.308	Cluster A
AAEL005766	Fructose-bisphosphate aldolase	40	**ADESTATCGKRFADI**	0.31	0.308	Cluster A
		240	**MVTAGQSCAKKPSAQ**	0.319	0.308	Cluster A
AAEL012135	Galectin	11	**QFAGNLSCTVEAGQI**	1.983	1.225	Cluster C
		307	**MNMGVPDCEGFESYS**	0.676	0.308	Cluster A
AAEL010386	Glucosyl/glucuronosyl transferases	2	********LCWLLLLSS**	4.025	1.225	Cluster C
		11	**LLLLSSLCIISVQNV**	1.76	1.225	Cluster C
		505	**HLLVRRVCRKKSSKP**	2.567	0.308	Cluster A
AAEL010464	Histone H1, putative	72	**EYFFHRACQICEEKM**	0.722	0.497	Cluster B
		75	**FHRACQICEEKMVED**	0.593	0.497	Cluster B
		315	**LHSCRYLCRAGATCI**	0.565	0.497	Cluster B
AAEL015573	Glycoside hydrolases	106	**FNEPLQTCLYSYEHD**	0.722	0.497	Cluster B

		444	GFYWIFRCYA*****	2.348	0.308	Cluster A
AAEL009237	Glycoside hydrolases	8	MKYVALVCLLLTVGF	2.446	1.225	Cluster C
		528	MLILRQLC*******	5.3	0.308	Cluster A
AAEL015020	Glycoside hydrolases	3	*****MKCFALVCLL	5.785	1.225	Cluster C
		8	MKCFALVCLLLLTVG	3.496	1.225	Cluster C
		529	MLILRQLC*******	5.3	0.308	Cluster A
AAEL017349	Heat shock cognate 70	18	AAVAVLTCTAEEKKE	0.924	0.308	Cluster A
AAEL013981	Hexamerin 2 beta	11	TVAAIALCLVALTSA	1.967	1.225	Cluster C
AGAP006452	hypothetical protein	14	RSLVAPLCFLLLASS	1.306	1.225	Cluster C
		29	WLVSDVDCAKKAAAS	0.567	0.308	Cluster A
		177	DYVAVLFCTDHENCP	0.314	0.308	Cluster A
AGAP003789	hypothetical protein	18	GVISAPTCGCCGSTK	0.31	0.308	Cluster A
		20	ISAPTCGCCGSTKKR	1.694	0.497	Cluster B
		198	AGIREAECEKSAMDV	0.386	0.308	Cluster A
AAEL009295	Lachesin	20	GVLLPLVCVAQRTPS	0.695	0.308	Cluster A
		113	TDAGIYQCQVVLSVT	1.529	1.225	Cluster C
AAEL003262	Leucine-rich transmembrane protein	1115	ANPVRCDCQARAFRR	0.602	0.497	Cluster B
		1246	FLLVVIICICRVRMN	0.776	0.308	Cluster A
		1248	LVVIICICRVRMNND	1.771	0.308	Cluster A
AAEL012554	Maltose phosphorylase	1209	FLGEYAACVCNTELN	0.852	0.497	Cluster B
		1429	DDQPAVRCYYRDGCV	0.433	0.308	Cluster A
		1435	RCYYRDGCVCE****	0.537	0.497	Cluster B
AAEL002861	Membrane protein, putative	89	QCRIVVNCCGPYRFF	0.814	0.308	Cluster A
		90	CRIVVNCCGPYRFFG	0.5	0.497	Cluster B
		415	TNLIEELCKNGFKFE	0.652	0.308	Cluster A
AAEL005610	Mitochondrial ATP synthase b cha	111	GPAVAAYCDKEIDRI	0.778	0.497	Cluster B
AAEL004423	Mitochondrial F0 ATP synthase D	105	REEISKFCKESEARI	0.583	0.497	Cluster B
AAEL014842	Multiple inositol polyphosphate ph	30	VHAQNIRCCEDYCYS	0.89	0.308	Cluster A
AAEL005733	Myosin heavy chain, nonmuscle or smooth muscle	794	MSWMQSWCRGYLARK	0.731	0.497	Cluster B
		1413	IESLNQKCVALEKTK	0.852	0.497	Cluster B

CPIJ015035	Myosin-IB	966	**DVPDIIECCIWILDV**	0.41	0.308	Cluster A
		967	**VPDIIECCIWILDVT**	1.388	1.225	Cluster C
		1024	**NLLVNQKCGQVANGN**	0.786	0.308	Cluster A
AAEL001411	Myosin heavy chain, nonmuscle or smooth muscle	361	**VEAIAKACYEKMFKW**	0.778	0.497	Cluster B
		408	**LNSFEQLCINYTNEK**	0.62	0.497	Cluster B
		828	**LQAEIELCAEAEEGR**	0.371	0.308	Cluster A
AAEL011905	Myosin I (Brush border myosin I)	724	**TYSKIITCQKYIRRY**	0.329	0.308	Cluster A
		966	**DVPDIIECCIWILNA**	0.381	0.308	Cluster A
AAEL012062	Na+/k+ atpase alpha subunit	321	**LLATVTVCLTLTAKR**	0.467	0.308	Cluster A
		915	**QWADLIICKTRRNSI**	0.486	0.308	Cluster A
AAEL012552	NADH-ubiquinone oxidoreductase	16	**VIVLGARCPTATQTA**	0.443	0.308	Cluster A
		84	**VAGNCRMCLVEVEKS**	1.028	0.497	Cluster B
		192	**RCIHCTRCIRFASEV**	0.528	0.497	Cluster B
		717	**ASPTMAKCVTAAKKQ**	1.481	0.308	Cluster A
AAEL011381	NADH-ubiquinone oxidoreductase	22	**ANVYVTNCLLKNVGA**	0.481	0.308	Cluster A
AAEL012616	Nadp transhydrogenase	9	**TRGMLRLCTYGGDAI**	1.579	1.225	Cluster C
		701	**GAAAVLTCVATYMHD**	0.343	0.308	Cluster A
		860	**AILSYIMCKAMNRSL**	0.743	0.308	Cluster A
AAEL008069	Notch	2	********MCERPACPQ**	1.138	0.308	Cluster A
		7	***MCERPACPQNSVRC**	0.481	0.308	Cluster A
		14	**CPQNSVRCSNGACIN**	1.562	1.225	Cluster C
		189	**TYPGGLECLYIIKAQ**	0.51	0.308	Cluster A
		494	**NAIEKISCLADGNWE**	0.414	0.308	Cluster A
		947	**PECIYAKCVSLPDDK**	0.787	0.497	Cluster B
		1560	**NGAVAPSCLPQYQEM**	0.704	0.497	Cluster B
		3276	**VLLIWMICSRANKRR**	1.2	0.308	Cluster A
		3397	**LVLIRQVCFKK********	1.71	0.308	Cluster A
AAEL006371	Oviductin	9	**SGRKLEDCSQHRDSG**	0.362	0.308	Cluster A
		95	**KMWPIEACFIALAIA**	1.57	1.225	Cluster C
AAEL012312	Proliferation-associated 2g4	53	**GASVKALCQKGDNQM**	0.319	0.308	Cluster A

	(Pa2g4/ebp1)	345	**GTNFDVNCFESEHSV**	0.343	0.308	Cluster A
AAEL012778	Protease m1 zinc metalloprotease	800	**MIISALGCSENKQFL**	0.452	0.308	Cluster A
AAEL008155	Protease m1 zinc metalloprotease	784	**VLINAMGCSQSKEQL**	0.343	0.308	Cluster A
AAEL012776	Protease m1 zinc metalloprotease	5	***MLKICVPLALLA**	4.421	1.225	Cluster C
		709	**LIALEWACNSDESCQ**	0.448	0.308	Cluster A
		780	**YLVDTISCVENGQSI**	0.452	0.308	Cluster A
AAEL012774	Protease m1 zinc metalloprotease	794	**MYISALGCSENKQFL**	0.567	0.308	Cluster A
AAEL008163	Protease m1 zinc metalloprotease	8	**MKLLFIGCFLSVVLA**	2.793	1.225	Cluster C
		791	**EIITALGCTKDTQSI**	0.343	0.308	Cluster A
AAEL012786	Protease m1 zinc metalloprotease	17	**AVILLVICVPISEAF**	0.4	0.308	Cluster A
AAEL013899	Protease m1 zinc metalloprotease	527	**CRIGQQACLEQAMSK**	0.333	0.308	Cluster A
		592	**YLMDSLACVGSREEQ**	0.376	0.308	Cluster A
AAEL008162	Protease m1 zinc metalloprotease	791	**LVISALGCAQNKDHL**	0.343	0.308	Cluster A
AAEL012779	Protease m1 zinc metalloprotease	542	**DLRSSIYCAGLVNAS**	0.31	0.308	Cluster A
		578	**DLIYALGCTENVELM**	0.476	0.308	Cluster A
AAEL001432	Protein disulfide isomerase	56	**VMFYAPWCGHCKKLK**	0.381	0.308	Cluster A
		398	**IEFYAPWCGHCKKLA**	0.713	0.497	Cluster B
AAEL002501	Protein disulfide isomerase	16	**SALVAVGCFFAGLAQ**	0.357	0.308	Cluster A
AAEL000859	Putative uncharacterized protein	25	**CESTALLCLKCADTD**	1.676	0.497	Cluster B
		187	**SLKVHTKCLMCKSQD**	0.759	0.497	Cluster B
		190	**VHTKCLMCKSQDGAK**	0.31	0.308	Cluster A
		248	**KNEVDSTCVTCSGEE**	0.62	0.497	Cluster B
		268	**KWLKCHQCKEADTST**	0.338	0.308	Cluster A
		372	**GTASSTPCVEPSQKK**	0.546	0.497	Cluster B
		412	**TDKTCATCVNEGCNG**	0.741	0.497	Cluster B
		494	**DGLTAKQCLTCAGEN**	0.667	0.497	Cluster B
AAEL005792	Putative uncharacterized protein	71	**EGNNMLVCCTKQDML**	0.562	0.308	Cluster A
		209	**HTSSIPACLWREKAK**	0.829	0.308	Cluster A
AAEL007845	Rab5	23	**GATQNKICQFKLVLL**	1.256	1.225	Cluster C
		211	**QSRQNSGCCSK******	2.041	1.225	Cluster C

		212	**SRQNSGCCSK*****	2.942	1.225	Cluster C
AAEL004902	Ras-related protein Rab-2A, putative	212	**GGQSSSGCC******	2.802	1.225	Cluster C
		213	**GQSSSGCC*******	2.893	1.225	Cluster C
AAEL013071	Ribophorin	17	**VFAAVIFCVQSAIDV**	0.543	0.308	Cluster A
		260	**DSRSNQACVKSYKTL**	1.512	1.225	Cluster C
AAEL010521	Ribophorin ii	655	**LALFTFLCGNRLLRA**	0.814	0.308	Cluster A
AAEL012736	Ribosomal protein L15	155	**VTGSPRPCTAP****	1.405	0.308	Cluster A
CPIJ007488	60S ribosomal protein	373	**DFLMIKGCCIGAKRR**	1.148	0.308	Cluster A
		374	**FLMIKGCCIGAKRRI**	1.148	0.497	Cluster B
AAEL013625	40S ribosomal protein S5	81	**KRFRKAQCPIVERLT**	1.438	1.225	Cluster C
AAEL003837	ryanodine receptor 3 brain	116	**NSDMYLACLSTSSSN**	0.348	0.308	Cluster A
		611	**LDVLCSLCVGNGVAV**	1.009	0.497	Cluster B
		1771	**YRAAHALCNHVDQKQ**	0.62	0.497	Cluster B
		2305	**SHQMVVACCRFLCYF**	0.314	0.308	Cluster A
		2306	**HQMVVACCRFLCYFC**	0.917	0.497	Cluster B
		2310	**VACCRFLCYFCRTGR**	1.231	0.497	Cluster B
		2313	**CRFLCYFCRTGRQNQ**	1.222	0.497	Cluster B
		3851	**ASIVARSCGEEEEEG**	0.352	0.308	Cluster A
		4231	**EIDFLLACCETNHDG**	0.319	0.308	Cluster A
		4232	**IDFLLACCETNHDGK**	0.87	0.497	Cluster B
		5104	**DFFPVGDCFRKQYED**	0.5	0.308	Cluster A
AAEL007926	Serine carboxypeptidase	18	**LFVLLGACRGVPRDG**	0.462	0.308	Cluster A
AAEL009682	Serine collagenase 1, putative	12	**TLVAAILCVLGAQAA**	0.567	0.308	Cluster A
		234	**ASLITQSCGNTAPTG**	0.329	0.308	Cluster A
AAEL002600	Serine protease	44	**CEHYLLKCCKVPKDL**	0.348	0.308	Cluster A
		45	**EHYLLKCCKVPKDLD**	0.602	0.497	Cluster B
		721	**VVLTAAHCVQNKKPH**	0.586	0.308	Cluster A
AAEL002595	Serine protease	126	**CANYLDTCCEKEQVL**	0.338	0.308	Cluster A
		127	**ANYLDTCCEKEQVLV**	1.545	1.225	Cluster C
		215	**VILTAAHCVANKQQD**	0.505	0.308	Cluster A

AAEL002629	Serine protease	9	**SRAVVLSCALLVFAV**	3.868	1.225	Cluster C
		68	**ACERGQRCVQRYLCT**	1.463	1.225	Cluster C
		102	**CVNYLAGCCYEEDII**	0.362	0.308	Cluster A
		103	**VNYLAGCCYEEDIIS**	1.056	0.497	Cluster B
		185	**VVLTASHCVQNKSPV**	0.448	0.308	Cluster A
AAEL011929	Serine-type enodpeptidase, putative	181	**SIITLADCRSRHSVA**	0.481	0.308	Cluster A
AAEL006627	Serine-type enodpeptidase, putative	181	**NIITLADCRNRHSVA**	0.433	0.308	Cluster A
		233	**IVSWGIPCGLGAPDV**	0.352	0.308	Cluster A
AAEL011917	Serine-type enodpeptidase, putative	10	**KSSALVVCLCLAVAS**	0.5	0.308	Cluster A
		12	**SALVVCLCLAVASAN**	0.976	0.308	Cluster A
		230	**VVSWGIPCGLGYPDV**	0.343	0.308	Cluster A
AAEL011913	Serine-type enodpeptidase, putative	234	**IVSWGIACAQGFPDV**	0.329	0.308	Cluster A
CPIJ011380	Serine-type enodpeptidase	214	**NIITLADCRNRHSVA**	0.519	0.308	Cluster A
AAEL011889	Serine-type enodpeptidase, putative	9	**KLLVLLVCAVVAVSA**	1.543	0.308	Cluster A
AAEL006902	Serine-type enodpeptidase, putative	10	**FFLAVMACLAVSQAA**	2.657	0.308	Cluster A
		287	**ELLLMMPCDN*****	2.705	0.308	Cluster A
AAEL006224	Short-chain dehydrogenase	23	**MSGQRNLCSQISSSR**	0.314	0.308	Cluster A
AAEL015065	Spectrin	2067	**DLTDPVRCNSIEEIK**	0.51	0.308	Cluster A
AAEL009634	Steroid dehydrogenase	12	**YDIFSGVCVFVVSVQ**	2.182	1.225	Cluster C
AAEL010330	Succinate dehydrogenase	5	***MALVCDLKMLLA**	4.099	1.225	Cluster C
		13	**DLKMLLACRGAFGQI**	1.224	0.308	Cluster A
		191	**YECILCACCSTSCPS**	2.852	0.497	Cluster B
		192	**ECILCACCSTSCPSY**	0.843	0.497	Cluster B
		196	**CACCSTSCPSYWWNG**	1.111	0.497	Cluster B
CPIJ004284	Sulfide quinone reductase	7	***MNSLRVCNVIRSSL**	1.181	0.308	Cluster A
		48	**VGGGAGGCSVAAKLS**	1.388	1.225	Cluster C
		332	**NVFAIGDCSASPNSK**	0.376	0.308	Cluster A
AAEL002107	Sulfide quinone reductase	7	***MYSLRVCNILRNGT**	0.971	0.308	Cluster A
AAEL006271	Superoxide dismutase (Cu-Zn)	12	**IVLAVVSCLASVYAS**	0.79	0.308	Cluster A
AAEL008687	Tar RNA binding protein (Trbp)	301	**STLPVAVCHGSGSTA**	0.324	0.308	Cluster A

AAEL008607	Tep3	914	**LIRMPYGCGEQNMLN**	0.31	0.308	Cluster A
		1409	**NEDCGNSCSIKSQKQ**	1.361	0.497	Cluster B
AAEL011641	Transferrin	209	**YPNLCELCQNPNECT**	0.917	0.497	Cluster B
		363	**CQTTSRWCTTSPEEK**	0.75	0.497	Cluster B
AAEL003872	Translationally-controlled tumor pr	161	**ESTPVLLCFKHGLEE**	1.176	0.308	Cluster A
AAEL013320	Translocon-associated protein, delta subunit	19	**VAVSASLCRASSCSN**	0.81	0.308	Cluster A
		24	**SLCRASSCSNPEVKS**	1.009	0.497	Cluster B
AAEL005614	Trypsin	4	******MKACIVLALCV**	5.669	1.225	Cluster C
		10	**ACIVLALCVVSAFAG**	0.529	0.308	Cluster A
		196	**PVVTLATCRSQWGTA**	0.443	0.308	Cluster A
AAEL008079	Trypsin-alpha, putative	7	***MPWSIECSTVIAFV**	3.843	1.225	Cluster C
		16	**TVIAFVVCLLVAAPI**	0.529	0.308	Cluster A
		43	**SNATGNACPHAVAIR**	1.364	1.225	Cluster C
		159	**VNRTCTLCGWGANST**	0.704	0.497	Cluster B
		204	**ALPTGQICAGVLAAG**	1.231	1.225	Cluster C
AAEL006642	Tubulin alpha chain	4	******MRECISVHVGQ**	0.624	0.308	Cluster A
		20	**GVQIGNACWELYCLE**	2.165	1.225	Cluster C
		129	**IRKLADQCTGLQGFL**	1.736	1.225	Cluster C
		213	**NEAIYDICRRNLDIE**	1.876	1.225	Cluster C
		295	**VAEITNACFEPANQM**	2.12	0.497	Cluster B
		305	**PANQMVKCDPRHGKY**	1.938	0.308	Cluster A
		316	**HGKYMACCMLYRGDV**	2.124	1.225	Cluster C
		347	**TIQFVDWCPTGFKVG**	1.419	0.308	Cluster A
		376	**AKVQRAVCMLSNTTA**	1.711	1.225	Cluster C
AAEL002851	Tubulin beta chain	12	**VHIQAGQCGNQIGAK**	1.433	0.308	Cluster A
		127	**VRKEAESCDCLQGFQ**	1.248	1.225	Cluster C
		129	**KEAESCDCLQGFQLT**	1.711	1.225	Cluster C
		211	**NEALYDICFRTLKLT**	1.364	1.225	Cluster C
		239	**TMSGVTTCLRFPGQL**	1.41	0.308	Cluster A
		303	**AKNMMAACDPRHGRY**	2.024	0.308	Cluster A

		354	**NNVKTAVCDIPPRGL**	1.843	1.225	Cluster C
AAEL005052	Tubulin beta chain	12	**VHLQAGQCGNQIGSK**	1.438	0.308	Cluster A
		129	**KESENCDCLQGFQLA**	1.562	1.225	Cluster C
		211	**NEALYDICMRTLRLA**	1.322	1.225	Cluster C
		239	**TMSGVTTCLRFPGQL**	1.267	0.308	Cluster A
		303	**SKNMMTACDPRHGRY**	1.786	0.308	Cluster A
		354	**NNVKVAVCDIAPRGL**	1.702	1.225	Cluster C
CPIJ007772	Vacuolar ATP synthase catalytic su	274	**DVIVYVGCGERGNEM**	0.324	0.308	Cluster A
AAEL008787	Vacuolar ATP synthase catalytic su	274	**DVIIYVGCGERGNEM**	0.314	0.308	Cluster A
AAEL011025	Vacuolar ATP synthase subunit ac	332	**NIVWIAECVAQKHRA**	0.748	0.308	Cluster A
AAEL005173	Vacuolar ATP synthase subunit c	147	**IAPNFHNCCIPCFLK**	1.12	0.497	Cluster B
		251	**NHGTNSSCGYCSHHT**	1.281	1.225	Cluster C
		254	**TNSSCGYCSHHTNSS**	0.639	0.497	Cluster B
AAEL006516	Vacuolar ATP synthase subunit h	298	**HCIAMVQCKVMKQLQ**	0.329	0.308	Cluster A
AAEL007777	Vacuolar ATP synthase subunit S1	15	**LGLALLVCSIQASDV**	0.795	0.308	Cluster A
AAEL006390	Vacuolar proton atpases	596	**EDHLKPGCAPSVLIM**	1.364	1.225	Cluster C
AAEL014053	Vacuolar proton atpases	13	**RSEEMALCQMFIQPE**	1.512	1.225	Cluster C
AAEL006023	Vanin-like protein 1, putative	351	**SLCQGSVCCNFTLNY**	0.529	0.308	Cluster A
AAEL001840	Zinc carboxypeptidase	10	**LWLPVLGCLLLVVLA**	2.545	1.225	Cluster C
AAEL008600	Zinc carboxypeptidase	3	*****MKCRSLVWLL**	4.967	1.225	Cluster C

Figure 4.1: Cholesterol and total protein content (A), Aminopeptidase and Alkaline phosphatase activity (B) in lipid raft fractions. Whole body BBMV was prepared and extracted with 1%Triton X-100 on ice for 30min with or without MBCD, and the membranes were floated in an Optiprep multistep gradient solution. After Optiprep step gradient ultracentrifugation for 4hrs at 4 °C and 270, 519g the gradient was fractionated from the top to the bottom. The cholesterol content of different Optiprep gradient fraction was determined by using an Amplex®Red cholesterol assay kit (Invitrogen, Carlsbad CA) according to the manufacturer's instructions. Cholesterol assays were done in 96-well flat-well plates (Costar) and fluorescence was measured by using a BioTek Synergy 4 plate reader at an excitation wavelength of 550 nm and an emission wavelength of 590 nm over 30 min (5min time point). Protein concentration of different gradient fractions was done with Coomassie assay (Bio-Rad, Hercules, CA). Fractionation of the gradient (12 x 1 mL) resulted in detection of a small protein peak observed within the 5–30% Optiprep zone (buoyant fractions 4–5), whereas the bulk of proteins were retained at the bottom of the gradient. Cholesterol is enriched in detergent insoluble and low density Optiprep gradient fraction.

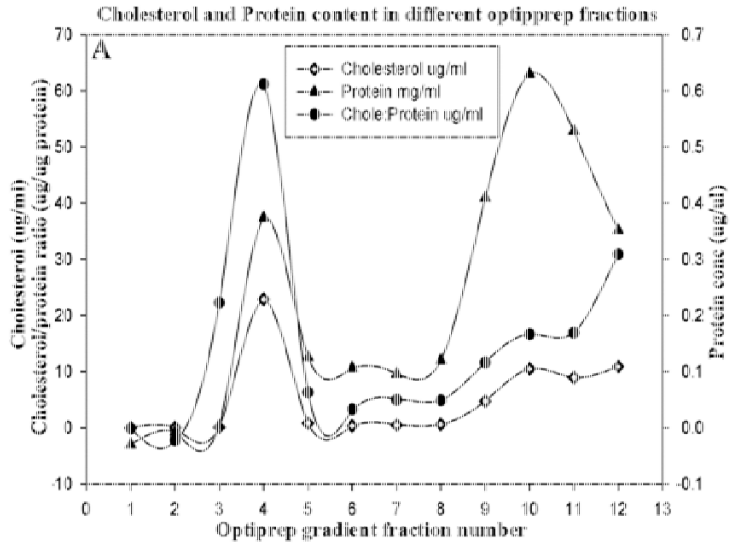
Cholesterol and Protein content in different optipprep fractions
A
Cholesterol ug/ml
Protein mg/ml
Chole:Protein ug/ml
Cholesterol (ug/ml)
Cholesterol/protein ratio (ug/ug protein)
Protein conc (ug/ul)
Optiprep gradient fraction number

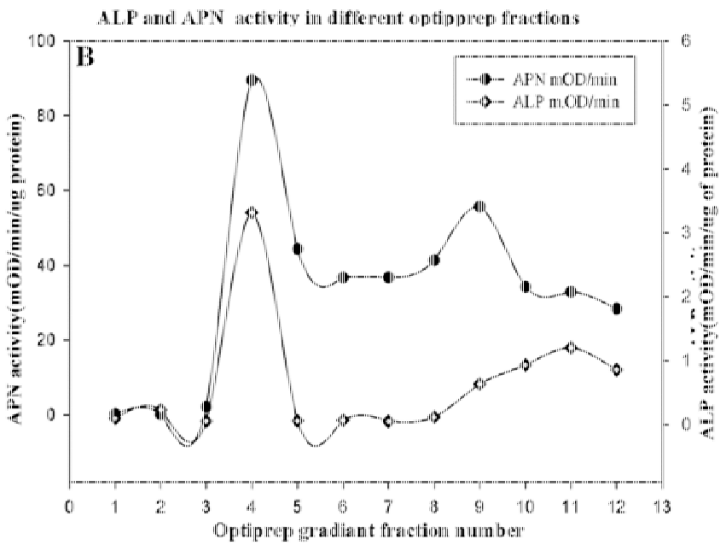
ALP and APN activity in different optipprep fractions
B
APN mOD/min
ALP mOD/min
APN activity(mOD/min/ug protein)
ALP activity(mOD/min/ug of protein)
Optiprep gradiant fraction number

Figure 4.2: Immunoblot analysis of Optiprep gradient fractions of the *A. aegypti* BBMV. Silver stained protein profile (A), and immunoblot of Flotillin-1 (B), APN1 (C) and Cry4Ba (D).

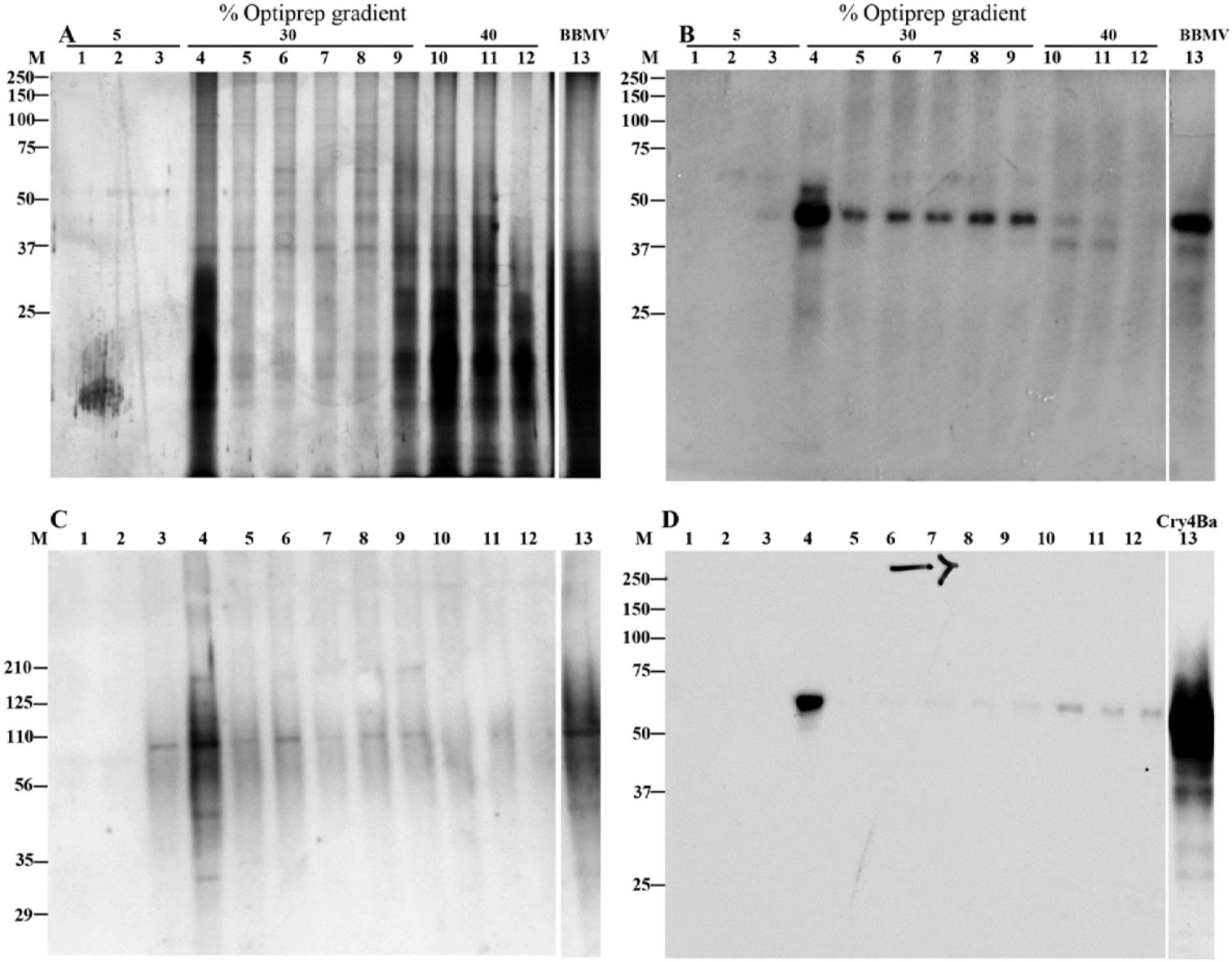
% Optiprep gradient
A
5
30
40
BBMV
M 1 2 3 4 5 6 7 8 9 10 11 12 13
250
150
100
75
50
37
25
% Optiprep gradient
B
5
30
40
BBMV
M 1 2 3 4 5 6 7 8 9 10 11 12 13
250
150
100
75
50
37
25
C
M 1 2 3 4 5 6 7 8 9 10 11 12 13
210
125
110
56
35
29
D
M 1 2 3 4 5 6 7 8 9 10 11 12 Cry4Ba 13
250
150
100
75
50
37
25

Figure 4.3. **Effect of MBCD on Protein, Cholesterol, Cry4Ba toxin, APN and ALP distribution in *Aedes* lipid raft fractions.** Isolation of lipid rafts from *A.aegypti* BBMV with pre incubation of MBCD followed by detergent solubilization. Triton X-100 insoluble complexes were prepared (see Materials and Methods) centrifuged through a 5%:30%:40% Optiprep step gradient and 1-ml fractions assayed for Cholesterol and total protein content (A), enzyme activity (B), AeFlot-1 immunoblot (C) and Cry4Ba toxin western blot (D). Treatment of BBMV with 20 mM MBCD had no effect the cholesterol and protein content of lipid raft fractions.

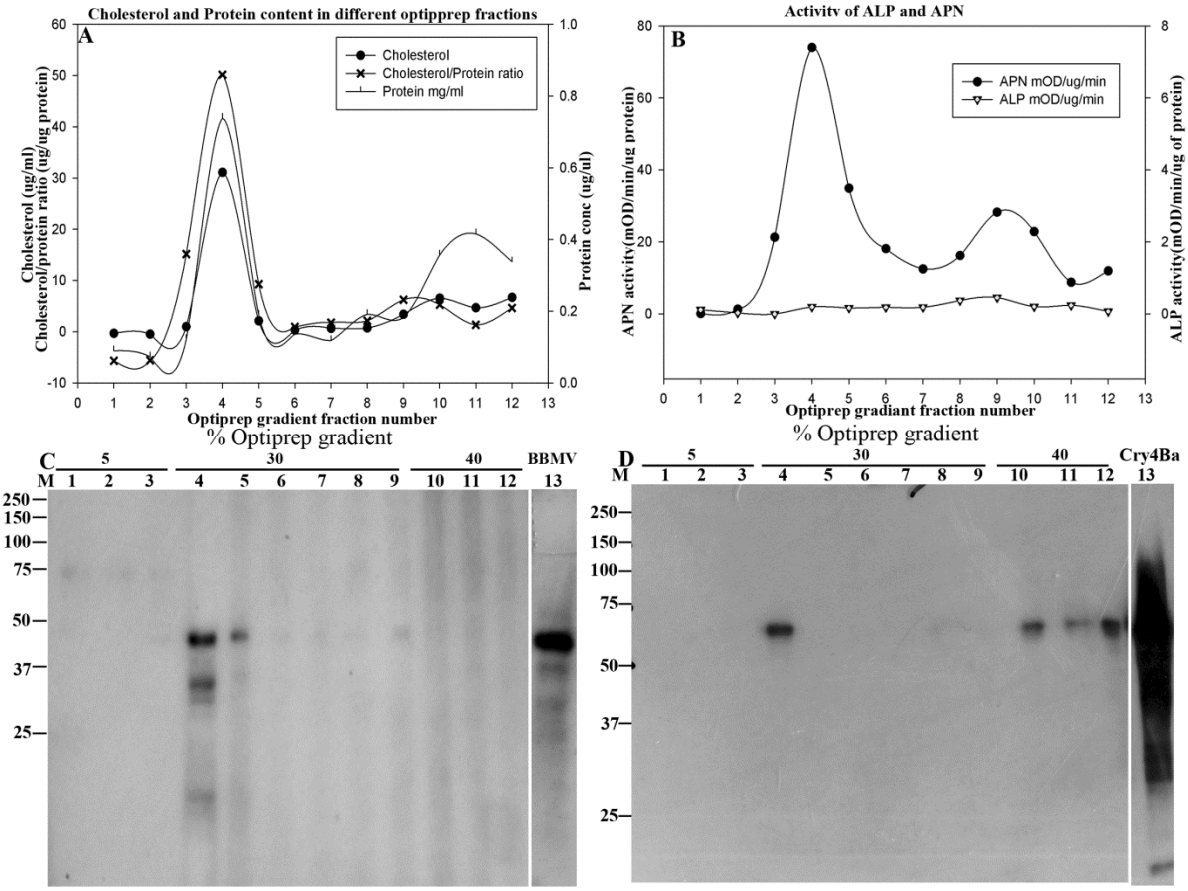
Cholesterol and Protein content in different optipprep fractions
A
Cholesterol
Cholesterol/Protein ratio
Protein mg/ml
Cholesterol (ug/ml)
Cholesterol/protein ratio (ug/ug protein)
Protein conc (ug/ul)
Optiprep gradient fraction number
% Optiprep gradient
Activitv of ALP and APN
B
APN mOD/ug/min
ALP mOD/ug/min
APN activity(mOD/min/ug protein)
ALP activity(mOD/min/ug of protein)
Optiprep gradiant fraction number
% Optiprep gradient
C
M
BBMV
D
Cry4Ba

Figure.4.4: Schematic representation of *Aedes* lipid rafts isolation and mass spectrometry analysis procedure.

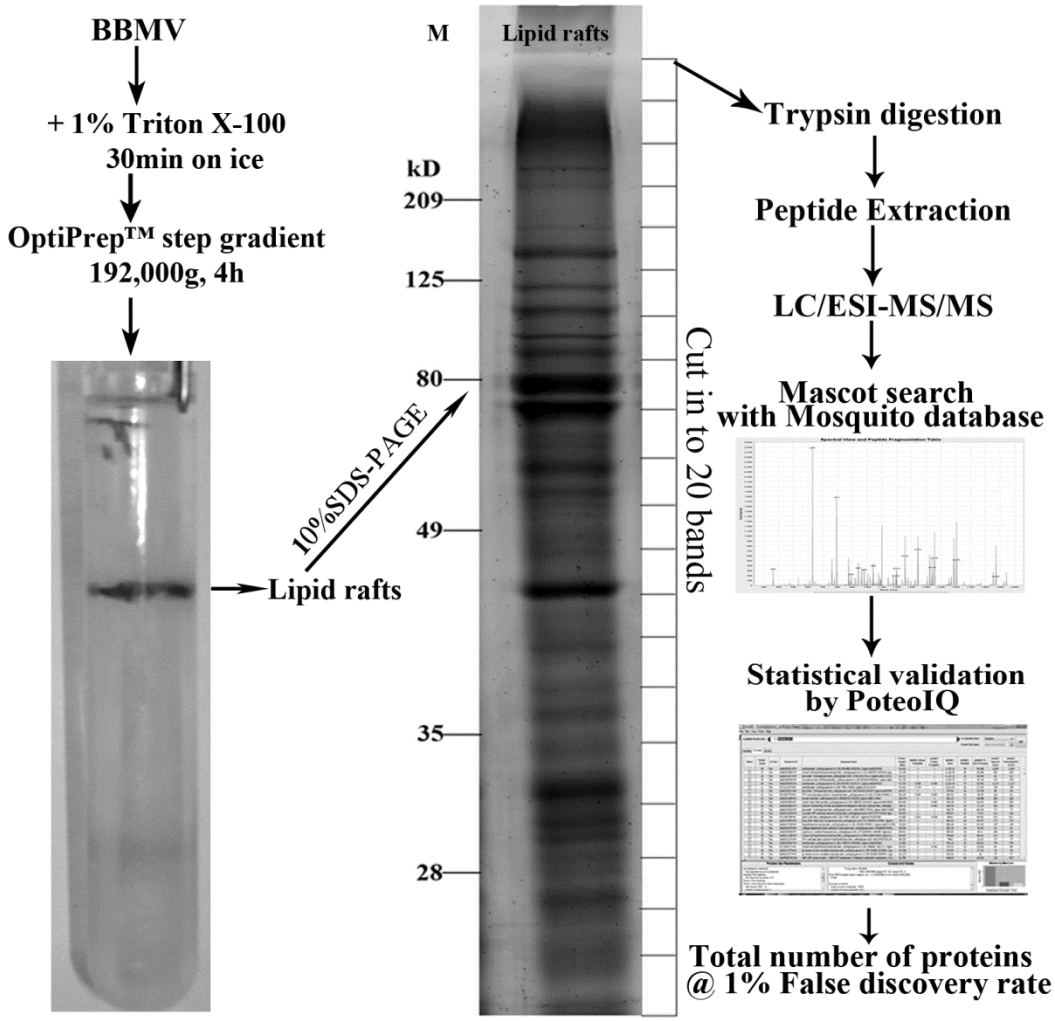
BBMV
+ 1% Triton X-100
30min on ice
OptiPrep™ step gradient
192,000g, 4h
Lipid rafts
10%SDS-PAGE
M
Lipid rafts
kD
209
125
80
49
35
28
Cut in to 20 bands
Trypsin digestion
Peptide Extraction
LC/ESI-MS/MS
Mascot search
with Mosquito database
Statistical validation
by PoteoIQ
Total number of proteins
@ 1% False discovery rate

Figure 4.5: **Classification of lipid rafts proteins. (A)** According to their pI and pI values were calculated using the ProtParam tool on the ExPASy server and **(B)** According to their molecular weight and molecular mass values (in kilodaltons) were calculated using the ProteoIQ tool.

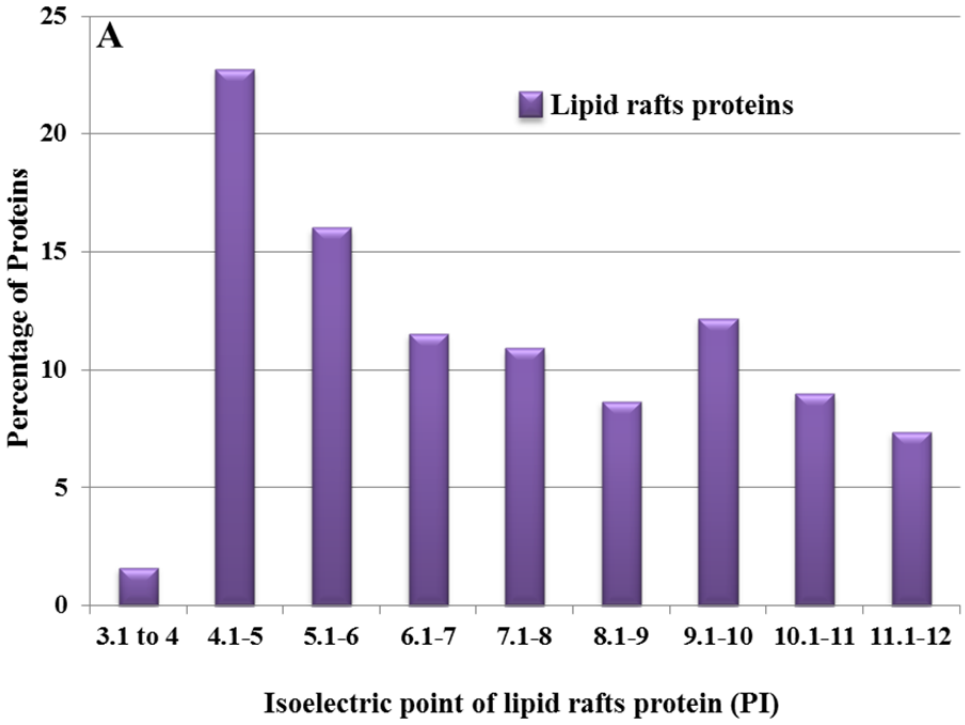
A
Lipid rafts proteins
Percentage of Proteins
25
20
15
10
5
0
3.1 to 4
4.1-5
5.1-6
6.1-7
7.1-8
8.1-9
9.1-10
10.1-11
11.1-12
Isoelectric point of lipid rafts protein (PI)

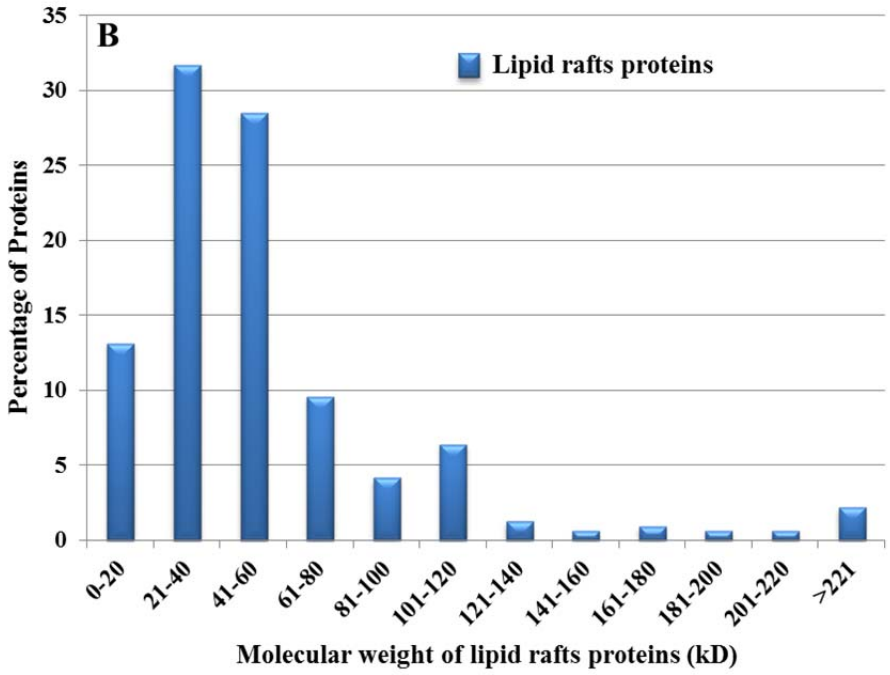
B
Lipid rafts proteins
Percentage of Proteins
35
30
25
20
15
10
5
0
0-20
21-40
41-60
61-80
81-100
101-120
121-140
141-160
161-180
181-200
201-220
>221
Molecular weight of lipid rafts proteins (kD)

Figure 4.6: Protein identification from *Aedes* lipid rafts preparation by LC-MS/MS analysis. Classification of *Aedes* lipid rafts proteins based on GO for cellular component (A), molecular function (B), and biological process (C). Numbers in percentages (%) correspond to the numbers of GO terms assigned for particular GO category.

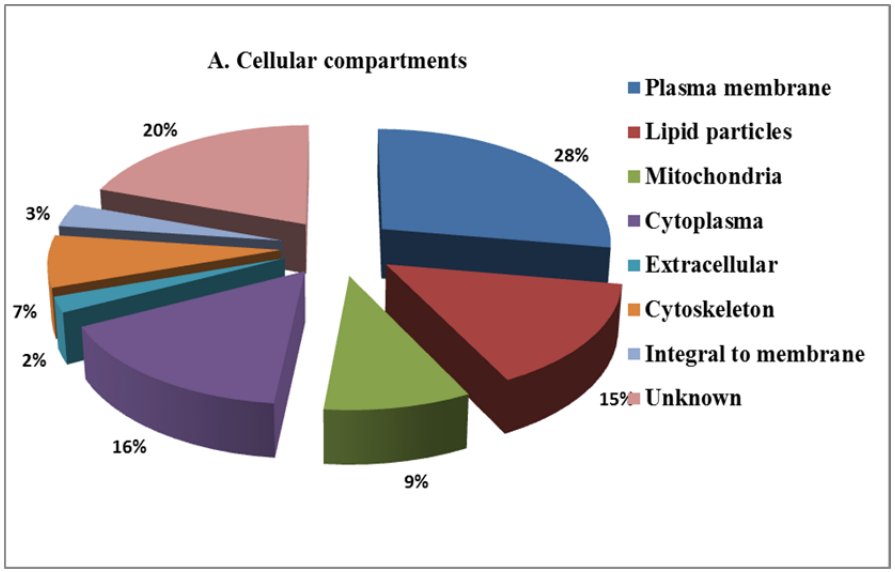
A. Cellular compartments
Plasma membrane
Lipid particles
Mitochondria
Cytoplasma
Extracellular
Cytoskeleton
Integral to membrane
Unknown
28%
15%
9%
16%
2%
7%
3%
20%

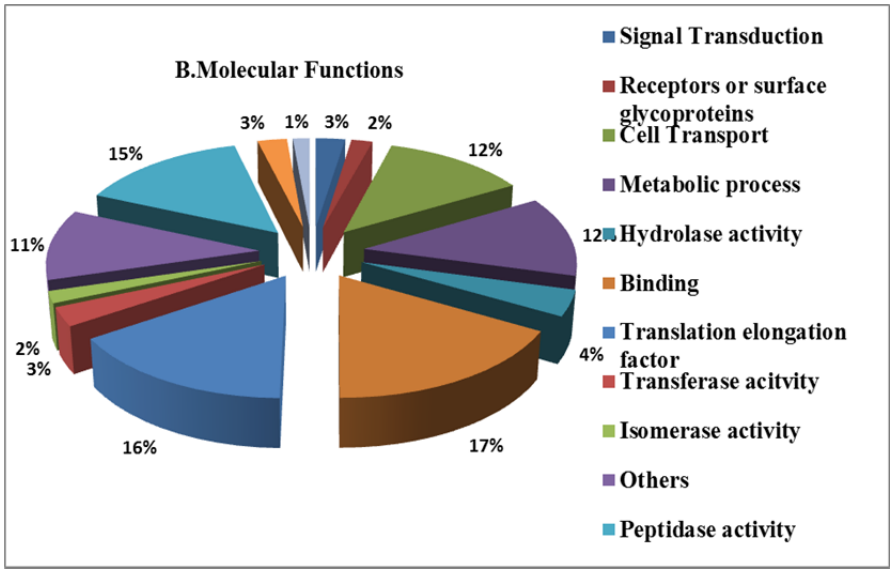
B.Molecular Functions
Signal Transduction
Receptors or surface glycoproteins
Cell Transport
Metabolic process
Hydrolase activity
Binding
Translation elongation factor
Transferase acitvity
Isomerase activity
Others
Peptidase activity
3%
1%
3%
2%
12%
12%
4%
17%
16%
3%
2%
11%
15%

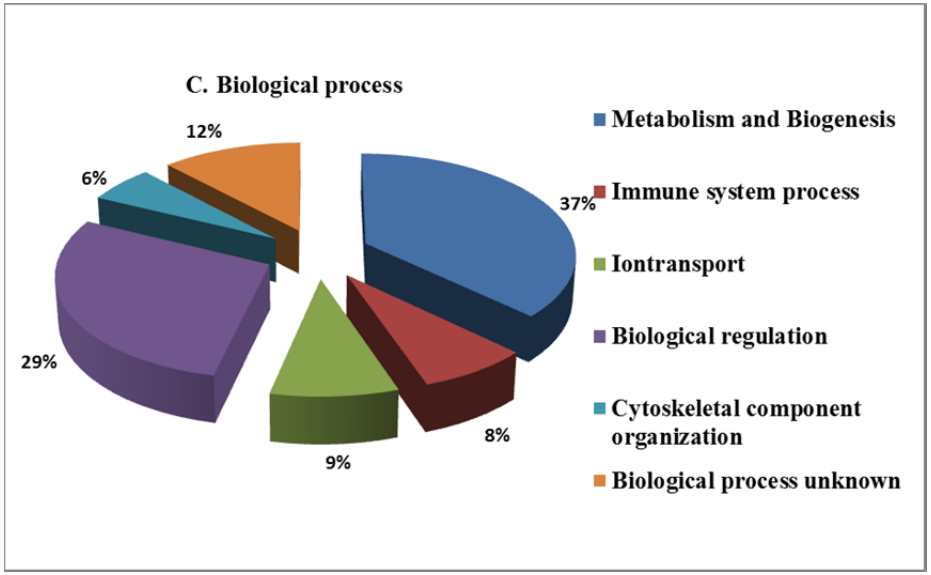
C. Biological process
Metabolism and Biogenesis
Immune system process
Iontransport
Biological regulation
Cytoskeletal component organization
Biological process unknown
37%
8%
9%
29%
6%
12%

CHAPTER 5

GENERAL DISCUSSION AND CONCLUSION

It is widely accepted that the primary action of *Bacillus thuringiensis* (Bt) Cry toxins is by their interaction with plasma membrane components of insect midgut epithelial cells, thereby forming pores in the apical microvilli membrane and finally leading to cell death. This is a well understood phenomenon in lepidopteran insects but in mosquitoes the precise mechanisms are poorly characterized.

The main concern is that insects are becoming resistant to Bt sprays and transgenic crops and it has been documented in some major insect species. Resistance against Bt toxins have been reported in the field populations of *Plutella xylostella* (Tabashnik, Cushing et al. 1990)*, Busseola fusca* (Van Rensburg 2007; Kruger, Rensburg et al. 2011) and *Helicoverpa zea* (Tabashnik, Gassmann et al. 2008). Although the mechanisms by which susceptible insects develop resistance differ, a point to consider is that insects can develop resistance to Bt toxins as observed with synthetic insecticide. However, when "mosquitocidal *Bacillus thuringiensis israelensis* (Bti)"- a mixture of Cry and Cyt toxins- is used, development of resistance in mosquitoes is slow and by no means comparable to the speedy development of resistance as observed with synthetic insecticides (Wirth, Georghiou et al. 1997). Still, a few laboratory selected strains of mosquitoes have shown the potential for development of resistance and laboratory selected *A. aegypti* larvae have shown up to 30-fold resistance to Bti (Paris, Tetreau et al. 2011). In this study, I have chosen to examine "Cry4Ba toxin" for three reasons: First,

comparatively, it has high toxic activity against *A. aegypti* larvae (Delecluse, Poncet et al. 1993); second, it contains the five conserved blocks which have structural homology to the core of activated Cry3Aa and Cry1Aa toxins (Boonserm, Davis et al. 2005), and third being its ability to bind similar receptors as lepidopteran active toxins (Soberon, Fernandez et al. 2007).

This dissertation research is aimed at characterizing Cry4Ba toxin interacting molecules from mosquito larval midgut by biochemical and proteomic approaches. Some of these novel approaches used to identify Bt binding proteins via 2-D electrophoresis based proteomic analyses of mosquito larval midgut proteins and also validating mass spectrometry identifications by immunoblotting and computational analyses. Use of these integrated approaches has resulted in the identification of several Cry4Ba binding proteins in *A. aegypti* larval midgut and some of them were similar to Cry toxin binding proteins reported previously through similar approaches (McNall and Adang 2003; Krishnamoorthy, Jurat-Fuentes et al. 2007). The comprehensive information on Cry4Ba binding proteins may help improve the understanding of mosquitocidal Bti toxin interaction with their target host. Successful cloning, and production of antisera of *Aedes* flotillin-1 (Aeflot-1) as a marker protein for lipid rafts, guided the purification of detergent resistant membranes (DRMs) from *A. aegypti* brush border membrane vesicles (BBMV). In addition, western blot analysis of BBMV from lepidopteran and coleopteran larvae can be detected by Aeflot-1 antibody. This finding demonstrates that Aeflot-1 antibody can be used as a marker protein to characterize lipid rafts in other group of insects as well. Additionally, proteomic analysis of Cry4Ba interacting lipid rafts revealed many membrane proteins which have potential implications in vector management and mosquito biology. This work demonstrated the utilities of proteomic-based approaches to examine the complex components of mosquito larval midgut and Bt toxin interactions with these components.

The identification of Cry4Ba toxin binding proteins and evidence for the involvement of lipid rafts in Cry4Ba toxicity were discussed in Chapters 2, 3 and 4 of this dissertation.

In chapter two, I have shown binding of ^{125}I-labeled Cry4Ba toxin to twelve different BBMV proteins a caveat being that proteins detected on blots are denatured. All these proteins were identified with high-confidence mascot scores using PMF alone or MS/MS spectral data. Compared to protein identities obtained from PMF data alone, MS/MS data analysis yielded superior identifications. One possible reason for this success could be an availability of well-annotated dipteran genome sequence databases coupled with powerful computational tools. It's reported that Cry4Ba toxin binds to Glycophosphatidylinositol (GPI)-aminopeptidase (APN) and three isoforms of GPI-alkaline phosphatases (ALPs). Other Cry4Ba binding proteins identified in my study are lipid raft associated flotillin, prohibitin and cytoplasmic side of plasma membrane associated V-ATPse, cytoskeletal protein actin, and less important serine proteases, mitochondrial porins and F_1F_0 ATP synthases subunits. There are several possible explanations for the toxin binding to the cytoplasmic side of proteins; as Cry4Ba makes pores in the midgut membrane which is a bilayer, it's possible only when toxin inserts and makes pores across the bilayer can toxin contact intracellular proteins. Otherwise mere toxin binding to GPI-anchored proteins which are on exoplasmic side, will not result in a membrane pore and ionic imbalance. Therefore, it is possible that the entire Cry4Ba toxin inserts into the lipid bilayer (Nair and Dean 2008) and then can access actin, V-ATPase (Beyenbach and Wieczorek 2006), flotillin-1 and other proteins which are localized on the cytoplasmic side of the membrane. In addition, Cry4Ba toxin binding to actin protein suggests the toxin's mode of action in cytoskeletal destabilization leads to loss of host cell shape and integrity (Shimada, Usui et al. 2001) and also possibly through apoptosis as reported previously (Loeb, Hakim et al. 2000).

Cry4Ba binding to mitochondrial proteins which involved several cellular processes. Mitochondrial membrane associated ATP synthase protein subunits which involves in ATP generation via H^+ transport (Chinopoulos and Adam-Vizi 2010), peptidase β subunit involves in cleavage of N-terminal signal sequences from proteins entering into the mitochondrion (Gakh, Cavadini et al. 2002) and porins which allow small metabolites such as ATP to diffuse across the mitochondrial membrane (Aiello, Messina et al. 2004). Cry4Ba also bound to two trypsin-like serine proteases of 30- and 42-kDa. The 30-kDa protein corresponds to the predicted size of the mature protein, while 42-kDa is closer to the size of a membrane secretory vesicle associated serine protease precursor (Shen, Edwards et al. 2000). We speculate that these trypsins might help in pulling the toxin close to the membrane by serving as a transient receptor which can lead to pore formation. Appearance of unexpected mitochondrial proteins on 2D gels is likely to reflect contamination of the BBMV preparations (Smith and Peters 1980). Nonetheless, this might have been anticipated because during homogenization process mitochondrial proteins are released, sometimes trapped in brush border membrane vesicles (Cutillas, Biber et al. 2005; Donowitz, Singh et al. 2007).

As presented in Chapter 3, we provided evidences showing presence of DRMs containing lipid rafts in BBMV derived from *A. aegypti* larval midgut. These DRMs were isolated by detergent extraction combined with gradient centrifugation. Published studies have reported the existence of lipid rafts in insects and their interaction with various cellular events including pathogen invasion (Rietveld, Neutz et al. 1999; Zhuang, Oltean et al. 2002; Eroglu, Brügger et al. 2003; Bravo, Gómez et al. 2004; Zhai, Chaturvedi et al. 2004; Avisar, Segal et al. 2005; Sousa, Carvalho et al. 2011). Flotillin-1, a lipid raft associated protein, is extensively used as a marker in biochemical characterization of mammalian DRMs/ lipid rafts (Bickel, Scherer et al.

1997; Morrow and Parton 2005; Stuermer 2010). Flotillin-1(called Aeflot-1) was successfully cloned from *A. aegypti* midgut and expressed in *E. coli*. Aeflot-1 protein sequence comparative analysis with other insect and vertebrate flotillin-1 sequences (Edgar and Polak 2001; Rivera-Milla, Stuermer et al. 2006) indicated similar protein characteristics. Importantly, antisera of Aeflot-1 specifically reacted with flotillin-1 protein from *A. aegypti* larvae and also cross reacts with flotillin-1 protein from members of Diptera, Coleoptera, and Lepidoptera. These results indicate apparent conservation of flotillin-1 protein structure, function and targeting to DRMs across arthropods, suggesting an important role for flotillin-1 in rafts-associated processes. The immunostaining of Aeflot-1 was observed at the apex of microvilli consistently along the posterior midgut and gastric caeca. It is interesting that other GPI-anchored ALPs (Fernandez, Aimanova et al. 2006) and APN (Chen, Aimanova et al. 2009) which are Cry toxin receptors also follow similar pattern of localization. Although it's physiological function in the insect midgut has not been characterized fully yet, to my knowledge this was the first report showing flotillin-1 localization in mosquito larval gut.

The use of anionic detergent extraction coupled with gradient flotation is a well-known concept in the mammalian cell biology field to investigate DRMs/lipid rafts. Although this procedure is relatively simple to prepare membrane fractions which are apparently resistant to detergent, it is important to ascertain the specificity of the methodology. Several lines of evidence through biochemical and western blot analyses suggest that *A. aegypti* BBMV has DRMs/rafts that are resistant to cold Triton X-100 solubilization. One of the most prominent markers of the DRMs is associated with low density fractions. First, we compared protein and cholesterol content, and found that the protein concentration was significantly low and cholesterol concentration and cholesterol to protein ratio was high in DRM fractions compared to

soluble high density fractions. Second, the enzymatic activities of ALP and APN were also highest in low density fraction (Radeva and Sharom 2004). Third, flotillin-1(Morrow and Parton 2005), and APN were specifically associated with prepared DRMs and were able to detect by western blot analysis (Dermine, Duclos et al. 2001; Gylfason, Knutsdottir et al. 2010).

We were interested in confirming the interaction of Bt Cry toxin with lipid rafts of the BBMV from the *A. aegypti* and to characterize those lipid rafts, if they proved to exist in this subcellular membrane fraction. The lipid rafts were extracted successfully from *A. aegypti* BBMV and fraction-4 identified as lipid raft enriched fractions due to the concentration of lipid raft specific marker proteins, APN, flotillin-1, and higher levels of cholesterol compared to other fractions. These findings corroborated the previous reports. Although plasma membrane is thought to be a platform for homogeneously distributed lipids and proteins, the concept of lipid rafts suggests that these sub domains are able to specifically sort proteins (Brown and Rose 1992). This differential enrichment of proteins in specific areas of the plasma membrane has been associated in vertebrate cells with some precise physiological functions (Brown and London 1998). The present study on insect DRMs further strengthens this statement, and the proteome analysis clearly reveals that compared with the whole BBMV proteome (Popova-Butler and Dean 2009), DRMs are enriched in selective proteins (Table 4.1).

Several experimental findings supported the importance of lipid rafts in mediating the action of Bt toxin. Cry1A toxin is concentrated into lepidopteran lipid rafts that facilitate rapid formation of pores and this can be possible only when lipid rafts are intact (Zhuang, Oltean et al. 2002). In addition, a previous study reported that the cadherin mediates the interaction of Cry1Ab toxin, lipid rafts and GPI-APN (Bravo, Gómez et al. 2004). Lepidopteran cells were resistant to Cry1Ca during G2-M phase of cell cycle because of absence of lipid raft domains in

the plasma membrane of Sf9 cells (Avisar, Segal et al. 2005). These toxin-host cell interactions rely on the presence of lipid rafts which provide flexibility in plasma membranes in the process of intoxication. Similarly, reduced levels of glycolipids have been detected in Bt-resistant larvae of *P. xylostella* (Kumaraswami, Maruyama et al. 2001) and glycolipids acts as a receptor for Bt toxins in nematodes and lepidopteran caterpillars (Griffitts, Haslam et al. 2005). In the present investigation, the Cry4Ba toxin was also shown to associate with DRMs, exhibiting similarities with other Bt toxins. It is possible that interactions with GPI-anchored proteins in lipid rafts help in coordinating the toxin oligomers in the process of pore formation across lipid bilayer in mosquito larval midgut cells.

The major goal of the research presented in chapter 4 was to characterize the proteome of lipid rafts prepared from *Aedes* larval BBMV. Using a combination of in-gel trypsin digestion coupled with peptide extraction and LC- MS/MS analysis, we were able to identify 312 proteins in this lipid raft fraction**,** a much larger number than in most previous studies of BBMV lipid rafts from other system (Nguyen, Amine et al. 2006; Gylfason, Knutsdottir et al. 2010). Among the total list of identified proteins, 36 hits were conserved hypothetical proteins not matching to any known proteins in the Diptera database. From the Gene Ontology (GO) predictions, for the subcellular location of the raft proteins, it is clear that the lipid raft fraction contains contamination by the ER, the nuclear envelope, and the mitochondria. Although numerous mitochondrial or vacuolar proteins have been identified in the lipid rafts proteome, some of the proteins have plasma membrane association *viz* V-ATPases (Wieczorek, Huss et al. 2003; Ryu, Kim et al. 2010), ATP synthases (Bae, Kim et al. 2004), voltage-dependent anion channels or porin (Bàthori, Parolini et al. 1999). Surprisingly a high diversity of ribosomal proteins were identified in our study (Table 4.1), a results in concordance with similar lipid rafts proteomic

studies (Zhang, Shaw et al. 2008; Williamson, Thompson et al. 2010). Ribosomal proteins may represent ribosomes that are attached to the cytoskeleton or association of ribosomal proteins with lipid rafts. We also identified several cytoskeletal proteins (actin and tubulin) in lipid rafts. However, we cannot exclude the possibility of brush border membrane vesicles trapping free ribosomes during the BBMV preparation which might have stuck to the raft fractions during extraction. In addition, our proteome analysis of *A. aegypti* lipid rafts identified many proteins that have previously been identified in other lipid rafts (see above, Chapter 4). Although our study does not establish direct evidence for functional correlation to the Cry4Ba toxin mode of action, the identification of these known Cry toxin receptor proteins, coupled with the extensive analysis of Cry4Ba toxin co-purification with lipid rafts fraction followed by immunodetection, suggests that similar to lepidopteran active Cry toxins, mosquitocidal Cry4Ba interacts with lipid rafts. This conclusion supports the notion that in addition to structural similarity between different Cry toxins, mode of action is also conserved across different groups of insects, suggesting existence of similar receptors.

Given the number of GPI-anchored proteins identified in this study (Table 4.1) which could serve as putative toxin receptors, it is possible that in *Aedes* larvae Cry4Ba toxin binds first to the highly abundant GPI-anchored proteins in lipid rafts (APN/ALP/alpha-amylase [Table 4.1]) and then to cadherin (Figure 5.1) or vice versa. Nevertheless, no proven experimental evidence to date supports this hypothesis in *Aedes* or mosquitoes larvae in general.

Characterization of proteome composition of *A. aegypti* DRMs/rafts emphasizes that despite differences in biology of yeast and mammalian cells, the protein composition and structural properties are consistent with their ability to separate into different phases. The novel finding in our current research has been identification of the interaction between *A. aegypti* lipid

rafts and Cry4Ba toxin and these rafts are enriched in GPI-anchored proteins which are implicated in Bt toxicity. In addition, we identified several membrane proteins and signaling molecules which could serve as potential markers for Bt-resistance in insects and provide an early warning for future control problems arising due to Bt-resistance. This understanding should enhance the ability to prolong the use of Bti biopesticides and also to mitigate the potentially devastating effects of resistance in mosquito control programs as well as outbreak of mosquito borne diseases. Despite contamination of lipid rafts with organelle proteomes, the analysis presented in this dissertation has uncovered several candidate proteins which can lead to new avenues for future investigations. Hopefully, these findings will provide a greater understanding in elucidating initial and critical step in receptor binding and subsequent oligomer formation of pore-forming Cry toxins and also toward the uncovering the intracellular effects and interactions of this toxin effects and interactions. For future studies, it would be crucial to evaluate the role of these key proteins which were identified in a lipid rafts proteome in various mosquitocidal Bt Cry toxin interactions.

References

Aiello, R., A. Messina, et al. (2004). "Functional characterization of a second porin isoform in *Drosophila melanogaster*." J. Biol.Chem. **279**(24): 25364-25373.

Avisar, D., M. Segal, et al. (2005). "Cell-cycle-dependent resistance to *Bacillus thuringiensis* Cry1C toxin in Sf9 cells." J. Cell Sci. **118**(Pt 14): 3163-3171.

Bae, T. J., M. S. Kim, et al. (2004). "Lipid raft proteome reveals ATP synthase complex in the cell surface." Proteomics **4**(11): 3536-3548.

Bàthori, G., I. Parolini, et al. (1999). "Porin is present in the plasma membrane where it is concentrated in caveolae and caveolae-related domains." J. Biol. Chem. **274**(42): 29607-29612.

Beyenbach, K. W. and H. Wieczorek (2006). "The V-type H+ ATPase: molecular structure and function, physiological roles and regulation." J. Exp. Biol. **209**(4): 577-589.

Bickel, P. E., P. E. Scherer, et al. (1997). "Flotillin and epidermal surface antigen define a new family of caveolae-associated integral membrane proteins." J. Biol. Chem. **272**(21): 13793-13802.

Boonserm, P., P. Davis, et al. (2005). "Crystal structure of the mosquito-larvicidal toxin Cry4Ba and its biological implications." J. Mol. Biol. **348**(2): 363-382.

Bravo, A., I. Gómez, et al. (2004). "Oligomerization triggers binding of a *Bacillus thuringiensis* Cry1Ab pore-forming toxin to aminopeptidase N receptor leading to insertion into membrane microdomains." Biochim. Biophys. Acta **1667**(1): 38-46.

Brown, D. A. and E. London (1998). "Functions of lipid rafts in biological membranes." Annu. Rev. Cell Dev. Biol. **14**: 111-136.

Brown, D. A. and J. K. Rose (1992). "Sorting of GPI-anchored proteins to glycolipid-enriched membrane subdomains during transport to the apical cell surface." Cell **68**(3): 533-544.

Chen, J., K. G. Aimanova, et al. (2009). "Identification and characterization of *Aedes aegypti* aminopeptidase N as a putative receptor of *Bacillus thuringiensis* Cry11A toxin." Insect Biochem. Mol. Biol. **39**(10): 688-696.

Chinopoulos, C. and V. Adam-Vizi (2010). "Mitochondria as ATP consumers in cellular pathology." Biochim. Biophys. Acta **1802**(1): 221-227.

Cutillas, P. R., J. Biber, et al. (2005). "Proteomic analysis of plasma membrane vesicles isolated from the rat renal cortex." Proteomics **5**(1): 101-112.

Delecluse, A., S. Poncet, et al. (1993). "Expression of cryIVA and cryIVB Genes, Independently or in Combination, in a Crystal-Negative Strain of *Bacillus thuringiensis* subsp. *israelensis*." Appl. Environ. Microbiol. **59**(11): 3922-3927.

Dermine, J. F., S. Duclos, et al. (2001). "Flotillin-1-enriched lipid raft domains accumulate on maturing phagosomes." J. Biol. Chem. **276**(21): 18507-18512.

Donowitz, M., S. Singh, et al. (2007). "Proteome of murine jejunal brush border membrane vesicles." J. Proteome Res. **6**(10): 4068-4079.

Edgar, A. J. and J. M. Polak (2001). "Flotillin-1: gene structure: cDNA cloning from human lung and the identification of alternative polyadenylation signals." Int. J. Biochem. Cell Biol. **33**(1): 53-64.

Eroglu, Ç., B. Brügger, et al. (2003). "Glutamate-binding affinity of *Drosophila* metabotropic glutamate receptor is modulated by association with lipid rafts." Proc. Natl. Acad. Sci. U.S.A. **100**(18): 10219-10224.

Fernandez, L. E., K. G. Aimanova, et al. (2006). "A GPI-anchored alkaline phosphatase is a functional midgut receptor of Cry11Aa toxin in *Aedes aegypti* larvae." Biochem. J. **394**(1): 77-84.

Gakh, O., P. Cavadini, et al. (2002). "Mitochondrial processing peptidases." Biochim. Biophys. Acta **1592**(1): 63-77.

Griffitts, J. S., S. M. Haslam, et al. (2005). "Glycolipids as receptors for *Bacillus thuringiensis* crystal toxin." Science **307**(5711): 922-925.

Gylfason, G. A., E. Knutsdottir, et al. (2010). "Isolation and biochemical characterisation of lipid rafts from Atlantic cod (*Gadus morhua*) intestinal enterocytes." Comp. Biochem. Physiol. B, Biochem. Mol. Biol. **155**(1): 86-95.

Krishnamoorthy, M., J. L. Jurat-Fuentes, et al. (2007). "Identification of novel Cry1Ac binding proteins in midgut membranes from *Heliothis virescens* using proteomic analyses." Insect Biochem. Mol. Biol. **37**(3): 189-201.

Kruger, M., J. R. J. V. Rensburg, et al. (2011). "Resistance to Bt maize in Busseola fusca (Lepidoptera: Noctuidae) from Vaalharts, South Africa." Environ. Entomol. **40**(2): 477-483.

Kumaraswami, N. S., T. Maruyama, et al. (2001). "Lipids of brush border membrane vesicles (BBMV) from *Plutella xylostella* resistant and susceptible to Cry1Ac delta-endotoxin of *Bacillus thuringiensis*." Comp. Biochem. Physiol. B, Biochem. Mol. Biol. **129**(1): 173-183.

Loeb, M. J., R. S. Hakim, et al. (2000). "Apoptosis in cultured midgut cells from *Heliothis virescens* larvae exposed to various conditions." Arch. Insect Biochem. Physiol. **45**(1): 12-23.

McNall, R. J. and M. J. Adang (2003). "Identification of novel *Bacillus thuringiensis* Cry1Ac binding proteins in *Manduca sexta* midgut through proteomic analysis." Insect Biochem. Molec. Biol. **33**(10): 999-1010.

Morrow, I. C. and R. G. Parton (2005). "Flotillins and the PHB domain protein family: rafts, worms and anaesthetics." Traffic **6**(9): 725-740.

Nair, M. S. and D. H. Dean (2008). "All domains of Cry1A toxins insert into insect brush border membranes." J. Biol. Chem. **283**(39): 26324-26331.

Nguyen, H. T. T., A. B. Amine, et al. (2006). "Proteomic characterization of lipid rafts markers from the rat intestinal brush border." Biochem. Biophys. Res. Commun. **342**(1): 236-244.

Paris, M., G. Tetreau, et al. (2011). "Persistence of *Bacillus thuringiensis israelensis* (Bti) in the environment induces resistance to multiple Bti toxins in mosquitoes." Pest Manag. Sci. **67**(1): 122-128.

Popova-Butler, A. and D. H. Dean (2009). "Proteomic analysis of the mosquito *Aedes aegypti* midgut brush border membrane vesicles." J. Insect Physiol. **55**(3): 264-272.

Radeva, G. and F. J. Sharom (2004). "Isolation and characterization of lipid rafts with different properties from RBL-2H3 (rat basophilic leukaemia) cells." Biochem. J. **380**(Pt 1): 219-230.

Rietveld, A., S. Neutz, et al. (1999). "Association of sterol- and glycosylphosphatidylinositol-linked proteins with *Drosophila* raft lipid microdomains." J. Biol. Chem. **274**(17): 12049 - 12054.

Rivera-Milla, E., C. A. Stuermer, et al. (2006). "Ancient origin of reggie (flotillin), reggie-like, and other lipid-raft proteins: convergent evolution of the SPFH domain." Cell Mol. Life Sci. **63**(3): 343-357.

Ryu, J., H. Kim, et al. (2010). "Proteomic analysis of osteoclast lipid rafts: the role of the integrity of lipid rafts on V-ATPase activity in osteoclasts." J. Bone Miner Metab. **28**(4): 410-417.

Shen, Z., M. J. Edwards, et al. (2000). "A gut-specific serine protease from the malaria vector *Anopheles gambiae* is downregulated after blood ingestion." Insect Mol. Biol. **9**(3): 223-229.

Shimada, Y., T. Usui, et al. (2001). "Asymmetric colocalization of Flamingo, a seven-pass transmembrane cadherin, and Dishevelled in planar cell polarization." Curr. Biol. **11**(11): 859-863.

Smith, G. D. and T. J. Peters (1980). "Analytical subcellular fractionation of rat liver with special reference to the localisation of putative plasma membrane marker enzymes." Eur. J. Biochem. **104**(1): 305-311.

Soberon, M., L. E. Fernandez, et al. (2007). "Mode of action of mosquitocidal *Bacillus thuringiensis* toxins." Toxicon **49**(5): 597-600.

Sousa, I. P., C. A. M. Carvalho, et al. (2011). "Envelope lipid-packing as a critical factor for the biological activity and stability of alphavirus particles isolated from mammalian and mosquito cells." J. Biol. Chem. **286**(3): 1730-1736.

Stuermer, C. A. (2010). "The reggie/flotillin connection to growth." Trends Cell Biol. **20**(1): 6-13.

Tabashnik, B. E., N. L. Cushing, et al. (1990). "Field development of resistance to *Bacillus thuringiensis* in diamondback moth (Lepidoptera, Plutellidae)." J. Econ. Entomol. **83**(5): 1671-1676.

Tabashnik, B. E., A. J. Gassmann, et al. (2008). "Insect resistance to Bt crops: evidence versus theory." Nat. Biotech. **26**(2): 199-202.

Van Rensburg, J. B. J. (2007). "First report of field resistance by the stem borer, *Busseola fusca* (Fuller) to Bt-transgenic maize." S. Afr. J. Plant & Soil **24**(3): 147–151.

Wieczorek, H., M. Huss, et al. (2003). "The insect plasma membrane H+ V-ATPase: intra-, inter-, and supramolecular aspects." J. Bioenerg. Biomembr. **35**(4): 359-366.

Williamson, R., A. J. Thompson, et al. (2010). "Isolation of detergent resistant microdomains from cultured neurons: detergent dependent alterations in protein composition." BMC Neurosci **11**: 120.

Wirth, M. C., G. P. Georghiou, et al. (1997). "CytA enables CryIV endotoxins of *Bacillus thuringiensis* to overcome high levels of CryIV resistance in the mosquito, *Culex quinquefasciatus*." Proc. Natl. Acad. Sci. U.S.A. **94**(20): 10536-10540.

Zhai, L., D. Chaturvedi, et al. (2004). "*Drosophila* Wnt-1 undergoes a hydrophobic modification and is targeted to lipid rafts, a process that requires porcupine." J. Biol. Chem. **279**(32): 33220-33227.

Zhang, N., A. R. E. Shaw, et al. (2008). "Liquid chromatography electrospray ionization and matrix-assisted laser desorption ionization tandem mass spectrometry for the analysis of lipid raft proteome of monocytes." Anal. Chim. Acta **627**(1): 82-90.

Zhuang, M., D. I. Oltean, et al. (2002). "*Heliothis virescens* and *Manduca sexta* lipid rafts are involved in Cry1A toxin binding to the midgut epithelium and subsequent pore formation." J. Biol. Chem. **277**(16): 13863-13872.

Figure 5.1: Model of Cry4Ba toxin mechanism in *A. aegypti* larval midgut

Upon ingestion of Cry4Ba toxin crystalline inclusions by an *Aedes* larva, the crystals solubilizes in alkaline midgut environment releasing the biologically inactive protoxins, which cleaved by midgut proteases, resulting in the formation of active toxin monomer. Toxin binding probably occurs first with the primary receptor cadherin triggering cleavage of helix α1 in domain-I similar to lepidopteran active Cry toxins. This cleavage results in change of confirmation in toxin structure unfolding more hydrophobic sites leading to the formation of oligomeric toxins which then bind to most abundant GPI-anchored APN or ALP or amylase proteins in lipid rafts forming a pre-porecomplex. Due to change in hydrophobicity of pre-porecomplex which results in high affinity to the lipid bilayer finally leading to membrane insertion of oligomeric toxins and pore formation. Additionally, because Cry4Ba toxin binds to flotillin and other proteins which are present on the cytoplasmic side of lipid bilayer, it is possible that these proteins might paly key role in stabilizing the pore or destabilizing the membrane stability there by affecting the host midgut epithelial cells.

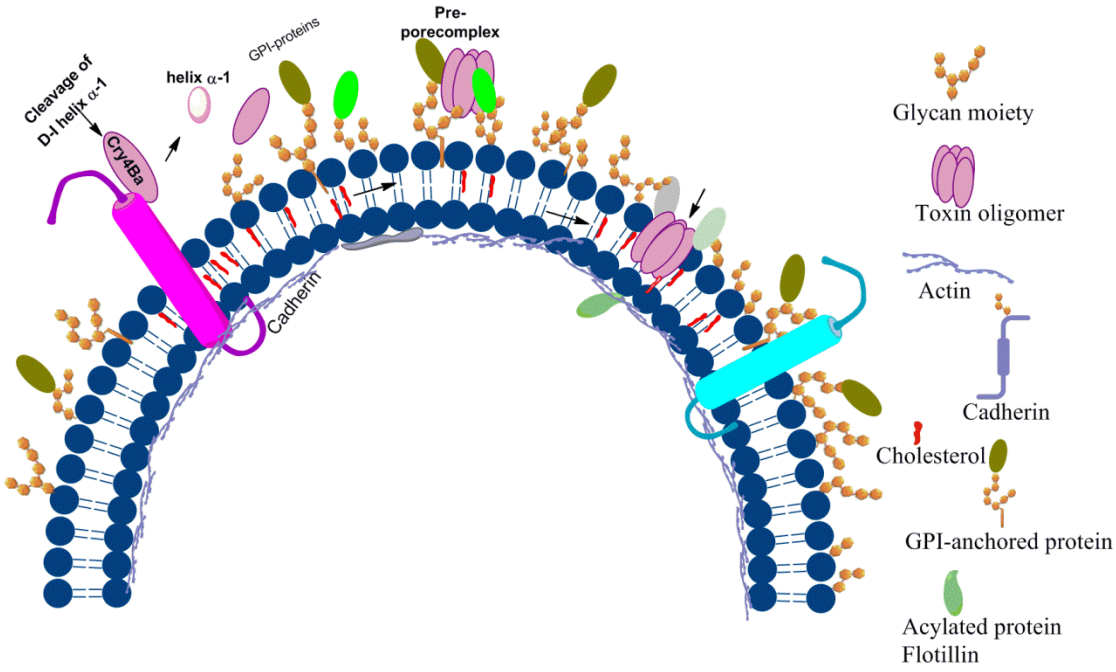
Cleavage of
D-I helix α-1
helix α-1
GPI-proteins
Pre-
porecomplex
Cry4Ba
Cadherin
Glycan moiety
Toxin oligomer
Actin
Cadherin
Cholesterol
GPI-anchored protein
Acylated protein
Flotillin